ROLE OF CARDIAC MAGNETIC RESONANCE IMAGING MEASURED MYOCARDIAL PERFUSION RESERVE IN ASYMPTOMATIC PATIENTS WITH AORTIC STENOSIS: A COMPARISON WITH EXERCISE TESTING

Thesis submitted for the degree of

Doctor of Philosophy

At the University of Leicester

by

Dr Anvesha Singh

MBChB, MRCP (UK)

Department of Cardiovascular Sciences

University of Leicester

November 2016

Abstract

Role of Cardiac Magnetic Resonance Imaging measured Myocardial Perfusion Reserve in asymptomatic patients with Aortic Stenosis: a comparison with Exercise Testing

Dr Anvesha Singh

Background: The management of asymptomatic patients with severe aortic stenosis (AS) is controversial. Cardiovascular Magnetic Resonance (CMR) imaging has been proposed as a potential prognostic marker that may help select patients for aortic valve replacement (AVR).

Aims: To establish: the reproducibility of novel CMR techniques; determinants of peak VO2 and MPR; effect of Ranolazine; and predictors of outcome in asymptomatic moderate-severe AS, and compare MPR to exercise testing as predictors of outcome.

Methods: The PRIMID-AS study was a multi-centre, prospective, observational study, with blinded analysis of imaging data. AS patients and controls underwent: trans-thoracic echocardiogram (TTE), symptom-limited cardiopulmonary exercise test (CPET), adenosine stress CMR at 3T and a CT calcium score, and were followed up for a minimum of 12 months, or until a primary endpoint occurred (symptom-driven AVR, MACE or cardiovascular death). Additionally a pilot study on the short-term effect of Ranolazine in asymptomatic patients with moderate-severe AS was carried out in 19 patients.

Results: 174 patients (age 66.2±13.34 years, 76% male, aortic valve area index 0.57±0.14 cm^2/m^2) were recruited as part of PRIMID-AS study, in addition to 23 age- and comorbidity-matched controls. Patients showed evidence of LV remodeling and impaired MPR, but preserved exercise capacity compared to controls, suggesting a state of 'compensation'. MPR and longitudinal strain were independently associated with age- and sex-corrected peak Vo_2, whilst extra-cellular volume (ECV) and AS severity were independently associated with MPR. A primary outcome occurred in 39 (22.4%) patients. MPR showed moderate association with outcome (area under curve (AUC)=0.62 (0.52-0.71, p=0.019), as did exercise testing (AUC=0.58 (0.49-0.67, p=0.071), with no significant difference between the two. Ranolazine did not improve diastolic function or MPR significantly.

Conclusions: MPR was associated with exercise capacity and symptom-onset in initially asymptomatic patients with AS, but with moderate accuracy and was not superior to symptom-limited exercise testing.

Acknowledgements

I have thoroughly enjoyed my time as a Clinical Research Fellow in the department of Cardiovascular Sciences, University of Leicester. I would like to thank the following people, without whose support, this thesis would not have been possible.

First and foremost, Professor Gerry McCann, my supervisor, who conceived the project and gave me the opportunity to undertake a PhD. He has been an encouraging, accessible and supportive supervisor throughout, who has also provided invaluable training in both clinical CMR and critical thinking, and continues to be a source of inspiration.

Dr Mark Horsfield, my co-supervisor, whose CMR Physics teaching and input in CMR analysis and interpretation has been invaluable.

The National Institute of Healthcare Research and Leicester Cardiovascular Biomedical Research Unit for funding the project (PDF 2011 Dr Gerald McCann) and myself.

The entire research team involved in making this project a success: the Cardiac Research Nurses: Sue Mackness and Robyn Lotto; the Cardiac Physiologists: Dr Anna-Marie Marsh and John McAdam; and the Cardiac MRI Radiographers for always being accommodating and fitting the long complex patient visits in. Also, the Research teams and PI's at the other centres, who helped achieve our recruitment target.

Dr Sarah Griffiths, our Trial Manager, whose input was invaluable. Rachel Zhang for her invaluable help with the statistical analysis for part of the thesis.

My fellow Research Fellows (Dr Jamal Khan, Dr Sheraz Nazir, Dr Prathap Kanagala) and BSc student (Soliana Bekele), who's support and company made the countless hours spent analysing the CMR images in a dark room a lot more fun.

Last but not the least, my parents for their continued support and encouragement, and most of all, my husband, Dr Gang Xu, for his unlimited support, understanding, encouragement and belief in me… and for being so proud of my achievements. And finally, my daughter Ria, who was born a week after the initial submission of this thesis!

Academic outputs resulting from this thesis

Prizes / Scholarships:

Early Career Award (Clinical) 2016. 19th Annual Society for Cardiovascular Magnetic Resonance (SCMR) Scientific Sessions, Los Angeles, USA. 27-30th January, 2016.

2016 Regional Scholarship Award. Society for Cardiovascular Magnetic Resonance (SCMR) Scientific Sessions, Los Angeles, USA. 27-30th January, 2016.

Young Investigator Award 2015. British Heart Valve Society (BHVS) Annual Meeting, Birmingham, UK. 16th October 2015.

BCS Travel Bursary. British Cardiovascular Society (BCS) annual conference 2015, Manchester, UK. 8-10th June 2015.

Publications:

Singh A, Steadman CD, Khan JN, Reggiardo G, McCann GP. Effect of late sodium current inhibition on MRI measured diastolic dysfunction in aortic stenosis: a pilot study. BMC Res Notes. 2016;9(1):64

Singh A, Horsfield MA, Bekele S, Khan JN, Greiser A, McCann GP. Myocardial T1 and extracellular volume fraction measurement in asymptomatic patients with aortic stenosis: reproducibility and comparison with age-matched controls. Eur Heart J Cardiovasc Imaging. 2015 Jul;16(7):763-70

Singh A, Steadman CD, Khan JN, Horsfield MA, Bekele S, Nazir SA, Kanagala P, Masca NG, Clarysse P, McCann GP. Intertechnique agreement and interstudy reproducibility of strain and diastolic strain rate at 1.5 and 3 Tesla: a comparison of feature-tracking and tagging in patients with aortic stenosis. J Magn Reson Imaging. 2015 Apr;41(4):1129-37

Singh A, Ford I, Greenwood JP, Khan JN, Uddin A, Berry C, Neubauer S, Prendergast B, Jerosch-Herold M, Williams B, Samani NJ, McCann GP. Rationale and design of the PRognostic Importance of MIcrovascular Dysfunction in asymptomatic patients with Aortic Stenosis (PRIMID-AS): a multicentre observational study with blinded investigations. BMJ Open. 2013;3(12):e004348

Singh A, Steadman CD, McCann GP. Advances in the Understanding of the Pathophysiology and Management of Aortic Stenosis: Role of Novel Imaging Techniques. Can J Cardiol. 2014 Sep;30(9):994-1003.

Manuscripts under review:

Singh A, Greenwood JP, Berry C, Dawson DK, Hogrefe K, Kelly DJ, Dhakshimamurthy V, Lang CC, Khoo JP, Sprigings D, Steeds RP, Jerosch-Herold M, Neubauer S, Prendergast B, Williams B, Zhang R, Hudson I, Squire IB, Ford I, Samani NJ, McCann GP. Comparison of exercise testing and CMR measured myocardial perfusion reserve for predicting outcome in asymptomatic aortic stenosis: the PRognostic Importance of MIcrovascular Dysfunction in Aortic Stenosis (PRIMID AS) study. (Submitted to EHJ).

Presentations:

International

Singh A, McCann GP. Gender differences in exercise capacity and LV remodeling in response to pressure overload in AS. (Poster presentation at **EuroCMR** 2016, Florence, Italy)

Singh A, Jersoch-Herold M, Greenwood JP, Berry C, Dawson DK, Lang CC, Kelly DJ, Sprigings D, Khoo JP, Hogrefe K, Steeds RP, Dhakshinamurthy VA, McCann GP. Myocardial Perfusion Reserve but not fibrosis predicts the onset of symptoms in initially asymptomatic patients with moderate to severe aortic stenosis. (Oral presentation in Early Career Award category at **SCMR** 2016, January, LA, USA)

McAdam J, **Singh A**, Marsh AM, Lai F, Greenwood JP, McCann GP. Echocardiographic and MRI assessment of myocardial strain and strain rates using speckle tracking and feature tracking in asymptomatic aortic stenosis. (Poster presentation at **ESC** 2015, London, UK)

Singh A, Khan JN, Steadman CD, Jerosch-Herold M, Nazir SA, Kanagala P, McCann GP. Effect of late sodium current inhibition on MRI measured diastolic dysfunction and myocardial perfusion reserve in aortic stenosis: a pilot study. JCMR 2015, 17(Suppl 1):P320 (Poster presentation at **SCMR/EuroCMR** 2015, February, Nice, France)

Singh A, Steadman CD, Khan JN, Nazir SA, Kanagala P, McCann GP. Inter-study reproducibility of Circumferential strain and strain rates at 1.5T and 3T: a comparison of Tagging and Feature Tracking. (Poster presentation at **SCMR** 2014, New Orleans, USA)

Singh A, Steadman CD, Bekele S, Khan JN, Nazir SA, Kanagala P, McCann GP. Inter-study reproducibility of Feature Tracking, Single and Multi-breath-hold Tagging in severe Aortic Stenosis. (Poster presentation at **EuroCMR** 2013, Florence, Italy)

Singh A, Bekele S, Gunarathne A, Khan J, Nazir SN, Steadman CD, Kanagala P, Horsfield MA, McCann GP. No difference in aortic distensibility and pulse wave velocity between bicuspid and tricuspid aortic stenosis. (Poster presentation at **EuroCMR** 2013, Florence, Italy)

Bekele S, **Singh A**, Khan JN, Nazir SA, Kanagala P, McCann GP. Determinants of exercise capacity in patients with asymptomatic aortic stenosis. (Poster presentation at **EuroCMR** 2013, Florence, Italy)

National

Singh A, McCann GP. A comparison of exercise testing and cardiovascular MRI to predict outcome in asymptomatic patients with moderate to severe Aortic Stenosis- a prospective UK multicentre trial. (Oral presentation Young Investigator Category at **BHVS** 2015, Birmingham, UK)

Singh A, Khan JN, Steadman CD, McCann GP. Effect of late sodium current inhibition on MRI measured diastolic dysfunction and myocardial perfusion reserve in aortic stenosis: A pilot study. (Moderated poster presentation at **BCS** 2015, June, Manchester)

Singh A, Steadman CD, Khan JN, Nazir SA, Kanagala P, McCann GP. Inter-study reproducibility of Circumferential strain and strain rates at 1.5T and 3T: a comparison of Tagging and Feature Tracking. (Poster presentation at **BSCMR** 2014, Southampton.)

Singh A, Steadman CD, Khan JN, Nazir SA, McCann GP. Inter-study reproducibility of strain measurements by cardiac MRI: A comparison of Feature Tracking, Single-breath-hold tagging and Multi-breath-hold Tagging. (Poster presentation at **BCS** 2013, London.)

Singh A, Bekele S, Gunarathne A, Khan JN, Nazir SA, Steadman CD, Horsfield MA, McCann GP. No significant difference in aortic distensibility and pulse wave velocity between bicuspid and tricuspid aortic stenosis. (Poster presentation at **BSCMR** 2013, Glasgow.)

Table of Contents

List of Figures

List of Tables

List of Abbreviations

AA	ascending aorta
AS	aortic stenosis
AUC	area under curve
AV	aortic valve
AVA(I)	aortic valve area (indexed to BSA)
AVC	aortic valve calcification
AVR	aortic valve replacement
AV Vmax	peak velocity across AV
(S/D)BP	(systolic / diastolic) blood pressure
BSA	body surface area
bSSFP	balanced steady-state free precession
CMR	cardiovascular magnetic resonance imaging
CPET	cardiopulmonary exercise test
CoV	coefficient of variation
CT	computed tomography
CW	continuous wave
DA	descending aorta
DPT	diastolic perfusion time
ECG	electrocardiogram
ECV	extracellular volume fraction
eGFR	estimated glomerular filtration rate
FOV	field of view
FT	Feature Tracking
GRE	gradient echo
Hct	haematocrit
HR	heart rate
ICC	intra-class correlation coefficient
LAV(I)	left atrial volume (indexed to BSA)
LGE	late gadolinium enhancement
LV	left ventricle
LVEDV(I)	left ventricular end-diastolic volume (indexed to BSA)
LVEF	left ventricular ejection fraction
LVESV(I)	left ventricular end-systolic volume (indexed to BSA)

LVH	left ventricular hypertrophy
LVM(I)	left ventricular mass (indexed to BSA)
LVOT	left ventricular outflow tract
LVRPP	left ventricular rate pressure product
LVSV(I)	left ventricular stroke volume (indexed to BSA)
MACE	major adverse cardiovascular events
MBF	myocardial blood flow
MOCO	motion-corrected
MOLLI	modified look-locker inversion recovery
MPG	mean pressure gradient
MPR(I)	myocardial perfusion reserve (index)
(NT-pro)BNP	(N-terminal pro-)brain natriuretic peptide
NYHA	New York Heart Association
PEDSR-C/L	peak early diastolic strain rate- circumferential / longitudinal
PET	positron emission tomography
PPG	peak pressure gradient
PSS-C/L	peak systolic strain- circumferential / longitudinal
PSSR-C/L	peak systolic strain rate- circumferential / longitudinal
PW	pulsed-wave
PWV	pulse wave velocity
ROC	receiver-operator characteristic curve
ROI	region of interest
RVEDV(I)	right ventricular end-diastolic volume (indexed to BSA)
SPAMM	spatial modulation of magnetisation
TAVI	trans-catheter aortic valve implantation
TDI	tissue Doppler imaging
TE	echo time
TI	inversion time
TR	temporal resolution
TTE	trans-thoracic echocardiogram
VAI	valvulo-arterial impedance

CHAPTER ONE

1 INTRODUCTION

Published (review article)**:**

Singh A, Steadman CD, McCann GP. Advances in the Understanding of the Pathophysiology and Management of Aortic Stenosis: Role of Novel Imaging Techniques. Can J Cardiol. 2014 Sep;30(9):994-1003.

1.1 Background

1.1.1 The normal Aortic Valve

The aortic valve (AV) lies between the left ventricle (LV) and the aorta and controls the outflow of blood from the heart. The normal AV has three equal sized cusps, which open fully to allow forward flow of blood during ventricular contraction, with an aortic valve area (AVA) of 3-4cm^2. During diastole the valve closes to prevent regurgitation. A bicuspid aortic valve is the most common congenital malformation, affecting 1-2% of the population(1). (Figure 1)

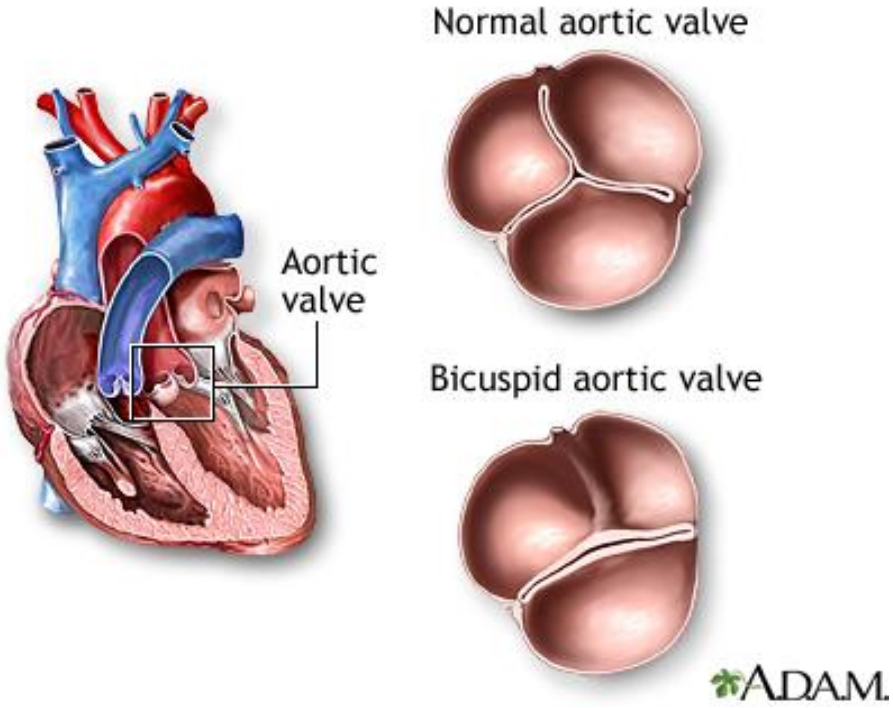

Figure 1. Anatomy of the aortic valve, with a tri-leaflet (top) and a bicuspd (bottom) aortic valves

(http://www.nlm.nih.gov/medlineplus/ency/imagepages/19893.htm)

1.1.2 Aortic Stenosis

Aortic stenosis (AS) is a reduction in the area of the aortic valve orifice to <2.5 cm^2 (Figure 2). AS is the commonest valve lesion requiring surgery in the western world(2) and is common in the elderly, with up to 3% of those over the age of 75 thought to have severe disease(3). With an aging population, the prevalence of AS is expected to double in the next 20 years(4).

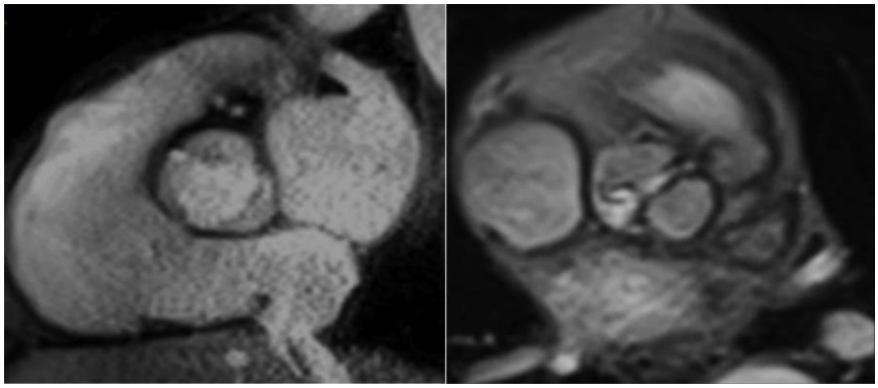

Figure 2. An example of a normal (left) and a stenosed (right) tri-leaflet aortic valve on Magnetic Resonance Imaging

1.1.3 Classification of severity

The severity of AS is classified according to the AVA and the pressure gradient across the valve. An increased pressure gradient results from the narrowed orifice (Table 1), with an increased pressure in the LV cavity required to drive flow into the aorta. Historically, AS severity was assessed invasively by cardiac catheterisation and calculation of the valve area using the Gorlin equation, but non-invasive assessment with trans-thoracic echocardiography (TTE) is now the established method(5).

Table 1. Classification of severity of Aortic Stenosis (European Society of Cardiology)

	Mild	Moderate	Severe
Peak velocity (m/s)	<3.0	3.0-4.0	>4.0
Peak Pressure Gradient (mmHg)	<36	36-64	>64
Mean Pressure Gradient (mmHg)	<25	25-40	>40
Aortic Valve Area (cm^2)	>1.5	1.0-1.5	<1.0

1.1.4 Aetiology

AS can be congenital or acquired. Congenital AS in childhood is most commonly caused by a unicuspid AV, while a bicuspid AV doesn't usually cause obstruction until adulthood. In adults, AS can result from secondary calcification of a congenitally bicuspid AV, primary degenerative calcification of a tri-leaflet valve, or can be post-inflammatory (rheumatic heart disease). Other rare causes include familial

hypercholesterolaemia, hyperuricaemia, Paget's disease, Fabry disease and hyperparathyroidism(6).

1.1.5 Natural history

Patients with a bicuspid AV tend to present earlier, in the 4th and 5th decade of life, whereas those with tri-leaflet valves present in the 6th or 7th decade(7). AS is a slowly progressive disease, with a long latent asymptomatic period, and good prognosis in this phase. It is often diagnosed following the discovery of an incidental ejection systolic murmur. Observational studies using both serial cardiac catheterisation and Doppler echocardiography have demonstrated that the rate of progression of AS severity and symptom development is highly variable amongst individuals(8). Eventually, when symptoms do develop, they are characterised by the triad of angina, dyspnoea and syncope.

1.2 Pathophysiology

AS is characterised by progressive narrowing of the AV, leading to chronic LV pressure overload. Concomitant arterial hypertension is also found in 35-51% of adults with AS(9), being commonly present in elderly patients with calcific AS, as well as that due to the reduced aortic elasticity and aortopathy associated with bicuspid aortic valves(10). The combined effect is to increase the afterload that can contribute to cardiac remodeling.

1.2.1 Cardiac remodeling

Cardiac remodeling is defined as 'genome expression, molecular, cellular and interstitial changes that are manifested clinically as changes in size, shape and function of the heart after cardiac injury'(11). AS is characterised by changes in LV wall thickness, mass and volume. The degree and pattern of response of the LV to chronic pressure overload in AS, however, is highly variable, and not directly related to the haemodynamic severity of AS(12, 13). Initial echo studies, and a more recent cardiovascular magnetic resonance (CMR) imaging study have identified various patterns of cardiac remodeling in response to the increased afterload(13-15)(Figure 3).

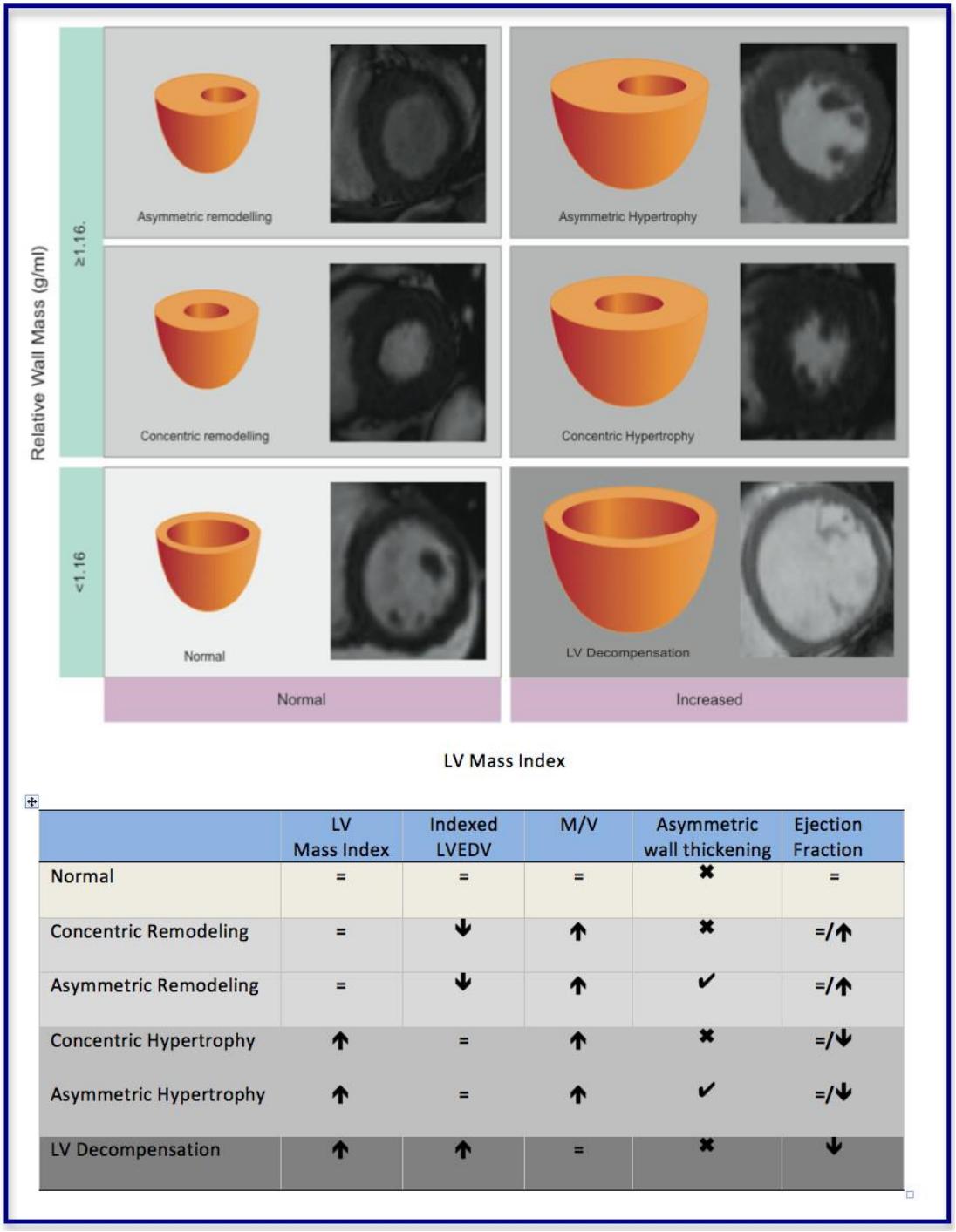

	LV Mass Index	Indexed LVEDV	M/V	Asymmetric wall thickening	Ejection Fraction
Normal	=	=	=	✖	=
Concentric Remodeling	=	↓	↑	✖	=/↑
Asymmetric Remodeling	=	↓	↑	✔	=/↑
Concentric Hypertrophy	↑	=	↑	✖	=/↓
Asymmetric Hypertrophy	↑	=	↑	✔	=/↓
LV Decompensation	↑	↑	=	✖	↓

Figure 3. Different patterns of cardiac remodeling identified in Aortic Stenosis(13)

1.2.1.1 Left ventricular hypertrophy (LVH) in AS

The increase in LV wall thickness in AS was traditionally thought to be an adaptive process that attempts to reduce wall stress, according to the Laplace equation(16). Wall stress is directly related to intra-cavity pressure and cavity size, and inversely related to wall thickness. However, in his study of patients with severe AS undergoing

echocardiography prior to aortic valve replacement (AVR), Kupari(12) demonstrated that increased LV mass was related to lower ejection fraction and a greater likelihood of heart failure, independent of the severity of AS. This finding, together with the observation in an experimental model of AS animals, that those who do not develop LVH are less likely to develop heart failure(17), suggests that LVH may be maladaptive rather than beneficial in AS. This has further been confirmed by Cioffi *et al.*, who found inappropriately high LV mass to be a predictor of adverse outcome in asymptomatic severe AS(18).

LVH is associated with a range of detrimental sequelae including: reduced myocardial perfusion(19), interstitial fibrosis and diastolic dysfunction(20). In AS, both myocyte apoptosis(21) and oncosis(22) (cell swelling before death) have been reported as being associated with adverse ventricular remodeling and the development of fibrosis.

1.2.2 Myocardial Blood Flow and Perfusion Reserve

Myocardial perfusion reserve (MPR) is defined as 'the maximal increase in myocardial blood flow (MBF) above its resting level for a given perfusion pressure when coronary vasculature is maximally dilated'(23). It is measured by calculating the ratio of MBF during hyperemia to resting MBF. In the absence of significant epicardial coronary artery disease, a reduction in MPR suggests the presence of microvascular dysfunction or deficiency(24).

As the LV remodels in response to the pressure overload in AS, the rate of myocyte hypertrophy exceeds that of the capillary angiogenesis, leading to a relatively reduced capillary density in the hypertrophied myocardium(25). With increased LV mass, there is increased oxygen demand at rest. The increase in resting MBF to match increased metabolic demand is therefore likely to be maintained by arteriolar vasodilation. However, the remodelled myocardium is unable to match the further increased demand on exercise, leading to reduced stress MBF and therefore reduced MPR. The ability to increase blood flow to the myocardium on exercise is most likely limited because vasodilation may already be near maximal(26), diastolic perfusion time (DPT)

will be limited further with increased heart rate and there is a rapid increase in LV end-diastolic pressure(27), which reduces the effective pressure gradient for perfusion. The inability of the hypertrophied myocardium to adequately increase its blood supply with increasing demand causes repetitive ischaemia(23), that may be responsible for the angina in patients with AS, despite normal epicardial coronary arteries, as well as ischaemic damage. Petersen's study of patients with hypertrophic cardiomyopathy demonstrated increased frequency of fibrosis with increasing wall thickness and decreasing hyperemic MBF, suggesting a possible pathophysiological link between repetitive hypoperfusion during stress and development of myocardial fibrosis(28). Reduced MPR in AS may therefore play a role in the development of both cell death and interstitial fibrosis from ischaemic necrosis.

1.2.3 Role of apoptosis

Apoptosis is defined as '*suicidal programmed cell death … characterized by preservation of mitochondrial and sarcolemmal integrity, nuclear chromatin condensation and removal by macrophages or neighboring cells'*(29). It is present in failing human hearts from multiple causes, with the reported apoptotic index of 0.12-35%. An increased rate of apoptosis has also been demonstrated in patients with severe AS, and is associated with reduced coronary and myocardial blood flow(21)(Figure 4). In another study, the apoptotic rate correlated directly with pre-operative New York Heart Association (NYHA) functional class, as well as post-operative duration of intensive care unit (ICU) stay, number of days of acute renal failure, and serum level of troponin-T at 24 hours after AVR for severe AS(30). The study by Hein provided the link between structure and function, where myocyte degeneration and cell death were found to be increased, with decreasing LV ejection fraction (EF)(22).

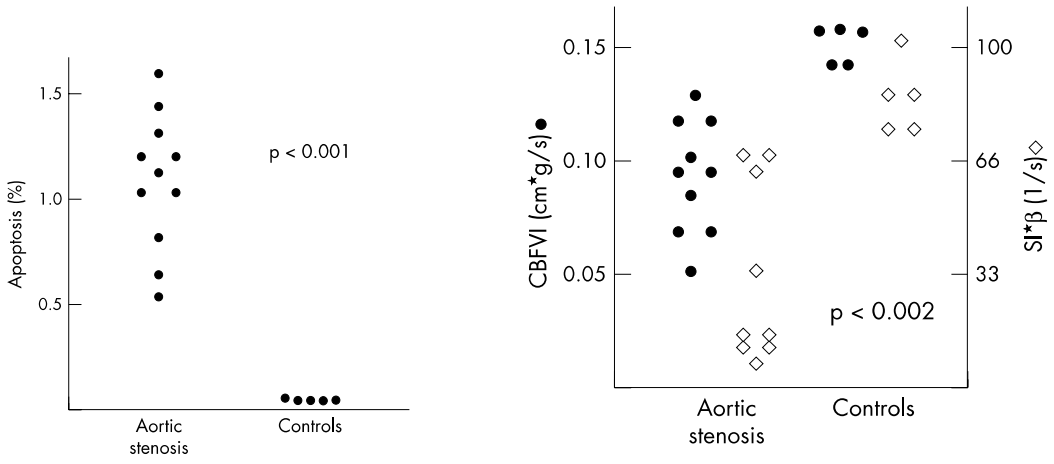

Figure 4. Difference in (a) myocyte apoptosis, (b) coronary blood flow velocity index (CBFVI) and SI*β (measure of myocardial flow), between AS patients and controls. (21)

1.2.4 Role of fibrosis

Reactive interstitial fibrosis is characterized by progressive onset and diffuse distribution, and is caused by increased collagen synthesis by myofibroblasts secondary to various stimuli, including inflammatory, endocrine and ischemic. Both interstitial and infiltrative fibrosis can lead to irreversible replacement fibrosis in the later stages of disease, characterized by cellular damage, necrosis and replacement of myocytes by collagen(31). Fibrosis plays an important role in the development of both diastolic and systolic dysfunction in AS. Extensive fibrosis is often present in patients with advanced heart failure, regardless of the aetiology. Fibrosis and myocyte damage appear to be the decisive morphological alterations in adverse LV remodeling in AS(22).

1.3 Risk stratification in AS

Many observational studies have attempted to identify prognostic markers to identify high-risk asymptomatic patients who may benefit from early surgery (Appendix-1).

1.3.1 Echocardiographic markers

Prospective studies have identified very severe AS (AVA <0.7-0.75 cm^2, (32, 33) or very high peak velocity of >5-5.5 m/s(34, 35)), rapid increase in velocity (>0.3 m/s per year)(36, 37) and heavy calcification of the valve(18, 37) as echocardiographic

predictors of adverse outcome. LVH(38), a high left ventricular mass index (LVMI)(18), increased left atrial (LA) area(39), reduced longitudinal LV strain(27, 39) as well as increased valvulo-arterial impedance (VAI)(39, 40), a marker of global afterload, have also been shown to predict adverse outcome in asymptomatic AS.

It should be noted, however, that echocardiographic measures of AS severity are poor discriminators between those who go on to develop symptoms and those that do not, compared to other parameters. In Amato's study(32), 10 out of 43 patients with AVA<0.7cm^2 remained asymptomatic, while 6 out of 23 with AVA>0.7cm^2 developed symptoms. Even in Otto's study of predictors of outcome(36), although there were statistically significant mean differences between the groups for measures of aortic stenosis severity, there was substantial overlap in individual hemodynamic values between the symptomatic and asymptomatic groups (Figure 5).

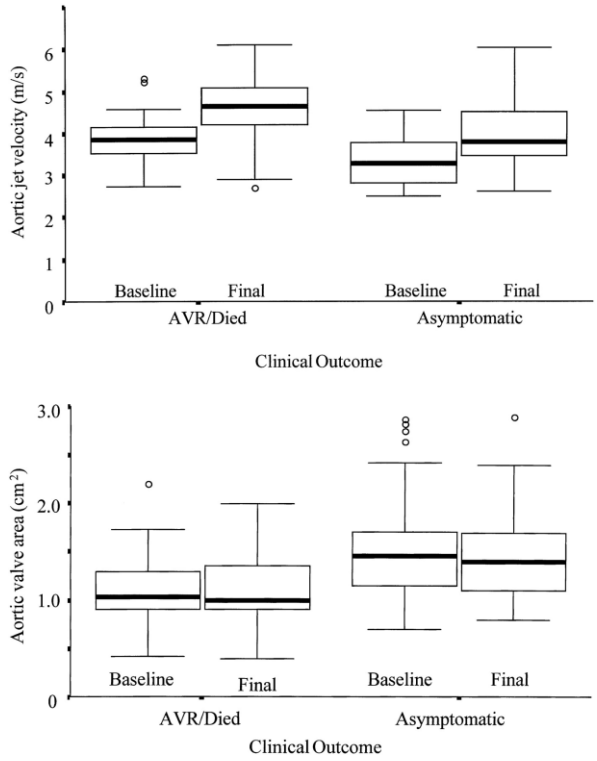

Figure 5. Aortic jet velocity (top) and aortic valve area (bottom) in subjects who developed symptoms requiring AVR or died compared with those who remained asymptomatic. (36)

1.3.2 Exercise testing

Traditionally, severe AS was regarded as an absolute contraindication to exercise testing because of the potential for complications(41). However, there have been several studies that have safely examined the role of carefully monitored exercise testing in eliciting symptoms and predicting outcome in apparently asymptomatic severe AS(32, 33, 36, 42). An abnormal response or symptoms on exercise testing have been shown to be predictive of adverse outcome in AS (Figure 6), though the definition of a positive test varies between studies.

A positive test has been defined as any one of: ST depression >1mm or 2mm in females, excessive dyspnoea, chest pain, syncope or a blunted increase in systolic BP <20mmHg. However, in Otto's study which included many patients with mild AS, asymptomatic flat or downsloping ST depression (>1 mm) was seen in 69% of all tests and was even more common in those with an abnormal resting electrocardiogram (ECG) (85%).

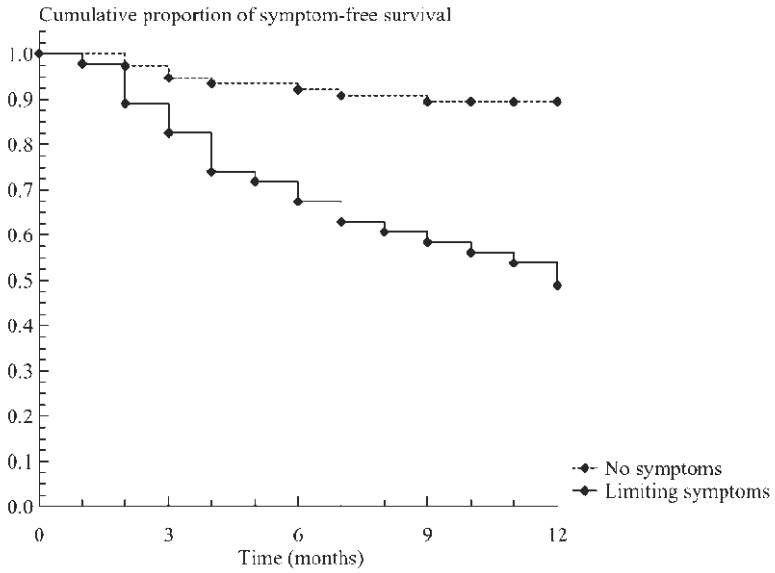

Figure 6. Symptom-free survival over 12 months in moderate-severe AS with and without a symptomatically positive ETT at baseline. (42)

The presence or absence of ST depression did not correlate with the presence of coronary artery disease at subsequent angiography(36). There is also substantial overlap in the BP response to exercise between patient groups(36, 42). In Das' study,

there was no additional benefit of ST changes or BP response to exercise-induced symptoms, for predicting outcome. ST segment depression occurred in 42% of patients who developed symptoms but also 20% of those who remained asymptomatic. In both Otto's and Lancellotti's studies(39), exercise parameters did not predict outcome on multivariate analysis.

Exercise testing appears to be a good tool for excluding imminent symptoms or other adverse outcome, but has a relatively low specificity (high false positive rate) for predicting outcome(32, 42, 43). For example, the positive predictive value of exercise testing was only 57% in the study by Das *et al.*, and even lower in the those >70 years of age(42). No trial has been done to assess whether a positive exercise test can actually improve outcome in asymptomatic patients with AS.

There is also a degree of subjectivity in interpreting positive symptoms, particularly breathlessness. This is reflected in Das' study where 83% of patients with exertional dizziness on exercise subsequently developed symptoms, where as only 54% with breathlessness and 50% with chest tightness did. In contrast, in Amato's study, where only dizziness and chest pain were used to define symptom-limited exercise test, all patients with symptoms on exercise reached an endpoint(32). It is therefore somewhat surprising that the latest American guidelines on valvular heart disease state that "*patients with symptoms provoked by exercise testing should be considered symptomatic*", despite acknowledging that "*it can be challenging to separate normal exercise limitations from abnormal symptoms due to AS, particularly in elderly sedentary patients*"(44), and both European and American guidelines now consider AVR as a class I recommendation in such patients (section 1.5.3).

1.3.3 BNP and NT-proBNP

A biomarker is defined as "*a biological molecule that can be identified in a particular disease and additionally may be able to assess the severity and prognosis or monitor the response to treatment of that disease state*"(45). Natriuretic peptides are endogenous cardiac hormones that are synthesized as pro-hormones, which are cleaved into the inactive N-terminal fragments (NT-proBNP) and the biologically

active hormone, before being released into circulation. The N-terminal fragments are often used as a surrogate for the biologically active hormone. Although brain (or B-type) natriuretic peptides (BNP) were originally identified in pig brain in 1988, the primary site of their synthesis is the ventricular myocardium(46). The release of BNP occurs in bursts, regulated by gene transcription, and the main stimulus for their release is myocyte stretch, though other factors such as endothelin-I, angiotensin-II and nitric oxide may also play a role.

BNP and NT-proBNP have been widely studied as potential markers for symptom development in AS(47-50). The increased myocardial wall stress caused by AS is thought to induce expression of these biomarkers, leading to increased levels being found in the bloodstream. Raised plasma concentrations of BNP and NT-proBNP have been shown to be related to AS severity, symptoms, LV function and associated with an increase risk of death or requirement for AVR, but also indicate higher peri-operative risk(45).

1.3.4 ECG and troponin

Recent studies have identified additional markers that have been shown to be associated with adverse outcome in AS. These include ECG markers of LVH with and without strain (defined as ST-depression and T-inversion in lateral leads), which have been shown to be independently predictive of adverse outcome including AVR and cardiovascular death in asymptomatic patients with AS(51, 52). LVH with strain on ECG has also been shown to be independently associated with CMR measures of focal and diffuse fibrosis and AS severity(52). In addition, plasma concentrations of high-sensitivity troponin-I have also been shown to be associated with LVMI and late gadolinium enhancement (LGE) in asymptomatic patients with AS, and independently associated with adverse outcome (AVR and cardiovascular death), independent of age, sex, systolic function and AS severity(53).

1.4 Role of Novel Imaging Techniques in AS

Cardiac imaging plays an important role in the management of patients with valvular heart disease, by providing a non-invasive and convenient tool for diagnosis and

monitoring. Echocardiography remains 'the key technique used to confirm the diagnosis of valvular heart disease, as well as to assess its severity and prognosis' (ESC guidelines 2012)(5). Three-dimensional TTE or trans-esophageal echocardiography can provide more accurate measurement of the aortic annulus prior to intervention. However, rest echocardiography is a poor discriminator in determining which asymptomatic patients will develop symptoms in the short term(54).

1.4.1 Stress Echocardiography

Doppler exercise echocardiography has an incremental prognostic value over resting echocardiographic and exercise electrocardiographic parameters alone(33). An increase in the exercise mean pressure gradient of >17-20 mmHg from baseline has been found to be an independent predictor of exercise capacity(55) as well as adverse outcome(33, 56) in patients with asymptomatic moderate to severe AS. In addition, absence of left ventricular contractile reserve, i.e., a decrease or a small increase in ejection fraction, and exercise pulmonary hypertension, are also associated with reduced exercise capacity and poor outcome(57).

The widespread dissemination of this technique is limited by the operator variability and difficulty in acquiring reliable echo images during / post-exercise. In routine clinical practice, stress testing is not often (<6%) performed in asymptomatic patients with severe AS, as shown in the Euro Heart Survey(58).

1.4.2 Tissue Doppler Imaging and Speckle Tracking

More advanced echocardiographic techniques including Tissue Doppler imaging (TDI) and speckle tracking allow early detection of diastolic and systolic dysfunction, though there is little validation of their prognostic value for clinical endpoints(5). TDI is a Doppler technique that allows quantification of the high amplitude but low-velocity myocardial velocities using a high-pass filter (>100 Hz). It integrates information about systolic and diastolic function, and has been validated against invasively measured LV filling pressures(59). Speckle tracking allows angle-independent determination of myocardial strain and strain rate through frame-by-frame tracking of natural acoustic markers within the myocardium in standard echocardiographic images(60).

Several studies have shown reduced myocardial deformation in patients with AS, despite normal EF(61-63). There may be a stepwise impairment in longitudinal, circumferential and radial myocardial deformation with increasing AS severity(63). Impaired longitudinal strain has also been associated with an abnormal response to exercise in asymptomatic patients with severe AS(27). In a small sub-group analysis of 18 patients, the investigators also demonstrated a relationship between longitudinal strain and cardiovascular events. More recently, global longitudinal strain, measured by speckle tracking, has been shown to be an independent predictor of outcomes in patients with severe asymptomatic AS, incremental to other echocardiographic markers (64).

Limitations of speckle tracking and TDI include the need for good image quality for accurate strain quantification, poor inter- and intra-observer variability and the test-retest repeatability of these measurements is not known in AS. In addition, TDI requires alignment with the myocardial plane of motion for accurate measurement.

1.4.3 Computed Tomography (CT)

CT can play a role in the assessment of AS by accurately quantifying the degree of aortic valve calcification (AVC), assessing the aortic root geometry as well as screening for significant coronary artery disease(65). AVC quantification, using both electron-beam CT and multi-detector CT (MDCT), has been validated against the amount of calcification detected by calcium weight or electron spectroscopy in excised aortic valves(66, 67). Various studies have also demonstrated a significant curvi-linear relationship between the degree of CT detected AVC and AS severity measured by echocardiography (Figure 7)(66, 68-70). MDCT detected AVC may also allow reclassification of patients. In a large cohort of patients, 29% were found to have discordant disease on echocardiography, out of whom about half of those with low gradient were classified as having severe AVC by MDCT(71). However, the impact on clinical outcome was not assessed in that study.

Recent reports have assessed the prognostic value of CT-measured AVC in patients with AS. One small study in 64 asymptomatic patients(72), suggested that CT-measured AVC is independently predictive of cardiac events including cardiac death, myocardial infarct, AVR and heart failure related hospitalisation. A larger study in 694 patients, which has been presented but not published, may confirm an association with increased mortality(73)(abstract only). It is intriguing to speculate that the most heavily calcified valves may be associated with greatest extent of LV remodeling.

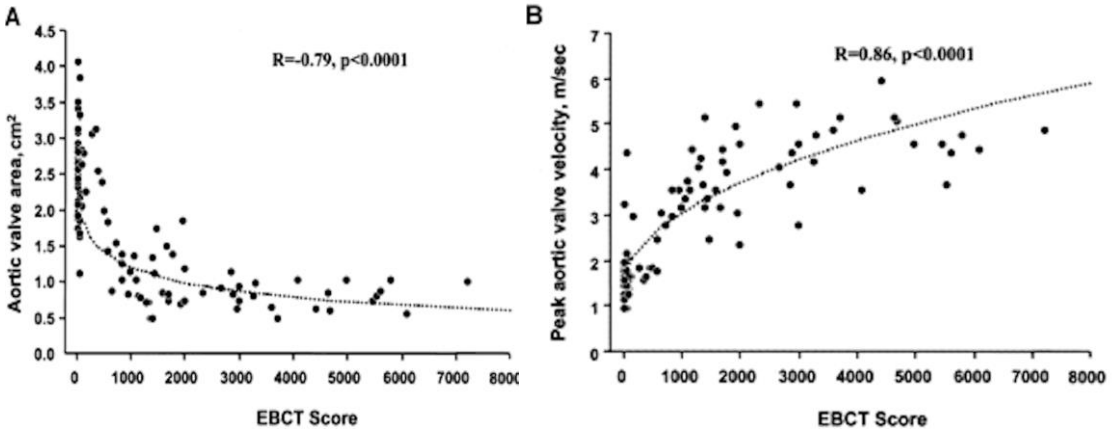

Figure 7. Association between Aortic Valve Calcification and A. Aortic valve area, B. Peak aortic velocity (EBCT: electron-beam computed tomography). (66)

CT-detected AVC has also been used a surrogate endpoint for disease activity in studies assessing the efficacy of statin therapy in calcific AS(74, 75). However, by the time AS has developed, it is likely that disease activity is too well established to be influenced by statins(74, 76). The role of subclinical coronary artery disease in the progression to symptoms in asymptomatic AS is unclear. CT coronary artery calcium score correlates with atherosclerotic plaque burden although underestimates this.

The limitations of CT include exposure to ionizing radiation, as well as the need for intravenous contrast and beta-blockers for CT coronary angiography. CT can also be prone to errors with arrhythmias and blooming artifacts, particularly in relation to the assessment of coronary disease, in the presence of severe calcification. The reproducibility of CT in AS also remains to be determined.

1.4.4 Positron Emission Tomography / CT

PET scanning employs tracers that consist of a positron emitter such as ^{18}F (fluorine), attached to a molecular vehicle that targets biochemical processes of interest. PET detectors are then used to build a 3D image of the positron emission events at the sites of tracer accumulation(77). Combined PET/CT scanning allows the combination of functional information from PET with accurate anatomical information from CT. PET/CT has been used to investigate inflammation and microcalcification, both of which are thought to be key mechanisms in the development and progression of AS.

The tracer ^{18}F-flurodeoxyglucose (^{18}F-FDG) is a glucose analogue that accumulates in areas of increased glucose usage, such as malignant cells with high cellular turnover, and macrophages with increased metabolic requirements in areas of inflammation. It can be used to target vascular inflammation. Increased ^{18}F-FDG uptake has been demonstrated in the aortic valves of patients with AS in two PET studies(78, 79). The degree of uptake increased with the severity of AS in a prospective study of 121 patients with a spectrum of disease.

^{18}F-Sodium Fluoride (^{18}F-NaF) targets exposed bone crystals, and is used to demonstrate areas of novel calcification, calcium remodelling and bone turnover. In one study, ^{18}F-NaF activity in the valves of patients with AS was found to progressively rise with increasing severity of AS(79). This study has established the concept that non-invasive imaging with PET/CT may be able to evaluate disease activity in AS. The association of increased ^{18}F-FDG activity with increasing AS severity was weaker than that for ^{18}F-NaF (Figure 8), suggesting that calcification is the predominant pathological process in AS, and perhaps a better target for future medical therapies. PET/CT also has potentially much wider applications, as new tracers are developed that target different pathways in the disease or LV remodeling process.

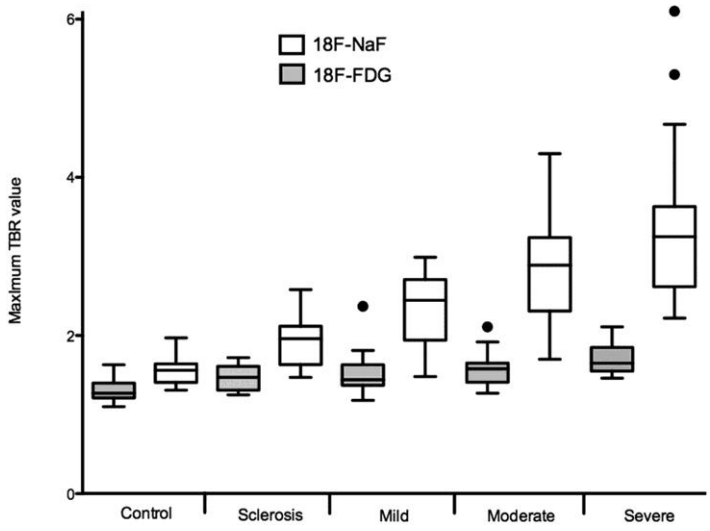

Figure 8. Uptake of ^{18}F-fluorodeoxyglucose (18F-FDG) and ^{18}F-sodium fluoride (^{18}F-NaF) according to the severity of AS. (79)

The limitations of PET/CT include the use of ionizing radiation, relatively expensive tracers, unknown scan-rescan reproducibility in AS and histological validation studies are also lacking at this time.

1.4.5 Cardiac Magnetic Resonance (CMR) Imaging

CMR is the gold standard non-invasive technique for the assessment of LV volumes, mass and function, and is the most accurate and reproducible technique for their quantification(80, 81). It has been validated against post-mortem studies of both animal and human hearts(82, 83). The accuracy of the technique and lack of ionizing radiation make CMR the ideal technique for the monitoring of progressive changes in ventricular mass and volumes, and assessing the effect of interventions in clinical trials. Additionally, CMR allows direct visualisation of aortic valve area, which has very good agreement with trans-oesophageal echocardiography(84). However, the main benefits in relation to the assessment of pathophysiology in AS, are the multiparametric capability of CMR combined with tissue characterisation of the myocardium.

1.4.5.1 Late Gadolinium Enhancement (LGE) and focal scarring

As outlined in section 1.2.4, fibrosis is a key determinant of both diastolic and systolic LV dysfunction in AS. Previously, the gold standard for detecting myocardial fibrosis

was endomyocardial biopsy, which has various disadvantages, including its invasive nature, sampling errors and its inability to assess the whole heart(31). Histological studies of patients with severe AS have shown that the extent of interstitial fibrosis is highly variable, ranging from 4% to 39%(85, 86).

LGE imaging is a technique optimised to detect myocardial infarction, with dead or scarred myocardium appearing bright and normal muscle black on inversion-recovery T1-weighted CMR images(87). However, LGE has been detected in almost all conditions associated with myocardial scarring and has been validated in necropsy studies in hypertrophic cardiomyopathy(88) and surgical biopsy studies in AS(89, 90).

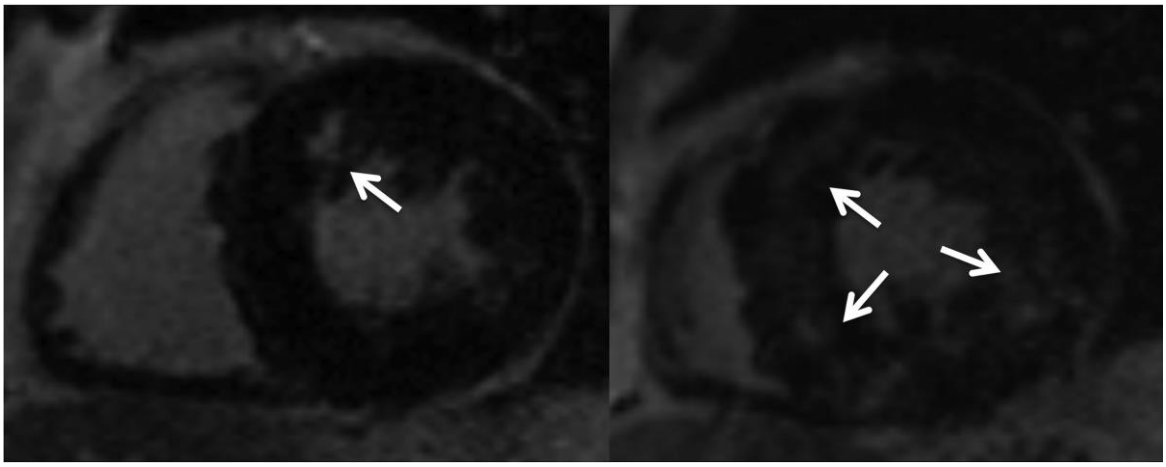

Figure 9. Examples of focal fibrosis demonstrated by Late Gadolinium Enhancement on MRI of patients with severe AS. Left: focal area of fibrosis at anterior right ventricle insertion point (arrow), Right: Patchy fibrosis throughout the myocardium.

LGE can be detected in 27-64% of patients with AS(25, 89, 91) (Figure 9). The extent of LGE has been shown to correlate with the extent of interstitial fibrosis on endomyocardial biopsy(89) and increases with increasing LVH(25, 91). The degree of LGE correlated more closely with the pre-operative NYHA class symptoms than the AVA or LV systolic function. LGE is also inversely associated with the degree of functional improvement post AVR(92) and all-cause mortality late after AVR(22, 89). In a larger study of 143 patients with AS, 50% of who subsequently underwent AVR, mid-wall fibrosis was a predictor of mortality, independent of ejection fraction, although the results were not adjusted for symptom status(93).

LGE relies on the higher signal intensity of abnormal myocardium compared to the 'normal appearing' myocardium, which needs to be 'nulled' by adjusting the inversion time. This technique is therefore insensitive to more homogenous changes seen with interstitial fibrosis.

1.4.5.2 T1 Mapping and Diffuse Myocardial Fibrosis

Diffuse interstitial fibrosis is associated with increased collagen content and increased myocardial extracellular volume fraction (ECV). T1 mapping is a novel technique that directly measures the T1 relaxation time of the myocardium, allowing quantification on a standardised scale(94) before (native) and after the administration of a bolus of gadolinium contrast.

Initial studies in AS employed a bolus and continuous infusion of low dose gadolinium contrast to achieve contrast agent concentration equilibrium between blood and myocardium(86). Taking 1-haematocrit (Hct) as the volume of distribution of the gadolinium (which is an extracellular agent) in blood, and knowing the changes in signal intensity of the myocardium and blood, allows calculation of the myocardial volume of distribution(95) (section 2.4.7.7). Both the equilibrium-contrast CMR (EQ-CMR) technique and the bolus-contrast (pseudo-equilibrium/ dynamic equilibrium) techniques have been validated against histological specimens, with good correlation demonstrated between ECV measured by CMR and collagen volume fraction on histology(86, 96, 97). EQ-CMR technique has also been compared to the bolus-contrast technique in a wide range of diseases and normal controls, with good agreement between the two techniques(97).

Native T1 values have been shown to be higher in patients with severe symptomatic AS compared to controls, and is moderately correlated with fibrosis on histology(98). However, there is marked overlap in native T1 values between asymptomatic patients with AS and controls. T1 values correcting for changes in the blood pool (partition coefficient and ECV methods) show better discrimination and excellent reproducibility

between healthy volunteers and patients with AS (Figure 10)(99, 100), though overlap remains.

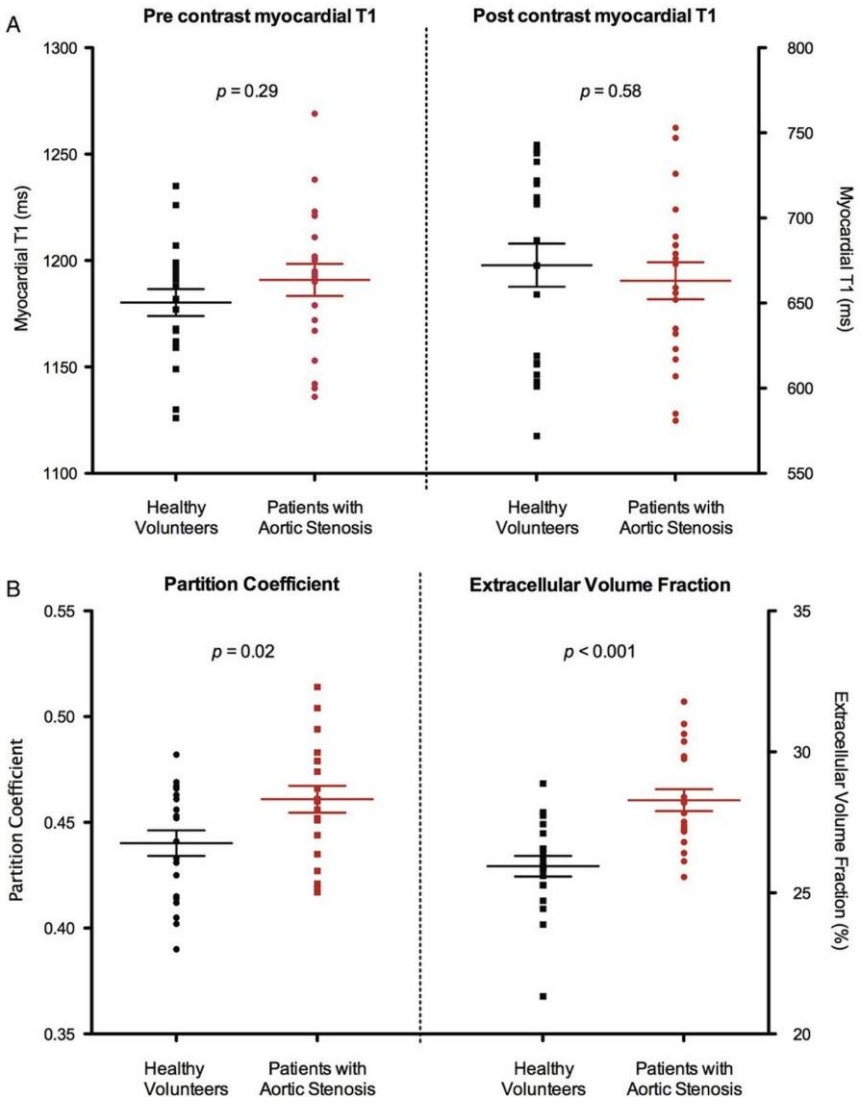

Figure 10. Ability of different T1 techniques to differentiate between AS and healthy controls: no significant difference using pre- (A) and post-contrast (B) myocardial T1 values, significant difference using Partition Coefficient (C) and ECV (D) techniques. (100)

Diffuse myocardial fibrosis, using EQ-CMR, has also been shown to be an independent predictor of exercise capacity in severe AS before AVR. Six months after AVR, diffuse fibrosis measured by T1 mapping did not significantly reduce(101) as has been found previously on histology(102).

T1 mapping therefore has the potential to detect increases in diffuse myocardial fibrosis before the onset of myocardial dysfunction, and may better identify asymptomatic patients at high risk, although further prognostic studies evaluating ECV are needed. There are multiple sequences and methods that can be used to quantify T1 in patients and there are variations with different field strengths. Strenuous efforts are being made by the CMR community to standardise this exciting technique so that it can be implemented in clinical practice(103).

1.4.5.3 MRI Spectroscopy

A recent study has used MR spectroscopy to demonstrate increased myocardial steatosis (increased myocardial triglyceride content) in severe AS compared to controls, regardless of symptomatic status, and was validated against histological samples from ten patients undergoing AVR(104). Myocardial steatosis was independently associated with systolic strain impairment in patients, despite normal EF. Steatosis is thought to cause myocardial dysfunction due the production of toxic metabolites such as diaclglycerol and ceramides(105). This finding provides new insights into the pathophysiological processes involved in AS, suggesting an additional mechanism, which may precede fibrosis, for the development of LV dysfunction, as well as a potential therapeutic target in future studies.

1.4.5.4 Myocardial Perfusion Reserve

Non-invasive methods of measuring coronary and myocardial flow include doppler echocardiography to assess coronary blood flow(21, 106) and PET and CMR to measure the absolute MBF. Although MBF at rest is similar in controls and patients with LVH secondary to hypertrophic cardiomyopathy(28) or AS(24), hyperaemic MBF is lower in patients than controls, resulting in a lower MPR in patients. In addition, Rajapan found MPR to be more severely impaired in the subendocardial layer than the subepicardium in patients with severe AS(24). The severity of this impairment was related to AS severity, haemodynamic load and diastolic perfusion time. Following AVR, increases in MPR were associated with diastolic perfusion time and increased AVA(107).

Myocardial perfusion measured by CMR allows non-invasive assessment of the microcirculation. It employs contrast agents as tracers and imaging of the first-pass of the contrast agent through the myocardium, which is a surrogate for myocardial blood flow. MPR measured by CMR has recently been shown to be an independent predictor of aerobic exercise capacity (age and sex-corrected peak VO_2) in 46 patients with severe isolated AS, and was inversely related to NYHA class symptoms (Figure 11)(108). In this study, MPR had univariate associations with filling pressure, LVMI, LGE, peak AV velocity and a borderline significant association with diastolic perfusion time(108). On multivariate analysis, LVMI and LGE were independently associated with MPR.

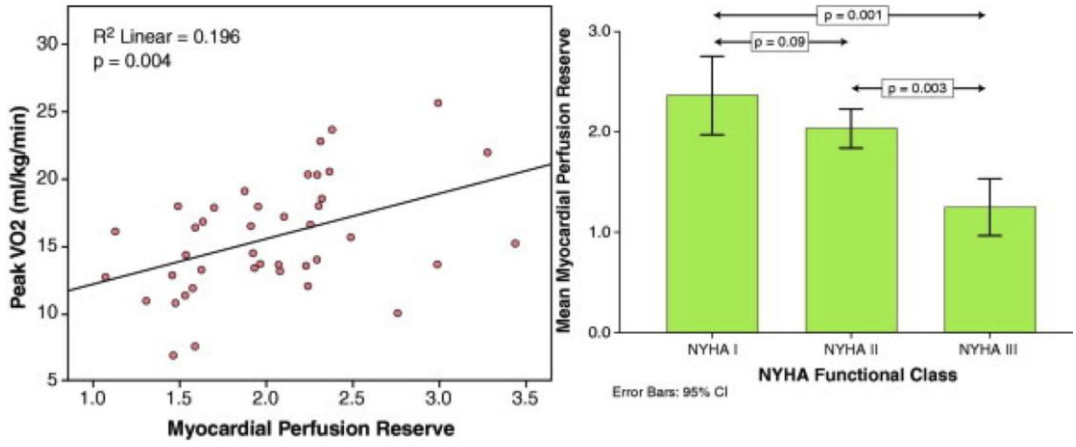

Figure 11. Relationship between Myocardial Perfusion Reserve and Peak VO_2 / NYHA class symptoms in patients with severe AS. (108)

MPR is therefore an attractive biomarker in AS given its strong relation to symptom status, functional capacity and its dependence on integrated measures of AS severity and LV remodeling. It is not yet known how MPR is affected by changes in interstitial fibrosis, nor indeed whether fibrosis precedes or results from microvascular dysfunction/insufficiency(22).

1.4.5.4.1 MBF and MPR quantification

The first-pass perfusion images acquired with CMR can be used for qualitative, semi-quantitative and quantitative assessment. In clinical practice, visual assessment of perfusion defect (qualitative) remains the mainstay. Both semi-quantitative and quantitative assessment involve generation of signal-intensity (SI) against time curves,

following manual contouring of the endocardial and epicardial borders as well as a blood pool region-of-interest (ROI). For semi-quantitative assessment, various parameters such as peak SI, up-slope parameter and area under the SI curve can be derived from these, at rest and hyperaemic stress, for calculation of myocardial perfusion reserve index (MPRI). Quantitative assessment allows absolute MBF and MPR to be calculated, and has been described using both model-dependent methods such as the 'lumped-compartment' model, or model-independent methods based on the 'central-volume principle', which in turn require the process of deconvolution to extract the transfer function for absolute MBF quantification. Multiple methods of this mathematical process of deconvolution have also been described, including the Fermi-function model and the model-independent deconvulution technique(109-111). Both methods of deconvolution have been validated against flow measured by injected microspheres in animal models, which is the gold standard for tissue perfusion assessment, with overall good to excellent correlations, using both single and dual-bolus techniques, and absolute MBF quantification correlating more closely than semi-quantitative methods(111).

However, quantification of MPR on CMR is limited by the relatively time-consuming method of SI-time curve generation, as well as complex mathematical derivation of MBF and a lack of universal agreement on the best method for its calculation. There is also scarce data on the reproducibility of MPR measurement using CMR, especially in patient groups. Further studies are therefore needed, assessing both its reproducibility and its prognostic value in predicting outcomes in asymptomatic AS.

1.5 Management of AS

1.5.1 Surgical management

The development of symptoms in AS heralds a malignant phase of the condition and prompt AVR results in a clear reduction in mortality(112)(Figure 12). Surgery in this situation is universally regarded as a class I indication (Table 2), despite the absence of randomised controlled trials(113, 114). Transcatheter aortic valve implantation

(TAVI) is an emerging alternative technique to surgical AVR, which is especially suitable for high-surgical-risk patients with severe symptomatic AS(115).

Table 2. Definition of classes of recommendation and levels of evidence (from European Society of Cardiology guidelines)

Class of recommendation	Definition	Level of Evidence	Data derived from
Class I	Evidence and/or general agreement that a given treatment or procedure is beneficial, useful, effective.	**A**	Multiple randomised clinical trials or meta-analyses.
Class II	Conflicting evidence and/or a divergence of opinion about the usefulness/efficacy of the given treatment or procedure.	**B**	A single randomised clinical trial or large non-randomised studies.
Class IIa	*Weight of evidence/opinion is in favour of usefulness/efficacy.*	**C**	Consensus of opinion of the experts / small studies, retrospective studies, registries.
Class IIb	*Usefulness/efficacy is less well established by evidence/opinion.*		
Class III	Evidence or general agreement that the given treatment or procedure is not useful/effective, and in some cases may be harmful.		

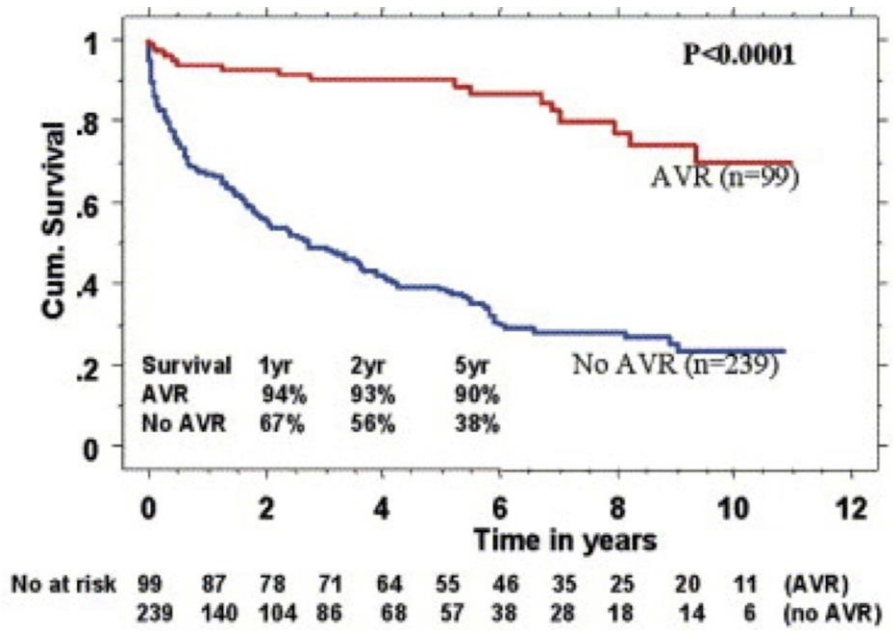

Figure 12. Kaplan-Meier survival curves comparing the outcome of asymptomatic severe aortic stenosis patients with and without aortic valve replacement (AVR). (112)

1.5.2 Medical management

There are currently no drugs of proven benefit that improve or reduce the progression of AS. Despite some experimental and retrospective studies suggesting the role of statins in slowing the progression of AS, large randomised controlled trials have failed to demonstrate a benefit in haemodynamic severity or clinical outcome in AS(74, 76, 116), and are therefore not recommended in the latest guidelines(44). Management of concurrent hypertension, which is common in AS, is recommended with standard anti-hypertensive therapy.

1.5.2.1 Novel medical therapies

As we gain greater understanding into the pathophysiology of symptom development and LV remodeling in AS, various potential therapeutic targets have been identified. New classes of drugs targeting these processes may slow down disease progression and improve prognosis in AS. These include: 1.) anti-osteoporosis drugs targeting micro-calcification and disease progression (ClinicalTrials.gov NCT02132026) (79, 117), 2.) drugs targeting LV remodeling (118), 3.) anti-steatosis agents(104) and 4.) drugs that could improve cardiac function and perfusion. Drugs that can improve myocardial function may prevent onset of symptoms, and especially in the elderly, decrease the need for intervention. Also a significant proportion of patients have residual symptoms post AVR/TAVI who may benefit from treatment.

1.5.2.1.1 Ranolazine

Ranolazine is a newly-licensed drug for the treatment of chronic stable angina(119, 120), that has been shown to improve both diastolic function and myocardial ischaemia in animal models and small clinical studies(121-124). It may therefore play a role in improving both diastolic function and myocardial perfusion in patients with AS and existing diastolic impairment / LVH.

1.5.3 Management Controversies

The management of patients with severe AS in the absence of symptoms remains one of the most controversial and debated areas in modern cardiology(125, 126). Registry data indicate that 15% of patients are asymptomatic at the time of surgery(58). There

is variation in clinical practice in the management of these patients because of arguments both for and against the traditional 'watch and wait' policy. There remains a small risk of sudden death in symptomatic patients (1-2% per annum)(127). Some patients, especially the elderly, may not recognise symptoms or may reduce their activities subconsciously to avoid symptoms. Shortly after the development of symptoms, the risk of sudden death and that of surgery itself can increase dramatically(128). Finally, the remodeling processes within the myocardium may be only partially reversible, which can lead to limited symptomatic improvement and intermediate long-term outcome post surgery(85, 129). However, early surgery is not without risk. There is peri-operative morbidity and mortality, as well as complications associated with the prosthetic valve itself, including endocarditis, bleeding complications and valve degeneration. Finally, in an elderly population, some patients may never develop symptoms related to AS in their lifetime.

This variation in clinical practice was reflected in the discrepancies between international guidelines on management of asymptomatic severe AS until recently (at the time of planning this study) (Table 3). This is partly because there has been no randomised trial that has assessed whether outcome can be improved in asymptomatic patients with a positive exercise test, or any other prognostic marker. For this reason, the American Heart Association/ American College of Cardiology guidelines had graded exercise-induced symptoms as a class IIb indication (can be considered, but weight of evidence does not support intervention) for AVR. However, somewhat surprisingly, both the latest European and American guidelines now class symptoms on exercise testing as a level-I recommendation. This is based on mainly observational studies, many with limitations, as discussed in section 1.6 below.

Table 3. Comparison of European and American guidelines on management of asymptomatic severe AS

Indication	ESC (2007)	AHA (2008 update)	ESC (2012)	AHA (2014)
Other Cardiac surgery	I (C)	I (C)	I (C)	I (B)
LVEF < 50%	I (C)	I (C)	I (C)	I (B)
Symptoms on ETT	I (C)	IIb (C)	I (C)	I (B)
Drop in BP on ETT	IIa (C)	IIb (C)	IIa (C)	IIa (B)
Rapid progression	IIa (C)	IIb (C)	IIa (C)	IIb (C)
Very severe AS	-	IIb (C)	IIa (C) >5.5 m/s	IIa (B) >5 m/s
LVH > 15 mm	IIb (C)	-	IIb (C)	-
Elevated natriuretic peptides	-	-	IIb (C)	-
Increase in exercise MPG >20 mmHg	-	-	IIb (C)	-
Complex arrhythmia on ETT	IIb (C)	-	-	-

LVEF = left ventricular ejection fraction, BP = blood pressure, ETT = exercise tolerance test, LVH = left ventricular hypertrophy, MPG = mean pressure gradient, ESC = European society of Cardiology, AHA – American heart association

The theoretical ideal time for surgery would be immediately prior to symptom development and before the irreversible aspects of cardiac remodelling take place. Understanding the pathophysiology and mechanisms which lead to symptom development and adverse events in AS, will help improve risk stratification of these patients. The ultimate aim in the management of asymptomatic patients with severe AS is to accurately identify those patients with incipient symptoms, so that intervention can be offered earlier, with low peri-operative risk.

1.6 Limitations of current research

There have been no randomised clinical trials to date assessing the effect of any of the above prognostic markers on outcome in asymptomatic patients with moderate to severe AS. Although most of the studies mentioned above are prospective in nature, there are still a number of limitations, as summarised in a recent editorial(54). These include non-blinded investigations influencing management decisions and a degree of selection bias in who gets referred for surgery, leading to the groups treated medically being different from those offered early surgery (as reflected by

more non-cardiac deaths in patients managed conservatively than in those operated on whilst asymptomatic(35, 38)). Finally, the majority of these studies used a composite of death and need for AVR as their endpoint. They have included asymptomatic patients having AVR based on the clinician's judgement, which is an extremely soft endpoint, since such patients are not at the same risk as those with symptoms, heart failure or death. They have also included symptomatic patients who then refuse surgery in the non-surgical group in the final endpoint analysis. These patients should ideally be excluded from endpoint analysis.

1.7 Summary

AS is a common disease in the western world, accounting for a great deal of morbidity and mortality, with its prevalence increasing with an ageing population. Whilst AVR is universally considered the best treatment once symptoms develop, the management of asymptomatic patients remains controversial, with variable clinical practice and differences in international guidelines until recently. This is because AS is characterised by a long and variable latent asymptomatic phase, with good prognosis until symptoms develop, and AVR itself is associated with peri- and post-operative morbidity and mortality, due to which a 'watch and wait' approach is recommended. However, there is a small risk of sudden cardiac death prior to symptom onset and some of the cardiac remodeling that occurs secondary to chronic pressure overload caused by AS, is thought to be irreversible. The ideal time of intervention therefore, would be just prior to the irreversible damage and onset of symptoms. Many observational studies have attempted to identify risk factors, including echocardiographic and exercise markers, though with some limitations. Recent advances in non-invasive imaging have allowed us to better quantify disease severity and to increase our understanding of the pathophysiological sequale of AS on the myocardium *in vivo*.

CMR is an attractive non-invasive imaging tool to assess patients with AS. In particular, MPR shows promise as a potential imaging biomarker for identifying high-risk patients with AS and has recently been shown to be a predictor of exercise capacity in AS. The increased afterload caused by the chronic pressure overload in AS

leads to LVH, with a relatively reduced capillary density and increased diastolic stiffness, leading to an inability to increase MBF during stress, resulting in reduced MPR and repetitive ischaemia during stress. This can lead to ischaemic necrosis and fibrosis within the myocardium, some of which can be irreversible.

The mechanisms responsible for exercise intolerance in AS are likely to be the same as those that lead to symptom development. A better understanding of the determinants of both exercise capacity and MPR in AS, will therefore improve our understanding of the pathophysiology of symptom development in AS. Better risk stratification of patients with AS will allow earlier intervention to be offered to those with imminent symptoms, in order to improve their management, with the ultimate aim of reducing both morbidity and mortality.

1.8 Aims

The main aim of this thesis was to establish robust prognostic markers in a moderately large multi-centre cohort of patients with moderate to severe AS, with particular focus on CMR and the assessment of MPR. Additionally, a proof-of-concept study was conducted to determine whether Ranolazine might improve MPR and diastolic strain rate in AS.

Specifically, the aims addressed in this thesis are:-

- to establish the reproducibility of contrast-enhanced CMR (MPR, T1 mapping) in AS.
- to establish the reproducibility of strain and strain rate measurement at 3T, compared to 1.5T.
- to establish the effect of Ranolazine on MPR and diastolic strain rate in asymptomatic AS.
- to establish differences in LV remodeling and exercise capacity in asymptomatic patients with moderate-sever AS and matched controls.
- to identify the determinants of MPR in asymptomatic AS.
- to identify the determinants of exercise capacity in asymptomatic AS.
- to establish the predictors of 1 year outcome in asymptomatic AS, and assess whether MPR is a better predictor than exercise capacity.

1.9 Original Hypotheses

1.9.1 Reproducibility of strain and strain rate

H_1: MRI measured strain and strain rate, using tagging and Feature Tracking, have good reproducibility (observer variability and test-retest repeatability) at 3T (CoV < 20%).

H_0: MRI measured strain and strain rate, using tagging and Feature Tracking, does not have good reproducibility at 3T (CoV > 20%).

1.9.2 Reproducibility of T1 / ECV

H_1: MRI-measured T1 / ECV using T1 mapping has good reproducibility (observer variability and test-retest repeatability) in moderate to severe AS (CoV < 20%).

H_0: MRI measured T1 / ECV does not have good reproducibility (CoV > 20%).

1.9.3 Reproducibility of MPR using MOCO *vs* raw image analysis

H_1: MPR measured using motion-corrected (MOCO) images is more reproducible (better observer variability and test-retest repeatability) than raw images.

H_0: Both MOCO and raw images are equally reproducible for measurement of MPR.

1.9.4 Effect of Ranolazine

H_1: Short-term treatment with Ranolazine leads to an improvement in MPR and diastolic strain rate in patients with moderate to severe AS.

H_0: Short-term treatment with Ranolazine does not lead to an improvement in MPR and diastolic strain rate in patients with moderate to severe AS.

1.9.5 Asymptomatic AS *vs.* controls

H_1: Asymptomatic patients with moderate to severe AS show evidence of LV remodeling and impaired exercise capacity compared to controls.

H_0: Asymptomatic patients with moderate to severe AS do not show evidence of LV remodeling and impaired exercise capacity compared to controls.

1.9.6 Determinants of exercise capacity

H_1: MPR is an independent predictors of peak VO_2 measured on CPET.

H_0: MPR does not predict peak VO_2 measured on CPET.

1.9.7 Determinants of MPR

H_1: MPR is related to LV mass and myocardial fibrosis in asymptomatic AS.

H_0: MPR is not related to LV mass or myocardial fibrosis in asymptomatic AS.

1.9.8 Predictors of outcome

H_1: MPR is a better predictor of outcome in moderate to severe AS than exercise testing.

H_0: MPR is not a better predictor of outcome in moderate to severe AS than exercise testing.

CHAPTER TWO

2 GENERAL METHODS

Published (PRIMID protocol paper):

Singh A, Ford I, Greenwood JP, Khan JN, Uddin A, Berry C, Neubauer S, Prendergast B, Jerosch-Herold M, Williams B, Samani NJ, McCann GP. Rationale and design of the PRognostic Importance of MIcrovascular Dysfunction in asymptomatic patients with Aortic Stenosis (PRIMID-AS): a multicentre observational study with blinded investigations. BMJ Open. 2013;3(12):e004348

2.1 Study Design

(i) The main study (PRIMID-AS: PRognostic Importance of MIcrovascular Dysfunction in asymptomatic patients with Aortic Stenosis) was a prospective, multi-centre, observational, cohort outcome study with blinded analysis of CMR data. Ten of the patients had the CMR scan performed twice, to allow test-retest reproducibility of contrast-enhanced CMR to be assessed. (ii) In addition, the Ranolazine study was a proof-of-concept single centre, open label, single group pilot study in 20 patients, with blinded endpoint (CMR) analysis, to assess whether Ranolazine may improve MPR and diastolic dysfunction in asymptomatic AS. (iii) Finally, 20 asymptomatic controls without valve disease were recruited to allow determination of age and sex-matched normal range for MPR and diffuse myocardial fibrosis. This would allow additional analysis by normal and reduced MPR.

2.2 Subject Selection

2.2.1 Recruitment

Patients were recruited from the cardiology outpatient department at Glenfield Hospital and surrounding hospitals in the Midlands. Additional centres were originally established in Leeds and Glasgow, with the later addition of Aberdeen, Dundee and Coventry, in order to increase the recruitment rate. In Leicester, patients were identified from the Biomedical Research Informatics Centre for Cardiovascular Science database, cardiology clinics, echocardiography and MRI reports. Their latest clinical echocardiogram report was screened for inclusion criteria, followed by review of their clinical notes / clinic letters for exclusion criteria. Those who were deemed eligible were posted a patient information sheet (PIS) with a reply envelope. Those who expressed an interest were checked for suitability and an appointment was arranged if applicable. Patients who had been sent a PIS were also approached in clinic if they hadn't sent the reply slip before their appointment.

2.2.2 Patient Inclusion Criteria (PRIMID-AS)

1. Moderate-severe aortic stenosis (2 or more of: AVA <1.5cm^2, peak pressure gradient >36mmHg, mean PG >25mmHg).

2. Asymptomatic.
3. Age >18 years and < 85 years.
4. Prepared to consider AVR if symptoms developed.
5. Ability to perform bicycle exercise test.

2.2.3 Patient Exclusion Criteria (PRIMID-AS)

1. History of coronary artery bypass graft (CABG), myocardial infarction (MI), angiographic coronary artery disease (>50% luminal stenosis if previously undertaken): Amended to history of CABG, or MI / coronary intervention within 6 months (for PRIMID-AS study only)
2. Persistent Atrial fibrillation or flutter
3. Severe Asthma.
4. Severe renal impairment eGFR <30ml/min.
5. Any absolute contraindication to CMR
6. Any absolute contraindication to Adenosine
7. Previous valve surgery/ Severe valve disease other than AS
8. Planned AVR
9. Significant LV systolic dysfunction (LVEF < 40%)
10. Other medical condition that limits life expectancy or precludes AVR
11. Participation in an interventional clinical trial

2.2.4 Healthy Volunteer Inclusion Criteria

1. Asymptomatic
2. Ability to perform bicycle exercise

2.2.5 Healthy Volunteer Exclusion Criteria

Points 1-6 as above (section 2.2.2), and in addition:-

- Presence of valvular heart disease (for regurgitant lesions more than mild on echocardiography)
- LV systolic dysfunction (EF < 50%)
- Uncontrolled hypertension >160/100mmHg. (Hypertension controlled on medication allowed)

- Obesity (BMI > 30)
- Chronic Obstructive Pulmonary Disease (clinical diagnosis)
- Other medical condition that limits life expectancy

2.2.6 Ranolazine study Inclusion Criteria

Points 1-3 of above (section 2.2.2), and in addition:-

- Evidence of diastolic dysfunction on echocardiography (MV inflow and or TDI) or LVH (maximum wall thickness ≥13mm)

2.2.7 Ranolazine study Exclusion Criteria

Points 1-6 of above (section 2.2.3), and in addition:-

- Hepatic impairment
- Concurrent administration of strong CYPA4 inhibitors
- Concurrent class I or III anti-arrhythmic administration
- QTc prolongation >470ms
- Hypersensitivity to Ranolazine
- Females of childbearing potential

2.3 Study Visits

Written informed consent was obtained from all patients prior to commencement of any investigations.

2.3.1 PRIMID-AS study visits and follow-up

The number of patient visits was kept to a minimum, and all investigations at the baseline visit (Figure 13) were carried out in a single visit in Leicester, and at other sites where facilities allowed. If necessary, the baseline visit was split. The baseline visit lasted 3.5 to 4 hours in total, with a break for lunch between the tests.

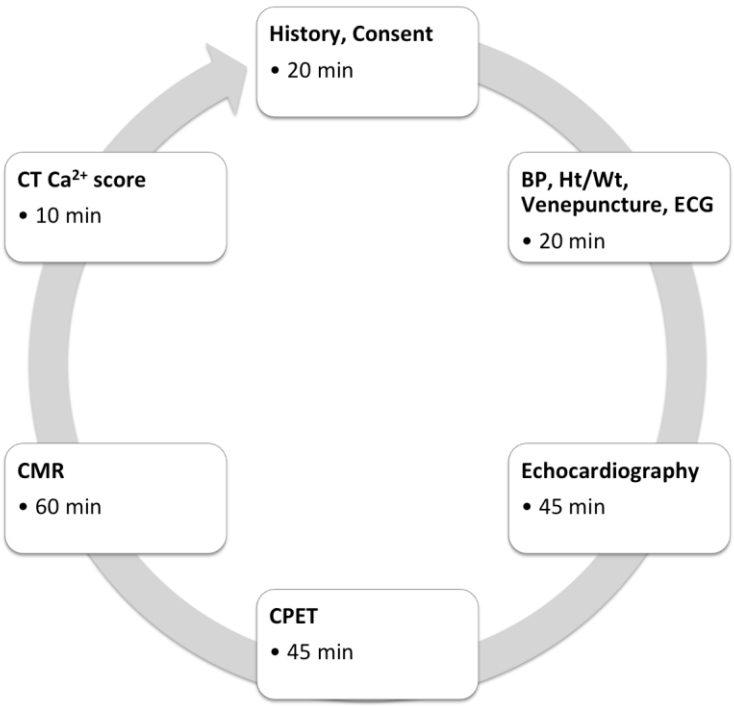

Figure 13. Baseline visit for PRIMID-AS

(BP=blood pressure, Ht=height, Wt=weight, ECG=electrocardiography, CPET=cardiopulmonary exercise test, CMR=cardiac magnetic resonance imaging, CT Ca^{2+} score=CT calcium score)

The patients were followed up at 6-monthly intervals, with the visits involving history taking and venepuncture for biomarker analysis. At the one-year visit, those patients who remained asymptomatic were invited for a repeat MRI scan in order to assess longitudinal CMR data in a sub-group of patients (Figure 14). The follow-up was stopped once the patient reached one of the pre-defined endpoints, or at the end of the study (minimum 12 months).

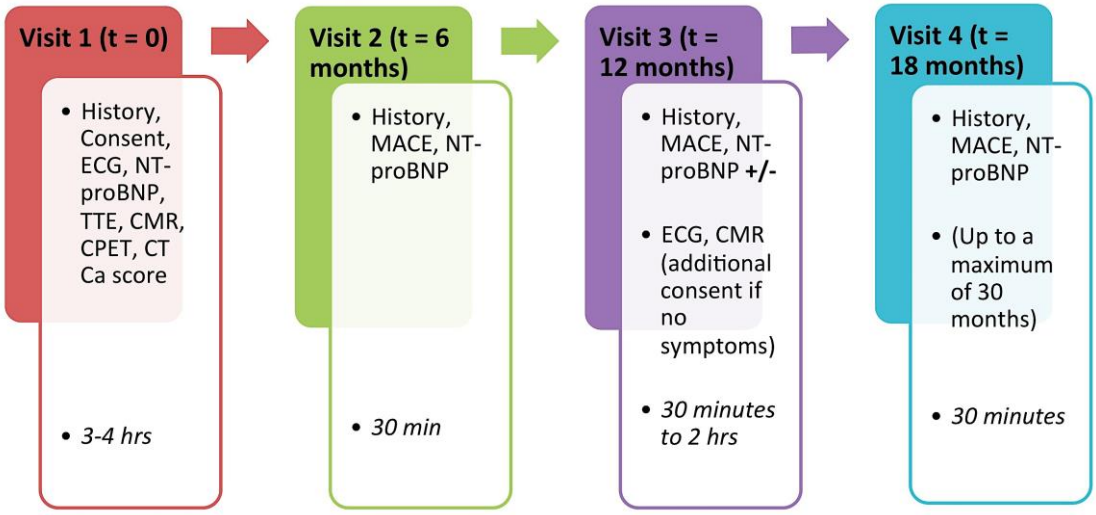

Figure 14. Study visits for PRIMID-AS study

(ECG=electrocardiogram, NT-proBP=N terminal pro-brain natriuretic peptide, TTE=trans-thoracic echocardiogram, CMR=cardiac magnetic resonance imaging, CPET=cardio-pulmonary exercise test, CT Ca score=CT calcium score, MACE=major adverse cardiovascular events)

2.3.2 Ranolazine study visits and follow-up

The visits for the Ranolazine study were very similar to that of the main study, with the exclusion of the CT and use of treadmill instead of the recumbent bicycle for the CPET. Patients were followed up at 2 weeks, 6 weeks and 10 weeks following initiation of 500 mg BD of Ranolazine (Figure 15). At 2 weeks, the dose was increased to 750 mg BD if tolerated and ECG and bloods remained normal. At the 6-week visit, the patient underwent all the tests performed at the baseline visit and Ranolazine was discontinued. At the 10-week visit, all the tests were repeated for the final time.

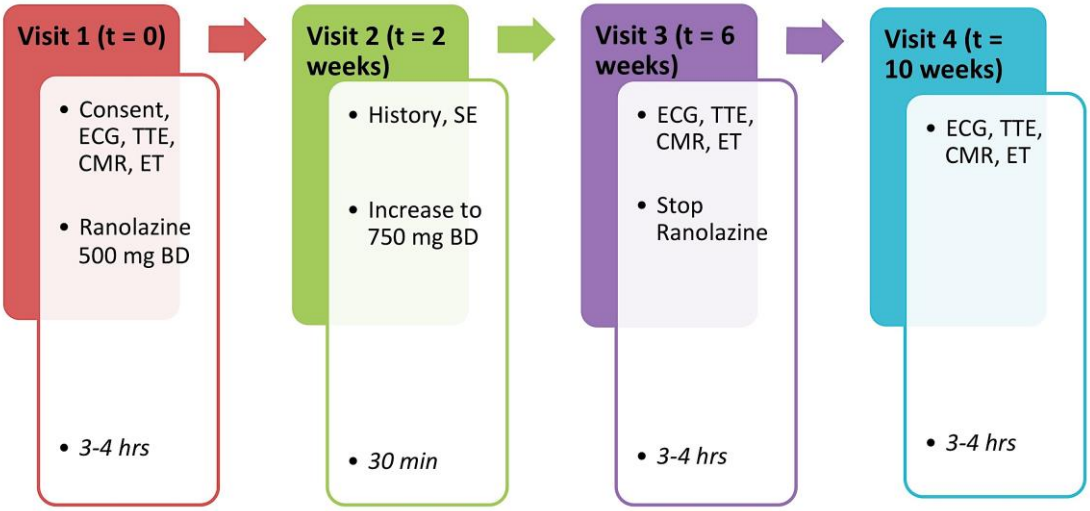

Figure 15. Study visits for the Ranolazine study

(Abbreviations as previous figure, and ET= exercise test)

2.4 Investigations

2.4.1 History Taking

Patients were interviewed to confirm the inclusion and exclusion criteria prior to written informed consent being obtained.

2.4.2 Venepuncture

Two intra-venous cannulae were placed in the ante-cubital fossae, to allow administration of contrast and adenosine for stress imaging, and 30 ml of blood was taken for full blood count, renal function, cholesterol, glucose and HbA1c. For the patients in the Midlands, nearly all of the cannulation and venepuncture was performed by myself. Twenty millilitres of the blood was transferred into EDTA tubes, which were centrifuged at 2000 revolutions per minute, for 20 minutes, at 4°C. Once separated, the plasma was pipetted into cryotubes in aliquots, labelled with the patient's study number and stored in a cryobox in an electronically monitored freezer at -80°C, for biomarker analysis at the end of the study. All the stored plasma samples from the different sites were transferred to Leicester for analysis at the end of the study, to avoid inter-assay bias.

2.4.3 Electrocardiography

A 12-lead standard ECG was undertaken by the research nurse or myself, to confirm sinus rhythm and document any signs of LVH (based on ECG voltage criteria). The following information was recorded:-

- Rhythm
- PR interval
- QRS interval
- Axis
- Sokolow (sum of S-wave in V1 and R-wave in V5 or V6, whichever is longer) and Cornell (sum of R-wave in aVL and S-wave in V3) voltage criteria for LVH

2.4.4 Trans-thoracic Echocardiography

TTE was performed by a British Society of Echocardiography (BSE) accredited echocardiographer in all subjects, according to International guideline recommendations. Standard 2D, colour flow, continuous-wave (CW) and pulsed-wave (PW) Doppler images were acquired in the parasternal long-axis, short-axis, apical 4-, 5-, 3- and 2-chamber views (Figure 16), as well as the sub-costal, supra-sternal and right parasternal views, if possible. A 3-lead ECG with clear QRS was attached. At least 3 cardiac cycles were recorded and stored for blinded, off line analysis using an Xcelera (Philips, Netherlands) workstation.

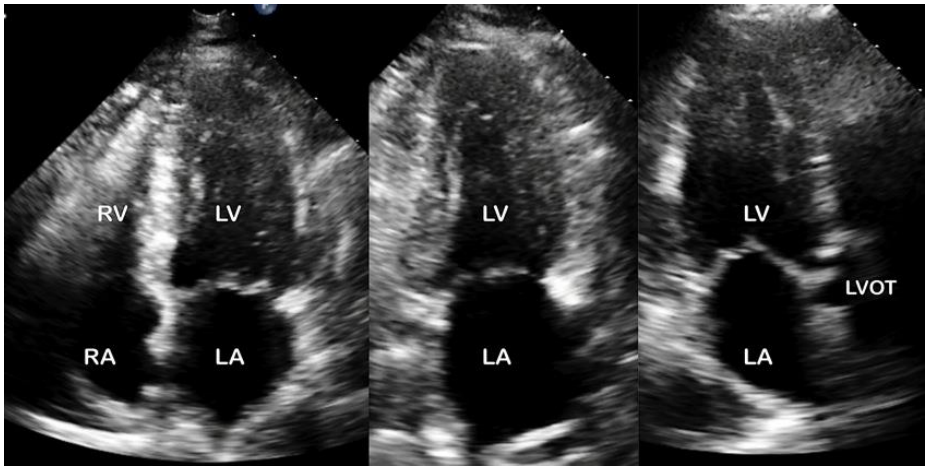

Figure 16. An example of apical 4-chamber (left), 2-chamber (middle) and 3-chamber (right) views on trans-thoracic Echocardiography.

(LA: left atrium, LV: left ventricle, LVOT: left ventricular outflow tract, RA: right atrium, RV: right ventricle)

2.4.4.1 Assessment of AS severity

CW Doppler through the aortic valve allowed measurement of peak velocity (AV Vmax) across the valve, with calculation of peak pressure gradient (PPG), mean pressure gradient (MPG) and AV velocity time integral (VTI). The pressure gradient across a stenotic valve is related to the jet velocity according to the Bernoulli equation, which has been simplified further to allow quick calculation of PPG(130) (Equation 1).

$$\mathbf{\Delta P} = 4 \times V^2$$

Equation 1: Modified Bernoulli equation used to calculate the pressure gradient across the aortic valve.

*(*ΔP = pressure drop across an obstruction, in mmHg; *V = maximal velocity at the obstruction, in m/s)*

Although the original equation was derived from the study of water flow in rigid tubes, and may not therefore accurately apply to pulsatile blood flow, the simplified Bernoulli equation has been validated against invasive haemodynamic measurements in various studies and correlates well with invasively measured gradients(131, 132). However, accurate measurement of the AV Vmax is dependent on the correct alignment of the Doppler interrogation angle to the flow, and small changes in this angle can lead to under-estimation of the peak velocity. Another important point of note is the difference in what is being measured using Doppler and catheterisation. While Doppler reports the maximal instantaneous gradient, catheter measurements traditionally report the peak-to-peak gradient (Figure 17). MPG represents an average of pressure gradients during the entire flow period, and Doppler measured MPG corresponds to that measured using catheterisation.

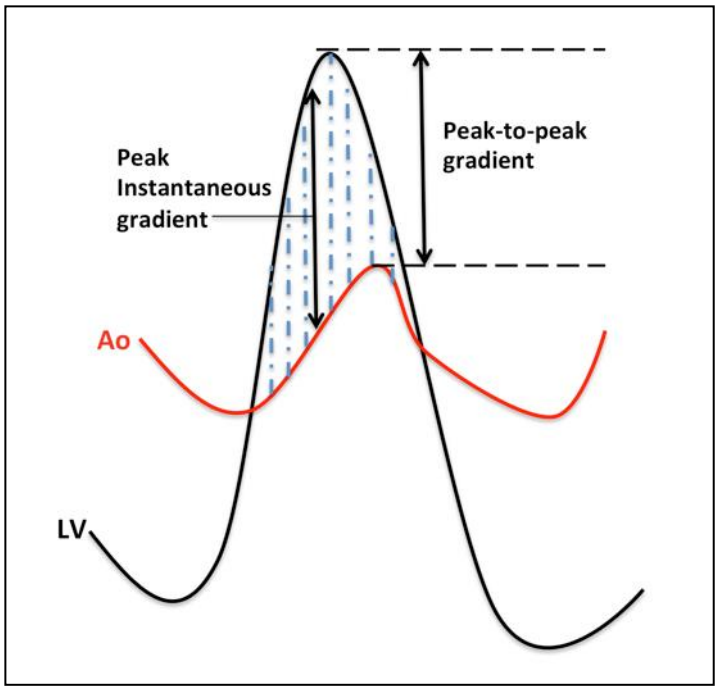

Figure 17. Schematic of aortic (Ao) and left ventricular (LV) pressures demonstrating the difference between peak-to-peak, peak instantaneous and mean pressure gradients (dashed blue lines).

PW Doppler through the left ventricular outflow track (LVOT) allowed measurement of the LVOT VTI. The LVOT diameter was measured on a zoomed parasternal long-axis view of the LVOT to calculate the LVOT area (Figure 18). Using these parameters, the aortic valve area (AVA) was calculated using the continuity equation(133) (Equation 2, Figure 19).

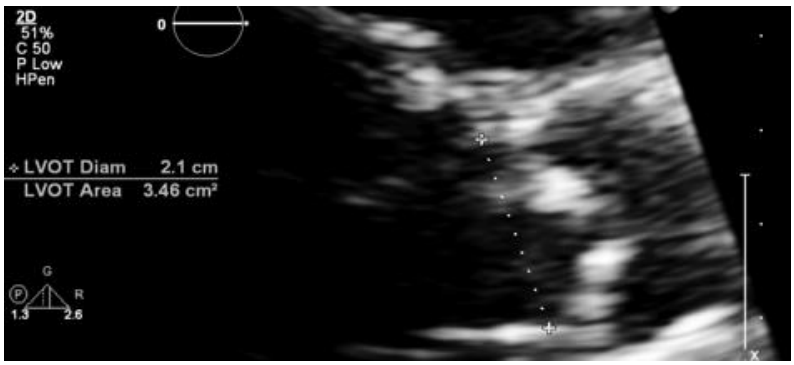

Figure 18. An example of LVOT diameter measurement (dashed line) on a zoomed-in parasternal long-axis view of the LVOT.

However, there are some limitations to this method as well. Calculation of the LVOT area assumes a circular shape of the LVOT, and small errors in LVOT diameter measurement can lead to large inaccuracies in the calculated area. Having said this, continuity equation AVA has been well validated against the previous gold standard method of assessing AVA using the Gorlin formula on invasive measures of pressure gradient and cardiac output(133, 134).

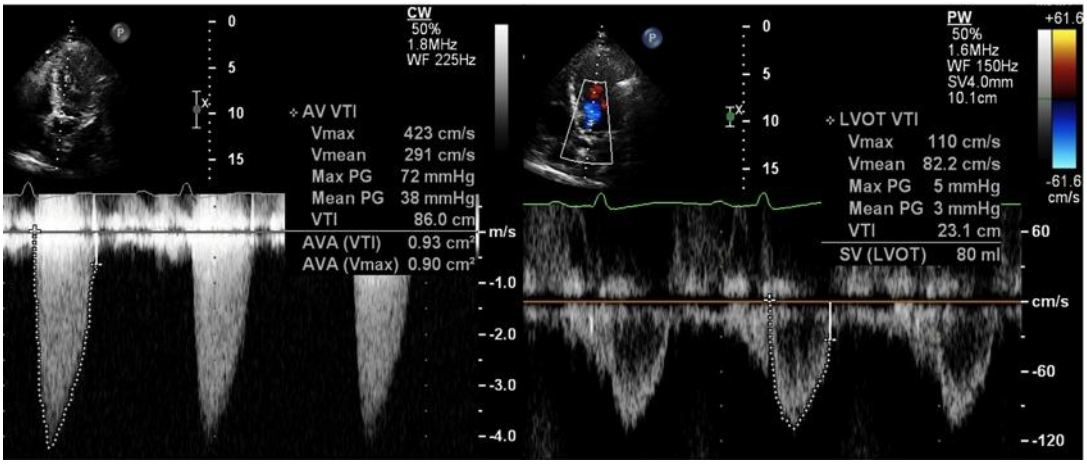

Figure 19. An example of continuous-wave Doppler through the aortic valve (left) with peak and mean pressure gradients displayed, and pulsed-wave Doppler through the LVOT (right), used for the calculation of Aortic Valve Area.

$$\mathbf{AVA} = \frac{LVOT_{area} \; x \; LVOT_{VTI}}{AV_{VTI}}$$

Equation 2. Calculation of AVA using the Continuity Equation

(AVA=aortic valve area in cm^2; LVOT area=left ventricular outflow tract area in cm^2; VTI=velocity time integral in cm; AV=aortic valve)

2.4.4.2 Assessment of Diastolic function

Diastolic function was assessed using mitral inflow velocities and tissue Doppler imaging (TDI), based on the British Society of Echocardiography guidelines. Pulsed-wave Doppler at the mitral valve tips, in the apical 4-chamber view, was used to determine the peak early diastolic filling velocity of the LV due to acceleration of blood across the mitral valve (E-wave), the late LV filling velocity due to atrial contraction (A-wave) and the deceleration time. The E/A ratio was then calculated (Figure 20).

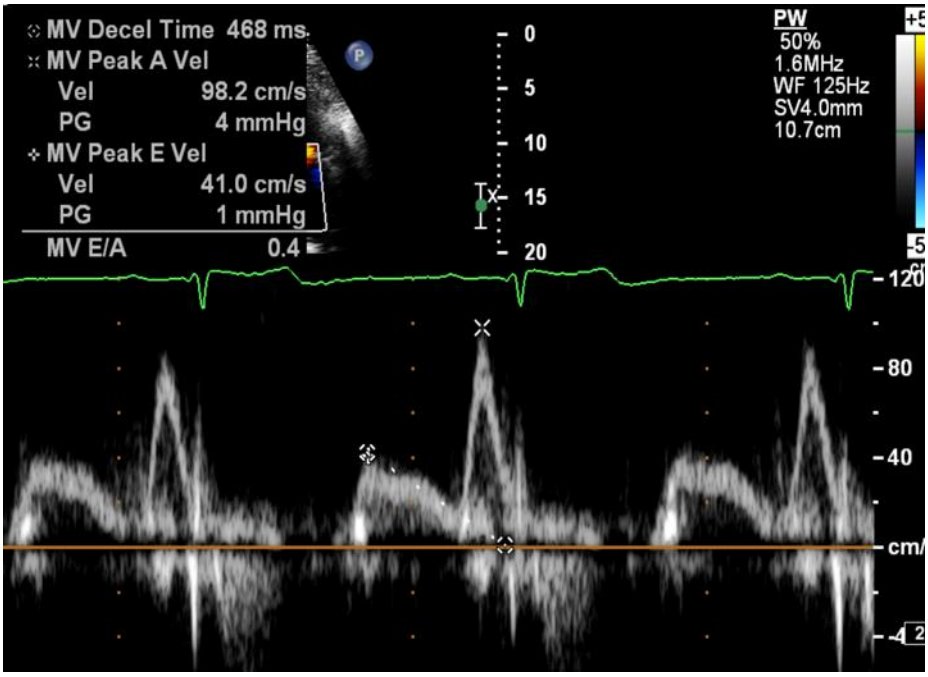

Figure 20. Pulsed-Wave (PW) doppler at the tips of the mitral valve showing the E-wave, A-wave, E/A ratio and the deceleration time.

TDI uses Doppler principles to measure the velocity of myocardial motion. Pulsed-wave TDI was used to determine the longitudinal velocities at the septal and lateral mitral annulus, in the apical 4-chamber view. The trans-mitral flow to mitral annular velocity ratio was calculated for the lateral and septal walls (lateral and septal E/E') (Figure 21).

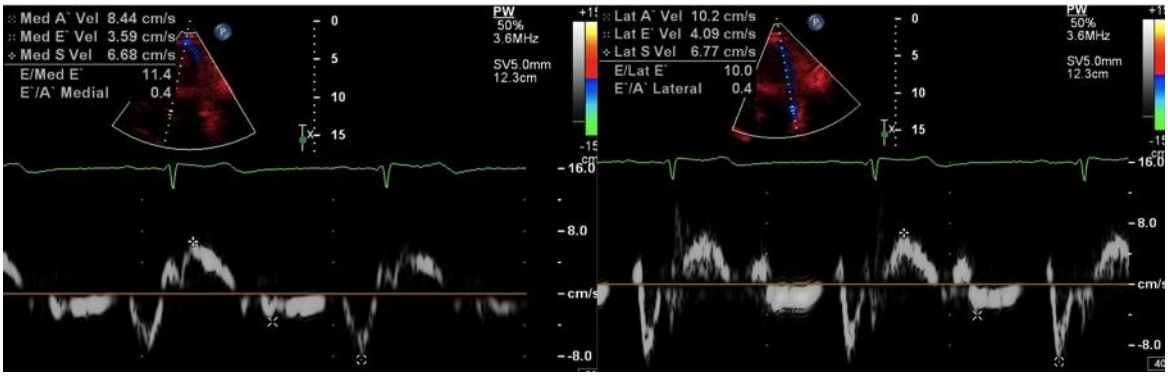

Figure 21. An example of PW TDI at the medial (left) and lateral (right) mitral annulus for calculation of E/e'

2.4.4.3 Left ventricular Rate Pressure Product and Diastolic Perfusion Time

The left ventricular rate pressure product (LVRPP) is a surrogate marker of myocardial oxygen consumption (Equation 3).

$$\textbf{LVRPP} = (PPG + SBP) \times HR$$

Equation 3: Calculation of LVRPP

(LVRPP = Left Ventricular Rate Pressure Product in mmHg.bpm.10^{-4}; PPG = peak aortic valve pressure gradient in mmHg; SBP = systolic blood pressure in mmHg; HR = heart rate in beats per minute)

Diastolic perfusion time (DPT), a major determinant of myocardial perfusion(135), was calculated using Equation 4, where LV ejection time (LVET) is the time between the opening and closing of the AV on continuous wave Doppler and the RR interval is the time between subsequent R-waves on ECG (Figure 22).

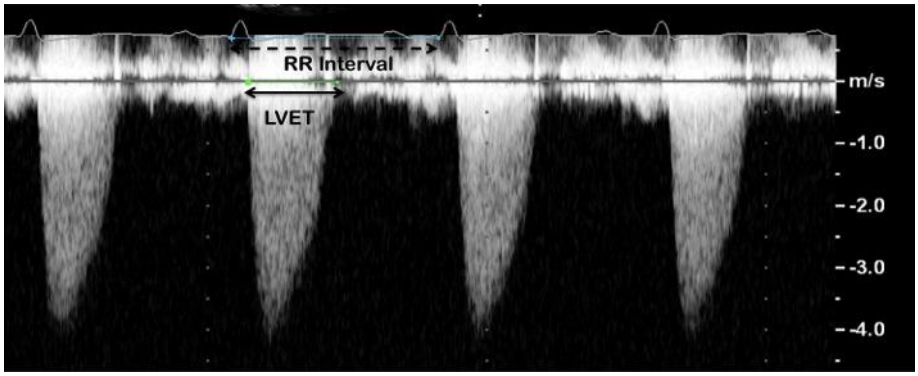

Figure 22. Measurement of left ventricular ejection time (LVET) and RR-interval on a continuous wave doppler across the aortic valve.

$$\textbf{DPT} = (RR\ interval - LVET) \times HR$$

Equation 4. Calculation of DPT

(DPT = diastolic perfusion time in s/min; LVET = left ventricular ejection time in seconds; HR = heart rate in beats per minute)

2.4.4.4 Valvulo-arterial Impedance

Valvulo-arterial impedance (VAI), a measure of global LV afterload, which combines the effect of both valvular and vascular (arterial) afterload in AS, was calculated as follows (Equation 5). It was calculated using the stroke volume derived from both TTE (LVOT Doppler) and CMR volumetric analysis.

$$VAI = \frac{SBP + MPG}{SVi}$$

Equation 5. Calculation of VAI

(VAI = valvulo-arterial impedance in mmHg/ml/m^2; SBP = systolic blood pressure in mmHg; MPG = mean pressure gradient across aortic valve in mmHg; SVi = stroke volume index)

2.4.5 Cardio-pulmonary Exercise Testing (CPET)

All PRIMID-AS patients underwent a recumbent bicycle, symptom-limited maximal exercise test, supervised by an Advanced Life Support trained physician, and assisted by a Cardiac Physiologist. All CPET was performed in an air-conditioned room at 18-20°C. Exercise was performed on an electrically braked semi-supine bicycle ergometer using a standardised 1 min incremental protocol, with the workload increment determined using the age, gender, height and weight of the patient(136) (Equation 6).

$$\textbf{Work Rate Increment} = *\frac{\textit{Peak Vo2} - {}^{\circ}\textit{Vo2 unloaded}}{100} \quad \textit{where:}$$

*__Peak Vo2__ (ml/min) = *(Height (cm) – age) x 20 (Males)*

(Height (cm) – age) x 14 (Females)

°__Vo2 unloaded__ = *150 + (6 x weight (kg))*

Equation 6. Formula used for calculation of Workload Increment per minute (in watts per minute)

The calculated increment was rounded up to the nearest five watts. This formula gives the predicted workload increment that would result in achieving maximum exercise at around 10 minutes (typically 10-20 watts per minute). The maximum predicted workload was therefore taken as ten times the calculated workload by the above-mentioned formula.

For the **Ranolazine** study, a treadmill was used instead of a bicycle, with the modified Bruce Protocol(137), as this was a sponsored study, with the study design being pre-

determined by the company. The subjects were exercised until they had achieved at least 85% of their maximal predicted heart rate.

2.4.5.1 Callibration

Before each test, the gas analyser was calibrated against a reference gas cylinder. The pneumotachograph, an airflow transducer, was volume calibrated using a 3L syringe.

2.4.5.2 Testing procedure

Baseline spirometry measurements were taken prior to testing. The subjects were then connected to a 12-lead ECG monitor (CASE system, GE, USA) and a 3-lead ECG for exercise echocardiography measurements. A facemask with an attached pnuemotachograph was placed on the individuals for ventilatory gas sampling. Before starting the exercise, all patients were read out the following definition of breathlessness: "*Breathlessness is defined as laboured or difficult breathing characterized by air hunger and an uncomfortable awareness of one's own breathing*."

A minimum of 1 minute of rest was completed before beginning exercise. The patient started pedalling at 0 watts for the first minute, with the workload increased by the pre-determined increment every minute. The speed of the pedalling was maintained at 60 revolutions per minute (range of 55-64 allowed). Expired ventilation (V_E), oxygen uptake (V_{O_2}) and carbon-dioxide production (V_{CO_2}) were continuously monitored, in addition to a 12-lead ECG and pulse oximetry, with BP recordings taken at baseline and then every 2 minutes during both the exercise and the recovery period. Computerized breath-by-breath measures of ventilation, oxygen uptake and carbon dioxide production were continuously monitored. Once the patient had reached their maximal exertion or any of the pre-determined reasons for terminating the test early (Table 4), the resistance was reduced to 25 watts and the patient asked to continue pedalling while the post-exercise Doppler data (TTE) was acquired from the apical view.

Table 4. Reasons for termination of exercise

a) Fatigue
b) Dyspnoea
c) Chest pain
d) Asymptomatic ST depression (> 5mm)
e) Significant cardiac arrhythmias i.e. VF/VT, heart block, ventricular ectopics > 1 in 4 consistently.
f) Hypertension (>250mmHg systolic, 120mmHg diastolic)
g) Fall in systolic pressure >20mmHg
h) Dizziness or faintness

The patient was then asked to stop pedalling and monitored until recovery of HR, BP and ECG. At the end of the test, the subjects were asked to scale their perceived level of effort and breathlessness using the Borg Rating of Perceived Exertion (RPE)(138) and the Borg CR10 Category Ratio scale(139), for subjective assessment (Table 5) and also asked their main reason for stopping.

Table 5. Borg scale (RPE = rating of perceived exertion)

RPE Scale (perceived exertion)		CR10 Category Ratio Scale (dyspnoea)	
6		0	Nothing
7	Very, very light	0.5	Very, very slight
8		1	Very slight
9	Very light	2	Slight
10		3	Moderate
11	Fairly light	4	Somewhat severe
12		5	Severe
13	Somewhat hard	6	
14		7	Very severe
15	Hard	8	
16		9	Very, very severe
17	Very hard	10	Maximal
18			
19	Very, very hard		
20			

2.4.5.3 Test Interpretation and Data Analysis

Care was taken by the supervising Physician to distinguish between truly limiting symptoms and quickly reversible mild dyspnoea/fatigue, by reading out a definition of 'true breathlessness' (as described above) to the patients prior to commencement of the test. The test was considered 'symptom-limited' if the patient stopped prematurely due to limiting breathlessness, chest tightness or dizziness at <80% of predicted maximal workload (***'strict definition'***). In addition, a more '***conventional definition***' of a positive test (symptoms at any stage) was also added, following publication of the new AHA/ACC guidelines on AS(44), that consider symptoms at any stage of exercise testing as an indication for AVR. In patients who stopped because of fatigue, the ETT was classed as negative or inconclusive if ≥80% or < 80% of the predicted workload was achieved respectively. This was because the purpose of the CPET was to elicit 'true' symptoms secondary to the AS, with the patients being exercised till symptoms developed or they reached their limit. Therefore, fatigue was not considered to be a 'symptom' as everyone would eventually experience this. The raw CPET data was averaged over 30 seconds for analysis and peak VO_2 and respiratory exchange ratio were calculated. Exercise duration, peak workload and maximum systolic blood pressure were also noted.

2.4.6 CMR Acquisition

Imaging was performed on 3-Tesla scanners, with an 18-channel phased array cardiac coil (Leicester), using retrospective ECG gating as a default (Table 6) for details at each site). We chose to use a 3T scanner because of the better signal-to-noise ratio and limits of agreement of MBF with microspheres(140) and better tag persistence compared to 1.5T with similar LV function analysis. All subjects were asked to fill in a standard safety questionnaire prior to scanning to ensure the absence of any contraindications to CMR. Patients were asked to abstain from caffeine intake for at least 12 hours prior to the adenosine stress. The scans typically took 1 hour to perform. The CMR protocol used in the main study is outlined in Figure 23.

Table 6. MRI scanner used at each site

Testing Site	Referring sites	3T Magnetic Resonance Scanner used
Leicester	Kettering Derby Coventry Grantham Northampton	Magnetom Skyra, Siemens, Erlangen, Germany
Leeds		Phillips Achieva TX, Phillips Healthcare, Best, The Netherlands
Glasgow		Magnetom Verio, Siemens, Erlangen, Germany
Aberdeen		Phillips Achieva TX, Phillips Healthcare, Best, The Netherlands
Dundee		Magnetom Trio, Siemens, Erlangen, Germany

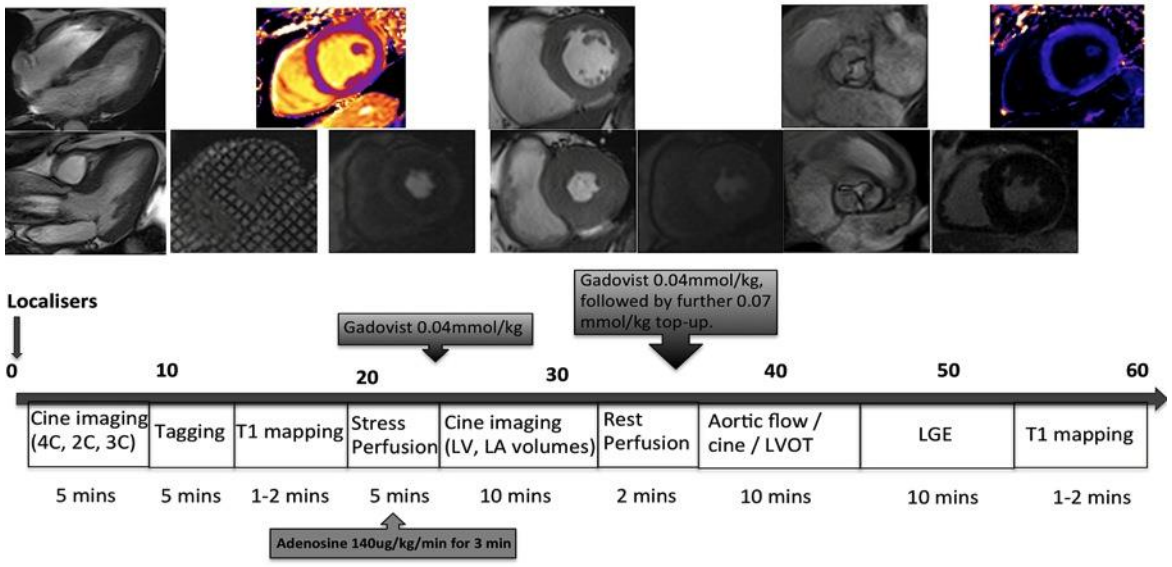

Figure 23. CMR Protocol used in PRIMID-AS study

(Abbreviations: 4/2/3C: 4/2/3 chamber, LV: left ventricular, LA: left atrial, LVOT: left ventricular outflow tract, LGE: late gadolinium enhancement)

2.4.6.1 Cine Imaging

Following the acquisition of the localiser images, magnetic field shim was applied over the heart before cine acquisition, to reduce B_0 field inhomogeneity. Balanced steady state free precession (bSSFP) cine images in the 2, 3 and 4 chamber views were acquired, with a slice thickness of 8 mm (typical parameters: matrix 256x204, field of

view (FOV) variable 300-360 x 360-420, TR 45 ms, TE 1.2 ms, flip angle 45°). The number of segments was altered according to the heart rate (HR<70 bpm: 14 segments, 70-80 bpm: 12 segments, 80-100 bpm: 11 segments).

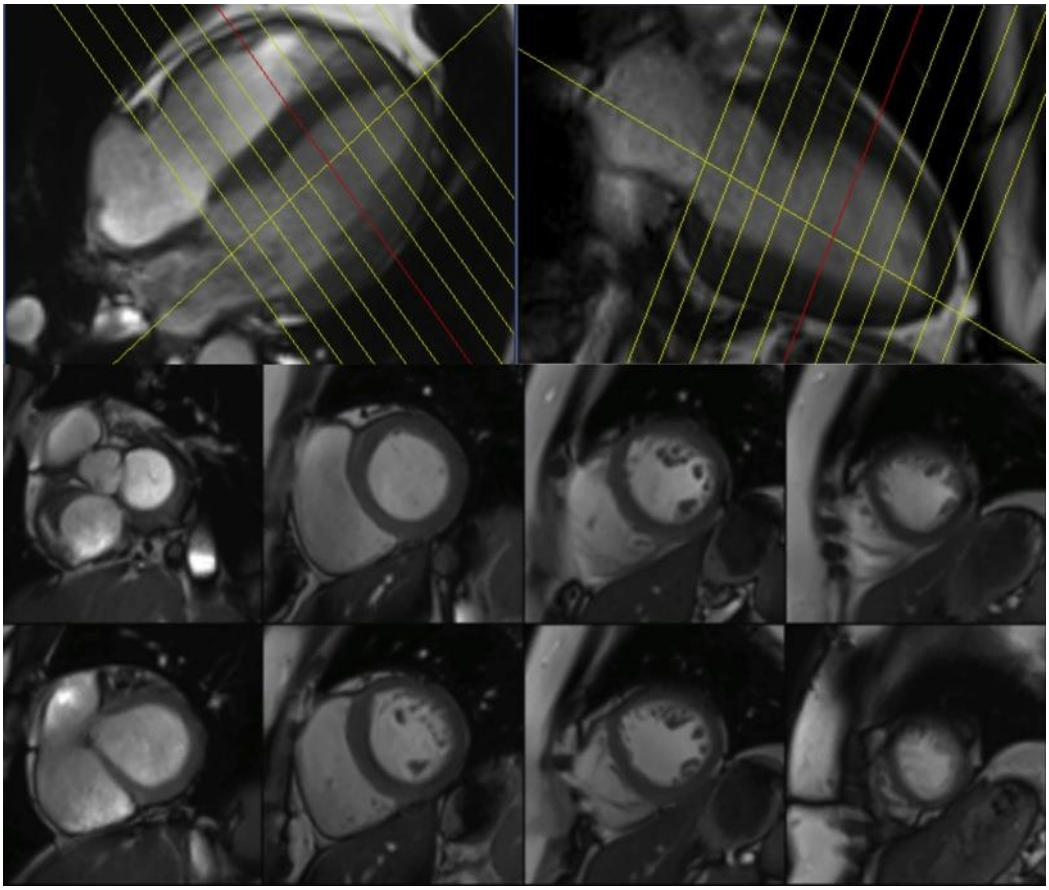

Figure 24. An example of the planning used for the short-axis SSFP cine stack shown on 4-chamber and 2-chamber slices (top panel), with examples of some short-axis slices (bottom panel).

For the short-axis cine stack, the first slice was planned at the mitral valve annulus, perpendicular to the inter-ventricular septum. Full coverage of the LV, with 1 slice every 10mm (slice thickness 8 mm, distance factor 25%) (Figure 24) was completed before acquisition of the left atrial (LA) stack. The transmitter-offset frequency was adjusted as necessary if off-resonance artefacts appeared within the LV or RV.

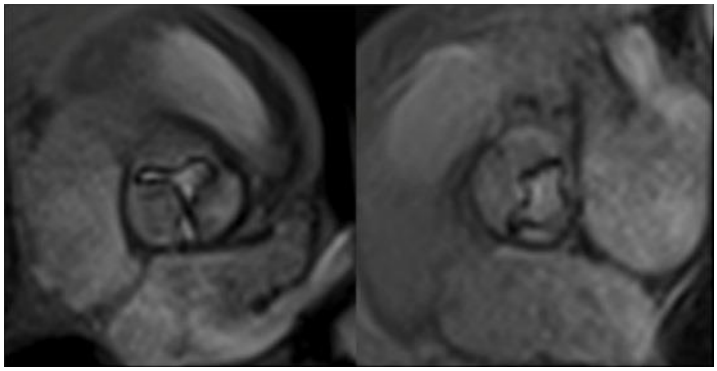

Figure 25. Examples of stills taken from aortic valve cine imaging, showing a tri-leaflet (left) and a bicuspid (right) aortic valve.

Cine imaging of the AV was acquired using a spoiled gradient echo (GRE) pulse sequence with a slice thickness of 6 mm (no gap), starting at the aortic annulus, and repeating every 3 mm until the AV orifice was no longer visible (Figure 25).

2.4.6.2 Myocardial Tissue Tagging

Myocardial tagged images were obtained using spatial modulation of magnetisation (SPAMM) imaging (typical parameters: matrix 224x198, slice thickness 8mm, grid tag spacing 8mm, TR 50 ms, TE 2.4ms, flip angle 10°, retrospective gating) at three short-axis slices (base, mid and apex) and one longitudinal slice (4-chamber) for calculation of circumferential and longitudinal strain and strain rates (Figure 26).

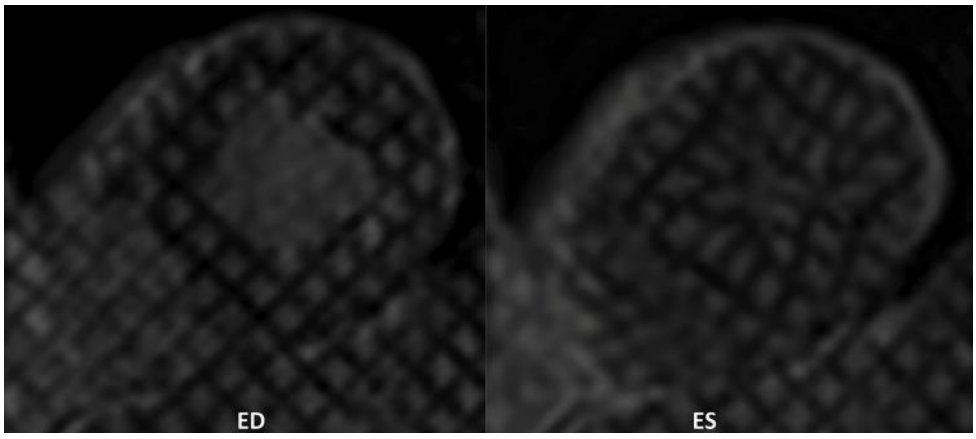

Figure 26. An example of tagged image at end-diastole (left) and end-systole (right).

The mid-short-axis slice was planned from the 4- and 3-chamber images at mid-systole, at the mid-point between the mitral annulus and the apex. The distance factor was altered (typically between 100-200%) to ensure that the LVOT was

excluded from the basal slice and the apical slice still contained some cavity (Figure 27).

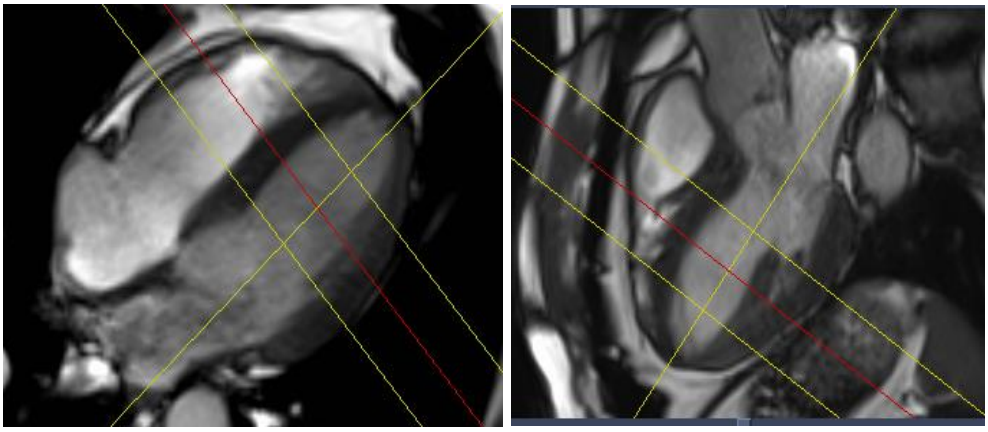

Figure 27. An example of planning of the basal, mid and apical slices for tagging and perfusion imaging.

2.4.6.3 Perfusion Imaging

A comprehensive adenosine stress and rest perfusion study was performed using a saturation recovery GRE sequence (typical parameters: matrix 224x134, slice thickness 8 mm, TR 176 ms, TE 1ms, flip angle 10°), for quantification of MBF and MPR. The smallest FOV was selected, while avoiding any wrap artefacts (Figure 28).

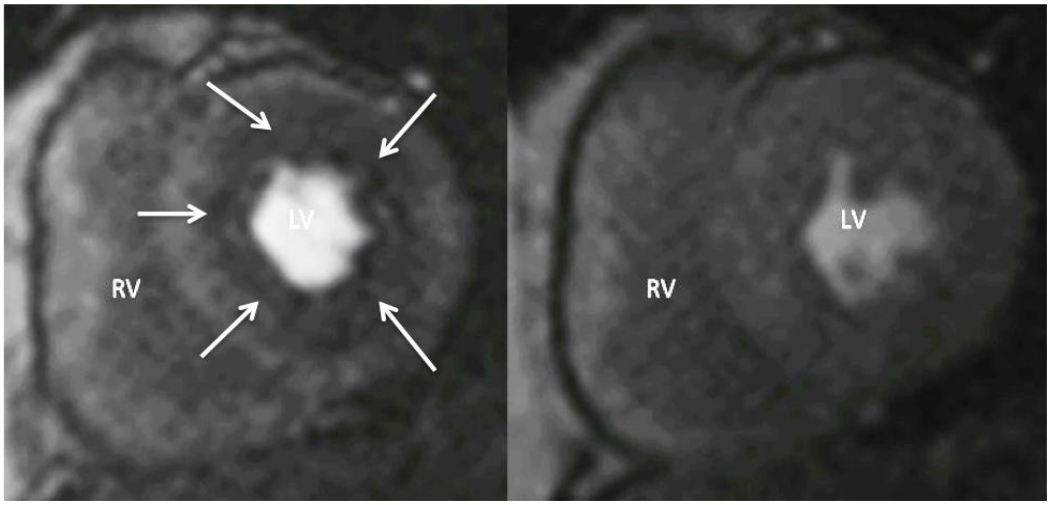

Figure 28. An example of stress (left) and rest (right) perfusion imaging, showing a global sub-endocardial perfusion defect at stress (white arrows).

Three short axis slices were acquired, with the slice positions copied from the tagged images. Stress imaging was performed after inducing pharmacological vasodilation with an infusion of adenosine at 140 mg/kg/minute for 3 minutes or until a

haemodynamic response and/or symptoms were achieved. The patient was closely monitored with recording of HR, BP and oxygen saturations every minute, as well as reporting of any symptoms. A bolus of gadolinium-based contrast agent (0.04mmol/kg of Gadovist, Bayer Pharma AG, Germany) was injected at a rate of 5 ml/second, followed by a 20 ml bolus of saline, just prior to image acquisition. First pass perfusion was assessed for the 3 slices, acquiring every heartbeat, using a saturation recovery gradient-echo sequence, during breath-hold. Rest perfusion images were acquired after a minimum of 10 minutes using identical parameters to the stress scans. A further 0.04mmol/kg of contrast was administered, followed by a top-up of 0.07mmol/kg to bring the total dose to 0.15mmol/kg for LGE imaging.

2.4.6.4 T1 Mapping

T1 data were acquired at the mid-ventricular short-axis slice pre-contrast and at least 15 minutes after the last contrast injection (bolus-contrast / dynamic-equilibrium technique(96, 97)), using a prototype, ECG-gated Modified Look-Locker Inversion recovery (MOLLI) sequence(141), with the 3(3)3(3)5 sampling pattern (typical parameters: matrix 256x192, slice thickness 8 mm, TE 1.1 ms, FoV 300 × 400 mm, flip angle 50°, minimum TI 120 ms, inversion time increment 80 ms). Multiple single-shot images in the same cardiac phase during end diastole were obtained in a single breath-hold. These images represent signal recovery following three preparation inversion pulses. Prior to acquisition of the MOLLI sequence, a tight field shim box was applied around the LV, the imaging volume was set at magnet iso-centre, and the FOV was increased to 400 mm, in order to reduce artefacts. The MOLLI sequence produces a series of 11 images with different inversion times, with data collected over 17 heartbeats. The Siemens software (Syngo MR D13) then employs a built-in post-processing image registration technique to produce a motion-corrected (MOCO) series of images, to account for mis-registration caused by breathing, patient movement or mis-triggering(142). In addition, the inline reconstruction software also produces a T1 parametric map (Figure 29), with pixel-by-pixel computation of the T1 values.

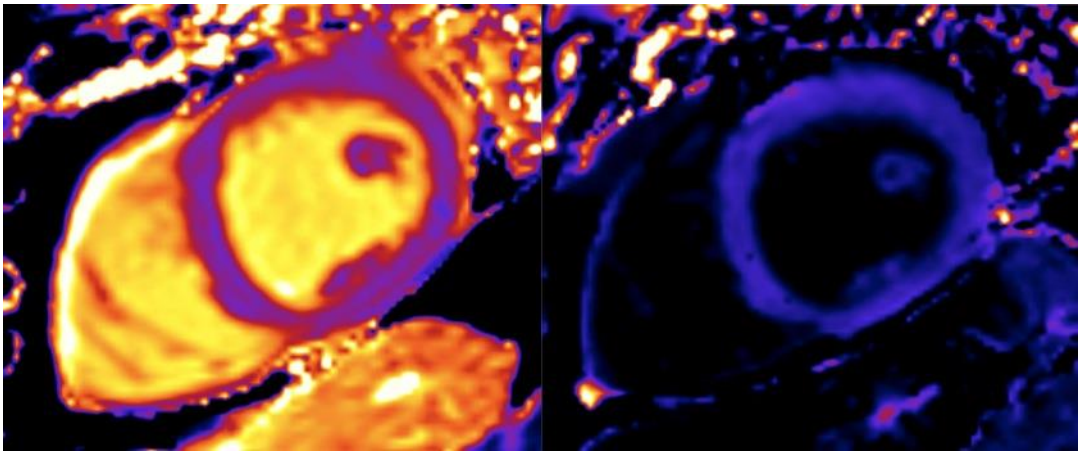

Figure 29. An example of a parametric colour map of the MOLLI sequence pre- (left) and post-contrst.

The MOLLI sequence was initially not available at the 3T scanner and so was not acquired in all of the study patients. This sequence was also not available for the Ranolazine study.

2.4.6.5 Late Gadolinium Enhancement

LGE imaging was performed at least 10 minutes after the last contrast injection, using an inversion recovery spoiled GRE sequence (typical parameters: matrix 256x192, slice thickness 8 mm, 2 mm gap, FOV 300x400, TR 2xRR interval, TE 2 ms). An inversion time (TI) scout was performed, in the mid short axis or 4-chamber slice position to identify the initial inversion time at which there was optimal nulling of the myocardium (typically 300 ms). Long-axis (2-, 3- and 4-chamber) as well as a full short-axis stack LV were acquired, copying the slice positions used in cine imaging (Figure 30). TI was altered by 10ms every 1-2 acquisitions. Any images showing enhancements of doubtful significance were repeated with the phase-encoding direction swapped or a slice planned through the region of enhancement, perpendicular to the current slice. If the patients were struggling with breath-holding, then single-shot images were acquired for the short-axis stack.

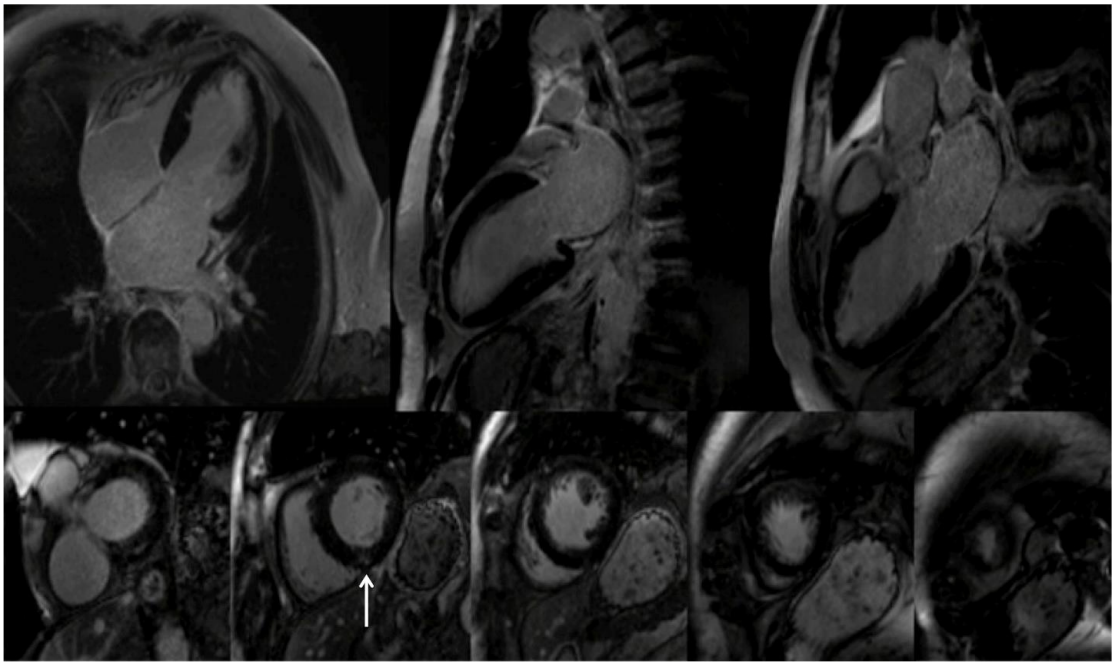

Figure 30. An example of LGE imaging showing long-axis (top panel) and short-axis (bottom panel) acquisitions, with inferior insertion point enhancement (white arrow).

2.4.6.6 Aortic cine and Phase Contrast Imaging

An SSFP cine (same parameters as cine imaging above) of the aorta at the pulmonary artery bifurcation level was acquired for calculation of aortic cross-sectional areas and distensibility. A retrospectively gated phase contrast velocity-encoded sequence was also performed at the same level, to calculate through-plane flow in the ascending and descending thoracic aorta in the transverse plane (typical parameters: matrix 256x176, VENC 250 cm/s, slice thickness 5 mm, reconstructed to 100-125 phases, TR 13 ms, TE 4 ms, flip angle 20°). A sagital oblique cine of the aortic arch was also acquired in order to calculate the pulse wave velocity (PWV) in this segment.

2.4.7 CMR Analysis

All CMR analysis was performed offline, blinded to the patient details, at the core lab, which was Leicester. I was responsible for the analysis of all CMR imaging.

2.4.7.1 LV Mass and Volumes

Analysis was performed on the short-axis cine stack using CMR 42 (Circle Cardiovascular Imaging, Canada) imaging software. LV epicardial and endocardial contours were manually drawn at end-diastole and end-systole (Figure 31), allowing

calculation of LV end-diastolic volume (LVEDV), LV end-systolic volume (LVESV), stroke volume (SV), LV ejection fraction (LVEF) and LV mass (LVM). Trabeculae and papillary muscles were included on the LV cavity measurement and excluded from LVM calculation, as this is the standard practice in our institution. This is because although inclusion of trabeculae in the LV cavity measurement can give higher volumes and lower mass, it has been shown to have higher inter-observer reproducibility and inter-examination repeatability than when they are excluded(143). LV mass/volume (LVM/LVEDV) ratio was calculated to estimate relative wall thickness. Values were also indexed to body surface area and denoted by the suffix 'I' for instance LVMI for left ventricular mass index.

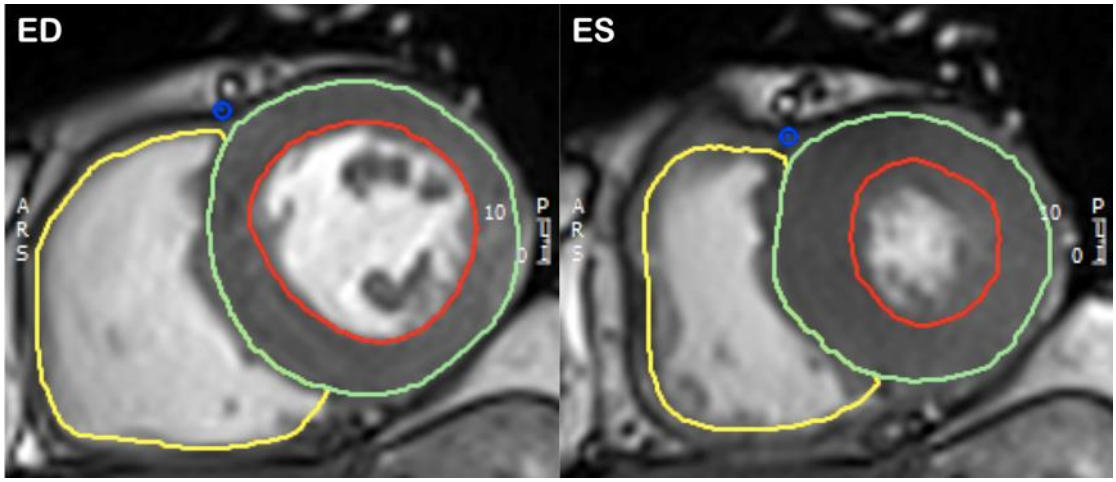

Figure 31. An example of epicardial (green), endocardial (red) and right ventricular (yellow) contours at end-diastole (ED) and end-systole (ES)

2.4.7.2 Left Atrial Volumes

LA volumes were manually contoured using CMR 42 (Circle Cardiovascular Imaging, Calgary, Alberta, Canada) software, and the volumes were indexed to body surface area giving the indexed LA volumes (LAVI).

2.4.7.3 Aortic Valve classification

The aortic valve cine images were used to quantify the AVA using planimetry, as well as to classify the valve morphology into a tri-leaflet or bicuspid (type 1-3) aortic valve(144)(Figure 32).

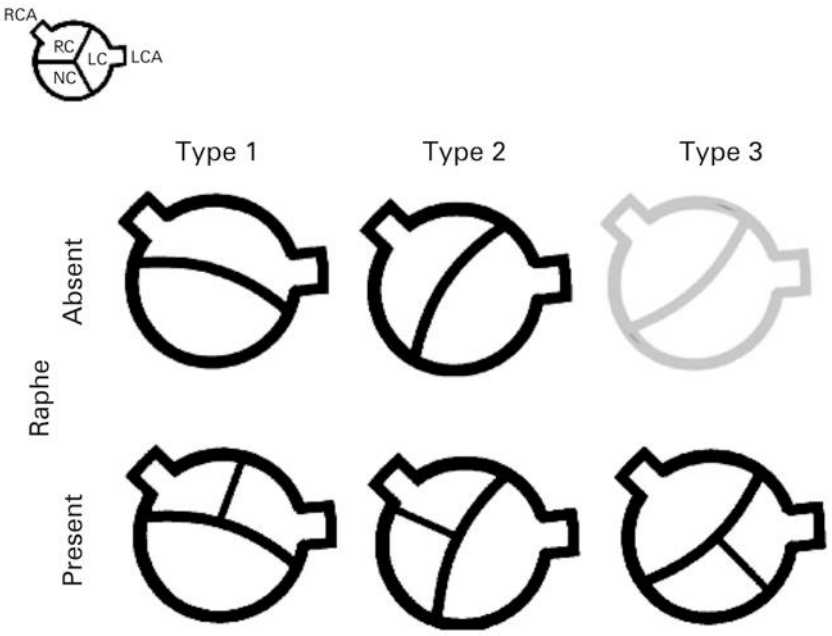

Figure 32. Classification of Aortic valve morphology. Top left: tri-leaflet valve. Bottom two rows: bicuspid valves ***(Type 1: fusion of RCC and LCC; Type 2: fusion of RCC and NCC; Type 3: fusion of LCC and NCC).*** **(144)**

(RCC = right coronary cusp, LCC = left coronary cusp, NCC = non-coronary cusp, RCA = right coronary artery, LCA = left coronary artery)

2.4.7.4 Myocardial Tissue Tagging

Tagged images were analysed using InTag (Creatis, Lyon, France), a plugin for the open source imaging software OsiriX (Pixmeo, Geneva, Switzerland). This software allows semi-automated quantification of myocardial motion following these steps: identification of the end-systole image, inputting tag spacing, manual tracing of the epicardial and endocardial borders (which is automatically propagated to all the phases) and indicating the anterior insertion point of the right ventricle. This was performed for each short-axis slice (base, mid and apex) to calculate the circumferential peak systolic strain (PSS), peak systolic strain rate (PSSR) and peak early diastolic strain rate (PEDSR) at each level, as well as globally (average of the three slices). Longitudinal strain and strain rates were calculated using the 4-chamber tagged sequence, with its analysis also requiring specification of the anterior and posterior mitral annulus and apex points.

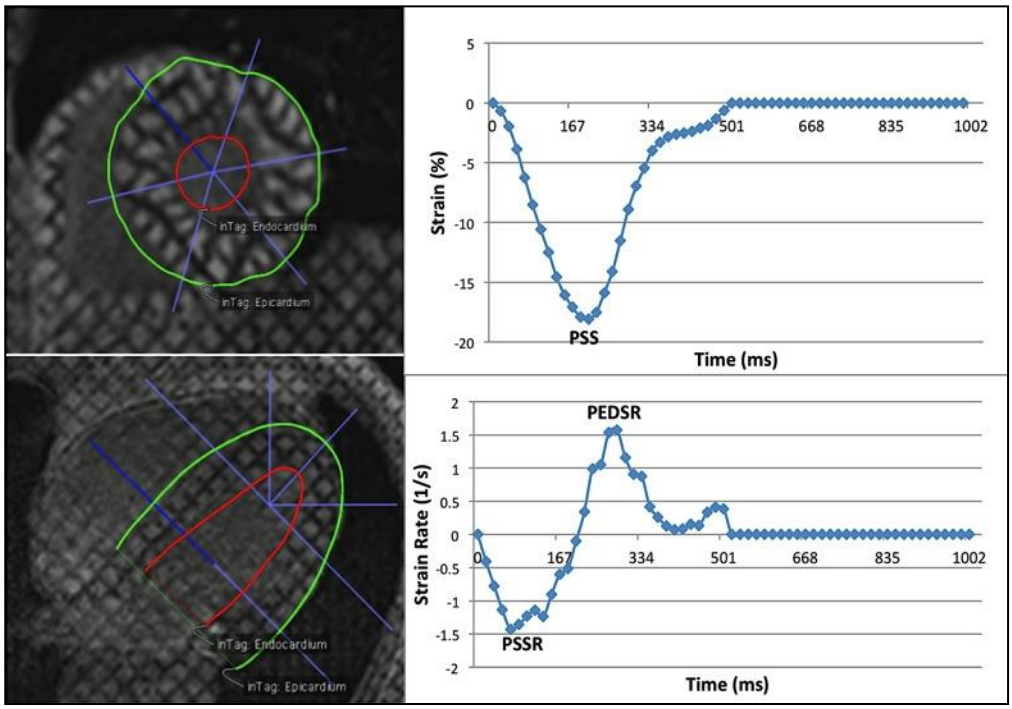

Figure 33. An example of the epicardial (green) and endocardial (red) contours on a short-axis and long-axis slice (left panel). Plot of strain and strain rate over time (right panel).

(PSS = peak systolic strain, PSSR = peak systolic strain rate, PEDSR = peak early diastolic strain rate)

The software generates output files containing data for circumferential (-C) and longitudinal (-L) strain. In order to obtain global strain values, the numerical data outputs were processed further using in-house Microsoft Excel spreadsheets (California, USA), to produce the average strain curves for each slice (Figure 33). Strain rates were calculated by dividing the difference between strains at consecutive time points by the time interval and plotting this against time.

2.4.7.5 Feature Tracking

Feature tracking (FT) is a relatively new technique for measuring strain and strain rates on CMR, that relies on automatic tracking of image features at the cavity-tissue interface of standard SSFP cine images, throughout the cardiac cycle, analogous to speckle tracking on echocardiography. Diogenes FT software (TomTec Imaging Systems, Munich, Germany) was used on the nearest slice from the short-axis cine stack corresponding to the tagged image slice position, representing the basal, mid and apical slices. Endocardial and epicardial contours were drawn on a single end-

diastolic phase and propagated automatically by the software to all phases, generating endocardial and epicardial strain and strain rate curves. If the contours did not track the borders well, the contour on the original phase was manually adjusted and re-propagated. No further post-processing was required, as the software generated both strain and strain rate graphs directly (Figure 34).

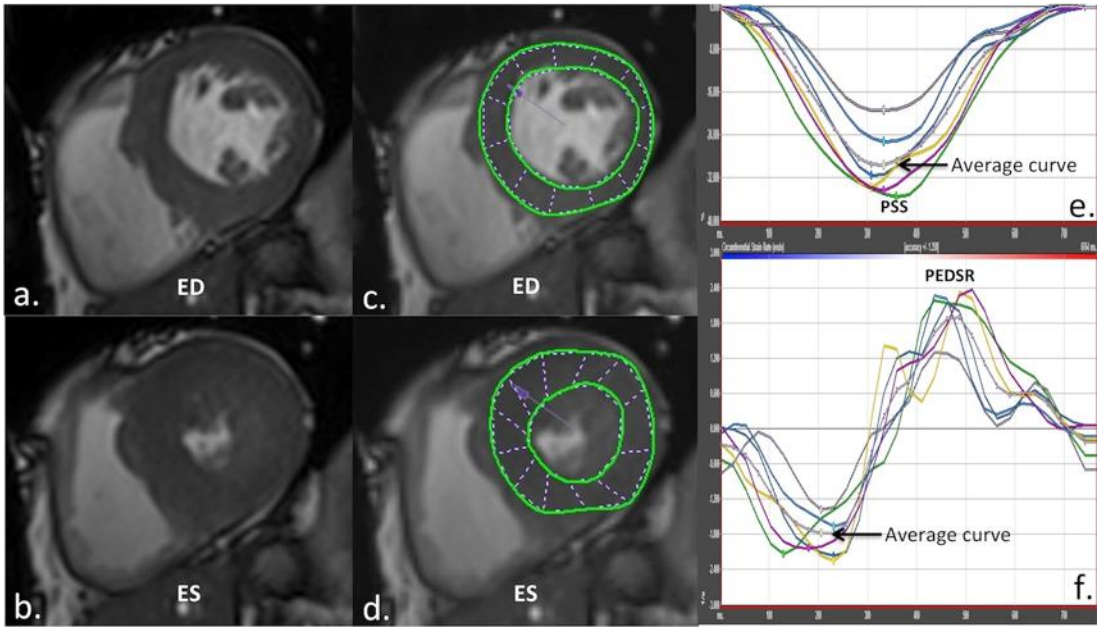

Figure 34. An example of feature tracking to generate typical strain and strain rate curves. a. SSFP cine image at end-diastole and b. end-systole, Epicardial and endocardial contours using FT software at c. end-diastole, and d. at end-systole, e. Circumferential strain curves and f. Circumferential strain rate curves generated by the FT software (segmental and average curves)

The **reproducibility** of strain analysis using both tagging and feature tracking was compared in ten patients, by calculating the inter- and intra-observer variability and test-retest repeatability of the two techniques, using Bland-Altman tests, before deciding on the technique to be used for the rest of the patients.

2.4.7.6 Perfusion Analysis

Perfusion analysis was performed using QMass v7.1 (Medis Medical Imaging Systems, Netherlands) imaging software. LV epicardial and endocardial contours as well as an LV blood pool region of interest were manually drawn, and propagated to all the phases of the perfusion sequence. The contours were then checked and manually moved / altered to ensure there was no cavity or pericardium within the defined

myocardial region and no papillary muscle within the LV cavity region of interest. The software produced signal intensity against time curves (Figure 35).

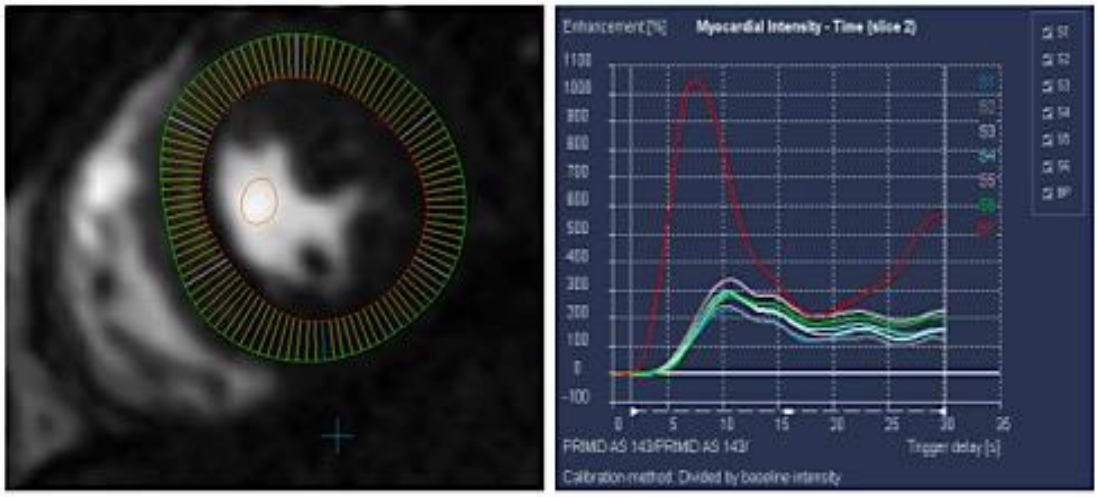

Figure 35. An example of epicardial (green), endocardial (red) and blood pool region of interest contours for perfusion analysis (left panel) and the associated graph of signal intensity against time in the blood pool (red) and myocardial segments (others) (right panel).

The result outputs were saved as text files and sent to Professor Michael Jerosch-Herold (Harvard Medical School, Boston, USA) for absolute myocardial blood flow (MBF) quantification. The measured arterial input, measured in arbitrary signal intensity units, was converted to a curve of percentage enhancement, by dividing by the baseline signal intensity in the blood pool before any contrast enhancement. A calibration curve of effective contrast enhancement versus the contrast enhancement extrapolated from the low R1 (contrast concentration) range was calculated by numerical simulation, using the sequence parameters, and a mean pre-contrast T1 value for blood of 1,450 ms. This calibration curve was then inverted, and used for correction of the observed % contrast enhancement in the blood pool. Saturation correction resulted in a 20-30% increase of the of the peak contrast enhancement of the arterial input function on average. The arterial input function, corrected for signal saturation, was used for MBF quantification by model-independent deconvolution(110). Transmural myocardial perfusion reserve (MPR) was calculated by dividing hyperaemic MBF by resting MBF.

In ten patients, this was done using the raw perfusion images as well as the MOCO images produced by using the software on the scanner. This was done to compare the inter- and intra-observer variability and test-retest repeatability using both techniques.

2.4.7.7 T1 mapping and ECV Calculation

Analysis was performed using CMR 42. LV epicardial and endocardial contours, as well as an LV blood pool region of interest (ROI), were manually drawn and propagated to all 11 images of the pre- and post-contrast MOCO MOLLI series (Figure 36). This generated average myocardial and blood pool, pre- and post-contrast T1 relaxation times. In addition, the parametric T1 map was also used to define the myocardial and blood pool ROIs to generate the T1 relaxation times, which was less time-consuming than propagating to the full MOLLI series. Both methods were used in ten patients by two observers, in order to compare the inter- and intra-observer variability and inter-technique agreement of the two methods. The test-retest repeatability was also calculated, in order to decide which method to utilise for the remainder of the patients.

The calculation of myocardial ECV requires the definition of regions of interest (ROI) for the myocardium and the blood pool, from which R1 (=1/T1) values are derived, which are used to calculate the partition coefficient (λ) and the ECV taking account of the blood Hct level(95) (Equation 7).

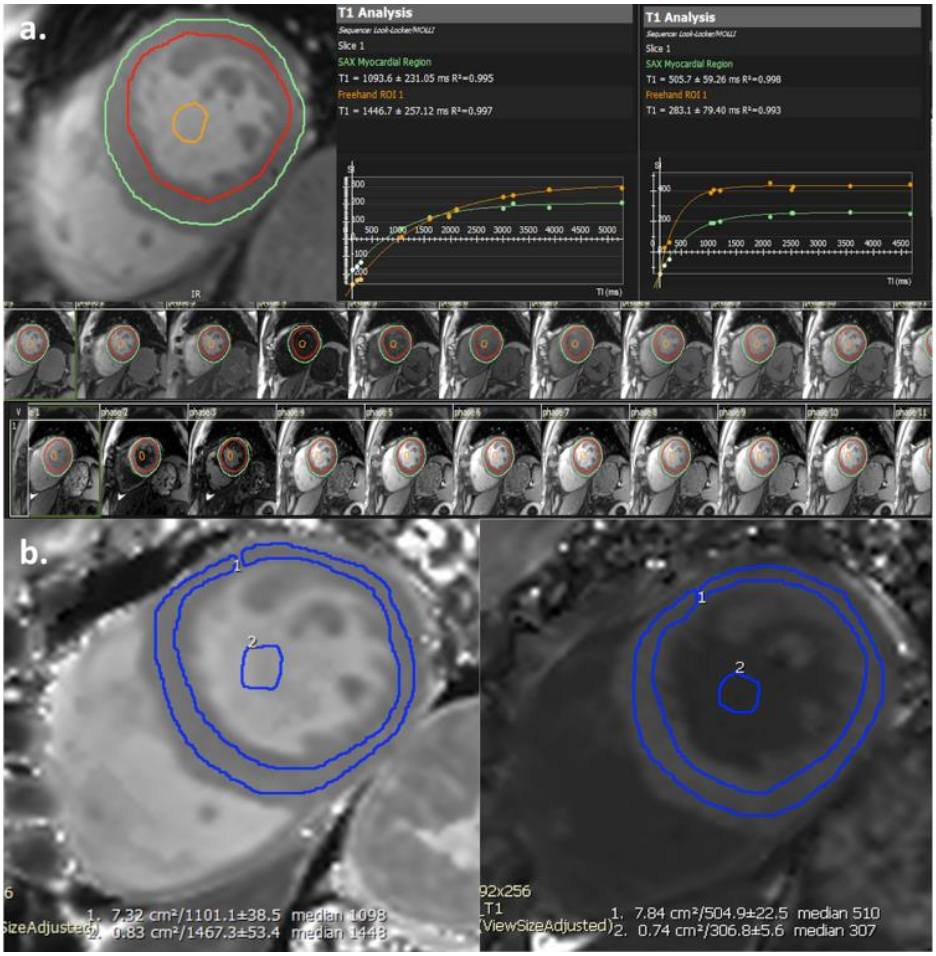

Figure 36. An example of outlining of the myocardial and blood pool regions of interest on a.) Full motion-corrected (MOCO) MOLLI series, with corresponding graphs showing the fitted relaxation curves produced pre- and post- contrast injection; and b.) T1 maps pre- (left) and post (right) contrast injection.

$$\lambda = \frac{\left(R1_{myo\ post} - R1_{myo\ pre}\right)}{\left(R1_{blood\ post} - R1_{blood\ pre}\right)} \qquad [1]$$

and

$$\mathrm{ECV} = \lambda\left(1 - \mathrm{hct}\right), \qquad [2]$$

Equation 7. Calculation of ECV

(λ = partition coefficient, R1 = reciprocal of T1, myo = myocardial, blood = blood pool, pre = pre-contrast, post = post-contrast, hct = haematocrit)

2.4.7.8 Late Gadolinium Enhancement

Two experienced observers visually assessed the LGE images for the presence or absence of focal fibrosis. This was qualitatively graded as infarct-pattern or non-infarct-pattern LGE, which was further categorised using a visual assessment scale (Table 7). Only grades 2 or above were considered significant, as subtle insertion point enhancement is a common non-specific finding, especially in the elderly.

Table 7. Visual assessment scale for non-infarct pattern LGE

Scale	Description
0	No enhancement
1	Subtle enhancement in 1 region within insertion point
2	Subtle enhancement in 1 region outside insertion point
3	Bright scar in 1 region
4	Clear scarring in multiple regions

Quantitative analysis was also performed using CMR 42 software. Epicardial and endocardial contours were traced on the short-axis LGE stack. A ROI was drawn in remote 'normal' looking myocardium on a single slice, and the percentage of LGE was automatically calculated as areas with signal intensity >5 standard deviation above the 'normal' ROI.

2.4.7.9 Aortic Distensibility and Pulse Wave Velocity

Ascending and descending maximum aortic cross-sectional areas were measured from the aortic cine at the pulmonary artery bifurcation level (Figure 37). Aortic distensibility was calculated using Equation 8.

$$\textbf{Distensibility} = (Amax - Amin) / (Amin \times PP)$$

Equation 8. Calculation of Aortic Distensibility in 10^{-3}mmHg^{-1}

(Amax = maximum aortic cross-sectional area in cm^2; Amin = minimum aortic cross-sectional area in cm^2; PP = pulse pressure (systolic BP- diastolic BP) in mmHg)

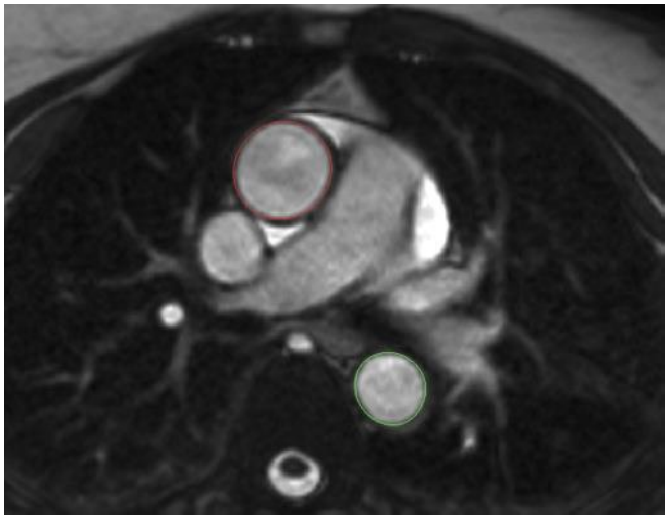

Figure 37. Single frame from an SSFP cine image of the ascending (red larger circle) and descending (green smaller circle) aorta, used for measurement of aortic dimensions and distensibility calculation

The PWV was assessed in the segment including the ascending aorta, the aortic arch and the proximal descending aorta up to the level of the pulmonary artery bifurcation (Figure 38), and calculated using Equation 9, where Δx is the distance around the aortic arch between the two sections through the ascending and descending aorta, and Δt is the transit time delay of two volume flow rate curves for the descending and ascending aorta. The sagittal oblique view of the aorta was used to measure the distance between the ascending and descending aorta (Δx), taking an average of the two distance measures for the outer and inner borders of the aortic lumen.

$$\mathbf{PWV} = \Delta x/\Delta t$$

Equation 9. Calculation of PWV

(PWV = pulse wave velocity in m/sec, Δx = distance around the arch in m; Δt = transit time delay of the volume flow rate curves for descending and ascending aortas in sec)

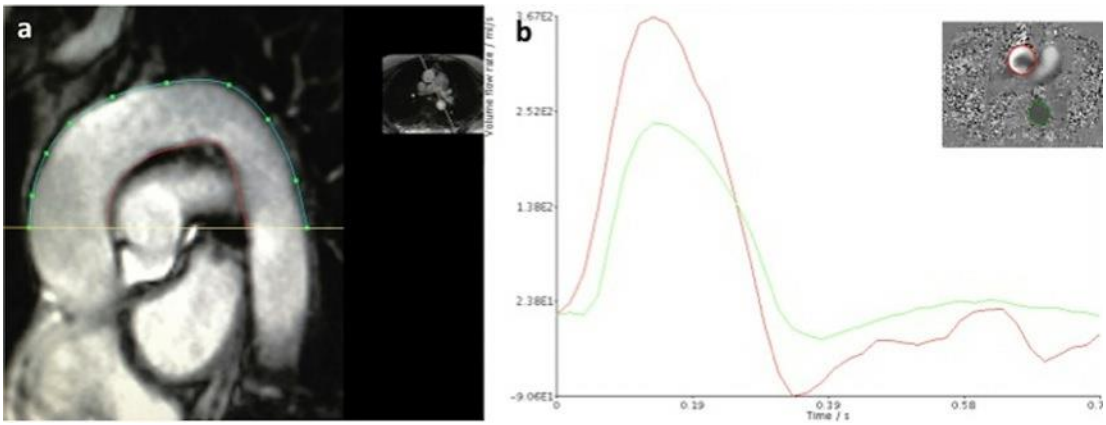

Figure 38. Pulse wave velocity calculation: a Sagittal oblique cine of the aorta for measurement of Δx (average of outer distance in green and inner distance in red), b. Aortic flow sequence used for calculation of Δt, i.e., the delay time between the volume flow rate curves (shown) in the ascending (red) and descending (green) aorta

An in-house software package was used to calculate Δt from the volume flow rate curves from the ascending and descending aorta. A maxium in the cross-correlation between these curves was used to find the transit time of the pressure wave around the arch.

2.4.8 CT Calcium Scoring

CT was performed on a multi-slice CT scanner with ECG gating, in a single breath-hold, for both AV and coronary artery calcium scoring. Coronary artery calcification was reported as present/absent and scored according to standard criteria. Results were not be fed back to clinicians given the lack of benefit of statins in patients with AS(76). We did consider CT coronary angiography but felt that the high radiation dose, administration of intravenous contrast and beta-blockers was not justified in patients who would not normally be investigated for coronary artery disease whilst asymptomatic.

2.5 Repeatability

Ten patients underwent a CMR twice within a week of their baseline visit, in order to calculate the test-retest repeatability of tagging, feature tracking, perfusion imaging and T1 mapping in patients with moderate to severe AS. All CMR analysis was done blinded to the patient and scan details.

2.6 Statistics

The statistical analysis plan for the Ranolazine sub-study is described in Chapter-4 (section 4.2.1). For the PRIMID-AS study and reproducibility, the statistical plan was as below.

2.6.1 Statistical Analysis: PRIMID-AS study

Baseline data was collected using electronic case-record forms under patients study ID's. All imaging data was blinded by the research nurse using unique TTE and CMR ID's generated by the CTU, and the images were placed in a folder for further analysis. All blinded CMR images were then analysed by myself, whilst the TTE images were analysed by a BSE-accredited Cardiac Physiologist (JM). The blinded imaging data were sent to the Robertson Centre for Biostatistics, University of Glasgow, for unblinding and statistical analysis for the main study. The interim statistical analysis for the Reproducibility Chapter was undertaken by myself using SPSS statistical package v20 (IBM, Chicago, USA), whilst the CTU performed the statistical analysis for the overall cohort for the Baseline, Determinants and Outcome chapters, after we developed a detailed statistical analysis plan together.

Normality was assessed using Kolmogorov-Smirnoff tests, histograms and Q-Q plots. Normally distributed data are expressed as mean±standard deviation. Non-parametric data are expressed as median (25%-75% interquartile range). Continuous variables were compared between patients and controls, and between patients with and without an outcome, using independent t-tests or Mann-Whitney tests, depending on the distribution. The Chi-squared test or Fisher's exact test, as appropriate were used to test for any differences for categorical variables.

For the **Reproducibility** Chapter, the method proposed by Bland and Altman(145), coefficient of variation (CoV) and two-way mixed-effect intra-class correlation coefficient (ICC) for absolute agreement(146) were used to assess inter-observer/intra-observer variability, test-retest repeatability and inter-technique agreement . In addition, paired t-tests were used to compare different analysis

techniques in patients, and independent t-tests were used to compare strain parameters between patient cohorts at 1.5T *vs*. 3T. Pearson's correlation coefficient was also used for assessment of correlation between techniques or scans.

Univariate **determinants** of MPR / MBF and exercise capacity (peak V_{O_2} and peak workload) were determined using regression analysis, and stepwise multivariate analysis was used to identify independent associations, after entering clinically and/or statistically significant univariate variables into the models.

Univariate and multivariate determinants of the primary and secondary **outcomes** were determined using Cox proportional hazards regression and stepwise selection. For multivariate analysis, sex was included in all models, in addition to: one measure of AS severity from echo, NT-proBNP, one CMR variable of LV remodeling, MPR and positive ETT. Kaplan-Meier curves were generated, using optimal cut-off for MPR, for event-free survival and compared using the log-rank test. The predictive accuracy of MPR and ETT for the primary outcome was assessed using logistic regressions and Receiver Operator Characteristic (ROC) analysis, with calculation of the area under the curves (AUC). The AUCs of MPR and ETT were compared using correlated ROC analysis. The MPR cut-point for predicting primary outcome was also selected to match the sensitivity of symptomatic CPET, and paired comparisons of the specificities of the two techniques were carried out using McNemar's Test. Additional sensitivity analyses were performed in patients with severe AS only.

2.6.2 Power Calculation

The study, with 170 subjects would have 80% power (binomial test) to show that MPR had superior overall accuracy (assumed 85%) to symptom-limited CPET, compared to the results of previous studies (76%) assuming an annual event rate of 29%(42).

CHAPTER THREE

3 REPRODUCIBILITY OF NOVEL CMR TECHNIQUES: OBSERVER VARIABILITY AND TEST- RETEST REPEATABILITY

Published:

Singh A, Steadman CD, Khan JN, Horsfield MA, Bekele S, Nazir SA, Kanagala P, Masca NG, Clarysse P, McCann GP. Intertechnique agreement and interstudy reproducibility of strain and diastolic strain rate at 1.5 and 3 Tesla: a comparison of feature-tracking and tagging in patients with aortic stenosis. J Magn Reson Imaging. 2015 Apr;41(4):1129-37

Singh A, Horsfield MA, Bekele S, Khan JN, Greiser A, McCann GP. Myocardial T1 and extracellular volume fraction measurement in asymptomatic patients with aortic stenosis: reproducibility and comparison with age-matched controls. Eur Heart J Cardiovasc Imaging. 2015 Jul;16(7):763-70

3.1 Introduction

It is important to establish the reproducibility of novel CMR techniques, which encompasses both the precision and reliability of the technique, before they can be widely applied to research and clinical settings. However, there is some confusion in the literature about the exact definitions of the various measures of 'variability', 'repeatability' and 'reproducibility'.

3.1.1 Definitions

Intra-observer variability is '*the amount one observer varies between observations when reporting more than once on the same material*'(147).

Inter-observer variability is '*the amount observers vary from one another when reporting on the same material'*(147).

Repeatability and reproducibility are components of precision of a measurement or technique.

Repeatability is defined as '*the closeness of agreement between independent results obtained with the same method on identical test material, under the same conditions (same operator, same apparatus, same laboratory and after short intervals of time)*'(148).

Reproducibility is defined as '*the closeness of agreement between independent results obtained with the same method on identical test material but under different conditions (different operators, different apparatus, different laboratories and/or after different intervals of time.'*(148).

3.1.2 Implications in cardiac imaging

In the case of cardiac imaging techniques, sources of variability can be introduced at multiple stages, including image acquisition (radiographer, protocol variability), image analysis (inter-observer, intra-observer variability, differences in post-processing techniques and software) as well as biological conditions related to the subjects

(diurnal variation, haemodynamic status). Test-retest repeatability assesses the whole of the data acquisition and analysis procedure, and good test-retest repeatability is particularly important when monitoring treatment effect or disease progression in longitudinal studies. The reproducibility of novel imaging techniques is often assessed in healthy volunteers but rarely in patient groups. It is important to assess test-retest repeatability of novel imaging techniques in disease groups as well as healthy controls, as there can be small differences in values between normal and abnormal, and the robustness of the technique at identifying the abnormal, as well as for serial assessment of patients relies on good reproducibility. We therefore sought to assess the reproducibility of novel CMR techniques in asymptomatic patients with AS.

3.2 Participants

The demographics for the original 10 patients who formed the 'repeatability cohort' (completed 2 scans within a week) are shown in Table 8. Due to an error with pump set-up for the first repeatability patient, an inaccurate contrast injection protocol was used during stress perfusion, and this patient was therefore excluded from the MPR repeatability analysis. An additional repeatability patient was recruited at a later date to make up the ten patients for this purpose.

Table 8. Demographic data for the original repeatability cohort

Parameter	**Value:** mean (std dev) or n(%)
Age (years)	67.3 ± 9.0
Gender (M)	8 (80%)
AV Vmax (m/s)	4.01 ± 0.70
PPG (mmHg)	66.2 ± 24.3
MPG (mmHg)	40.7 ± 17.1
AVA (TTE) (cm^2)	0.97 ± 0.29
AVA (CMR) (cm^2)	1.01 ± 0.14
SBP (mmHg)	155.3 ± 22.6
HR (bpm)	72.0 ± 8.6
HTN	4 (40%)
DM	1 (10%)
Hyperlipidaemia	1 (10%)
CAD	0 (0%)
ACEI/ARB	1 (10%)
Statin	6 (60%)
Beta-blocker	4 (40%)
Ca-channel blocker	1 (10%)
Aspirin / Clopidogrel	2 (20%)
Other anti-hypertensive	2 (20%)
Other cardiac meds	2 (20%)

Abbreviations: AVA = aortic valve area, AV Vmax = peak velocity across aortic valve, bpm = beats per minute, CAD = coronay artery disease, HR = heart rate, MPG = mean pressure gradient, PPG = peak pressure gradient, SBP = systolic blood pressure.

3.3 Reproducibility of myocardial deformation: a comparison between Tagging and FT at 1.5T and 3T

Myocardial tissue tagging requires acquisition of additional tagged sequences and time-consuming post-processing during analysis(149, 150). FT utilises the standard SSFP cine images acquired for functional analysis, and is also less time-consuming to analyse. FT has been compared to tagging in a large population of patients with Duchenne Muscular Dystrophy and healthy controls, showing high correlations with tagging for circumferential strain without significant bias(151). FT has also been shown to have good inter- and intra-observer variability in healthy volunteers(152) and patient groups(151, 153), as well as reasonable test-retest repeatability (coefficient of variation (CoV) ~20%) in healthy volunteers, when studied on the same day(154). The test-retest repeatability of FT had not been reported in any patient groups, nor compared to that of tagging.

In order to compare the repeatability of the two techniques available for myocardial deformation assessment at 3T and 1.5T field strengths, our cohort of 10 repeatability patients at 3T (median interval of 7 days) were compared to 8 previously recruited patients with AS, who had had two scans on a 1.5T scanner (median interval of 12 days).

3.3.1 Image acquisition and analysis

The methodology of image acquisition and analysis is as outlined in the Methods chapter (section 2.4.6 onwards). Tagged images were acquired using spatial modulation of magnetization (SPAMM) at 3T and complementary SPAMM (CSPAMM) at 1.5T (slice thickness 6mm, grid tag spacing 7 mm, TR 4.7ms, TE 2.3ms, flip angle 12°, temporal resolution 42ms, prospective gating). In addition to three short-axis slices (base, mid and apex), a 4-chamber tagged image was also acquired at 3T only. Identical parameters were used at scan-1 and 2. Analysis was performed offline, blinded to patient details and whether it was the first or second scan.

Circumferential peak systolic strain (PSS-C) and peak early diastolic strain rate (PEDSR-C) were calculated for each short-axis slice and globally (average of base, mid, apex). Global longitudinal PSS (PSS-L) and PEDSR (PEDSR-L) were calculated using an average of 4-, 3- and 2-chamber cine images using FT, and compared to the 4-chamber tagged image at 3T. For inter-observer variability, two observers performed FT and tagging analysis on a sample of five patients from 1.5T and five from the 3T cohort, using a mixture of scans from visit one and visit two. For scan-1, FT results from the endocardial contour only, as well as an average of the epicardial and endocardial values, were examined. For test-retest repeatability, only the average of epicardial and endocardial values was used.

3.3.2 Demographic data

Table 9. Comparison of the repeatability cohort at 1.5T and 3T

Variable	1.5 T group (n=8)	3T group (n=10)
Age (years)	66.6 (8.3)	67.3 (9.0)
Male (n, (%))	6 (75%)	8 (80%)
SBP (mmHg)	130.8 (5.9)*	155.2 (22.6)
DBP (mmHg)	75.4 (10.6)	77.6 (11.0)
Echo		
PPG (mmHg)	77.3 (11.8)	66.2 (24.3)
MPG (mmHg)	47.0 (6.0)	40.7 (17.1)
CMR		
AVA (cm^2)	0.71 (0.19)*	1.01 (0.14)
LVEDVI (ml/m^2)	101.8 (20.8)*	82.9 (15.8)
LVMI (g/m^2)	73.4 (15.7)*	58.6 (7.8)
LVEF (%)	54.4 (4.1)*	59.1 (4.2)

Result are mean (standard deviation) values. Abbreviations: SBP: systolic blood pressure, DBP: diastolic blood pressure, PPG: peak pressure gradient, MPG: mean pressure gradient, AVA: aortic valve area, CMR: cardiac magnetic resonance imaging, LVEDVI: left ventricular end-diastolic volume indexed, LVMI: left ventricular mass indexed, LVEF: left ventricular ejection fraction.
*Significant difference on independent t-test ($p<0.05$).

Demographics of the subjects are presented in Table 9. The patients studied at 1.5T had more severe AS, greater left ventricular volumes and mass, and slightly lower ejection fraction than those studied at 3T.

3.3.3 Analysis duration

The average time taken to analyse a patient's full data set was 25 minutes using FT, and 30 minutes using tagging. However, an additional 20 minutes per patient was required for post-processing to extract average PSS and PEDSR values from the tagging dataset, so that the total time for tagging analysis was approximately double that required for FT.

3.3.4 Reproducibility of Circumferential PSS and PEDSR

3.3.4.1 Inter-technique agreement

FT using the endocardial contours alone resulted in significantly higher global PSS-C and PEDSR-C values than both tagging and FT with average of endocardial and epicardial values, at both field strengths (Table 10). FT using an average of endocardial and epicardial values resulted in values much closer to those obtained from tagging, although they remained significantly higher for all measures except PEDSR-C at 1.5T (95% CI -0.63 to 0.07, p = 0.10).

Table 10. Global circumferential strain and strain rate values for Tagging and Feature Tracking using endocardial only and average of endocardial and epicardial values

Field Strength	Parameter	Tagging	FT (Endo only)	FT (Epi/Endo average)
1.5T	**PSS-C**	-17.02 ± 3.42*†	-28.68 ± 3.39†	-20.95 ± 1.89
	PEDSR-C	1.01 ± 0.31*	1.78 ± 0.54†	1.29 ± 0.34
3T	**PSS-C**	-17.74 ± 3.02*†	-30.18 ± 5.63†	-21.35 ± 3.95
	PEDSR-C	0.84 ± 0.28*†	1.93 ± 0.55†	1.33 ± 0.38

Results for baseline scan displayed. Abbreviations: FT: Feature Tracking, PSS: peak systolic strain, PEDSR: peak early diastolic strain rate, Endo: Endocardial contour, Epi/Endo: Average of endocardial and epicardial contours. * Statistically significant difference compared to FT (endo only) ($p<0.05$), † Statistically significant difference compared to FT (epi+endo average) ($p<0.05$).

Agreement between FT and tagging for global circumferential values was poor at 1.5T, with non-significant correlations, very wide limits of agreement using BA tests and significant bias for FT giving higher values (Table 11). At 3T the agreement tended to be better, with higher correlations, but the values remained significantly higher with FT and the limits of agreement remained wide.

3.3.4.2 Inter-observer variability

The inter-observer variability of PSS-C and PEDSR-C using both tagging and FT at both field strengths was good. CoV's for PSS-C/PEDSR-C were 4.3%/6.1% for FT at 1.5T; 4.1%/6.2% for FT at 3T; 4.4%/3.7% for tagging at 1.5T and 5.2%/5.8% for tagging at 3T. (Intra-observer variability was not assessed separately, as test-retest repeatability was performed by the same observer, and therefore encompasses this in its assessment.)

3.3.4.3 Test-retest repeatability

The test-retest repeatability results are shown in Table 12 and the corresponding Bland-Altman plots in Figure 39. There were no significant differences in PSS-C or PEDSR-C between scan one and scan two, for either tagging or FT and at 1.5T or 3T. The test-retest repeatability of global PSS-C and PEDSR-C were better with FT compared to tagging at both 1.5T and 3T, with narrower limits of agreement on Bland-Altman plots and lower CoVs. When the apical slice was excluded, repeatability of PSS-C and PEDSR-C were similar for FT and tagging at 1.5T. However at 3T, although repeatability of PSS-C was good for both techniques, it was better for FT. repeatability of PEDSR-C at 3T was moderate to poor with both techniques, with no improvement after apical slice exclusion.

Table 11. Inter-technique agreement between Tagging and FT: Comparison of global and regional Circumferential strain and strain rates at 1.5T and 3T

Parameter	Region	Tagging average value (Mean ± SD)	FT Average value (Mean ± SD)	Paired Mean difference (SD) (Tagging-FT)	BA Limits of agreement	ICC	CoV%
1.5 Tesla Field Strength							
PSS-C	**Global**	**-17.02 ± 3.42***	**-20.95 ± 1.89**	**3.93 (4.01)**	**-3.92 to 11.78**	**-0.06**	**21.1**
	Basal	-17.82 ± 3.83	-18.48 ± 1.29	0.66 (4.32)	-7.80 to 9.12	-0.38	23.8
	Mid	-18.13 ± 3.39	-19.20 ± 3.47	1.08 (4.22)	-7.20 to 9.35	0.40	22.6
	Apical	-15.11 ± 4.77*	-25.16 ± 2.63	10.05 (6.53)	-2.75 to 22.85	-0.23	32.4
PEDSR-C	**Global**	**1.01 ± 0.31**	**1.29 ± 0.34**	**-0.28 (0.42)**	**-1.10 to 0.54**	**0.23**	**36.5**
	Basal	0.92 ± 0.32	1.04 ± 0.23	-0.11 (0.35)	-0.80 to 0.57	0.32	35.6
	Mid	0.98 ± 0.32	1.14 ± 0.38	-0.15 (0.40)	-0.93 to 0.63	0.53	37.5
	Apical	1.12 ± 0.46*	1.69 ± 0.59	-0.57 (0.65)	-1.84 to 0.70	0.30	45.9
3 Tesla Field Strength							
PSS-C	**Global**	**-17.74 ± 3.02***	**-21.35 ± 3.95**	**3.61 (3.37)**	**-2.99 to 10.22**	**0.54**	**17.2**
	Basal	-18.19 ± 3.39	-20.00 ± 2.76	1.81 (2.90)	-3.88 to 7.50	0.66	15.2
	Mid	-19.05 ± 4.71	-20.93 ± 5.43	1.88 (4.64)	-7.22 to 10.97	0.73	23.2
	Apical	-15.96 ± 2.88*	-23.12 ± 4.75	7.15 (4.68)	-2.01 to 16.32	0.20	23.9
PEDSR-C	**Global**	**0.84 ± 0.28***	**1.33 ± 0.38**	**-0.49 (0.31)**	**-1.09 to 0.11**	**0.44**	**28.4**
	Basal	0.84 ± 0.35*	1.16 ± 0.29	-0.32 (0.20)	-0.70 to 0.07	0.71	19.7
	Mid	0.81 ± 0.37*	1.21 ± 0.45	-0.40 (0.46)	-1.29 to 0.50	0.43	45.3
	Apical	0.87 ± 0.34*	1.63 ± 0.51	-0.76 (0.44)	-1.63 to 0.11	0.32	35.6

Abbreviations: as Table 10. BA=Bland-Altman. Average of epicardial and endocardial contours used for FT. *significant difference compared to FT value ($p<0.05$). Paired mean differences and limits of agreement are using Bland-Altman technique.

Table 12. Test-retest repeatability of Circumferential strain and strain rate using Tagging and FT on 1.5T and 3T

Technique	Parameter	Region	Average value†	Paired Mean difference (SD)	BA Limits of agreement	R	CoV
1.5 Tesla Field Strength							
Tagging	**PSS-C**	Global	-16.86 ± 2.78	-0.33 (2.20)	-4.64 to 3.98	0.78*****	**13.0**
		Basal/Mid	-17.68 ± 2.82	-0.59 (1.75)	-4.02 to 2.84	0.89*****	**9.9**
	PEDSR-C	Global	1.00 ± 0.31	0.02 (0.19)	-0.35 to 0.38	0.82*****	**18.8**
		Basal/Mid	0.94 ± 0.28	0.04 (0.12)	-0.19 to 0.27	0.92*****	**12.5**
FT	**PSS-C**	Global	-20.88 ± 2.26	-0.14 (1.93)	-3.93 to 3.64	0.70	**9.2**
		Basal/Mid	-18.62 ± 2.23	-0.44 (1.82)	-4.00 to 3.12	0.69	**9.8**
	PEDSR-C	Global	1.24 ± 0.31	0.11 (0.17)	-0.23 to 0.45	0.86*****	**14.0**
		Basal/Mid	1.04 ± 0.22	0.10 (0.12)	-0.14 to 0.34	0.88*****	**11.9**
3 Tesla Field Strength							
Tagging	**PSS-C**	Global	-17.59 ± 2.86	-0.30 (3.31)	-6.79 to 6.20	0.36	**18.9**
		Basal/Mid	-18.51 ± 3.16	-0.23 (3.19)	-6.49 to 6.03	0.54	**17.3**
	PEDSR-C	Global	0.82 ± 0.26	0.05 (0.28)	-0.50 to 0.60	0.46	**34.3**
		Basal/Mid	0.79 ± 0.24	0.07 (0.27)	-0.47 to 0.61	0.49	**34.6**
FT	**PSS-C**	Global	-20.94 ± 3.43	-0.82 (2.07)	-4.88 to 3.25	0.86*	**9.9**
		Basal/Mid	-20.06 ± 3.37	-0.80 (2.49)	-5.68 to 4.08	0.78*	**12.4**
	PEDSR-C	Global	1.23 ± 0.37	0.20 (0.32)	-0.43 to 0.82	0.61	**25.9**
		Basal/Mid	1.10 ± 0.34	0.17 (0.32)	-0.46 to 0.80	0.54	**29.3**

Abbreviations: as Table 10, BA=Bland-Altman, R on Pearson's correlation, CoV=Coefficient of variation. Average of epicardial and endocardial contours used for FT. **No significant difference between scan-1 and scan-2 values on paired sample t-test**; *Statistically significant correlation ($p<0.05$), †Average of all values from scan 1 and 2.

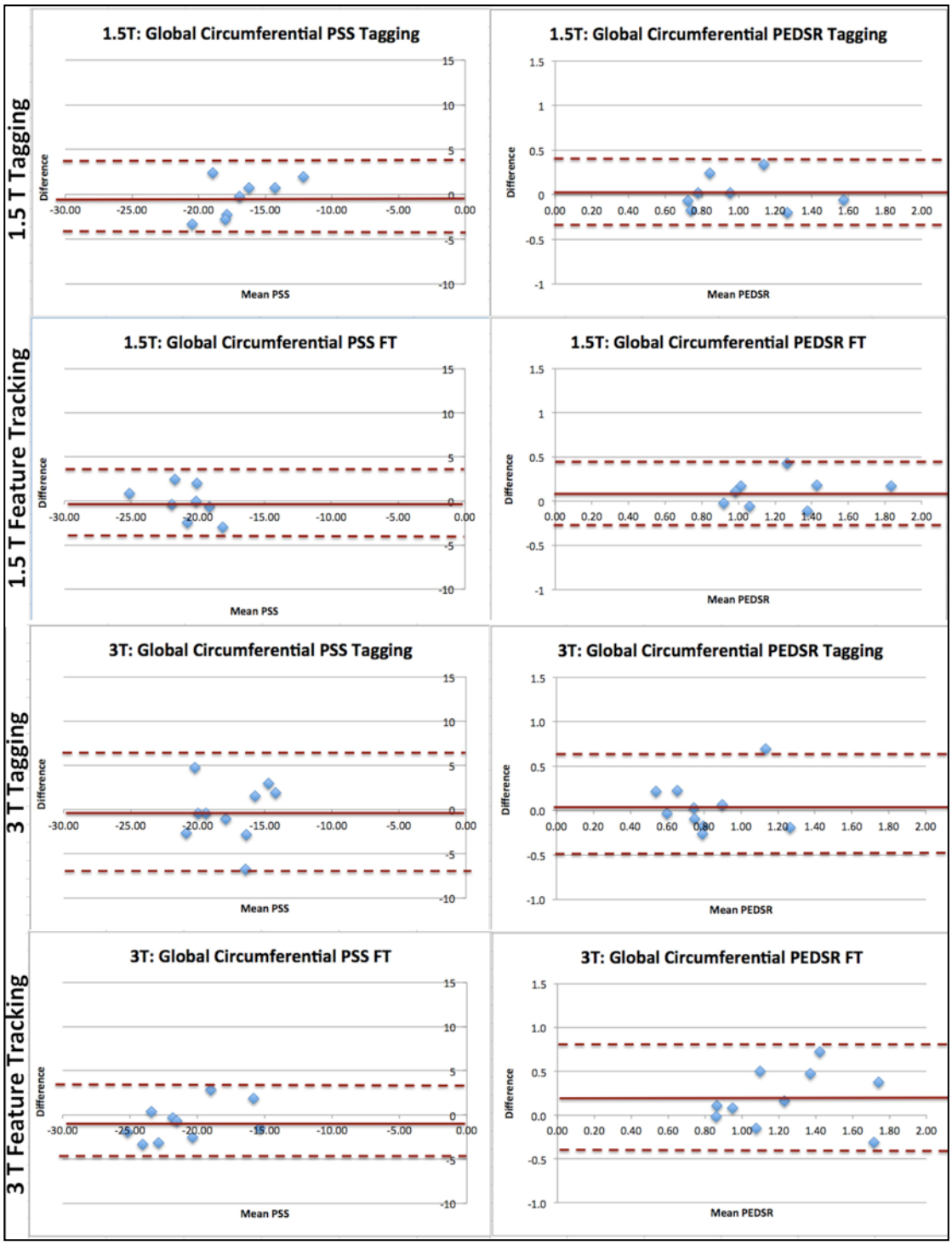

Figure 39. Bland-Altman plots for test-retest repeatability of Global Circumferential PSS and PEDSR, using tagging and Feature Tracking at 1.5T and 3T

3.3.5 Reproducibility of longitudinal PSS and PEDSR

3.3.5.1 Inter-technique agreement

The inter-technique agreement of longitudinal strain and strain rates was only available at 3T, as longitudinal tagging was not acquired at 1.5T. Agreement was moderate at 3T, with CoV of 22.9% and 29.9% for PSS-L and PEDSR-L respectively, with significantly higher values with FT compared to tagging. Agreement was similar for PSS-L when only 4C was used for FT, but worse for PEDSR-L.

3.3.5.2 Inter-observer variability

The inter-observer variability of PSS-L and PEDSR-L was better with FT (CoV's 8.4%/10.5% at 1.5T and 5.8%/11.8% at 3T) than tagging at 3T (CoV 15.1% for PSS-L, 24.1% for PEDSR-L).

3.3.5.3 Test-retest repeatability

Results are displayed in Table 13 and Figure 40. There was no significant difference in the longitudinal strain and strain rate values between scan one and scan two using either technique. Using Bland-Altman analysis, the test-retest repeatability of PSS-L was good with FT at 1.5T and 3T and moderate with tagging at 3T. Repeatability of PEDSR-L was moderate to poor, and similar for tagging and FT. It was similar for PSS-L when only 4C was used for FT, but worse for PEDSR-L.

Table 13. Test-retest repeatability of Longitudinal strain and strain rates on 1.5T and 3T scanner field strengths

Technique	Parameter	Average value	Paired Mean difference (SD)	Limits of agreement	R (Pearson's Correlation)	CoV
1.5 Tesla Field Strength						
FT	**PSS-L**	-16.72 ± 2.25	-0.64 (1.73)	-4.03 to 2.75	0.72*	**10.4**
	PEDSR-L	1.03 ± 0.24	0.05 (0.35)	-0.63 to 0.72	0.06	**33.8**
3 Tesla Field Strength						
FT	**PSS-L**	-16.47 ± 3.07	0.39 (2.69)	-4.88 to 5.65	0.64*	**16.3**
	PEDSR-L	0.94 ± 0.24	0.14 (0.28)	-0.41 to 0.70	0.29	**30.1**
Tagging	**PSS-L**	-11.05 ± 3.10	0.69 (2.49)	-4.20 to 5.58	0.69*	**22.6**
	PEDSR-L	0.66 ± 0.18	0.00 (0.19)	-0.37 to 0.38	0.49	**28.9**

Abbreviations: as Table 10, L: longitudinal. Average of epicardial and endocardial contours used for FT. **No significant difference between scan-1 and scan-2 values on paired sample t-test (p>0.05)**; *Statistically significant correlation (p<0.05).

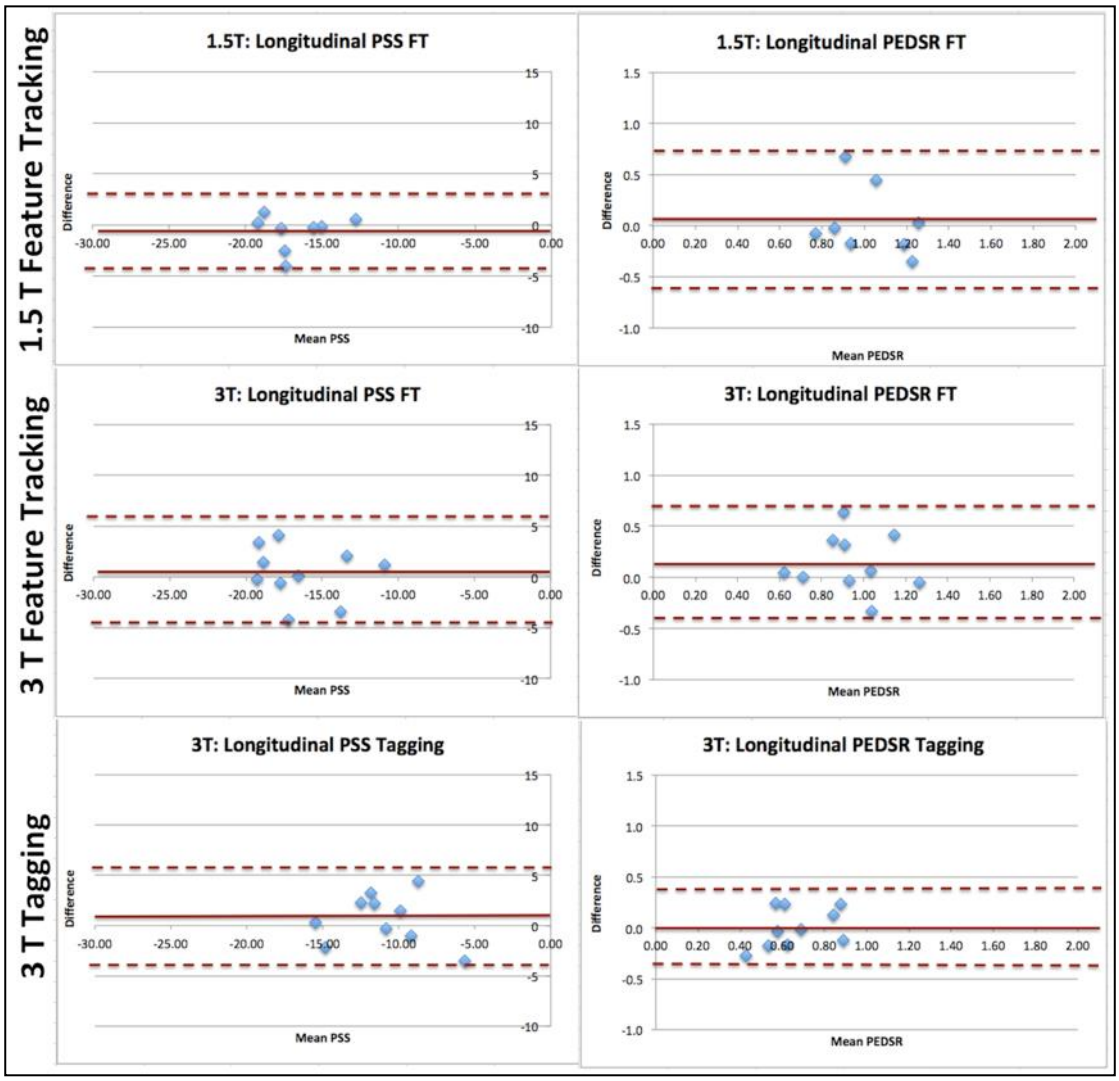

Figure 40. Bland-Altman plots for test-retest repeatability of Longitudinal PSS and PEDSR, using tagging and Feature Tracking at 1.5T and 3T. (Note- longitudinal tagging not done at 1.5T)

3.3.6 Discussion

FT derived strain values were higher in comparison to tagging. This was regardless of field strength and whether only endocardial, or both endocardial and epicardial contours were used for FT. This has been noted previously for longitudinal and radial strains in healthy volunteers(155), and for regional circumferential PSS in septal, anterolateral and inferior segments in patients with hypertrophic cardiomyopathy(156).

The higher strain values with FT compared to tagging in our patients are in contrast to those reported in patients with Duchene Muscular Dystrophy(151), which suggested good agreement for PSS between the techniques. However, strain was only measured on a single mid-ventricular slice, using harmonic phase (HARP), which is consistent with our regional results that showed no significant differences in the mid slice and worse agreement at the apex. It is unlikely that the different tagging quantitative software used in that study alone would explain the difference, since strain measurements using InTag and HARP have been shown to have good agreement(149). The poor agreement for apical slices is likely to be secondary to poor tracking associated with LVH in AS, leading to near cavity obliteration, loss of tags and partial volume effects, especially if the slice is planned too apically.

Agreement of global and regional strain tended to be better at 3T than 1.5T, though a positive bias remained for FT. There have been no studies that have compared agreement between FT and tagging at different field strengths. The intra-observer variability of FT in healthy volunteers was found to be slightly better at 3T compared to 1.5T, for circumferential PSS (CoV 13.3% *vs.* 17.2%)(157). The slightly better agreement at 3T may be related to increased signal to noise at the higher field strength. Although 3T imaging results in longer T1 values leading to intrinsically better tag persistence(158) it is unlikely to explain the better agreement in this study, since at 1.5T a CSPAMM sequence was used, which gives better tag persistence than SPAMM(159).

Other work from our group has also shown that endocardial-only contouring for FT is quicker to analyse in patients with myocardial infarction, and correlated significantly with infarct size, segmental area at risk and myocardial salvage index(150). In addition, given that it is primarily subedocardial myocardial dysfunction that is affected in AS, we decided to use the endocardial contours for further assessment of myocardial deformation using FT.

Our results in AS patients show that FT and tagging strain measures are not interchangeable. This is irrespective of whether regional or global strain values are obtained and independent of field strength. Values obtained with the average of endocardial and epicardial contours on FT are considerably lower, and closer to those obtained by tagging, than with endocardial contouring only.

The test-retest repeatability of FT PSS was excellent, particularly at 1.5T, and comparable to that of tagging. In a study of healthy volunteers, circumferential PSS using FT at mid-level was the most reproducible, with a CoV of 20.3%, with a CoV of 26.4% for longitudinal strain(154). This compares to CoV's of 9-12% in our cohort of patients studied 7-12 days apart. AS patients are characterised by pressure overload leading to LVH(13) and the resultant increase in wall thickness could account for the better repeatability of FT due to reduced partial volume effects. Additionally, differences in the pulse sequences between scanner manufacturers, and in image quality, are likely to have an important bearing on analysis with FT.

The test-retest repeatability of all circumferential parameters on both tagging and FT tended to be higher at 1.5T compared to 3T. Although the image quality was generally good at both field strengths the greater incidence of minor artefacts due to field inhomogeneity at 3T leading is likely to lead to poorer tracking. In addition, we choose a SPAMM sequence at 3T for tagging to minimise off-resonance artefacts but this may not perform as well as the CSPAMM sequence used at 1.5T(159, 160).

Prior to our study, there had only been one previous report assessing the test-retest repeatability of tagging (CSPAMM), which demonstrated lower CoV's of 4.8-5.5% for PSS in 12 healthy volunteers at 1.5T(161) than our results in AS patients. These findings indicate the importance of using the appropriate standard deviation of the patient population under investigation for calculation of sample sizes for prospective trials, to avoid underestimation, or indeed overestimation of, the required sample size for FT(154).

Diastolic function is difficult to assess on MRI, and this is one of the major limitations compared to echocardiography. AS is characterised by LVH, myocardial fibrosis and abnormalities of diastolic function. PEDSR is a load independent measure of myocardial relaxation(162). The repeatability of global circumferential PEDSR was good at 1.5T, particularly when apical slices were excluded, for both FT and tagging (CoV~12%), but relatively poor at 3T and for longitudinal strain.

3.3.7 Limitations

The number of patients studied was small, but it is rare for true test-retest repeatability to be reported in patient groups. We have only assessed repeatability of the circumferential and longitudinal strain parameters since these appear to have the best observer variability. We have quantified tagging using open source software and the results may not apply to other available software packages. Since different patients were studied at 1.5T and 3T, and there was a difference in the pulse sequence used (CSPAMM at 1.5T and SPAMM at 3T), this was not a pure comparison between field strengths, and some of the variation in our results may be due to differences in the patient populations. Furthermore, longitudinal strain was not measured using tagging at 1.5T, which limits our inter-technique comparison of longitudinal strain. The results may not be generalizable to other pulse sequences, scanner manufacturers or other patient groups.

3.3.8 Conclusions

In conclusion, PSS and PEDSR values derived using FT are higher than those using tagging, with the differences being most marked in apical slices. The test-retest repeatability of circumferential PSS is excellent using FT and good using tagging at 1.5T and 3T. The repeatability of circumferential PEDSR assessed by FT and tagging at 1.5T is good when only basal and mid slices are used but moderate to poor at 3T. Tagging appears to offer no significant advantages over FT for the assessment of strain and diastolic strain rate in patients with AS.

3.3.9 Implications for this thesis

Given that FT can be used to calculate strain and strain rate directly from standard cine images, without lengthy post-processing, and its reproducibility is at least as good as that of tagging, I decided to use FT for further assessment of myocardial deformation as part of this thesis. I also chose to use the endocardial-only contours for further assessment in AS for reasons mentioned above. Based on these findings, in future studies where the primary outcome relates to the assessment of circumferential PEDSR, measurement at basal and mid slices at 1.5T would be recommended. However, for the PRIMID-AS study, the primary measure of interest was MPR and therefore the study was conducted at 3T, as there is higher signal to noise at 3T and it is therefore thought to be better for MBF and MPR assessment.

3.4 Reproducibility of T1 mapping using MOLLI at 3T: parametric map *vs.* full MOLLI series of images

3.4.1 Background

The most widely-used technique for myocardial T1 quantification is the Modified Look-Locker Inversion Recovery (MOLLI) sequence(141). While the inter- and intra-observer variability of ECV measurement has consistently been shown to be excellent, there is scarce data assessing test-retest repeatability, especially in patient groups. True test-retest repeatability of ECV has mainly been assessed in healthy volunteers with no co-morbidities(100, 163, 164). Previous studies have employed various methods of defining the myocardial regions of interest (ROIs) to obtain average myocardial T1 values, including outlining the epicardial and endocardial borders on the full series of images with multiple inversion times produced by the scanner(94, 96), as well as outlining on a single T1 parametric maps(97, 100, 164) or R1(95) maps produced by the scanner or in-house software. Analysing a single T1 map generated inline on the scanner has the advantage of being less time-consuming and may be less prone to variation than analysing the full MOLLI series (typically 11 images). No previous study had directly compared these two techniques.

I sought to assess the test-retest repeatability, inter-observer and intra-observer variability of T1 quantification and ECV measurement using MOLLI at 3T, by outlining the myocardium on the T1 maps generated inline after motion correction as well as each of the 11 images in the MOLLI series.

3.4.2 Image acquisition and analysis

As described in the Methods chapter (section 2.4.6.4), T1 data was acquired using the MOLLI sequence(141), at the mid short-axis level pre- and ~15 minutes post contrast. Blood was taken to determine the Hct level. Identical parameters were used on the scan-1 and 2.

Mean blood and myocardial T1 values were obtained from the parametric maps of mean T1 value produced by the scanner, as well as the raw data of T1 values at different inversion times or the 'full MOCO MOLLI series' in the repeatability cohort (n=10) for comparison of test-retest repeatability of the two analysis methods. Two observers (AS and SB) analysed scan-1 and one observer (SB) repeated the contours on scan-1, using both techniques, for the inter-observer and intra-observer variability. One observer (AS) also analysed scan-2 in order to assess the test-retest repeatability. We also compared the effect of heart rate (HR) correction in 10 patients, by generating T1 values with and without HR-correction (built-in option in the analysis software) from the MOLLI series of images, as no HR-correction was applied when the T1 maps were calculated on the scanner console.

3.4.3 Inter-observer and intra-observer variability

Table 14 shows the inter-observer and intra-observer variability results for native (pre-contrast) myocardial T1 and ECV, using the T1 maps and full MOLLI series for analysis. Variability was excellent using the T1 maps for assessment and good using the full MOLLI series.

3.4.4 Test-retest repeatability

The test-retest repeatability results are shown in Table 14. Overall, repeatability using the T1 map was better than that of the full MOLLI series, with lower CoVs and narrower Bland-Altman limits of agreement (Figure 41).

Table 14. Inter-observer, intra-observer and test-retest repeatability of T1 map and full MOLLI series analysis techniques

Parameter	Mean ± SD value	CoV (%)	Mean ± SD difference	BA limits of agreement
INTER-OBSERVER VARIABILITY				
	T1 map			
Myocardial T1 (ms)	1081.38 ± 26.39	**0.34**	-2.31 ± 3.69	-9.54 to 4.92
ECV	0.235 ± 0.016	**2.31**	0.000 ± 0.005	-0.011 to 0.011
	MOLLI series			
Myocardial T1 (ms)	1130.12 ± 54.83	**5.53**	-10.65 ± 62.53	-133.21 to 111.91
ECV	0.246 ± 0.020	**10.35**	0.003 ± 0.025	-0.047 to 0.053
INTRA-OBSERVER VARIABILITY				
	T1 map			
Myocardial T1 (ms)	1080.13 ± 27.67	**0.52**	0.18 ± 5.63	-10.85 to 11.21
ECV	0.235 ± 0.018	**1.83**	-0.001 ± 0.004	-0.010 to 0.007
	MOLLI series			
Myocardial T1 (ms)	1130.54 ± 53.73	**5.35**	-11.49 ± 60.49	-130.05 to 107.07
ECV	0.248 ± 0.020	**9.72**	0.000 ± 0.024	-0.047 to 0.047
TEST-RETEST REPEATABILITY				
	T1 map			
Myocardial T1 (ms)	1086.61 ± 22.67	**1.77**	-8.16 ± 19.27	-45.94 to 29.62
ECV	0.234 ± 0.018	**6.52**	0.002 ± 0.015	-0.027 to 0.032
	MOLLI series			
Myocardial T1 (ms)	1118.42 ± 55.40	**8.52**	34.05 ± 95.33	-152.79 to 220.89
ECV	0.239 ± 0.029	**12.98**	0.011 ± 0.031	-0.049 to 0.072

Abbreviations: MOLLI = modified Look-Locker Inversion Recovery, ECV = extracellular space volume fraction, SD = standard deviation, CoV = coefficient of variation, BA = Bland Altman.

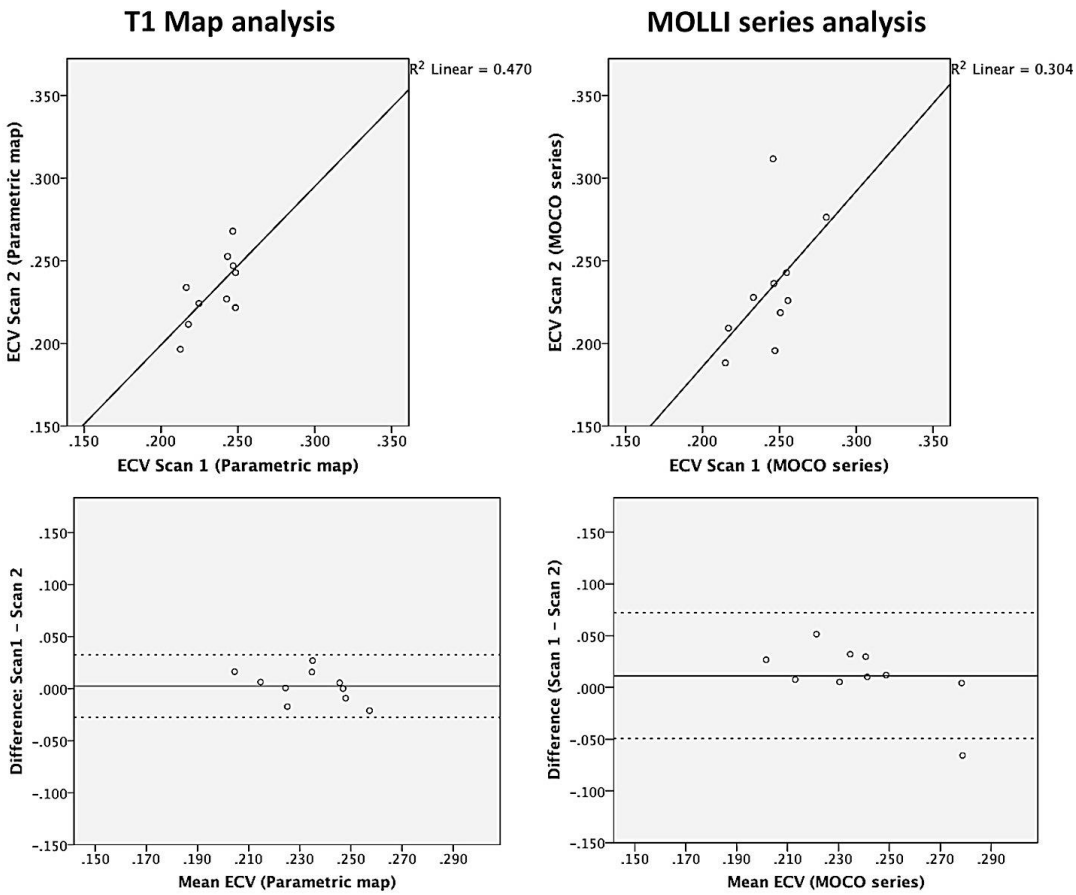

Figure 41.Scatter plots and Bland-Altman plots for test-retest repeatability of ECV in moderate-to-severe aortic stenosis.

3.4.5 Inter-technique agreement

Looking at the inter-technique agreement (Table 15), the CoVs were good (<10%) for agreement between the two methods, but there was a small negative bias for the T1 map technique, which gave slightly lower raw T1 values compared to the full MOLLI series (mean native T1 = 1086.61 ± 22.67 *vs.* 1118.42 ± 55.40, p = 0.04 and mean ECV = 0.234 ± 0.018 *vs.* 0.239 ± 0.029, p>0.05).

Table 15. Inter-technique agreement between Parametric map and full MOCO series analysis for native T1 and ECV calculation

INTER-TECHNIQUE VARIABILITY						
	Mean value Parametric Map	Mean ± SD value MOCO series	CoV	Mean ± SD difference	BA Limits of Agreement	r-value
Native T1	1086.61 ± 22.67°	1118.42 ± 55.40	**5.97**	-31.81 ± 65.77	-160.71 to 97.10	-0.295
ECV	0.234 ± 0.018	0.239 ± 0.029	**8.25**	-0.005 ± 0.019	-0.043 to 0.033	0.77*

Abbreviations as in Table 14. °p = 0.044 on paired t-test between parametric map and MOCO value, R-value for Pearson's correlation, *p<0.05

3.4.6 Effect of HR correction

There was no significant difference between T1 values or ECV on paired t-test (T1 = 1101.39 ± 42 *vs.* 1086.19 ± 20, p=0.132; ECV = 0.233 ± 0.04 *vs.* 0.230 ± 0.04, p=0.134 with and without HR-correction respectively), and significant correlations were present on Pearson's correlation.

3.4.7 Discussion

This is the first study to assess test-retest repeatability of ECV measurement in patients with AS. Additionally, we compared values obtained from different post-processing methods. While test-retest repeatability of T1 mapping has previously been assessed in healthy volunteers and one small study of 7 patients with amyloidosis(164) using ShMOLLI and multi-breath-hold T1 mapping, this is the first study to assess it in patients with AS. Our values using T1 maps compare favourably with those previously demonstrated for healthy volunteers with MOLLI at 3T. For native myocardial T1, previous CoVs have varied been between 2.5% and 8.4%(163, 165), compared to 1.8% in this report. For ECV, the CoV was 6.4%

in Liu's study(163), compared to ours of 6.5%. Therefore the high reproducibility of T1 and ECV does suggest that this technique could be used reliably for serial monitoring of AS patients.

3.4.8 Limitations

The numbers were relatively small, but similar to other studies assessing test-retest repeatability of CMR measured parameters. The flip angle used in the earlier version of the MOLLI prototype used for this study was higher than the current recommendation (35°), which may have led to underestimation of the absolute T1 value(166), but as the same protocol was used in all subjects studied, we do not believe this affects the validity of the results.

3.4.9 Conclusions

In conclusion, the test-retest repeatability of T1 quantification using MOLLI is excellent in patients with AS, and is higher when outlining the myocardium on a single T1 map rather than on each individual MOLLI image.

3.4.10 Implications for this thesis

Based on these results, the T1 map was utilised for any further quantification of ECV as part of this thesis.

3.5 Reproducibility of MPR at 3T: a comparison of MOCO *vs.* raw image analysis

3.5.1 Background

There have not been many studies looking at test-retest repeatability of quantitative MBF and MPR analysis, especially at 3T. Most studies looking at reproducibility have looked at healthy volunteers at a younger age(167, 168), and amongst patient groups, this has mainly been assessed in patients with coronary artery disease (CAD)(169). Others have assessed the reproducibility of semi-quantitative methods of MPRI calculation in both healthy controls and CAD(168-170).

3.5.2 Participants

Out of the original 10 patients who had two MRI scans, one was unanalysable due to contrast arriving too early in the LV cavity for quantitative blood flow analysis. The remaining original 9 patients were therefore used for inter- and intra-observer variability analysis. For the purposes of test-retest repeatability, an additional patient was recruited at a later date, due to an error with contrast injection during stress perfusion acquisition on scan-2 of one of the original cohort. All 10 were used for inter-technique assessment (MOCO *vs.* raw).

3.5.3 Image acquisition and analysis

Stress and rest first pass perfusion images were acquired at 3 short-axis slices (base, mid and apex), as described in the Section 2.4.6.3. As described, we used the bolus contrast technique rather than dual-bolus technique used by some centres, as this is the standard practice at our centre, and also because this is easier for the patients, with shorter scan times. Also, MPR reather than the absolute MBF was the primary measure of interest in our study, and therefore the signal saturation correction would affect both stress and rest MBF eually and not have a major impact on MPR values. The Siemens scanner automatically produces motion-corrected (MOCO) images in addition to the raw images, in order to account for the breathing movements. We therefore decided to look at the

reproducibility of contouring on both the raw set of images as well as the MOCO images.

3.5.4 Time taken for analysis

The average time taken to contour the raw images was 22 minutes, compared to 10.6 minutes for the MOCO images, due to less manual adjustment required.

3.5.5 Inter-technique agreement (MOCO *vs.* raw)

The signal intensity curves produced using MOCO images were smoother compared to the raw images (Figure 42). The results of comparison between MOCO and raw images is summarised in Table 16. There was no significant difference in the mean values of MPR, stress MBF and rest MBF obtained using the raw and MOCO images on paired t-test, and the two techniques showed excellent correlation. The CoV's were slightly higher for MPR compared to MBF.

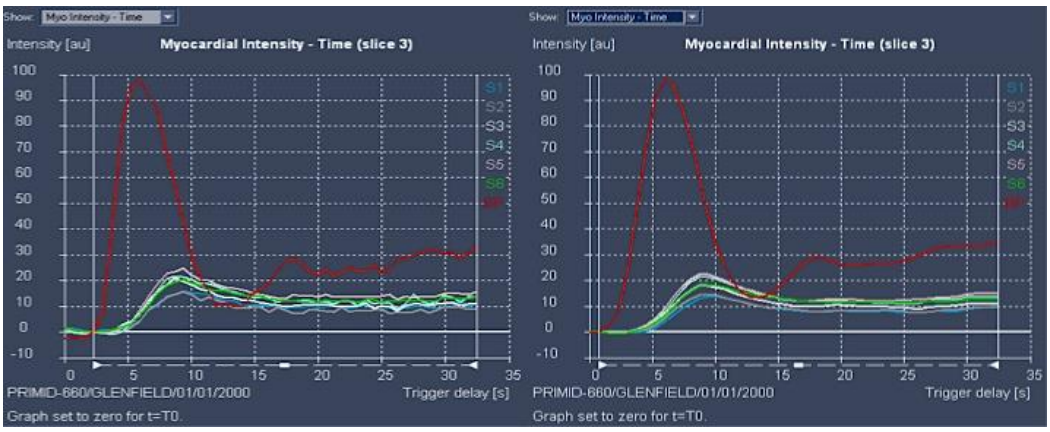

Figure 42. An example of the signal intensity curves obtained using raw images (left) and MOCO images (right) in the same patient, with MOCO images giving smoother curves

3.5.6 Inter-observer and intra-observer variability

The results for intra-observer and inter-observer variability for quantification of global MPR, stress MBF and rest MBF are summarised in Table 17. As can be seen, significant correlations were present for all parameters measured. Overall, intra-observer variability was good (CoV of ≤15%) and similar for MOCO and raw image analysis. The inter-observer variability was similar for most measures except MOCO MPR and stress MBF, for which the COV's were slightly higher, though still <20%.

Table 16. Inter-technique agreement between MOCO and raw perfusion image analysis for MPR and MBF

Parameter	MOCO average value (Mean ± SD)	Raw Average value (Mean ± SD)	p-value (paired t-test)	ICC	r-value	Paired Mean difference (SD) (MOCO-raw)	BA Limits of agreement	CoV%
Global MPR	2.249 ± 0.823	2.290 ± 0.843	0.80	0.92*	0.83*	-0.041 (0.486)	-0.992 to 0.911	21.39
Stress MBF	2.100 ± 0.946	2.124 ± 0.842	0.79	0.98*	0.96*	-0.024 (0.282)	-0.577 to 0.529	13.35
Rest MBF	0.948 ± 0.255	0.959 ± 0.265	0.73	0.97*	0.93*	-0.011 (0.095)	-0.197 to 0.176	9.97

Abbreviations: MPR=myocardial perfusion reserve, MBF=myocardial blood flow, MOCO=motion-corrected, SD=standard deviation, ICC=intra-class correlation coefficient, BA=Bland Altman, CoV=coefficient of variation. R-value on Pearson's correlation. * $p<0.05$.

Table 17. Intra-observer and inter-observer variability of quantification of MPR and MBF, using MOCO and raw perfusion images

Technique	Parameter	Mean ± SD	ICC	r-value	Paired Mean difference (SD)	BA Limits of agreement	CoV
INTRA-OBSERVER VARIABILITY							
MOCO	**MPR**	2.144 ± 0.810	0.96*	0.97*	0.246 (0.225)	-0.195 to 0.687	**10.49**
	Stress MBF	2.059 ± 0.923	0.98*	0.99*	0.131 (0.216)	-0.292 to 0.554	**10.48**
	Rest MBF	0.985 ± 0.268	0.95*	0.93*	-0.063 (0.106)	-0.270 to 0.144	**10.72**
Raw	**MPR**	2.248 ± 0.899	0.96*	0.93*	0.130 (0.345)	-0.545 to 0.806	**15.34**
	Stress MBF	2.147 ± 0.884	0.99*	0.98*	0.029 (0.172)	-0.308 to 0.365	**8.00**
	Rest MBF	0.998 ± 0.282	0.95*	0.91*	-0.057 (0.127)	-0.306 to 0.191	**12.72**
INTER-OBSERVER VARIABILITY							
MOCO	**MPR**	2.299 ± 0.805	0.94*	0.88*	-0.065 (0.418)	-0.884 to 0.754	**18.17**
	Stress MBF	2.158 ± 0.916	0.96*	0.93*	-0.067 (0.367)	-0.786 to 0.652	**17.00**
	Rest MBF	0.953 ± 0.257	0.97*	0.94*	0.000 (0.091)	-0.178 to 0.179	**9.56**
Raw	**MPR**	2.292 ± 0.871	0.97*	0.94*	0.042 (0.297)	-0.541 to 0.624	**12.96**
	Stress MBF	2.197 ± 0.924	0.99*	0.99*	-0.071 (0.158)	-0.380 to 0.239	**7.19**
	Rest MBF	0.986 ± 0.257	0.91*	0.83*	-0.034 (0.157)	-0.341 to 0.273	**15.88**

Abbreviations: as in Table 16. R-value on Pearson's correlation. * $p<0.05$.

3.5.7 Test-retest repeatability

The results of the test-retest repeatability of MPR and MBF quantification using MOCO (Figure 43a) and raw perfusion images are summarised in Table 18. There was no significant difference in the mean MPR or MBF values between scan-1 and scan-2 on paired t-tests. However, no significant correlations were found between the measured values between the two scans, and the Bland-Altman limits of agreement were wide, with high CoV's, especially for MPR and stress MBF.

Table 18. Test-retest repeatability of quantification of MPR and MBF using MOCO and raw perfusion images

Parameter	Average value (Mean ± SD)	R-value	ICC	Paired Mean difference (SD)	BA Limits of agreement	CoV
MOCO image analysis						
MPR	2.248 ± 0.616	-0.08	-0.19	-0.133 (1.332)	-2.744 to 2.478	**59.26**
Stress MBF	2.059 ± 0.660	0.07	0.14	-0.141 (1.235)	-2.562 to 2.280	**60.00**
Rest MBF	0.949 ± 0.265	0.56	0.73	-0.033 (0.289)	-0.599 to 0.533	**30.44**
Raw image analysis						
MPR	2.268 ± 0.537	-0.16	-0.37	-0.314 (1.243)	-2.751 to 2.122	**54.81**
Stress MBF	2.121 ± 0.537	-0.09	-0.22	-0.295 (1.179)	-2.607 to 2.017	**55.61**
Rest MBF	0.967 ± 0.221	0.24	0.42	-0.003 (0.345)	-0.680 to 0.674	**35.72**

Abbreviations: as in Table 16. R-value on Pearson's correlation. No significant difference in MPR or MBF values between scan-1 and scan-2 on paired t-tests ($p>0.05$).

On looking more closely at the MPR values for scan-1 and scan-2, there were two patients in which there was a marked discrepancy, both of whose perfusion scans already had contrast present in the RV in the first frame that was acquired, which was likely due to early contrast injection in relation to the breathing instructions and start of image acquisition by the radiographer. I therefore re-calculated the CoV's after excluding these two patients, which brought down the CoV's to **41.2% / 40.3% / 36.6%** for MPR / stress MBF / rest MBF respectively using MOCO images (Figure 43b), and **25.0% / 33.9% / 43.3%** using the raw images.

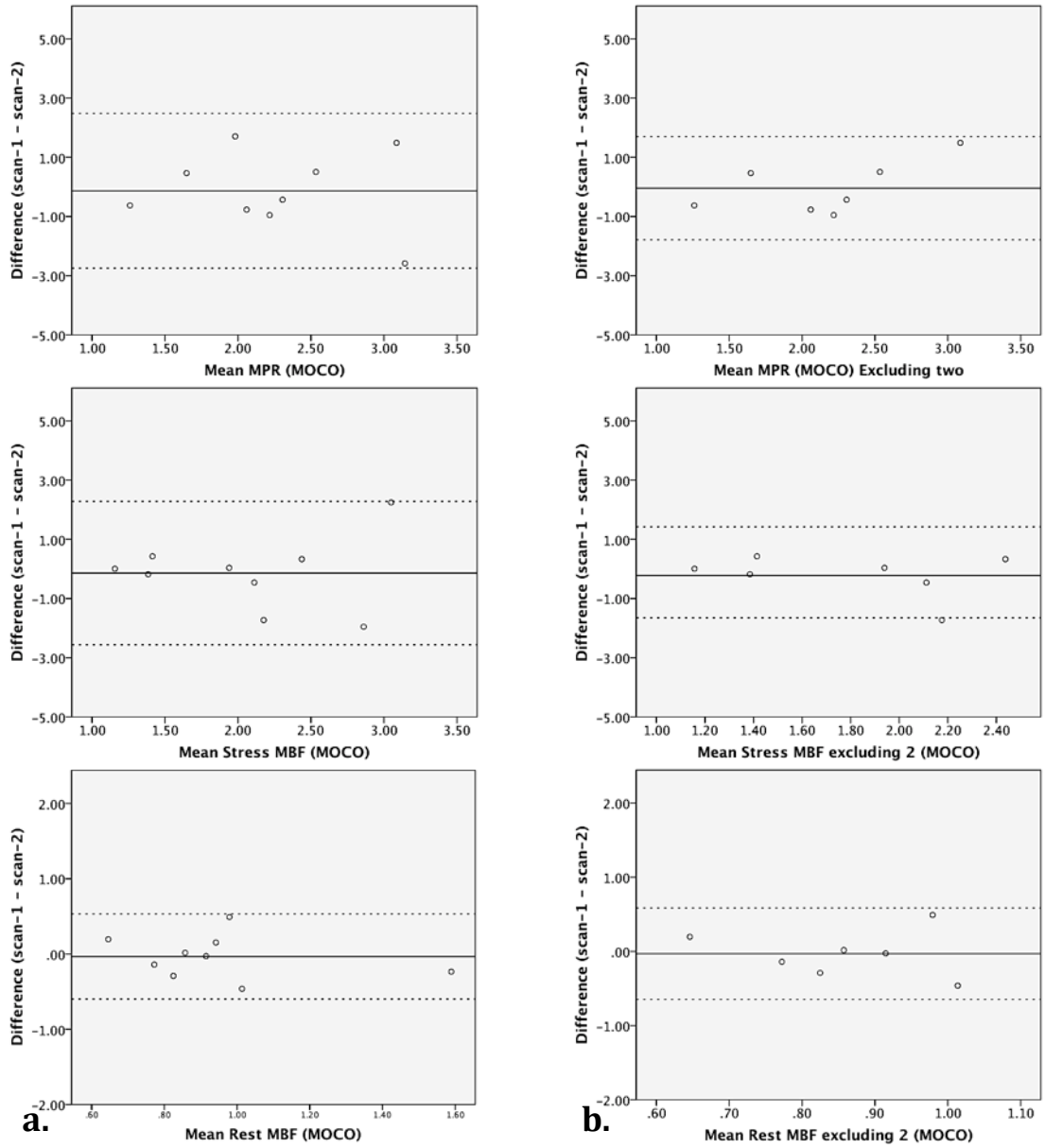

Figure 43. Bland-Altman plots for test-retest repeatability of MPR, stress MBF and rest MBF using MOCO images for a.) all patients (left column), b.) excluding two patients (right column)

3.5.8 Discussion

This is the first time that reproducibility (intra-observer, inter-observer variability and test-retest repeatability) has been assessed in patients with AS, using two sets of images for contouring.

3.5.8.1 MOCO vs. raw image analysis

This is the first direct comparison of raw images *vs.* MOCO image analysis for quantification of MBF and MPR that we are aware of. We have shown excellent correlation between the values obtained by the two methods, with smoother signal intensity curved, and half the time taken to contour using MOCO images.

3.5.8.2 Intra-observer and inter-observer variability

The intra-observer and inter-observer variability were found to be good to moderate, and not much different between raw and MOCO images. Our CoV's for intra-observer variability for MBF and MPR of around 10% for MOCO and 8-15% for raw images compares favourably to the only other study to have reported this for quantitative MBF analysis by Larghat *et al*(168) in 11 healthy controls (CoV of 18.4%, 14.1% and 13.4% for MPR, stress MBF and rest MBF respectively). The inter-observer variability in that study was 13.3% / 13.6% / 15.2% for MPR, stress MBF and rest MBF respectively, compared to our values of 18% / 17% / 10% for MOCO and 13% / 7% / 16% using raw images. Another study that looked at the intra- and inter-observer variability of MBF quantification using Fermi-constrained deconvolution method reported ICC's of 0.80-0.85 for intra-observer and 0.55-0.73 for inter-observer variability(171), compared to which, our ICC's were much higher (>0.90).

3.5.8.3 Test-retest repeatability

The test-retest repeatability was found to be poor in our cohort of patients. Previous studies reporting test-retest repeatability of quantitative MBF/MPR have mainly utilised Fermi-constrained deconvolution method, and have reported COV's of 21-35% for global MPR, 27-41% for stress MBF and 16-26% for rest MBF(154, 168, 169). The only study looking at test-retest repeatability using the model-independent deconvolution method was on a subset of the MESA cohort(172). This study only reported stress and rest MBF and not MPR, and had a very long interval of 334±158 days between the two scans, which therefore is a major limitation. The calculated CoV from that paper was 20% for stress MBF and 16% for rest MBF.

The re-calculated COV's after exclusion of the two patients with contrast present in the RV in the first frame acquired, brought most of the CoV's much closer to previously published values. Early contrast injection in relation to the breathing instructions and start of image acquisition can lead to inaccurate baseline correction, as even a small amount of contrast present in the LV cavity can lead to over-correction. Although every effort was made to standardise the scanning, with identical protocols used between scans, an element of variability is unavoidable in the exact timing of radiographers' instructions / acquisition and contrast injection. The majority of the previous studies were also performed at 1.5T(168, 169, 172) compared to ours at 3T, which may account for some difference in repeatability, though the intra- and inter-observer variability's were similar. In order to account for the signal saturation effect due to the non-linear relationship between enhancement and contrast concentration in the blood pool, theses effects need to be either corrected (as in our study) or avoided. Strategies that try and avoid this problem include(110): 1.) lower contrast doses (though at the price of lower contrast-to-noise in the myocardium, 2.) dual-contrast sequences (acquisition of low-resolution low-T1 blood pool and high-resolution high-T1 myocardial data with each RR-interval) and 3.) dual-bolus contrast injection (utilising a low-dose bolus to image blood-pool and overcoming the signal saturation effects in the LV, followed by a high-dose bolus to image the myocardial contrast enhancement, whilst still maintaining adequate myocardial signal)(167, 169). We used a relatively low contrast concentration but with the bolus-method in our study, which may partly explain the poorer repeatability. Further work comparing the reproducibility of bolus *vs.* dual-bolus technique in the same cohort of patients may be able to test this hypothesis.

3.5.9 Conclusions

Quantitative MBF and MPR assessment using both MOCO and raw images demonstrated good intra- and inter-observer variability. The test-retest repeatability was found to be moderate to poor for the overall cohort, and best

for rest MBF. This calls into question the utility of quantitative MBF / MPR as a reliable outcome measure in interventional clinical trials, using the current complex post-processing and quantification techniques. There is clearly a need for simplification and semi-automation of post-processing, as well as a more standardised approach to absolute MBF quantification, which would hopefully lead to better reproducibility of this important CMR technique.

3.5.10 Implications for this thesis

Given that the MOCO analysis correlated very well with the raw image analysis, but took half the time to contour, we decided to utilise the MOCO images (where available) for further MPR analysis for the rest of the thesis.

CHAPTER FOUR

4 EFFECT OF RANOLAZINE ON CMR MEASURED DIASTOLIC FUNCTION AND MYOCARDIAL PERFUSION RESERVE IN ASYMPTOMATIC AS- A PROOF OF CONCEPT STUDY

Published:

Singh A, Steadman CD, Khan JN, Reggiardo G, McCann GP. Effect of late sodium current inhibition on MRI measured diastolic dysfunction in aortic stenosis: a pilot study. BMC Res Notes. 2016;9(1):64

4.1 Background

As outlined in chapter-1, AS is characterised by pressure overload hyperterophy, diastolic dysfunction and myocardial fibrosis leading to systolic dysfunction as a late phenomenon. Microvascular dysfunction is common and with reduced myocardial perfusion reserve which may be associated with angina even with normal coronary arteries. There are currently no proven medical therapies in AS.

Ranolazine is a newly licensed drug for the treatment of chronic stable angina(119, 120). The mechanisms of action of Ranolazine are not fully understood, but it is thought to inhibit late sodium channel activation, decreasing intracellular calcium concentration, shortening the action potential duration, but without significant effects on heart rate or blood pressure. In experimental models, Ranolazine has been shown to improve diastolic dysfunction in isolated myocytes(121-123) and reduce progressive remodelling in a dog model of heart failure(173). In small pilot studies of patients with angina, Ranolazine decreased reversible ischaemia on scintigraphy(124) and improved some echocardiographic parameters of diastolic and systolic function, but not others (174). However, a recently published randomised trial of Ranolazine in patients with heart failure with preserved EF (HFpEF) (n=20) failed to demonstrate improvement in echocardiographic measures of diastolic function(175). It may therefore improve diastolic function and/or myocardial perfusion in patients with AS and existing diastolic dysfunction/ LVH. The mechanism of action for the improved MBF is thought to be secondary to the lower intra-cellular calcium concentration leading to improved myocyte relaxation and improved diastolic wall stiffness, leading to reduced extravascular compression of the microvasculature. This leads to an increased trans-myocardial pressure gradient secondary to an increased diastolic perfusion time and decreased LVEDP, leading to less ischaemia.

4.2 Study methods

The inclusion and exclusion criteria, study methods and follow-up information are described in the Methods chapter (sections 2.2.6 and 2.3.2). As mentioned previously, this pilot study was a sponsored study, and therefore the methodology had been already finalised before the assessment of reproducibility as part of my thesis. If we were to re-design such a study, we would recommend scanning at 1.5T instead, possibly using CSPAMM.

4.2.1 Statistical analysis and power calculation

In a previous group of 8 AS patients tested 2 weeks apart, diastolic strain rate was 0.73±0.22 and 0.71±0.21 with paired mean difference of 0.04 and SD of 0.16. Sixteen patients with analysable images would allow us to detect a difference of 0.12 in diastolic strain rate with 80% power, $p<0.05$ and 2-tailed. To allow for drop-outs and unanalysable image quality, we planned to recruit 20 patients. Statistical tests were performed using SPSS 20.0 software (Statistical Package for the Social Sciences, Chicago, IL).

Normality was assessed using the Shapiro-Wilk test, histograms and Q-Q plots. Continuous data are expressed as mean (standard deviation). Paired-samples t-tests were used to compare parameters between different visits. In addition, repeated measure analysis of variance (ANOVA) was used to compare parameters across the three visits for the primary endpoint. The results were further analysed after splitting the patients according to the median peak pressure gradient (PPG) and MPR, into low and high-PPG/MPR subgroups, and patient characteristics between sub-groups were compared using independent t-test.

4.3 Patient recruitment

A total of 45 Patient Information Sheets were sent out after screening. Twenty patients were consented for the study (Figure 44). Of these, 1 was excluded after consenting due to the incidental finding of previously unknown atrial fibrillation.

Four patients withdrew from the study before visit-3, and therefore did not undertake follow-up investigations. One was because of the finding of a regional perfusion defect on MRI, suggesting significant coronary artery disease, 2 were due to drug intolerance and 1 for non-compliance with study medication. Another 2 patients did not complete the last visit, although they took the drug for the prescribed period and had a baseline and visit-3 assessments. Therefore, 15 patients completed visits 1 to 3, and 13 patients completed all four visits. There were 2 patients who continued on the lower dose of Ranolazine (500mg BD) due to experiencing side effects with the higher dose (insomnia and dizziness), but who were happy to complete the course at the lower dose.

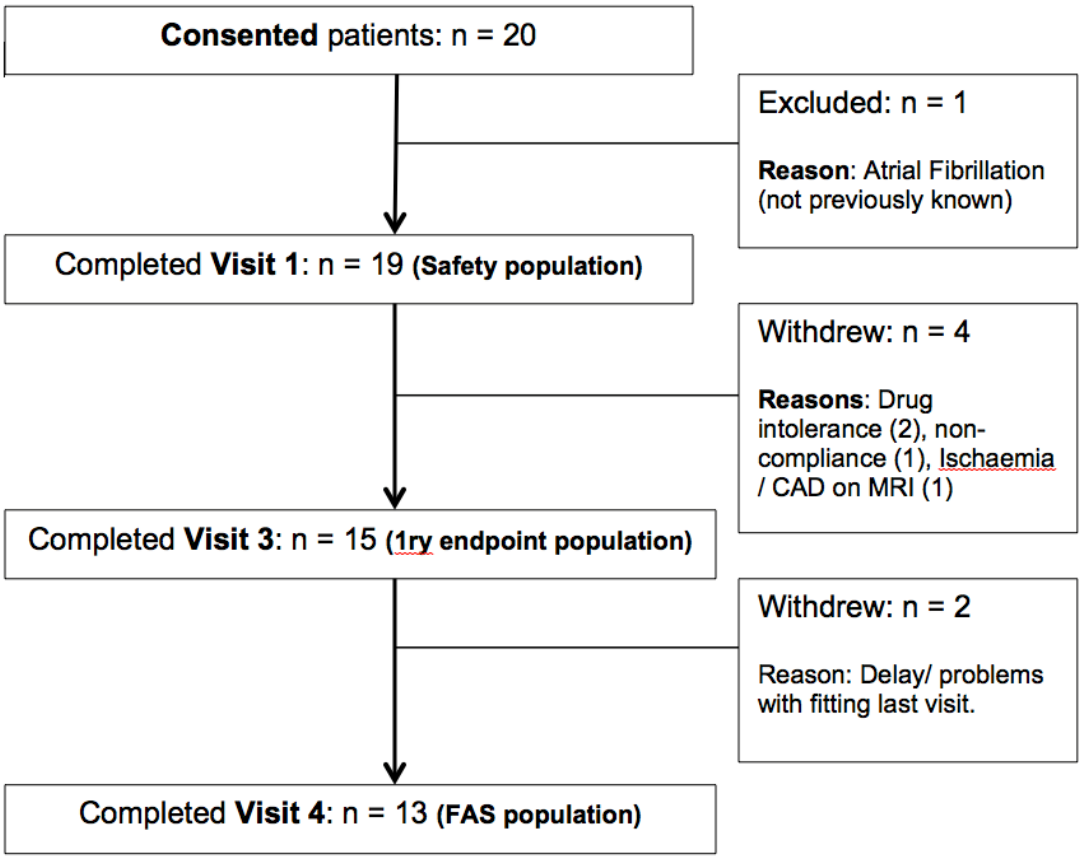

Figure 44. Flowchart showing recruitment for Ranolazine study

(1ry endpoint = primary endpoint, FAS = full analysis set)

4.4 Study population definitions

The "**safety population**" includes all enrolled patients having taken at least one dose of study drug (**n=19**). The '**primary endpoint' population** is defined as all enrolled patients who took the study drug for 6 weeks and had at least two measurements of diastolic strain rate (baseline and week-6) (**n=15**). The **Full-Analysis-Set** (FAS) population is defined as all enrolled patients who took at least one dose of the drug and completed the study, with three measurement of diastolic strain rate (baseline, week-6 and week-10) (**n=13**).

4.5 'Primary endpoint' Population

4.5.1 Demographic data

The demographic data for the 'primary endpoint population' (n=15) is shown in Table 19.

4.5.2 Primary endpoint- PEDSR

The results for global circumferential PEDSR (average of basal, mid and apical) as well as individual slices, measured on MRI Tagging, are shown in Table 20. In order to calculate global values, analysable data on all three slices was available for 13 patients. There was a trend for the global PEDSR to increase from the baseline value to week-6, though this was not statistically significant.

Table 19. Demographic data for 'primary endpoint' population (n=15)

Parameter		Value
Age (years)		65.9 ± 9.67
Gender ratio (male/female, n (%))		12 / 3 (80.0 / 20.0)
BMI (kg/m^2)		29.3 ± 3.36
Smoking History (n, %)	Current	0 (0.0)
	Former	6 (40.0)
	Never	9 (60.0)
Heart Rate (bpm)		74.5 ± 11.8
Systolic Blood Pressure (mmHg)		153.0 ± 23.6
Diastolic Blood Pressure (mmHg)		81.7 ± 11.1
Echocardiographic Data		
Peak pressure gradient (mmHg)		48.8 ± 12.4
Mean Pressure Gradient (mmHg)		27.1 ± 7.5
Aortic Valve Area (cm^2)		1.26 ± 0.31
E/A		0.77 ± 0.16
Average Septal E/e'		12.94 ± 3.91
Average Lateral E/e'		10.65 ± 3.49
Resting LVRPP (mmHg.bpm)		14424.3 ± 3054.0
Exercise LVRPP (mmHg.bpm)		36041.3± 5235.1
Cardiac MRI Data		
LVMI (g/m^2)		66.72 ± 15.35
LVEDVI (ml/m^2)		85.02 ± 15.92
LVEF(%,)		58.29 ± 3.81

BMI: body mass index, LVRPP: left ventricular rate pressure product, LVMI: left ventricular mass indexed to body surface area, LVEDVI: left ventricular end diastolic volume indexed to body surface area, LVEF: left ventricular ejection fraction

Table 20. Tagging measured PEDSR for 'Primary endpoint' Population (n=15)

Region	Number analysable	Baseline	Week-6	p (paired t-test)
Base	15	0.818 ± 0.231	0.893 ± 0.305	0.475
Mid	14	0.829 ± 0.135	0.841 ± 0.153	0.791
Apex	13	0.756 ± 0.232	0.790 ± 0.229	0.501
Global	13	0.79 ± 0.151	0.86 ± 0.181	0.198

4.5.3 Secondary endpoints

The results for the secondary endpoints are shown in Table 21. There was no significant change demonstrated in global MPR, NT-proBNP or echocardiographic measures of diastolic dysfunction between baseline and week-6. The apical PSS increased significantly from -15.30±3.12 to -17.67±4.00, though there was no significant change in the basal, mid or global values.

The total exercise duration increased from 10.47±3.68 minutes to 11.60±3.25 minutes, which was of borderline significance (p=0.06), with a trend for the maximal HR and SBP to be lower at week-6. Although there was no change in the resting LVRPP, the exercise LVRPP decreased from 36041 to 34517 mmHg.bpm at week-6, though this trend was not statistically significant.

Table 21. Secondary endpoint measures for 'primary endpoint' population (n=15)

Parameter		Number analysable	Baseline	Week-6	p (paired t-test)
MRI Parameters					
PSS (%)	Base	15	-17.65 ± 3.86	-17.60 ± 4.26	0.958
	Mid	14	-19.31 ± 3.04	-18.44 ± 4.09	0.352
	Apex	13	-15.30 ± 3.12	-17.67 ± 4.00	**0.038***
	Global	15	-17.44 ± 2.57	-17.53 ± 3.98	0.907
PSSR (1/s)	Base	15	-0.965 ± 0.246	-0.991 ± 0.195	0.727
	Mid	14	-1.048 ± 0.195	-1.108 ± 0.215	0.376
	Apex	13	-0.944 ± 0.279	-1.043 ± 0.297	0.288
	Global	15	-0.99 ± 0.203	-1.04 ± 0.208	0.436
Stress MBF		15	2.73 ± 0.695	2.51 ± 0.717	0.301
Rest MBF		15	1.03 ± 0.185	1.00 ± 0.178	0.587
MPR		15	2.68 ± 0.634	2.52 ± 0.614	0.452
LVEDV (ml)		15	173.7 ± 47.64	170.1 ± 59.02	0.624
LVESV (ml)		15	73.3 ± 25.26	74.3 ± 29.38	0.509
EF (%)		15	58.3 ± 3.81	56.7 ± 4.81	0.080
Exercise Parameters					
Resting HR (bpm)		15	74.5 ± 11.8	74.4 ± 13.7	0.963
Resting SBP (mmHg)		15	153.0 ± 23.6	147.2 ± 17.3	0.208
Exercise duration (min)		15	10.47 ± 3.68	11.60 ± 3.25	**0.062**
Max HR (bpm)		15	143.5 ± 10.7	139.6 ± 15.5	0.273
Max SBP (mmHg)		15	182.9 ± 20.5	174.5 ± 25.8	0.133
Resting LVRPP (mmHg.bpm)		15	14424.3 ± 3054.0	14514.1 ± 3591.6	0.903
Exercise LVRPP (mmHg.bpm)		15	36041.3 ± 5235.1	34516.9 ± 6538.4	0.313
Biomarker					
NT-proBNP (pmol/L)		15	48.54 ± 82.43	51.64 ± 73.28	0.715
Echocardiographic Parameters					
E/A		15	0.773 ± 0.163	0.783 ± 0.169	0.765
Septal E/e'		15	12.94 ± 3.91	13.79 ± 2.86	0.258
Lateral E/e'		15	10.65 ± 3.49	10.62 ± 3.43	0.979

Abbreviations as Table 19 & PSS: peak systolic strain, PSSR: peak systolic strain rate, MBF: myocardial blood flow, MPR: myocardial perfusion reserve, LVESV: left ventricular end systolic volume, HR: heart rate, SBP: systolic blood pressure. *p<0.05

4.6 FAS population

4.6.1 Primary endpoint

For the 13 patients who completed the final visit, 4 weeks after stopping Ranolazine, the results of global and regional PEDSR are shown in Table 22. There was a non-significant trend for the PEDSR to increase from the baseline value after administration of Ranolazine and then return towards the original value on stopping the drug (Figure 45).

Table 22. Tagging measured global PEDSR for FAS Population (n=13)

Region	Number analysable	Baseline	Week-6	Week-10
Base	12	0.860 ± 0.206	0.939 ± 0.281	0.899 ± 0.282
Mid	12	0.839 ± 0.140	0.851 ± 0.155	0.760 ± 0.184
Apex	11-12	0.793 ± 0.229	0.795 ± 0.251	0.751 ± 0.261
Global	11	0.82 ± 0.130	0.87 ± 0.193	0.81 ± 0.211

(All p-values >0.05 using both paired t-tests and repeated measures ANOVA analysis)

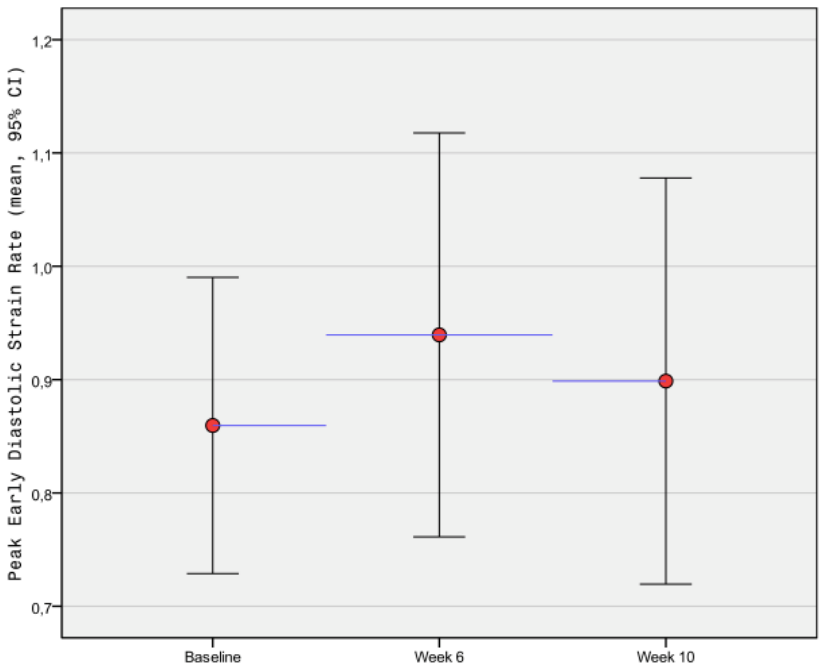

Figure 45. Trend in PEDSR with study visit for the Basal slice (FAS Population)

4.6.2 Secondary endpoints

The results for the secondary endpoints for the FAS population are shown in Table 23. The overall trend was for the global PSS and global PSSR to increase at week-6, which was largely driven by the increase in apical values. The PSSR tended to return close to the baseline value at week-10. There was no significant change in MPR, though the trend was for it to decrease slightly at week-6.

For the exercise parameters, the total exercise time increased by nearly a minute between baseline and week-6 but this increase was sustained at week-10. There was a trend for the maximal HR and SBP to be lower at week-6 compared to baseline, despite longer exercise duration, with these values increasing slightly again at week-10 but still remaining lower than at baseline. There was also a trend for the exercise LVRPP to decrease from the baseline value at week-6, and increase slightly again at week-10. There was no change in the resting values of HR, SBP or LVRPP. The total exercise duration for all patients exercised at each visit showed a similar trend (Figure 46): 10.73 minutes at baseline (n=19), 12.03 minutes at week-6 (n=15, p=0.071), and 11.99 minutes at week-10 (n=13, p=0.727).

The mean NT-proBNP value tended to increase with each visit, with the difference being statistically significant between baseline and week-10. The echocardiographic parameters did not demonstrate any significant changes, except a significant increase noted in septal E/e' between baseline and week-10 (p=0.046).

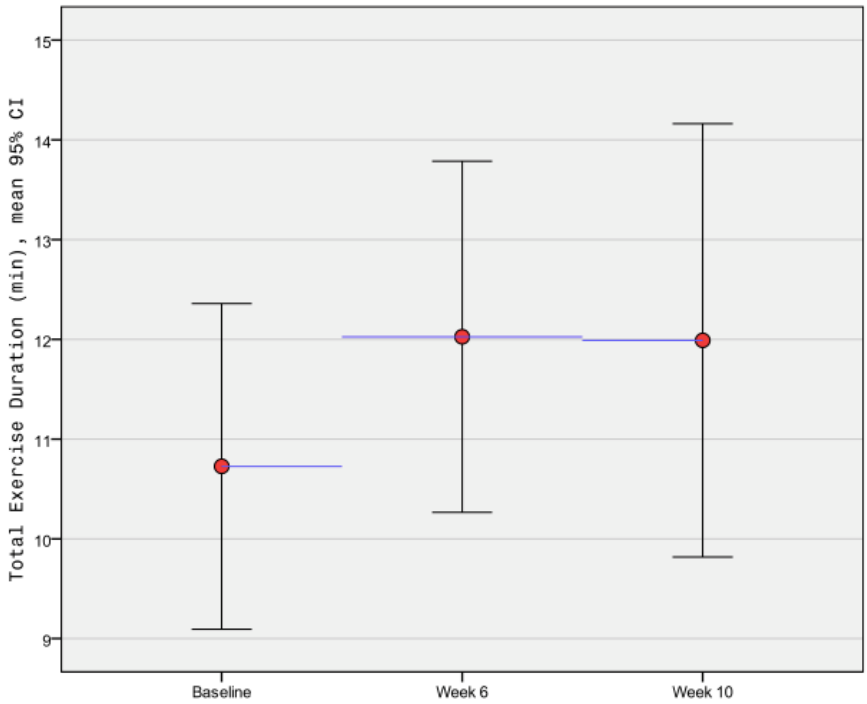

Figure 46. Total Exercise Duration with study visit for all patients tested at each visit

Table 23. Secondary endpoint measures for FAS Population (n=13)

Parameter		Number analysable	Baseline	Week-6	Week-10
MRI Parameters					
PSS (%)	Base	12	-18.52 ± 3.48	-19.02 ± 2.90	-19.10 ± 5.03
	Mid	12	-19.79 ± 2.98	-19.39 ± 3.14	-19.30 ± 3.32
	Apex	11-12	-15.55 ± 3.30*	-18.48 ± 3.74	-17.33 ± 4.64
	Global	12	-18.05 ± 2.43	-18.93 ± 2.63	-18.57 ± 3.38
PSSR (1/s)	Base	12	-1.008 ± 0.256	-1.028 ± 0.189	-0.993 ± 0.219
	Mid	12	-1.066 ± 0.205	-1.150 ± 0.203	-1.030 ± 0.142
	Apex	11-12	-0.941 ± 0.285	-1.083 ± 0.307	-0.979 ± 0.258
	Global	12	-1.01 ± 0.21	-1.08 ± 0.21	-1.00 ± 0.18
Stress MBF		11	2.80 ± 0.786	2.40 ± 0.664	2.54 ± 0.454
Rest MBF		11	1.05 ± 0.192	0.99 ± 0.208	1.04 ± 0.230
MPR		11	2.69 ± 0.726	2.45 ± 0.559	2.52 ± 0.579
LVEDV (ml)		13	174.31 ± 44.17	173.08 ± 60.22	172.00 ± 59.58
LVESV (ml)		13	72.46 ± 22.47	74.69 ± 29.89	74.15 ± 26.14
Exercise Parameters					
Resting HR (bpm)		13	74.1 ± 12.0	73.5 ± 13.2	72.0 ± 11.7
Resting SBP (mmHg)		13	155.9 ± 24.0	148.5 ± 17.9	146.2 ±25.0
Exercise duration (min)		13	10.88 ± 3.94	11.85 ± 3.39	11.99 ± 3.59
Max HR (bpm)		13	142.2 ± 11.0	136.5 ± 13.7	140.6 ± 12.7
Max SBP (mmHg)		13	183.9 ± 20.6	174.5 ± 24.2	179.3 ± 15.1
Resting LVRPP (mmHg.bpm)		13	14639.7 ± 3228.3	14735.9 ± 3773.6	14512.6 ± 3131.8
Exercise LVRPP (mmHg.bpm)		13	36342.3 ± 5351.4	34285.9 ± 6902.7	35604.6 ± 4787.5
Biomarker					
NT-proBNP (pmol/L)		13	52.82 ± 87.88†	57.57 ± 77.22	70.94 ± 77.06
Echocardiographic Parameters					
E/A		13	0.742 ± 0.143	0.765 ± 0.171	0.775 ± 0.159
Septal E/e'		13	12.57 ± 3.81†	13.50 ± 2.95	13.84 ± 3.85
Lateral E/e'		13	10.93 ± 3.48	10.90 ± 3.37	11.03 ± 2.75

Abbreviations as Table 21. * $p<0.05$ compared to week-6, † $p<0.05$ compared to week-10

4.7 Sub-group analysis by Peak Pressure Gradient

Sub-group analysis was carried out by dividing the patients into two groups according to the median PPG (51.4 mmHg) as follows:-

Group A (Low PPG)**:** PPG ≤ 51.4 (n = 8)

Group B (High PPG)**:** PPG > 51.4 (n = 7)

The demographic and baseline data for the subgroups is shown in Table 24. The low-PPG subgroup was younger and had lower mean PPG and MPG, as well as higher E/A.

4.7.1 PEDSR in low and high PPG subgroups

The results for the primary endpoint for the FAS population according to the PPG-subgroups are shown in Table 25. There was a tendency for the PEDSR to increase from baseline to week-6, with a return towards baseline at week-10 in the high-PPG subgroup, at the basal and mid-level, and this increase at week-6 was statistically significant for the mid slice (p=0.002). When only an average of the basal and mid slice was taken, there was a statistically significant increase in PEDSR from 0.79±0.16 to 0.87±0.16 (p=0.020) at week-6, in the high-PPG subgroup, with a drop back to 0.79±0.20 (p=0.31) at week-10. These trends were not present for the low-PPG group.

Table 24. Baseline data for sub-groups according to PPG

Parameter		Low PPG (n = 8)	High PPG (n = 7)
Age (years)		61.0 ± 8.8*	71.4 ± 7.7
Gender ratio (male/female, n (%))		5 / 3 (62.6 / 37.5)	7 / 0 (100 / 0)
BMI (kg/m^2)		29.8 ± 2.8	28.7 ± 4.1
Smoking History (n, %)	Current	0 (0.0)	0 (0)
	Former	3 (37.5)	3 (42.9)
	Never	5 (63.5)	4 (57.1)
Heart rate (bpm)		71.3 ± 12.6	78.3 ± 10.5
Systolic blood pressure (mmHg)		148.3 ± 21.0	158.4 ± 26.8
Diastolic blood pressure (mmHg)		80.9 ± 13.3	82.7 ± 8.8
Echocardiographic Data			
Peak pressure gradient (mmHg)		40.7 ± 8.8*	60.2 ± 5.7
Mean Pressure Gradient (mmHg)		21.7± 5.0*	33.4 ± 4.2
Aortic Valve Area (Echocardiographic) (cm^2)		1.33 ± 0.31	1.18 ± 0.31
E/A		0.85 ± 0.18*	0.68 ± 0.09
Average Septal E/e'		13.69 ± 4.32	12.09 ± 3.50
Average Lateral E/e'		10.66 ± 2.43	10.64 ± 4.64
Resting LVRPP (mmHg.bpm)		13424.5 ± 3112.4	15567.0 ± 2757.6
Exercise LVRPP (mmHg.bpm)		36477.1 ± 5409.5	37919.9 ± 5387.2
Cardiac MRI Data			
LVMI (g/m^2)		62.4 ± 17.7	71.6 ± 11.5
LVEDVI (ml/m^2)		83.92 ± 15.30	86.29 ± 17.74
LVEF (%)		58.9 ± 4.3	57.6 ± 3.3
Global PEDSR (1/s)		0.83 ± 0.17	0.78 ± 0.15
Global MPR		2.83 ± 0.70	2.51 ± 0.56
Exercise Test			
Exercise time (min)		11.5 ± 3.5	10.4 ± 4.1
Peak HR (bpm)		146.0 ± 7.2	141.1 ± 14.1
Peak SBP (mmHg)		185.6 ± 15.4	181.3 ± 26.0

Abbreviations as Table 21. * statistically significant difference between sub-groups ($p<0.05$)

Table 25. Sub-group analysis of PEDSR for FAS Population according to PPG

Slice	Number analysable	Baseline	Week-6	Week-10
Group A (Low PPG)				
Base	5	0.95 ± 0.12	0.87 ± 0.14	0.97 ± 0.37
Mid	5	0.92 ± 0.08	0.81 ± 0.15	0.77 ± 0.18
Apex	3	0.86 ± 0.18	0.97 ± 0.04	0.91 ± 0.23
Global	5	0.93 ± 0.87	0.85 ± 0.11	0.89 ± 0.23
Group B (High PPG)				
Base	7	0.79 ± 0.24	0.99 ± 0.35	0.85 ± 0.22
Mid	7	0.75 ± 0.13*	0.86 ± 0.16	0.75 ± 0.20
Apex	6	0.73 ± 0.28	0.65 ± 0.21	0.66 ± 0.27
Global	7	0.78 ± 0.15	0.92 ± 0 .34	0.75 ± 0.21

* $p<0.05$ compared to week-6

4.7.2 Secondary endpoint

The results for the exercise parameters according to the PPG subgroups are shown in Table 26. For the low-PPG group there was no significant change in exercise capacity or LVRPP. Exercise LVRPP showed a non-significant decrease at week-6 and increase again at week-10 in the high-PPG subgroup, despite no change in total exercise duration. There was no significant change in MPR noted between visits for either sub-group.

Table 26. Sub-group analysis of secondary endpoints for FAS Population according to PPG

	Number analysable	Baseline	Week-6	Week-10
Group A (Low-PPG)				
Exercise time (min)	5	12.2 ± 2.9	13.0 ± 3.1	13.0 ± 3.5
Exercise LVRPP (mmHg.bpm)	5	36059.9 ± 6466.1	36494.4 ± 9458.1	36266.7 ± 7390.9
Group B (High-PPG)				
Exercise time (min)	7	10.0 ± 4.0	10.3 ± 3.7	10.7 ± 3.8
Exercise LVRPP (mmHg.bpm)	7	36611.9 ± 5404.8	32577.6 ± 5271.0	35158.0 ± 2969.7

All $p>0.05$

4.8 Subgroup analysis by MPR

The median MPR for the 'primary endpoint' population was 2.79. The patients were divided into two groups according to their MPR, as follows:-

Group A (Low MPR)**:** MPR < 2.79 (N = 7)

Group B (High MPR)**:** MPR ≥ 2.79 (N = 8)

The demographic data for the subgroups is shown in Table 27. Other than the global MPR being significantly lower in group-A, the groups were well matched.

4.8.1 PEDSR in low and high MPR subgroups

There was a trend for global PEDSR to increase with Ranolazine treatment in the low-MPR group, and then return towards baseline at week-10 (Table 28). When all patients who had a baseline and 6-week scans were included (n=15), the increase in PEDSR was close to reaching statistical significance for the basal slice (0.78±0.29 to 1.10±0.25, p=0.09). This trend however, was absent in the high-MPR sub-group.

4.8.2 Secondary endpoints

The results for the exercise parameters according to the MPR subgroups are shown in Table 29. There was a trend for the exercise LVRPP to reduce at week-6 in the low-MPR group, despite not much change in total exercise duration. There was no change in either exercise duration or exercise LVRPP in the high-MPR subgroup.

Table 27. Baseline data for sub-groups according to MPR

Parameter		**Low MPR** (n = 7)	**High MPR** (n = 8)
Age (years)		63.6 ± 10.3	67.9 ± 9.3
Gender ratio (male/female, n (%))		6 / 1 (85.7 / 14.3)	6 / 2 (75.0 / 25.0)
BMI (kg/m^2)		29.3 ± 4.3	29.3 ± 2.6
Smoking History (n, %)	Current	0 (0.0)	0 (0)
	Former	4 (57.1)	2 (25.0)
	Never	3 (42.9)	6 (75.0)
Heart Rate (bpm)		78.6 ± 9.4	71.0 ± 13.2
Systolic Blood Pressure (mmHg)		153.0 ± 29.3	153.0 ± 19.6
Diastolic Blood Pressure (mmHg)		83.7 ± 11.3	80.0 ± 11.4
Echocardiographic Data			
Peak pressure gradient (mmHg)		50.5 ± 13.0	49.2 ± 12.7
Mean Pressure Gradient (mmHg)		27.4 ± 7.5	27.0 ± 8.1
Aortic Valve Area (cm^2)		1.31 ± 0.40	1.20 ± 0.21
E/A		0.79 ± 0.17	0.76 ± 0.17
Average Septal E/e'		11.19 ± 1.01	14.48 ± 4.89
Average Lateral E/e'		9.34 ± 2.90	11.80 ± 3.73
Resting LVRPP (mmHg.bpm)		15400.5 ± 2627.3	13570.2 ± 3309.1
Exercise LVRPP (mmHg.bpm)		38888.7 ± 4365.0	34449.0 ± 5656.8
Cardiac MRI Data			
LVMI (g/m^2)		68.2 ± 13.9	65.4 ± 17.3
LVEDVI (ml/m^2)		81.59 ± 17.33	88.03 ± 15.07
LV Ejection Fraction (%)		58.3 ± 3.3	58.3 ± 4.4
Global PEDSR (1/s)		0.82 ± 0.17	0.80 ± 0.16
Global MPR		2.16 ± 0.44*	3.13 ± 0.38
Exercise Test			
Exercise time (min)		10.7 ± 3.3	11.2 ± 4.2
Peak HR (bpm)		146.6 ± 12.8	141.3 ± 8.9
Peak SBP (mmHg)		189.6 ± 23.3	178.4 ± 17.2

Abbreviations as for Table 21. * $p<0.05$ compared to High-LVMI subgroup.

Table 28. Sub-group analysis of PEDSR for FAS Population according to MPR

Region	Number analysable	Baseline	Week-6	Week-10
Group A (Low-MPR)				
Base	6	0.86 ± 0.22	1.10 ± 0.27	0.93 ± 0.21
Mid	5	0.83 ± 0.15	0.88 ± 0.12	0.81 ± 0.19
Apex	5	0.89 ± 0.20	0.86 ± 0.15	0.89 ± 0.25
Global	6	0.88 ± 0.80	1.03 ± 0 .30	0.86 ± 0.15
Group B (High-MPR)				
Base	6	0.86 ± 0.22	0.78 ± 0.18	0.86 ± 0.36
Mid	6	0.82 ± 0.14	0.80 ± 0.17	0.70 ± 0.19
Apex	4	0.62 ± 0.23	0.62 ± 0.26	0.59 ± 0.25
Global	6	0.80 ± 0.19	0.75 ± 0.12	0.76 ± 0.28

All p>0.05.

Table 29. Sub-group analysis of secondary endpoints for FAS Population according to MPR

	Number analysable	Baseline	Week-6	Week-10
Group A (Low-MPR)				
Exercise time (min)	6	11.0 ± 3.6	11.2 ± 3.8	11.5 ± 3.6
Exercise LVRPP (mmHg.bpm)	6	39148.9 ± 3052.2	35417.1 ± 7042.9	36882.7 ± 5799.2
Group B (High-MPR)				
Exercise time (min)	6	11.8 ± 3.7	11.7 ± 3.7	11.8 ± 4.2
Exercise LVRPP (mmHg.bpm)	6	33615.0 ± 6402.4	33085.4 ± 7839.0	34357.3 ± 4188.5

All p>0.05

4.9 Results summary

For the primary endpoint, there was a non-significant trend for PEDSR to increase from the baseline value to a higher value after 6 weeks of oral Ranolazine, and then reduce to a lower value at week-10, after stopping Ranolazine. On sub-group analysis, these trends were more apparent in the high-PPG (with a statistically significant increase in PEDSR at week-6 for the mid-slice and the average of basal

and mid slice values) and low-MPR sub-groups. The total exercise duration showed a trend towards increasing at week-6, with a lower exercise LVRPP. The trend for the exercise LVRPP to reduce at week-6 was mirrored in the same sub-groups that demonstrated an increase in PEDSR (high-PPG and low-MPR).

4.10 Discussion

4.10.1 PEDSR

This was a small prospective, open-label blinded end-point single-centre pilot study that aimed to assess the effects of Ranolazine on diastolic function and MPR in patients with moderate to severe AS and evidence of diastolic dysfunction at recruitment. There was no conclusive evidence in these data that Ranolazine improved PEDSR, though some interesting trends were demonstrated. However, there was a statistically significant increase in circumferential PEDSR demonstrated for the mid slice, and the average of basal and mid slice values in the high-PPG subgroup. Patients in this subgroup tended to be older, male and with reduced E/A.

The effect of Ranolazine in improving diastolic function has previously been demonstrated in both animal models(122, 176) and experimental in-vitro studies in human myocytes(121, 123). The exact mechanism for this effect is not entirely clear, but is thought to be related to the late Na^+ current inhibition by Ranolazine, leading to a decrease in intra-cellular-Na^+ dependent intracellular calcium concentration(121). There have only been a few small clinical studies assessing the effect of Ranolazine on diastolic function. In a study of ischaemic heart disease patients with previous MI (n=15), Ranolazine infusion improved regional diastolic function, measured by 2-dimensional invasive LV angiograohy in non-infarcted ischaemic segments(177). Another small study of patients with stable angina (n=22) demonstrated improvement in some echocardiographic parameters of diastolic function, but not others(174). A case report documented improvement in ischaemic burden and symptoms in a patient with patent grafts

but on-going ischaemia, most likely due to microvascular and diastolic dysfunction(178). Finally, a recently published randomised trial of Ranolazine in patients with heart failure with preserved EF (n=20) failed to demonstrate improvement in echocardiographic measures of diastolic function(175). A limitation in all the above-mentioned studies may be their small sample sizes.

The lack of statistical significance in our study may not reflect a lack of efficacy. The sample size of the study was small, with only fifteen patients having analysable tagging images for the primary endpoint, compared to an anticipated 16 at inception. Since the study commenced, we have also shown, as part of this thesis, that PEDSR may be less reproducible using tagging (SPAMM) at 3T, as used in this study, compared to CSPAMM tagging at 1.5T that was used to estimate the sample size(179). (Although we also showed FT to be more reproducible than tagging, the methodology had already been pre-set by the sponsor and the data acquisition and analysis for the Ranolazine sub-study had already been completed using Tagging prior to this.) Additionally, on discontinuation, mean PEDSR tended to return towards the baseline value, suggesting a possible genuine effect of Ranolazine. Sub-group analysis also demonstrated interesting differences, with mean PEDSR showing some improvement in the low-MPR and high-PPG subgroups. The suggestion that Ranolazine may have greater efficacy in improving diastolic function in those with more advanced disease (reduced perfusion reserve(108)) and ischaemia is purely a hypothesis at this stage. Finally, the maximum dose of Ranolazine used in our study was 750 mg bd (with two patients continuing on 500 mg bd), which is lower than the dose of 1000 mg bd used in most other studies mentioned above, which may partially account for the lack of efficacy.

4.10.2 MPR

Our study did not demonstrate improvement in global MPR in the overall population following 6 weeks of Ranolazine therapy. In a previous open-label pilot study of patients with coronary artery disease and perfusion defects on exercise

SPECT myocardial perfusion imaging (n=20), 4 weeks of treatment with Ranolazine led to an improvement in myocardial perfusion pattern and severity(124). This is thought to occur due to reduced diastolic wall stiffness caused by the late Na^+ current inhibition by Ranolazine, leading to reduced extra-vascular compression of the coronary microcirculation, and improved myocardial blood flow. However, another study by the same group using vasodilator stress (n=18), failed to show an improvement in myocardial perfusion(180). Exercise testing induces true ischaemia by a supply/demand mismatch, whereas vasodilator-stress induced perfusion defects result from regional heterogeneity in blood flow, which may not activate the late Na^+ current. In a more recent pilot study of patients with microvascular angina, Ranolazine did not lead to an improvement in coronary flow reserve, measured by Doppler echocardiography, in response to adenosine or cold pressor test(181).

4.10.3 Exercise testing

The total exercise time did show an increase at week-6, which was close to reaching statistical significance. This observation lends weight to the hypothesis that the small increase in PEDSR seen may be significant. We cannot discount that the increase in exercise capacity was related to improved technique on the treadmill, as there was no reduction in duration at week-10. However, the increase in exercise duration at week-6 was associated with a slightly reduced peak heart and blood pressure compared to baseline, and therefore a slightly lower exercise LVRPP (a measure of myocardial work), that were not sustained at week 10. There was also a trend for the exercise LVRPP to decrease from baseline to week-6, and then increase again at week-10, in the same subgroups that demonstrated an improved PEDSR at week-6 (high-PPG and low-MPR). No such changes were noted for resting LVRPP or resting HR / SBP.

Ranolazine may therefore increase myocardial efficiency during exercise, and the mechanism for this may be related to an improvement in PEDSR. Ranolazine has previously been shown to increase exercise duration in multiple studies of

patients with chronic stable angina(119, 120, 182). In the study of patients with heart failure with preserved ejection fraction (HFpEF), Ranolazine improved the V_E/V_{CO_2} slope, an index of ventilatory response to exercise, as well as the exercise duration(175). As mentioned in the Methods chapter, due to a fault in the gas analyser equipment, we were unfortunately unable to accurately quantify such measures of exercise capacity for this pilot study.

4.10.4 Limitations

The major limitation of this study is its small sample size, with a risk of a type II statistical error. However the study was always planned as a pilot and the primary purpose was to assess the effect size. Although this was also an open-label study, without placebo control, we did have the blinded endpoint analysis, which mitigates bias in measurement of the imaging endpoints.

4.10.5 Conclusions

In this small, proof-of-concept, pilot study, Ranolazine did not show a significant improvement in diastolic dysfunction or MPR, in patients with moderate to severe AS. However, some interesting signals were seen, with a trend towards an improved exercise capacity, despite lower exercise LVRPP with Ranolazine, suggesting improved myocardial efficiency, possibly due to subtle changes in diastolic function. Given the low power of the current study, a larger study in patients with severe AS and diastolic dysfunction is warranted and preferably conducted at 1.5T, with consideration of feature tracking to avoid data loss with tagging.

CHAPTER FIVE

5 BASELINE DATA: COMPARISON OF ASYMPTOMATIC PATIENTS WITH MODERATE TO SEVERE AS AND HEALTHY CONTROLS

5.1 Introduction

Patients with AS were compared to age and gender matched controls without valve disease. We aimed to establish normal values of MPR and other CMR parameters in matched controls, as most data on healthy controls are on younger controls with no co-morbidities. However, we wanted to see the incremental effect of AS on these parameters, and so deliberately chose not to exclude common co-morbidities such as treated hypertension and diabetes from our control cohort. We also wanted to confirm that LV remodeling occurs at this early asymptomatic stage of AS.

5.2 Patient Recruitment

Patients were recruited between April 2012 and October 2013. Initial recruitment was slower than anticipated, and therefore various measures were put in place to increase recruitment. This included relaxation of the exclusion criteria (from history of coronary disease to myocardial infarction within six months), addition of a Trial Manager, regular newsletter for the sites and the addition of new sites (Aberdeen, Dundee and Coventry), which dramatically improved recruitment from April 2013 (Figure 47).

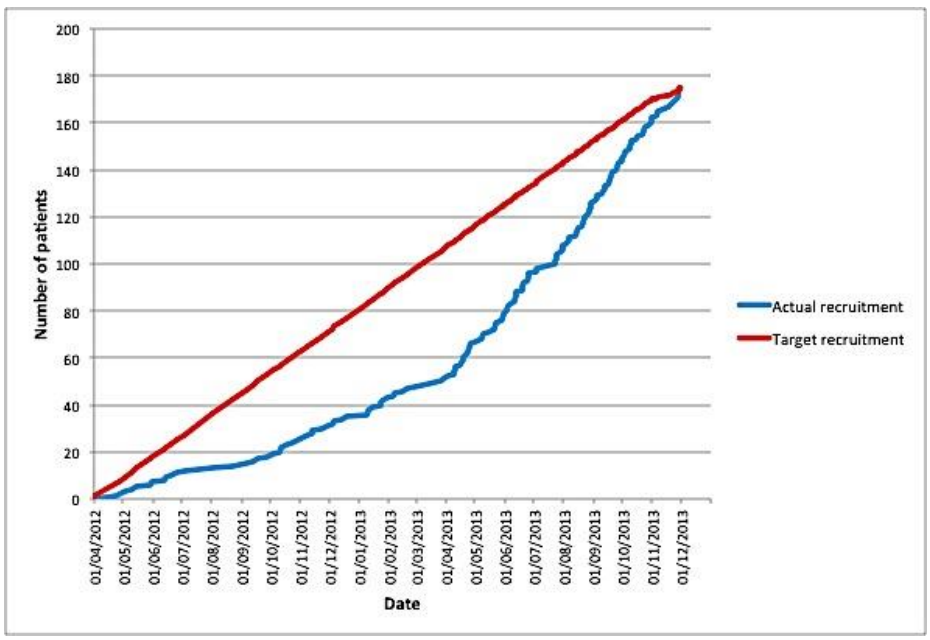

Figure 47. Recruitment graph

A total of 183 patients were consented to participate in the study. Nine of these were withdrawn for various reasons, as listed in Table 30. The final number of patients included in analysis was 174 (Figure 48). All the baseline visits for the regional sites (Kettering, Northampton, Grantham, Derby and Coventry) were performed in Leicester (n=126).

Table 30. Reasons for withdrawal from study

Type of withdrawal	Reason
Clinician (n=2)	Didn't meet inclusion criteria on echo after consent
Clinician (n=2)	Thought to be symptomatic on assessment after consent
Clinician (n=1)	Atrial fibrillation discovered after consent
Clinician (n=1)	Unable to cycle
Clinician (n=1)	MRI not performed
Patient (n=2)	Claustrophobic

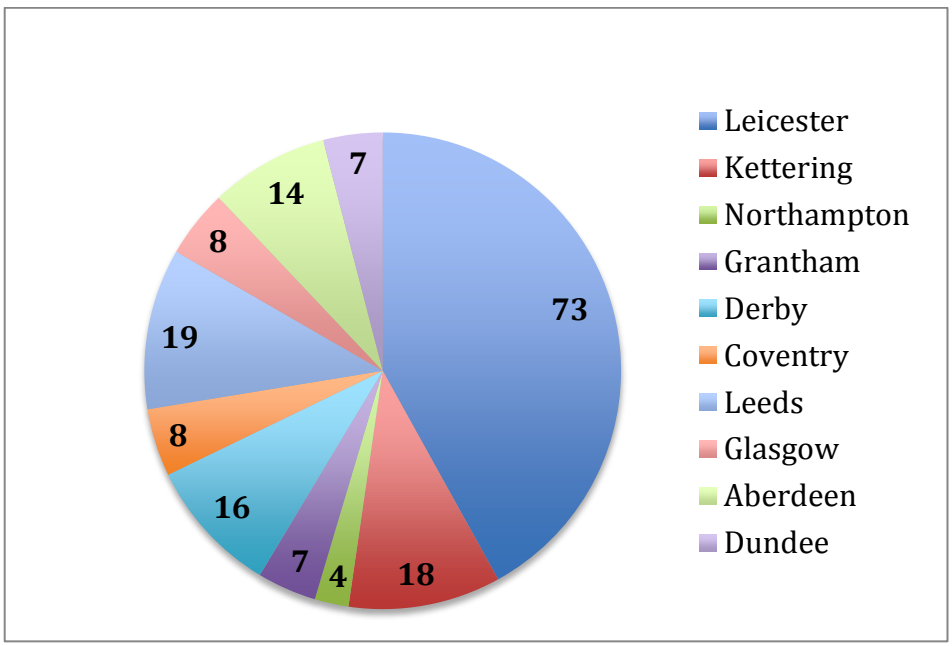

Figure 48. Recruitment numbers according to site

5.3 Healthy control recruitment

Healthy controls were recruited at a single centre (Leicester) through advertisement with posters and word of mouth. The initial aim had been to recruit twenty asymptomatic, age-matched controls without significant valve disease. Patients with common co-morbidities such as treated hypertension and diabetes were not excluded, so as to allow the assessment of the incremental effect of AS. However, four out of the first twenty controls had to be excluded due to unexpected findings on the tests (Table 31). In addition, due to the fault with the gas-analyser mentioned in Methods, some of the gas-exchange CPET data had to be excluded, as not all controls were able to return for a repeat CPET. A further seven controls were also recruited. The final numbers of usable healthy control data were: 23 controls in total and 19 with usable CPET data.

Table 31. Reasons for exclusion of Controls

Type of withdrawal	Reason
Clinician	LBBB on resting ECG
Clinician	Frequent atrial ectopics / runs of atrial tachycardia
Clinician	Broad complex tachycardia during CPET (asymptomatic)
Clinician	LVH with strain pattern on ECG, moderate LVH on CMR

5.4 Demographic data

The demographic data for the AS patients and healthy controls are displayed in Table 32. There was no significant difference in the age, gender distribution and resting haemodynamics between patients and controls. There was a greater incidence of hypertension and hyperlipidaemia in the patient group, though the resting SBP and proportion of statin use was similar. The incidence of diabetes was similar. NT-proBNP level was significantly higher in patients with AS. There was no significant difference in levels of haemoglobin, haematocrit, HbA1c or eGFR.

Table 32. Demographic data for patients and controls

	AS Patients (n=174)	Healthy Controls (n=23)	p-value
Age (years)	66.2 ± 13.3	68.3 ± 8.8	0.331
Male (n (%))	133 (76.4)	16 (69.6)	0.471
BSA (m^2)	2.0 ± 0.21	1.9 ± 0.18	0.615
BMI (kg/m^2)	28.0 ± 4.2	26.6 ± 3.5	0.129
Resting HR (bpm)	70.3 ± 11.4	72.6 ± 8.2	0.358
Resting SBP (mmHg)	146.9 ± 21.1	154.1 ± 25.0	0.136
Diabetes (n (%))	25 (14.4)	2 (8.7)	0.747
Hypertension (n (%))	93 (53.4)	6 (26.1)	0.014*
Hyperlipidaemia (n (%))	92 (52.9)	5 (21.7)	<0.001*
ACE-I/ARB (n (%))	77 (44.3)	5 (21.7)	0.044*
Beta-blocker (n (%))	54 (31.0)	1 (4.3)	0.006*
Statin	105 (60.3)	10 (43.5)	0.123
NT-proBNP (pmol/L)	56.5 (19.2, 152.5)	16.5 (0.30, 43.0)	<0.001*
Hb (g/dL)	14.2 ± 1.2	14.2 ± 1.2	0.835
Hct	0.425 ± 0.035	0.430 ± 0.036	0.544
HbA1c (%)	5.9 ± 0.81	6.1 ± 0.67	0.289
eGFR (ml/min)	88 ± 28.6	81 ± 20.4	0.286

Abbreviations: BSA=body surface area, HR=heart rate, SBP/DBP=systolic/diastolic blood pressure, ACE-I=angiotensin converting enzyme inhibitor, ARB=angiotensin II receptor blocker, NT-proBNP=N terminal brain natriuretic peptide, Hb=haemoglobin, Hct=haematocrit, eGFR=estimated glomerular filtration rate.

5.5 Echocardiographic and electrocardiographic data

The echocardiographic data for patients and controls is displayed in Table 33. All measures of AS severity were higher in patients compared to controls. Although there was no significant difference in E/A, the septal and lateral E/e' were significantly lower in controls. The longitudinal systolic strain and strain rate measured by speckle tracking were significantly reduced in patients with AS, but there was no significant difference in longitudinal diastolic strain rate. The resting LVRPP, was significantly higher in patients, though the difference in VAI did not

reach statistical significance. Only 10-18% of the patients with AS met the ECG criteria for LVH, using Sokolow / Cornell criteria, compared to none of the controls.

Table 33. Echocardiographic and electrocardiographic data for patients and controls

	AS patients (n=174)	Healthy Controls (n=23)	p-value
AV Vmax (m/s)	3.86 ± 0.56	1.35 ± 0.27	<0.001*
MPG (mmHg)	35.4 ± 12.5	4.2 ± 1.7	<0.001*
AVAI (cm^2/m^2)	0.57 ± 0.14	1.71 ± 0.36	<0.001*
E/A	0.88 ± 0.29	0.84 ± 0.23	0.499
Septal E/e'	12.28 ± 4.86	10.67 ± 3.34	0.049*
Lateral E/e'	9.88 ± 3.72	8.07 ± 2.97	0.026*
DPT (ms)	615.6 ± 157.5	599.7 ± 101.6	0.517
Longitudinal PSS (%)	-18.18 ± 2.76	-19.61 ± 2.25	0.020*
Longitudinal PSSR (1/s)	-1.00 ± 0.20	-1.16 ± 0.19	<0.001*
Longitudinal PEDSR (1/s)	0.79 ± 0.21	0.85 ± 0.21	0.174
Resting LVRPP ($mmHg.bpm.10^{-4}$)	1.37 ± 0.29	1.09 ± 0.23	<0.001*
VAI (Echo) ($mmHg/ml/m^2$)	3.96 ± 1.06	3.67 ± 0.76	0.220
Sokolow criteria (n(%))	18 (10.3)	0 (0)	0.138
Cornell criteria (n(%))	31 (17.8)	0 (0)	0.029*

Abbreviations: AV Vmax=peak aortic jet velocity, MPG=mean pressure gradient, AVAI=aortic valve area indexed to BSA, DPT=diastolic perfusion time, PSS=peak systolic strain, PSSR=peak systolic strain rate, PEDSR=peak early diastolic strain rate, LVRPP=left ventricular rate pressure product, VAI=valvulo-arterial impedance

5.6 CPET data

All patients with the exception of two completed the CPET (1 due to previous knee replacement, 1 due to equipment unavailability at the start). Gas-exchange data of the first 30 patients had to be excluded from analysis due to the faulty gas analyser. This left 142 patients with full CPET data, and 172 with exercise parameters without the gas-exchange data.

Table 34. CPET data for patients and controls

	AS patients (n=172)	**Healthy Controls** (n=23)	**p-value**
Exercise duration (min)	8.50 ± 2.01	9.10 ± 1.70	0.182
% predicted HR (%)	86.8 ± 11.8	93.2 ± 7.3	0.001*
Rise in SBP (mmHg)	41.0 ± 22.3	54.0 ± 19.4	0.016*
Exercise LVRPP ($mmHg.bpm.10^{-4}$)	3.52 ± 0.73	3.17 ± 0.42	0.002*
Peak VO_2 (ml/kg/min)	17.6 ± 5.6	18.9 ± 4.1	0.327
% Predicted VO_2 (%)	72.8 ± 17.3	76.3 ± 15.2	0.403
Peak workload achieved (W)	110 ± 40.1	125 ± 38.2	0.110
% Predicted workload (%)	86.4 ± 27.4	98.5 ± 23.7	0.050
Peak RER	1.12 ± 0.14	1.12 ± 0.08	0.999
Positive test (strict) (n(%))	19 (11.0)	1 (4.5)	0.040*
Positive test (conventional) (n(%))	55 (32.0)	2 (9.1)	<0.001*
Reason for stopping (n(%)):			0.468
Chest pain	4 (2.3)	0 (0.0)	
Dyspnoea	43 (25.0)	2 (9.1)	
General fatigue	22 (12.8)	5 (22.7)	
Leg fatigue	73 (42.4)	12 (54.5)	
Arrhythmia	1 (0.6)	0 (0.0)	
Hypertension	1 (0.6)	0 (0.0)	
Other	28 (16.3)	3 (13.6)	

Abbreviations: HR=heart rate, SBP=systolic blood pressure, LVRPP=left ventricular rate pressure product, VO2=oxygen uptake, RER=respiratory exchange ratio.

Table 34 demonstrates the exercise data for patients and controls. The controls achieved a higher percentage predicted heart rate, a greater rise in systolic blood pressure on exercise, but with a lower exercise LVRPP. Controls also achieved a greater workload and percentage predicted workload, though this did not reach statistical significance (p = 0.11 and 0.05 respectively). However, there was no significant difference seen in the total exercise duration, peak VO_2 and percentage predicted VO_2 between patients and controls. The proportion of AS patients with a positive test using the strict definition was 11%, compared to 32% using the conventional definition. Only 2 of the controls were classified as 'symptom-

limited', both stopping due to dyspnoea. The commonest reason for stopping for both patients and controls was fatigue, and the commonest symptom was dyspnoea.

5.7 CMR data

CMR was successfully acquired in all included patients and controls without complication.

5.7.1 Volumetric, myocardial deformation and distensibility data

Left and right ventricular volumetric analysis was possible in all patients. Left atrial short-axis stack was acquired in only 168 patients due to time constraints secondary to artefacts necessitating repeated imaging of certain slices, or in order to quicken the scan for patients poorly tolerating it. Assessment of distensibility was possible in 167 patients, while PWV was calculated in 165, due to artefacts. Myocardial deformation analysis was not possible in one patient due to prospectively acquired poor quality images.

Patients with AS had greater LV, RV and LA volumes and LV mass, as well as greater mass/volume (Table 35). The stroke volumes were also higher, with significantly lower EF (though still within the normal range). Longitudinal strain and strain rate (systolic and diastolic) were significantly lower in patients than controls. However, there were no significant differences in circumferential strain and strain rate values (systolic or diastolic). Aortic distensibilty was lower in controls than AS patients, reaching statistical significance for the ascending aorta. There was no significant difference in PWV.

Table 35. CMR volumetric, myocardial deformation and distensibility data for patients and controls

	AS patients (n=174)	Healthy Controls (n=23)	p-value
LVEDVI (ml/m^2)	87.58 ± 18.27	78.16 ± 9.40	<0.001*
LVESVI (ml/m^2)	38.28 ± 10.65	32.11 ± 5.03	<0.001*
LVSV (ml)	97.0 ± 23.2	89.0 ± 12.0	0.011*
LVSVI (ml/m^2)	49.31 ± 9.31	46.02 ± 5.97	0.027*
LVEF (%)	56.7 ± 4.95	58.9 ± 3.67	0.044*
LVMI (g/m^2)	57.69 ± 13.85	44.31 ± 7.20	<0.001*
LV mass/volume (g/ml)	0.66 ± 0.11	0.57 ± 0.08	<0.001*
LAVI (ml/m^2)	54.96 ± 14.76	46.83 ± 8.57	<0.001*
RVEDI (ml/m^2)	88.23 ± 15.15	82.31 ± 9.12	0.011*
VAI (MRI) (mmHg/ml/m^2)	3.81 ± 0.82	3.50 ± 0.74	0.078
Longitudinal PSS (%)	-18.48 ± 3.02	-20.43 ± 3.16	0.004*
Longitudinal PSSR (1/s)	-1.09 ± 0.24	-1.21 ± 0.25	0.034*
Longitudinal PEDSR (1/s)	1.09 ± 0.28	1.22 ± 0.31	0.038*
Circumferential PSS (%)	-28.10 ± 4.66	-29.45 ± 3.78	0.183
Circumferential PSSR (1/s)	-1.73 ± 0.39	-1.81 ± 0.32	0.396
Circumferential PEDSR (1/s)	1.67 ± 0.41	1.69 ± 0.41	0.867
AA distensibility (10^{-3}mmHg^{-1})	1.92 ± 1.19	1.34 ± 0.73	0.002*
DA distensibility (10^{-3}mmHg^{-1})	2.11 ± 1.48	1.67 ± 1.07	0.168
PWV (m/s)	8.40 ± 3.56	8.31 ± 2.35	0.881

Abbreviations: LVEDVI=left ventricular end-diastolic volume indexed to BSA, LVESVI=left ventricular end systolic volume indexed to BSA, LVSV=left ventricular stroke volume, LVSVI=LVSV indexed to BSA, LVEF=left ventricular ejection fraction, LVMI=left ventricular mass indexed to BSA, LAVI=left atrial volume indexed to BSA, RVESVI=right ventricular end diastolic volume indexed to BSA, VAI=valvulo-arterial impedance, PSS=peak systolic strain, PSSR=peak systolic strain rate, PEDSR=peak early diastolic strain rate, AA=ascending aorta, DA=descending aorta, PWV=pulse wave velocity

5.7.2 Contrast enhanced CMR

5.7.2.1 Myocardial blood flow and perfusion reserve

MPR calculation was not possible in nine patients as a result of problems with blood flow quantification due to artefacts or contrast being present in the first frame, in either or both the stress (n=8) and rest (n=5) perfusion images. Both global MPR and stress MBF were significantly lower in patients than controls, while there was no significant difference in resting MBF (Table 36). Total MBF, which is derived by multiplying MBF by the LVMI, was higher in patients at rest, given their higher LV mass, whereas it remained lower at stress (though not reaching statistical significance).

Table 36. CMR perfusion and fibrosis data for patients and controls

	AS patients (n=174)	**Healthy Controls** (n=23)	**p-value**
CMR Perfusion data			
Global MPR	2.27 ± 0.70	3.16 ± 0.65	<0.001*
Global stress MBF (ml/min/g)	2.16 ± 0.70	3.17 ± 0.54	<0.001*
Global rest MBF (ml/min/g)	0.98 ± 0.27	1.03 ± 0.25	0.421
Total stress MBF (ml/min/m^2)	122.36 ± 44.66	140.88 ± 32.57	0.068
Total rest MBF (ml/min/m^2)	55.54 ± 16.54	45.43 ± 10.73	<0.001*
CMR Fibrosis data			
LGE present (n,%)	82 (47.1)	5 (21.7)	0.025*
% LGE (%)	4.20 ± 3.76	2.00 ± 2.21	<0.001*
Native myocardial T1 (ms)	1131.9 ± 69.54	1092.3 ± 34.29	<0.001*
ECV (%)	24.82 ± 2.43	25.05 ± 2.57	0.680

Abbreviations: MPR=myocardial perfusion reserve, MBF=myocardial blood flow, LGE=late gadolinium enhancement, ECV=extracellular volume fraction

5.7.2.2 Late gadolinium enhancement

LGE images were acquired in all patients, but were non-analysable due to artefacts or incomplete LV coverage in 4 patients. There was a greater frequency and amount of focal fibrosis (measured on LGE) in patients than controls (Table 36). Amongst patients, significant non-ischaemic pattern LGE (grade 2-4: see

Table 7) was present in 60 patients. Infarct-pattern LGE was present in 26 patients, out of which 4 also had additional non-ischaemic pattern LGE. All LGE in healthy controls were grade-2 non-ischaemic pattern. Subtle insertion point only enhancement (grade-1) was found in an additional 33 patients and 4 controls, but was not considered a significant finding.

5.7.2.3 T1 mapping and extracellular volume

Assessment of diffuse interstitial fibrosis was possible in 121 patients, as T1 mapping was unavailable for 53 scans. ECV calculation was possible for a total of 117 patients, due to post-contrast T1 mapping being absent (n=2) or haematocrit being unavailable (n=2). Although native myocardial T1 was significantly higher in patients, there was no significant difference in ECV between patients and controls in our study.

5.8 Summary and Discussion

In summary, patients and controls were well matched for age, gender and resting haemodynamics, despite there being a higher incidence of co-morbidities and cardiovascular medication use amongst patients.

5.8.1 Echocardiographic and exercise parameters

The echocardiographic data confirmed AS amongst patients, who also demonstrated evidence of diastolic dysfunction (higher septal and lateral E/e'), compared to controls. There have not been many studies directly comparing exercise capacity between AS patients and matched controls. In combination with the exercise data, our AS cohort demonstrated higher LVRPP (myocardial work) at rest and during exercise, as expected, despite achieving significantly lower % predicted HR and rise in SBP on exercise than controls, which has been shown before(183, 184).

The peak workload was non-significantly lower in the AS group due to a wide range of values and high standard deviations in both patients and controls,

though the %predicted workload was close to reaching statistical significance (p=0.05). This is similar to the results in Donal *et al's* study of 207 AS patients, where no difference in peak workload or total exercise duration was found between age- and gender-matched controls and the overall patient group(184). On the contrary, in Clynes's study, peak workload was significantly lower in the 14 asymptomatic patients with AS (majority severe) who completed a bicycle ETT compared to matched controls, as was their total exercise duration(183). However, the majority of their patients had severe AS and controls had no known co-morbidities, which may explain the differences. Somewhat surprisingly, no significant difference was seen in the peak VO_2 or % predicted VO_2 between our patients and controls, which is contrary to the findings in Clyne's study in the cohort who performed a treadmill CPET. Some of these differences may partly be due to an older cohort of controls being used in our study, as VO_{2max} is thought to decline by 10% per decade with age(185). In fact, the peak VO_2 achieved by the patients (26.7) and controls (36.3) in Clyne's study (mean age in their 40's) was much higher than our cohort (mean age in 60's), though this was using treadmill rather than bicycle test. In Donal's study on older subjects (mean age around 67 years), there was also no difference in total exercise duration between patients and matched controls using bicycle ETT. An alternative explanation for the similarities between our patients and controls may be that these asymptomatic patients are still in a state of compensated hypertrophy, despite moderate to severe AS.

Two of the healthy controls also stopped exercise due to symptoms of 'dyspnoea', which highlights one of the limitations of exercise testing in the real-world elderly population, with the subjective nature of describing the reasons for terminating exercise. This, in combination with the wide range of peak workloads achieved, may partly explain previously observed the low specificity of a positive exercise test in predicting outcome in this group of relatively elderly patients(32, 42, 43). The determinants and mechanisms relating to exercise limitation are further explored in Chapter-6.

5.8.2 LV remodeling

The chronic pressure overload caused by AS is known to cause initially adaptive and then maladaptive LVH, as well as changes within the myocardial extracellular matrix(129). The CMR data demonstrated evidence of clear LV remodeling amongst the patient group compared to controls (12-19% higher LV volumes and 30% higher mass). This was despite all patients being asymptomatic, and many with only moderate AS, confirming the presence of LV remodeling even at this early stage of the disease process, as demonstrated in the schematic in Figure 49.

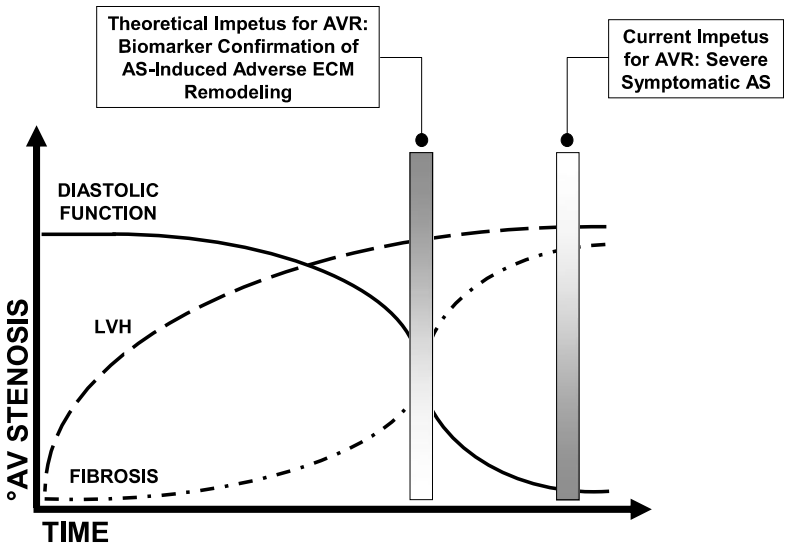

Figure 49. Schematic demonstrating the changes of LV remodeling with chronic pressure overload in AS (reproduced from (129))

5.8.3 Aortic stiffness parameters

There was no difference in PWV or DA distensibility between AS patients and controls, whilst the AA distensibility was higher in patients than controls. A possible reason for the lower AA distensibility in our control group could be higher pulse pressures in this group of older controls with hypertension. There have not been many studies comparing measures of aortic elasticity / stiffness between AS patients and controls. Most studies have compared younger patients with bicuspid AV (BAV) without significant disease to controls, and found lower distensibility and higher PWV in these patients, using both TTE and CMR(10, 186). In one TTE study comparing patients with BAV stenosis (n=32, mean AVA

1.34±0.59cm^2) to controls, although aortic stiffness index was significantly higher in patients, there was no difference found in aortic root distensibility(187). Other studies comparing degenerative AV disease to controls have shown mixed reports. No difference in PWV was shown when comparing controls to patients with aortic sclerosis (n=62) in a TTE study(188), as well as to elderly patients with severe AS (n=40) in an invasively measured cardiac catheterisation study(189). Markers of AS severity did not predict PWV in this study either. On the other hand, increased aortic stiffness index (measured on TTE) was demonstrated in 12 patients with severe AS undergoing AVR(190), whilst Liu et al also showed higher PWV in 30 patients with degenerative AS compared to matched controls(118). A limitation of most of these studies have been their small sample size, and not many studies have employed CMR to compare parameters between AS and controls.

5.8.4 Myocardial perfusion

To our knowledge, this is the first study directly comparing CMR measured MBF/MPR in asymptomatic AS patients to controls. MPR and stress MBF were significantly lower in patients with AS than controls, with no significant difference in the rest MBF. This finding is consistent with the only other study comparing MBF in AS to controls, which was done using PET(24). TTE studies assessing coronary flow reserve (CFR) have also shown similar findings of lower CFR in AS than controls(21, 191). A previous study at our centre measuring MPR by CMR in severe (mostly symptomatic) AS demonstrated slightly lower values of MPR (2.03±0.55) and markedly reduced stress MBF (1.77±0.47), though there were no controls in that study. These data would suggest a linear progression of pathology with increasing severity of AS, and support the hypothesis of a relatively greater degree of capillary dilatation at rest to compensate for the increased LV mass with increasing severity of AS, leading to normal resting MBF. This is thought to be due to a relative reduction in capillary density due to increased rate of cellular hypertrophy in comparison to capillary angiogenesis(23, 192). As a result, there is an inability to increase MBF adequately on stress, resulting in the lower MPR in

patients. This hypothesis is further supported by our finding of a significantly higher 'total rest MBF' in patients than controls, which was not different when normalised to per unit of muscle mass. The determinants and mechanisms of MPR are further explored in Chapter-6.

5.8.5 Myocardial deformation

The myocardial deformation data demonstrated impaired longitudinal strain and strain rates in AS compared to controls, but no difference in circumferential values. This has been well described in the literature, with many studies showing impaired long-axis function or global longitudinal strain (GLS) in patients with AS and preserved EF, compared to controls(27, 193, 194). GLS has also been shown to be associated with LVMI(193, 194), AS severity(193), reduced exercise capacity(27) and a predictor of outcome(27, 39, 64, 111) in AS.

There have not been many studies comparing multi-directional strain and strain rates between AS and controls. In one TTE study by Lafitte *et al*, GLS was significantly reduced in asymptomatic severe AS patients compared to controls, with no difference in circumferential or radial strain(27). On the contrary, another TTE study comparing myocardial deformation in different grades of AS to aortic sclerosis showed an incremental fall in longitudinal as well as circumferential and radial parameters with increasing AS severity, though they included symptomatic patients as well. There was a suggestion in that study of longitudinal function being affected before circumferential, with no difference in circumferential values between aortic sclerosis and mild AS on post-hoc analysis, as well as symptomatic patients demonstrating more impaired multidirectional function than asymptomatic. A study by Delgado et al comparing severe AS (mostly symptomatic) to controls also found significantly lower longitudinal and circumferential parameters in patients than controls, though interestingly, the difference was not significant for circumferential strain between hypertensive controls and AS patients, nor for radial strain between any groups(61).

One explanation for these findings might be that the subendocardial myocardial fibres are known to be orientated longitudinally, whilst the circumferential fibres are located in the mid-wall of the myocardium. As a result, any impairment of myocardial perfusion via microvascular ischaemia, which tends to affect the sub-endocardium first leads to selective impairment in the longitudinal function. An animal model study using aortic banding to create pressure-overload demonstrated impaired sub-endocardial blood flow in dogs with LVH, compared to the sub-epicardium and controls, which was associated with abnormal sub-endocardial contractile function(195). Another study using a pig model of acute pressure overload demonstrated earlier impairment in longitudinal strain, with preserved radial strain, at lower increase in LV afterload(196).

5.8.6 LGE and T1 mapping

Focal fibrosis (LGE) was significantly more prevalent in patients with AS, though ECV was not significantly different. As described in the Introduction, LGE has been found to be present in 27-65%(25, 89, 91, 93, 101) of patients with AS, with the amount of LGE being reported between 3.0-7.3% of the LV mass, compared to the prevalence being 47% in out cohort. The amount of LGE in our cohort was 4.2%, compared to 7.3% in Flett's study(101), though their cohort consisted of severe and mostly symptomatic patients with AS. Also of note, some LGE was also found in our control group (all grade-2 or below), compared to none in the controls studied by Flett. This is again likely to be due to the presence of co-morbidities including hypertension and diabetes being excluded in their cohort.

We have already published data from this work showing that ECV was not significantly increased in asymptomatic patients with AS, compared to age and sex-matched controls(197). This finding is contrary to others who have demonstrated significantly higher T1 and ECV in patients with AS than healthy controls(98-100). However, the healthy control groups in most studies were not age-matched to the patient group(100, 163, 164), and controls with any history of hypertension, diabetes or other cardiovascular risk factors were excluded(98,

101). A correlation between age and ECV has been demonstrated in one study(95), but not in others(99, 101). We age-matched and deliberately included controls with common co-morbidities, since we wanted to see the true incremental effect of AS. One recent study also did not demonstrate any significant difference in the native T1 value between AS and controls (1191 ± 34 *vs.* 1180 ± 28 ms respectively, p=0.29), and although the ECVs were higher in the AS group, their controls were significantly younger(100). In Bull's study, where the controls were age-matched to the patient population, there was no difference in native T1 values between controls and patients with moderate AS. There was also a large overlap between moderate and asymptomatic severe AS, as well as a significant difference between asymptomatic severe AS and symptomatic severe AS(98). More recently it has been shown that native T1 is also influenced by changes in the intravascular compartment, and doesn't just reflect interstitial fibrosis. Mahmod's *et al*(169) performed T1 mapping at rest and during adenosine vasodilator stress in patients with severe AS and demonstrated that although resting T1 values were significantly higher in AS than controls, this difference was no longer significant on hyperaemic stress. Even though T1 increased in both, the ΔT1 was significantly blunted in AS. This would also further support the above-mentioned hypothesis of near maximal vasodilation in AS at rest, leading to a more blunted response at stress.

5.9 Conclusions

In conclusion, patients with AS demonstrated evidence of higher myocardial workload (LVRPP), LV remodeling, impaired longitudinal function, reduced stress MBF / MPR, and a greater degree of focal myocardial fibrosis than matched controls, despite being asymptomatic. However, there was no significant difference in exercise capacity (VO_2), circumferential strain / strain rates, rest MBF and ECV.

CHAPTER 6

6 DETERMINANTS OF EXERCISE CAPACITY AND MYOCARDIAL PERFUSION IN AS

6.1 Introduction

The mechanisms leading to reduced exercise capacity in AS are likely to be the similar to those that lead to symptom development; reduced exercise capacity has also been shown to be a poor prognostic marker in AS(32, 33, 42). Understanding the determinants of exercise limitation is therefore vital to increasing our understanding of the pathophysiology of disease progression and symptom development in AS. Reduced MPR is likely to play an important role in limiting exercise capacity in these patients. In fact, it was shown to be the only independent predictor of peak VO_2 in patients with severe AS undergoing AVR, and was inversely proportional to NYHA class symptoms(108). However, there is scarce data on the determinants of MBF and MPR in asymptomatic patients with moderate to severe AS.

6.2 Determinants of exercise capacity

6.2.1 Associations with age and sex corrected peak VO_2

As mentioned in Chapter-5, VO_2 data was available for 142 of the patients. The univariate associations of age and sex-corrected peak VO_2 in these patients is shown in Table 38 and Table 39.

Peak VO_2 was directly correlated with AVAI, longitudinal and circumferential strain, MPR and PWV, while inversely correlated with NT-proBNP, VAI, LV mass/volume, rest MBF, coronary calcium score and Cornell LVH criteria on ECG.

Table 38. Univariate associations of age and sex-corrected peak VO2: anthropometric, echocardiographic and CT variables

Variable	Estimate (95% CI)	p-value
Log (NT-proBNP) (log pmol/L)	-0.52 (-0.96, -0.07)	0.023*
AVAI (cm^2/m^2)	7.42 (1.96, 12.88)	0.008*
MPG (mmHg)	-0.02 (-0.08, 0.04)	0.477
AV Vmax (m/s)	-0.65 (-1.98, 0.69)	0.340
Septal E/e' (cm/s)	0.05 (-0.13, 0.24)	0.566
Lateral E/e' (cm/s)	0.09 (-0.17, 0.34)	0.507
PSS-L (TTE) (%)	-0.66 (-0.97, -0.34)	<0.001*
PSSR-L (TTE) (1/s)	-4.00 (-8.59, 0.58)	0.086
PEDSR-L (TTE) (1/s)	2.56 (-2.44, 7.55)	0.312
VAI (TTE) (mmHg/ml/m2)	-1.28 (-2.00, -0.57)	0.001*
AV Ca^{2+} score (500 Agatston)	0.08 (-0.16, 0.32)	0.529
Coronary Ca^{2+} score (500 Agatston)	-0.42 (-0.76, -0.07)	0.019*
Cornell criteria LVH (mm)	-0.10 (-0.19, -0.00)	0.042*
Sokolow criteria LVH (mm)	-0.01 (-0.09, 0.08)	0.867

Abbreviations: AV Vmax=peak aortic jet velocity, MPG=mean pressure gradient, AVAI=aortic valve aread indexed, PSS=peak systolic strain, PSSR=peak systolic strain rate, PSEDSR=peak early diastolic strain rate, L=longitudinal, VAI=valvulo-arterial impedance, AoV Ca^{2+} score=aortic valve calcium score, LVH=left ventricular hypertrophy, TTE=trans-thoracic echocardiogram. (*p<0.05).

All tables: Estimates correspond to change in the mean of the variable being tabulated per unit change in the variable of interest unless otherwise indicated.

For stepwise multivariate analysis, the following variables were entered into the model (p<0.10 on univariate analysis and/or clinically significant): age, gender, log(NT-proBNP), AVAI, PSS-L(TTE), PSSR-L(TTE), VAI(TTE/CMR), LVMI, LV mass/volume, PSS-C(CMR), LVEF, MPR, rest MBF, stress MBF, native T1, ECV, LGE%, PWV and Cornell criteria.

The independent associates of age and sex-corrected peak V_{O_2} were gender, PSS-L(TTE) and MPR (Table 40).

Table 39. Univariate associations of age and sex-corrected peak VO_2: CMR variables

Variable	Estimate (95% CI)	p-value
VAI (CMR) (mmHg/ml/m2)	-1.02 (-2.04, -0.01)	0.049*
LVEDVI (mL/m^2)	-0.00 (-0.05, 0.04)	0.838
LVESVI (mL/m^2)	-0.04 (-0.12, 0.04)	0.329
LAVI (mL/m^2)	0.02 (-0.04, 0.07)	0.530
LVEF (%)	0.16 (-0.00, 0.33)	0.056
LVMI (g/m^2)	-0.06 (-0.12, 0.00)	0.054
LV mass/volume (g/mL)	-8.3 (-15.5, -1.04)	0.025*
MPR (ratio)	1.64 (0.51, 2.77)	0.005*
Rest MBF (mL/min/g)	-5.04 (-7.86, -2.22)	0.001*
Stress MBF (mL/min/g)	0.17 (-0.99, 1.34)	0.769
LGE presence (Y vs N)	0.83 (-0.74, 2.40)	0.298
% LGE (%)	-0.18 (-0.39, 0.03)	0.094
Native T1 (ms)	-0.01 (-0.02, 0.01)	0.278
ECV (%)	0.06 (-0.31, 0.42)	0.756
PSS-C (CMR) (%)	-0.17 (-0.33, -0.00)	0.045*
PSSR-C (CMR) (1/s)	-0.46 (-2.42, 1.49)	0.641
PEDSR-C (CMR) (1/s)	1.57 (-0.47, 3.61)	0.130
PSS-L (CMR) (%)	-0.18 (-0.45, 0.09)	0.196
PSSR-L (CMR) (1/s)	0.65 (-2.53, 3.84)	0.685
PEDSR-L (CMR) (1/s)	-1.20 (-4.05, 1.66)	0.409
PWV (m/s)	0.30 (0.08, 0.52)	0.009*

Abbreviations: VAI=valvulo-arterial impedance, LVED/SVI=left ventricular end-diastolic/systolic volume indexed to BSA, LAVI=left atrial volume indexed to BSA, LVEF=LV ejection fraction, LVMI=LV mass indexed to BSA, MBF=myocardial blood flow, MPR=myocardial perfusion reserve, LGE=late gadolinium enhancement, ECV=extracellular volume fraction, PSS=peak systolic strain, PSSR=peak systolic strain rate, PSEDSR=peak early diastolic strain rate, C=circumferential, L=longitudinal, PWV=pulse wave velocity. (*p<0.05)

Table 40. Multivariate associations of age and sex-corrected peak VO_2

Variable	HR (95% CI)	p-value
Gender (M)	5.27 (2.62, 7.92)	<0.001
PSS-L (TTE)	-0.39 (-0.75, -0.03)	0.039
MPR	2.00 (0.69, 3.31)	0.004

Abbreviations: as above.

6.2.2 Associations with age and sex corrected peak workload

The univariate associations of age and sex-corrected peak workload are shown in Table 41 and Table 42. This was positively associated with MPR and negatively with NT-proBNP, lateral E/e' and rest MBF.

Table 41. Univariate associations of age and sex corrected peak workload: anthropometric and echocardiographic variables

Variable	Estimate (95% CI)	p-value
Log (NT-proBNP)	-3.32 (-5.97, -0.67)	0.014*
AVAI	0.87 (-32.2, 30.49	0.957
MPG	-0.15 (-0.49, 0.20)	0.404
AV Vmax	-3.77 (-11.5, 3.95)	0.336
VAI Echo	-0.48 (-4.67, 3.70)	0.820
Septal E/e'	-0.83 (-1.94, 0.27)	0.138
Lateral E/e'	-1.77 (-3.26, -0.29)	0.020*
PSS-L (TTE)	-1.29 (-3.03, 0.44)	0.143
PSSR-L (TTE)	-12.4 (-35.7, 11.0)	0.296
PEDSR-L (TTE)	-2.71 (-27.7, 22.3)	0.831
Change in MPG on exercise	0.38 (-0.03, 0.79)	0.068

Abbreviations: AV Vmax=peak aortic jet velocity, MPG=mean pressure gradient, AVAI=aortic valve aread indexed, PSS=peak systolic strain, PSSR=peak systolic strain rate, PSEDSR=peak early diastolic strain rate, L=longitudinal, VAI=valvulo-arterial impedance, TTE=trans-thoracic echocardiogram. (*p<0.05) Units as above.

For stepwise multivariate analysis, the following variables were entered into the model (p<0.10 on univariate analysis and/or clinically significant): age, gender, log(NT-proBNP), lateral E/e', LVMI, LV mass/volume, VAI(CMR), PSS-C(CMR), MPR, rest/ stress MBF, native T1, ECV, LGE% and change in MPG on exercise.

The independent associations of peak workload were log(NT-proBNP) and VAI(CMR), in addition to age and gender (Table 43).

Table 42. Univariate associations of age and sex corrected peak workload: CMR variables

Variable	Estimate (95% CI)	p-value
VAI (CMR)	-3.25 (-8.97, 2.47)	0.263
LVEDVI	0.03 (-0.22, 0.28)	0.797
LVESVI	-0.08 (-0.51, 0.36)	0.724
LAVI	-0.00 (-0.31, 0.31)	0.999
LVEF	0.64 (-0.26, 1.55)	0.163
LVMI	0.03 (-0.31, 0.37)	0.872
LV mass/volume	-4.38 (-44.2, 35.39)	0.828
MPR	6.92 (0.25, 13.59)	0.042*
Rest MBF	-23.0 (-39.8, -6.12)	0.008*
Stress MBF	0.24 (-6.50, 6.99)	0.943
LGE presence	-3.29 (-12.1, 5.48)	0.460
LGE %	-0.80 (-1.99, 0.39)	0.186
ECV	-0.71 (-2.96, 1.53)	0.529
PSS-C (CMR)	-0.83 (-1.77, 0.12)	0.085
PSSR-C (CMR)	-3.96 (-15.2, 7.27)	0.487
PEDSR-C (CMR)	0.53 (-11.1, 12.1)	0.928
PSS-L (CMR)	0.05 (-1.49, 1.59)	0.948
PSSR-L (CMR)	9.51 (-8.54, 27.6)	0.300
PEDSR-L (CMR)	-13.4 (-29.9, 3.19)	0.113

Abbreviations: VAI=valvulo-arterial impedance, LVED/SVI=left ventricular end-diastolic/systolic volume indexed to BSA, LAVI=left atrial volume indexed to BSA, LVEF=LV ejection fraction, LVMI=LV mass indexed to BSA, MBF=myocardial blood flow, MPR=myocardial perfusion reserve, LGE=late gadolinium enhancement, ECV=extracellular volume fraction, PSS=peak systolic strain, PSSR=peak systolic strain rate, PSEDSR=peak early diastolic strain rate, C=circumferential, L=longitudinal, PWV=pulse wave velocity. (*p<0.05). Units as above.

Table 43. Multivariate associations of age and sex corrected peak workload

Variable	HR (95% CI)	p-value
Age	-1.27 (-1.70, -0.85)	<0.001
Gender (M)	38.84 (27.59, 50.10)	<0.001
Log(NT-proBNP)	-4.36 (-6.80, -1.91)	0.001
VAI (CMR)	-7.00 (-13.1, -0.86)	0.027

Abbreviations: as above.

6.3 Determinants of myocardial perfusion

6.3.1 Associations with MPR

As outlined in chapter-5, MPR was quantifiable in 165 patients. The univariate associations of global MPR are listed in Table 44 and Table 45. MPR was inversely related to age, NT-proBNP, AS severity, LV mass/volume, ECV, AoV and coronary calcium scores, VAI (CMR) and resting LVRPP. It was directly related to longitudinal strain and diastolic strain rate on echo and exercise LVRPP. We deliberately excluded other exercise parameters, as a low MPR is likely to impair exercise tolerance, rather than the other way round.

Table 44. Univariate associations of MPR: anthropometric, echocardiographic and CT variables

Variable	Estimate (95% CI)	p-value
Age (per year)	-0.02 (-0.03, -0.01)	<0.001*
Gender (M)	0.11 (-0.14, 0.37)	0.380
NT-proBNP	-0.11 (-0.16, -0.05)	<0.001*
AV Vmax	-0.37 (-0.55, -0.18)	<0.001*
MPG	-0.01 (-0.02, -0.01)	0.001*
AVAI	0.89 (0.13, 1.66)	0.022*
Septal E/e'	-0.02 (-0.05, 0.01)	0.128
Lateral E/e'	0.03 (-0.01, 0.07)	0.110
PSS-L (TTE)	-0.07 (-0.11, -0.02)	0.005*
PSSR-L (TTE)	-0.22 (-0.84, 0.40)	0.477
PEDSR-L (TTE)	0.80 (0.20, 1.40)	0.009*
VAI (TTE)	-0.08 (-0.18, 0.02)	0.123
AoV Ca^{2+} score	-0.05 (-0.08, -0.02)	0.002*
Log (AoV Ca^{2+} score)	-0.17 (-0.30, -0.05)	0.007*
Log (Coronary Ca^{2+} score)	-0.09 (-0.15, -0.03)	0.002*

Abbreviations: AV Vmax=peak aortic jet velocity, MPG=mean pressure gradient, AVAI=aortic valve aread indexed, PSS=peak systolic strain, PSSR=peak systolic strain rate, PSEDSR=peak early diastolic strain rate, L=longitudinal, VAI=valvulo-arterial impedance, AoV Ca^{2+} score=aortic valve calcium score, TTE=trans-thoracic echocardiogram. (*p<0.05). Units as above.

Table 45. Univariate associations of MPR: CMR variables

Variable	Estimate (95% CI)	p-value
VAI (CMR)	-0.22 (-0.35, -0.09)	0.001*
LVEDVI	0.00 (-0.00, 0.01)	0.480
LVEF	0.01 (-0.01, 0.03)	0.402
LV mass/volume	-1.55 (-2.48, -0.63)	0.001*
LVMI	-0.00 (-0.01, 0.00)	0.259
Stress MBF	0.69 (0.58, 0.80)	<0.001*
Rest MBF	-0.94 (-1.31, -0.56)	<0.001*
LGE presence	0.04 (-0.17, -0.26)	0.694
LGE %	-0.02 (-0.05, 0.01)	0.237
Native T1 (ms)	0.00(-0.00, 0.00)	0.432
ECV	-0.08 (-0.13, -0.03)	0.002*
AA distensibility	0.09 (-0.01, 0.18)	0.066
PWV	-0.02 (-0.05, 0.01)	0.190
PSS-C (CMR)	-0.01 (-0.03, 0.02)	0.545
PSSR-C (CMR)	0.15 (-0.13, 0.43)	0.281
PEDSR-C (CMR)	0.13 (-0.14, 0.40)	0.349
PSS-L (CMR)	-0.00 (-0.04, 0.03)	0.863
PSSR-L (CMR)	0.20 (-0.25, 0.65)	0.374
PEDSR-L (CMR)	0.23 (-0.16, 0.62)	0.240

Abbreviations: VAI=valvulo-arterial impedance, LVEDVI=left ventricular end-diastolic volume indexed to BSA, LVEF=LV ejection fraction, LVMI=LV mass indexed to BSA, MBF=myocardial blood flow, LGE=late gadolinium enhancement, ECV=extracellular volume fraction, AA=ascending aorta, PWV=pulse wave velocity, PSS=peak systolic strain, PSSR=peak systolic strain rate, PSEDSR=peak early diastolic strain rate, C=circumferential, L=longitudinal. (*p<0.05). Units as above.

Table 46. Multivariate associations of MPR

Variable	HR (95% CI)	p-value
AV Vmax	-0.40 (-0.52, -0.27)	<0.001
ECV	-0.09 (-0.17, -0.02)	0.018

Abbreviations: as above.

For stepwise multivariate analysis, clinically and/or statistically significant univariate variables ($p<0.10$) were entered into the model, after removing any co-linear variables (e.g., including the most significant of AV Vmax, MPG and AVAI): age, gender, log(NT-proBNP), AV Vmax, septal/lateral E/e', VAI(CMR), LV Mass/Volume, LVMI, LGE presence/%, native T1, ECV, AA distensibility, AV Ca^{2+} score and log (coronary Ca^{2+} score). Myocardial deformation parameters were excluded from multivariate analysis, as again, a low MPR is likely to cause impaired strain, rather than the other way round.

AV Vmax and ECV remained independently associated with MPR (Table 46).

6.3.2 Associations with rest MBF

The univariate associations of rest MBF are shown in Table 47 and Table 48. Rest MBF was directly correlated with markers of myocardial deformation and LVEF, and it was negatively correlated with LA/LV volumes, LVMI and %LGE. There was no correlation with measures of AS severity, except CMR-derived VAI.

For stepwise multivariate analysis, the following variables were entered into the model: age, gender, log(NT-proBNP), AV Vmax, septal E/e', VAI (CMR), LVEDVI, LAVI, LVEF, LVMI, LGE %, native T1, ECV, AV Ca^{2+} score and log (coronary Ca^{2+} score).

The independent associations of rest MBF were female gender, septal E/e', LAVI and log (coronary Ca^{2+} score) (Table 49).

Table 47. Univariate associations of rest MBF: anthropometric, echocardiographic and CT variables

Variable	Estimate (95% CI)	p-value
Age	-0.00 (-0.00, 0.00)	0.801
Gender (M)	-0.21 (-0.30, -0.11)	<0.001*
Log (NT-proBNP)	-0.00 (-0.02, -0.02)	0.964
AV Vmax	0.03 (-0.04, 0.10)	0.433
MPG	0.00 (-0.00, 0.00)	0.538
AVAI	-0.20 (-0.49, 0.09)	0.185
Septal E/e'	0.00 (-0.01, 0.01)	0.422
Lateral E/e'	0.00 (-0.01, 0.02)	0.787
PSS-L (TTE)	-0.00 (-0.02, 0.01)	0.727
PSSR-L (TTE)	-0.33 (-0.56, -0.10)	0.006*
PEDSR-L (TTE)	0.12 (-0.11, 0.36)	0.307
VAI (TTE)	0.03 (-0.01, 0.07)	0.111
AoV Ca^{2+} score	-0.00 (-0.02, 0.01)	0.504
Log (AoV Ca^{2+} score)	-0.02 (-0.07, 0.03)	0.494
Log (Coronary Ca^{2+} score)	0.02 (-0.01, 0.04)	0.158

Abbreviations: AV Vmax=peak aortic jet velocity, MPG=mean pressure gradient, AVAI=aortic valve aread indexed, PSS=peak systolic strain, PSSR=peak systolic strain rate, PSEDSR=peak early diastolic strain rate, L=longitudinal, VAI=valvulo-arterial impedance, AoV Ca^{2+} score=aortic valve calcium score, TTE=trans-thoracic echocardiogram. (*p<0.05). Units as above.

Table 48. Univariate associations of rest MBF: CMR variables

Variable	Estimate (95% CI)	p-value
VAI (CMR)	0.07 (0.02, 0.12)	0.008*
LVEDVI	-0.00 (-0.01, -0.00)	0.004*
LAVI	-0.00 (-0.01, -0.00)	0.006*
LVEF	0.01 (0.00, 0.02)	0.013*
LV mass/volume	-0.11 (-0.48, 0.25)	0.534
LVMI	-0.00 (-0.01, 0.00)	0.004*
LVMI group (high *vs.* low)	-0.05 (-0.13, 0.03)	0.228
Stress MBF	0.14 (0.09, 0.20)	<0.001*
MPR	-0.14 (-0.19, -0.08)	<0.001*
LGE presence	0.07 (-0.01, 0.15)	0.081
LGE %	-0.01 (-0.02, -0.00)	0.016*
Native T1 (ms)	-0.00(-0.00, 0.00)	0.060
ECV	0.01 (-0.02, 0.03)	0.638
AA distensibility	0.00 (-0.04, 0.04)	0.976
PWV	-0.01 (-0.02, 0.00)	0.183
PSS-C (CMR)	-0.00 (-0.01, 0.01)	0.555
PSSR-C (CMR)	-0.13 (-0.23, -0.03)	0.014*
PEDSR-C (CMR)	0.17 (0.07, 0.27)	<0.001*
PSS-L (CMR)	-0.02 (-0.03, -0.00)	0.010*
PSSR-L (CMR)	-0.28 (-0.44, -0.11)	0.001*
PEDSR-L (CMR)	0.31 (0.17, 0.45)	<0.001*

Abbreviations: VAI=valvulo-arterial impedance, LVEDVI=left ventricular end-diastolic volume indexed to BSA, LAVI=left atrial volume indexed to BSA, LVEF=LV ejection fraction, LVMI=LV mass indexed to BSA, MBF=myocardial blood flow, MPR=myocardial perfusion reserve, LGE=late gadolinium enhancement, ECV=extracellular volume fraction, AA=ascending aorta, PWV=pulse wave velocity, PSS=peak systolic strain, PSSR=peak systolic strain rate, PSEDSR=peak early diastolic strain rate, C=circumferential, L=longitudinal. (*p<0.05). Units as above.

Table 49. Multivariate associations of rest MBF

Variable	HR (95% CI)	p-value
Gender (M)	-0.37 (-0.50, -0.23)	<0.001
Septal E/e'	0.01 (0.00, 0.03)	0.026
LAVI (CMR)	-0.01 (-0.01, -0.00)	<0.001
Log (coronary Ca^{2+} score)	0.03 (0.01, 0.05)	0.007

Abbreviations: as above.

6.3.3 Associations with stress MBF

Table 50. Univariate associations of stress MBF: anthropometric, echocardiographic and CT variables

Variable	Estimate (95% CI)	p-value
Age	-0.02 (-0.03, -0.01)	<0.001*
Gender (M)	-0.30 (-0.55, -0.05)	0.020*
Log (NT-proBNP)	-0.12 (-0.17, -0.06)	<0.001*
AV Vmax	-0.31 (-0.50, -0.12)	0.002*
MPG	-0.01 (-0.02, -0.00)	0.005*
AVAI	0.37 (-0.41, 1.14)	0.351
Septal E/e'	-0.01 (-0.04, 0.02)	0.479
Lateral E/e'	0.04 (-0.00, 0.07)	0.051
PSS-L (TTE)	-0.07 (-0.11, -0.02)	0.003*
PSSR-L (TTE)	-0.79 (-1.41, -0.18)	0.012*
PEDSR-L (TTE)	1.07 (0.48, 1.66)	<0.001*
VAI (TTE)	-0.01 (-0.11, 0.09)	0.878
AoV Ca^{2+} score	-0.05 (-0.08, -0.02)	0.002*
Log (AoV Ca^{2+} score)	-0.17 (-0.29, -0.05)	0.006*
Log (Coronary Ca^{2+} score)	-0.07 (-0.13, -0.01)	0.015*

Abbreviations: AV Vmax=peak aortic jet velocity, MPG=mean pressure gradient, AVAI=aortic valve aread indexed, PSS=peak systolic strain, PSSR=peak systolic strain rate, PSEDSR=peak early diastolic strain rate, L=longitudinal, VAI=valvulo-arterial impedance, AoV Ca^{2+} score=aortic valve calcium score, TTE=trans-thoracic echocardiogram. (*p<0.05). Units as above.

Table 51. Univariate associations of stress MBF: CMR variables

Variable	Estimate (95% CI)	p-value
VAI (CMR)	-0.10 (-0.24, 0.03)	0.122
LVEDVI	-0.00 (-0.01, 0.00)	0.491
LAVI	-0.01 (-0.02, -0.00)	0.004*
LVEF	0.03 (0.01, 0.05)	0.012*
LV mass/volume	-1.61 (-2.53, -0.68)	<0.001*
LVMI	-0.01 (-0.02, -0.00)	0.004*
LVMI group (high *vs.* low)	-0.22 (-0.43, -0.00)	0.047*
Rest MBF	0.99 (0.61, 1.36)	<0.001*
MPR	0.70 (0.59, 0.81)	<0.001*
LGE presence	0.16 (-0.06, 0.37)	0.148
LGE %	-0.04 (-0.07, -0.01)	0.003*
Native T1 (ms)	-0.00(-0.00, 0.00)	0.711
ECV	-0.06 (-0.11, -0.01)	0.025*
AA distensibility	0.12 (0.03, 0.21)	0.013*
PWV	-0.04 (-0.07, -0.00)	0.026*
PSS-C (CMR)	-0.01 (-0.04, 0.01)	0.234
PSSR-C (CMR)	-0.09 (-0.37, 0.19)	0.529
PEDSR-C (CMR)	0.47 (0.22, 0.73)	<0.001*
PSS-L (CMR)	-0.04 (-0.07, 0.00)	0.054
PSSR-L (CMR)	-0.31 (-0.75, 0.14)	0.178
PEDSR-L (CMR)	0.78 (0.41, 1.15)	<0.001*

Abbreviations: VAI=valvulo-arterial impedance, LVEDVI=left ventricular end-diastolic volume indexed to BSA, LAVI=left atrial volume indexed to BSA, LVEF=LV ejection fraction, LVMI=LV mass indexed to BSA, MBF=myocardial blood flow, MPR=myocardial perfusion reserve, LGE=late gadolinium enhancement, ECV=extracellular volume fraction, AA=ascending aorta, PWV=pulse wave velocity, PSS=peak systolic strain, PSSR=peak systolic strain rate, PSEDSR=peak early diastolic strain rate, C=circumferential, L=longitudinal. (*p<0.05). Units as above.

Univariate associations with stress MBF are shown in Table 50 and Table 51. Stress MBF was inversely related to age, NT-proBNP, AS severity, AV / coronary Ca^{2+} scores, LAVI, PWV, LV mass, %LGE and ECV, while it was directly associated

with female gender, parameters of myocardial deformation, systolic function and AA distensibility.

For stepwise multivariate analysis, the following variables were entered into the model: age, gender, log(NT-proBNP), AV Vmax, septal/lateral E/e', LAVI, LVEF, LV Mass/Volume, LVMI, LGE %, native T1, ECV, AA distensibility, PWV, AV Ca^{2+} score and log (coronary Ca^{2+} score). The independent associations of stress MBF were age, AV Vmax and LVEF (Table 52).

Table 52. Multivariate associations of stress MBF

Variable	HR (95% CI)	p-value
Age	-0.02 (-0.03, -0.00)	0.009
AV Vmax	-0.38 (-0.49, -0.27)	<0.001
LVEF (CMR)	0.03 (0.01, 0.06)	0.008

Abbreviations: as above.

6.4 Discussion

6.4.1 Exercise capacity

Studies assessing the determinants of exercise capacity in AS have looked at various measures of 'maximal exercise capacity' including total exercise time (150, 198, 199), peak VO_2 (108, 200, 201) and positive ETT (variable definitions)(27, 55, 184). We chose to look at age- and sex-corrected peak VO_2 as this is the most objective assessment of aerobic exercise capacity. In addition, we also looked at determinants of age- and sex-corrected peak workload, due to missing gas exchange data in 30 patients.

6.4.1.1 Age and sex-corrected peak VO2

We found MPR and PSS-L (TTE) to be independently associated with age- and sex-corrected peak VO_2. This is in partial agreement with the few studies that have looked at this, and have found age, VAI(200), MPR(108), gender and PSS-L (basal)(201) to be amongst multivariate determinants of peak VO_2 in AS.

Somewhat surprisingly, Dulgheru *et al*'s group did not correct for age and gender, despite peak VO_2 being associated with both in their studies, and also being well recognised to be lower in females and decrease with age.

The only other study looking at CMR associations of peak VO_2 also showed univariate associations with age, gender, rest MBF and MPR, and no associations with LGE or LVEF, similar to our findings(108). In contrast, we also found univariate associations with LV mass/volume and AVAI, which may partly be due to our larger sample size and wider range of severity of AS included. Most studies have not found resting measures of AS severity to be associated with exercise capacity, with the exception of Das *et al* (198), where EOA was associated with total exercise time in a similar cohort of patients to ours, though again, no correction for age/gender was used, and they did not perform multivariate analysis, which probably explains this discrepancy.

Our findings provide interesting insights into the mechanism of exercise limitation in these 'asymptomatic' patients with AS. Even at this early stage of disease, a normal resting MBF is maintained, thought to be due to vasodilation which may be near maximal in some, which in turn reduces their ability to increase MBF on exercise, leading to the lower MPR (as demonstrated in Chapter-5 compared to controls). The increase in HR caused by exercise leads to reduced diastolic perfusion time, which may further impair myocardial perfusion(19, 195). This in turn leads to subendocardial dysfunction/ischaemia, with a reduction in cardiac output and a reduced exercise capacity. The finding of PSS-L also being independently associated with peak VO_2 also supports this hypothesis, as subendocardial ischaemia affects the longitudinal fibres first, leading to impairment of longitudinal function before circumferential or global function is affected, therefore, those with a lower MPR leading to a lower PSS-L will be not be able to increase cardiac output appropriately and to increase workload.

6.4.1.2 Age and sex-corrected peak workload

All univariate associations with peak workload (MPR, rest MBF and NT-proBNP) were also associated with peak VO_2, except lateral E/e'. NT-proBNP and VAI (CMR) were independently associated with age- and sex-corrected peak workload as a measure of exercise capacity. No other study has specifically looked at predictors of peak workload in AS.

BNP is secreted by the LV in response to increased wall stress, and has been shown to be associated with AS severity, symptoms, LV function and outcome in AS(45). It may therefore imply that those with an elevated NT-proBNP represent those with increased wall stress, at the verge of 'decompensation' and symptom development, and NT-proBNP is therefore a determinant of exercise capacity because pressure overload and remodeling. One other CMR study looking at determinants of a 6-minute walk test in severe AS also found BNP and % diffuse fibrosis to be independent associated, after age and sex were also entered into the model(101). We did not find markers of focal or diffuse fibrosis to be associated with exercise capacity in our cohort despite the independent association with MPR. This may again be due to our cohort being at an earlier 'compensated' stage of disease compared to the severe, mostly symptomatic AS patients studied in their study.

VAI, which is a measure of global LV afterload that incorporates the valvular and arterial load on the LV, has been associated with LV function, symptom onset and outcome in AS(40, 202). VAI was also found to be a multivariate association of peak VO_2 in Dulgheru's study of a similar cohort of patients, though they did not correct for age and sex(200). The increased afterload on the LV in AS requires the LV to generate higher pressures at rest in order to maintain cardiac output, thus increasing the myocardial oxygen demand at rest, which may in turn impair their ability to increase flow adequately during exercise, and therefore lead to reduced exercise capacity. The increased LV wall stress would also in-turn lead to increased NT-proBNP production. VAI has also been shown to be inversely

correlated with longitudinal function in AS(203), and would further support the hypothesis linking VAI, MPR and longitudinal function as mechanisms for reduced exercise capacity.

It is important to acknowledge that some of the previous findings may have been due to the effects of gender, as female patients are known to have smaller stroke volumes with more concentric remodeling(204), which can in turn leads to higher VAI compared to males, possibly suggesting a greater severity of AS for a given PPG in females. A major strength of our study compared to previous studies, is the fact we have measured TTE, CMR and CPET variables in all patients, and corrected for age and gender. Other parameters that have been shown to be independently associated with exercise capacity in AS include change in MPG / PSS-L / LVEF on exercise (measures of valve compliance and contractile reserve)(55, 184), which we either did not assess or find in our study.

6.4.2 Blood flow and perfusion reserve

There have been very few studies looking at determinants of MBF and MPR using CMR in patients with AS.

6.4.2.1 MPR

The only other study looking at CMR-measured absolute MBF and MPR quantification was done at our centre in patients with severe AS(108), and found gender, AV Vmax, MPG, septal E/e', LV mass/volume, LVMI and LGE to be univariate associations of MPR, out of which LGE and LVMI remained independently associated on multivariate analysis. Another study assessed CMR-measured semi-quantitative MPRI in severe AS, and found similar univariate associtaions: AVA, LVMI, LGE presence (but not %) and PSS-C though multivariate analysis was not performed(205). Similar to those studies, we also found univariate associations with measures of AS severity (AV Vmax, MPG, AVAI) and remodeling (LV mass/volume). Other studies that have used PET or Doppler TTE to assess MPR or CFR in AS have also found markers of AS severity (PPG / AVA /

EOA)(24, 206, 207), rest LVRPP(24, 191), DPT(24), NT-proBNP, and pulmonary artery systolic pressure(191) to be associated with MPR/CFR.

Compared to our previous study in severe AS patients undergoing AVR(108), LGE and LVMI were not found to be independently associated with MPR in our cohort of asymptomatic patients, where as, for the first time, we have shown ECV to be independently associated with MPR. Of note, T1 mapping was not assessed in Steadman's study, in fact, no other study has assessed T1 mapping and MPR in patients with AS. One of the reasons for LVMI and LGE not being associated wiih MPR may be the earlier stage of disease in our cohort (all asymptomatic). Whilst LGE may represent more irreversible replacement fibrosis, which is associated with post-AVR outcomes in severe disease, it may not be a predictor of MPR or symptoms in the earlier stages of AS. ECV however, is thought to represent diffuse interstitial fibrosis, which occurs earlier, may be reversible, and can lead to impaired MPR via the relatively reduced arteriolar/ capillary density associated with the LV remodeling and interstitial fibrosis seen in AS. Ours is by the far the largest cohort of AS patients to date who have had determinants of MPR/MBF assessed (previous sample sizes: 20-77(24, 207)). The larger sample size has allowed us to include more variables in the multivariate model without the risk of over-fitting, but this may also account for differences seen compared to previous studies.

6.4.2.2 Rest and stress MBF

Rest MBF has previously been shown to be associated with gender, rest LVRPP(108), measures of AS severity (MPG, EOA)(206) and LVMI(24) in AS. We found septal E/e' (a measure of LV filling pressure), LAVI, female gender and log (coronary Ca^{2+} score) to be independently associated with rest MBF, but not markers of AS severity. As mentioned above, the increased global afterload in AS leads to increased myocardial oxygen demand at rest, which is maintained by increased rest MBF (as demonstrated by the positive correlation of rest MBF with both septal E/e' and VAI). Somewhat surprisingly, there was a negative

correlation with LAVI, which may be a spurious result as the effect size was small, but it may also represent more advanced stage of remodeling. Our patient cohort represent a varied severity of AS, and therefore some may be at an earlier compensated phase, whilst others may be at the later stage of impending decompensation, which might account for the differences seen compared to previous studies. It is hard to physiologically account for the positive correlation with coronary Ca^{2+} score, which is likely to represent a spurious result.

Associations of stress MBF has only been reported in one other study in AS, and included AVA and hyperaemic DPT(24). Similar to this, we also found AS severity (AV Vmax) to be independently associated, in addition to age and LVEF. This may again be due to these patients being in a state of compensation, with supra-normal systolic function (as discussed further in Section 7.7.2.2), and preserved ability to increase MBF on exercise. The 'supra-normal' contractile function is probably able to better increase the cardiac output during stress. It is also possible however, that LVEF is co-linear with other variables in the model, such as age and gender, as younger female patients would have a higher LVEF (59.2 ± 4.49% *vs.* 55.9 ± 4.84% in our females and male patients respectively, $p<0.05$).

6.4.3 Potential novel therapeutic targets

The above findings provide interesting insights into the pathophysiology of exercise limitation and myocardial perfusion in these patients, as well as identifying potential therapeutic targets, which could delay disease progression and symptom onset, thereby reducing the number of AVR/TAVI needed. These asymptomatic patients with moderate-severe AS exhibit early LV remodeling, with the valve obstruction leading to increased LV filling pressures and global afterload, as well as possible diffuse interstitial fibrosis. These changes lead to reduced capillary density but increased myocardial oxygen demand at rest, which is most likely maintained through near-maximal capillary dilatation. There is therefore a reduced ability to increase MBF on exercise, leading to a reduced MPR and subendocardial myocardial ischaemia on exercise, with consequently

reduced longitudinal function. These changes also lead to reduced exercise capacity, and probably the eventual onset of symptoms once the compensatory mechanisms fail.

The renin-angiotensin system (RAS) is thought to play an important role in regulating LVH and myocardial fibrosis, and its inhibition has been shown to reduce fibrosis and improve diastolic function in hypertensive patients(208). Our findings suggest that anti-fibrotic therapy in AS could potentially lead to improved MPR, and therefore improved exercise capacity in AS. A recent placebo-control trial of Ramipril in asymptomatic patients with moderate-severe AS showed significant reduction in LVMI compared to placebo after one year of treatment, though no change was demonstrated in MPRI, T1 or exercise tolerance(118). However, MPRI was only assessed in a third of the cohort (so could represent a type-II error), ECV was not calculated, and the cohort were at an early stage of disease (like ours), and may therefore not have had a high enough burden of fibrosis to show improvement in such a short period of time.

Another novel therapeutic target in AS includes calcium metabolism, and although we did not show AV calcification to be a multivariate association, it was a univariate association of both MPR and stress MBF in our cohort. A study investigating the role of anti-osteoporosis drugs in AS is currently under way(117) to see if targeting this pathway may alter disease progression in AS (NCT02132026).

The role of Ranolazine, a late-sodium channel inhibitor, that leads to decreased intra-cellular Ca^{2+} concentration and has been shown to improve diastolic function and myocardial perfusion in small studies, has already been explored in AS as part of this thesis (Chapter-4). Although the findings were not statistically significant, it merits further investigation in a larger cohort of patients, perhaps with more advanced disease.

6.5 Conclusion

Our data looking at determinants of exercise capacity and myocardial perfusion in asymptomatic patients with moderate-severe AS provides interesting insights into the pathophysiology of exercise limitation and symptom development, and identifies potential therapeutic targets for the future. We have shown a link between increased global afterload caused by the AS, reduced MPR, impaired longitudinal function and reduced exercise capacity, even in the early compensated phase of the disease. This is the largest cohort of such patients to date to have TTE, CPET and CMR assessment, and determinants of age- and sex-corrected exercise capacity looked at, which is an added strength of our study.

CHAPTER SEVEN

7 A COMPARISON OF EXERCISE TESTING AND STRESS CMR TO PREDICT OUTCOME IN ASYMPTOMATIC PATIENTS WITH AS

7.1 Introduction

This chapter describes the results of the main PRIMID-AS study, the full methods for which have been described in chapter-2. The main aim of the PRIMID-AS study was to compare MPR with symptom limited exercise testing as predictors of outcome in asymptomatic patients with moderate to severe AS.

7.2 Primary and secondary outcomes definitions

The recruitment flowchart with follow-up data is shown in Figure 50. All included patients were followed up for a minimum of 12 months, or until a pre-defined outcome was reached, and a maximum of 30 months. The median follow-up time was 374 (IQR 351-498) days.

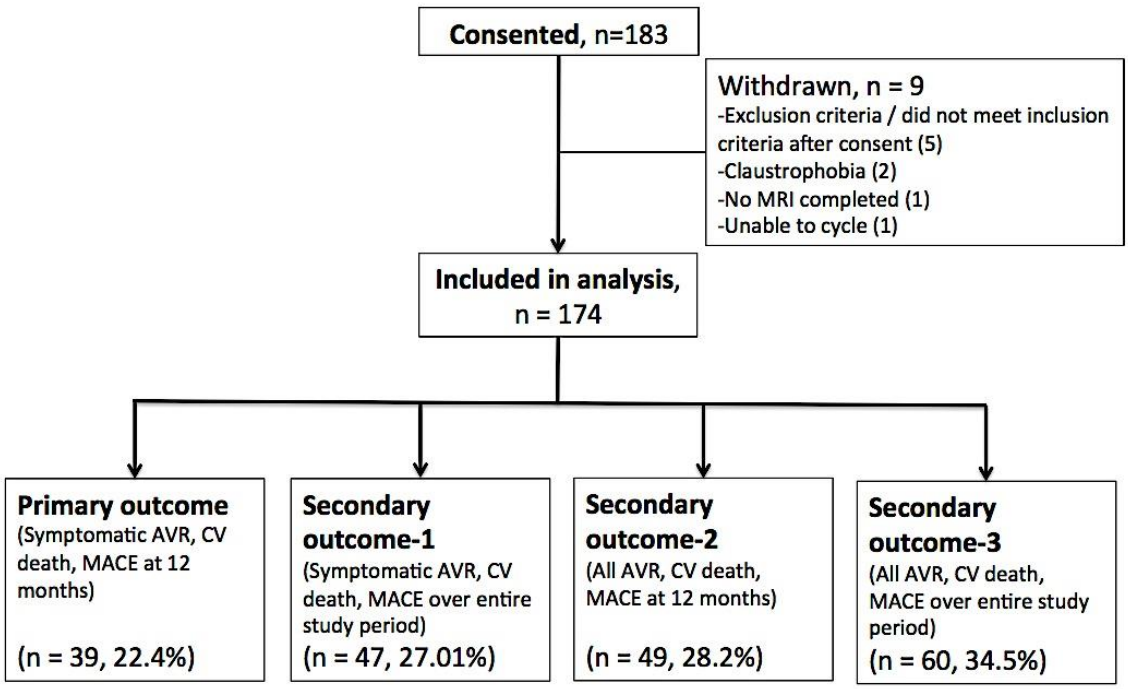

Figure 50. Recruitment and outcomes reached

A ***primary outcome*** (symptom-driven AVR, cardiovascular death and MACE at 12 months) occurred in 39 patients (22.4%), all of who developed typical symptoms and 1 died within 12 months (after development of symptoms).

We decided to look at a further three secondary outcomes, as the outcomes were assessed at two time periods: 12 months from recruitment (pre-defined primary outcome) as well as the total duration of the study. For the secondary outcomes, the numbers were:

-***Secondary outcome-1*** (composite primary endpoint over entire study period) = 47 (27.01%): 46 developed symptoms, 2 deaths (1 sudden cardiac death (SCD) and 1 after symptom onset).

-***Secondary outcome-2*** (all AVRs, deaths, MACE at 12 months) = 49 (28.2%): 39 developed symptoms, 1 death (after symptom onset), 10 AVR before symptoms at Clinician's discretion.

-***Secondary outcome-3*** (all AVRs, deaths, MACE over entire study period) = 60 (34.5%): 46 developed symptoms, 2 deaths (1 SCD and 1 after symptom onset), 13 AVR before symptoms.

The decision to refer for AVR was at the discretion of the clinician looking after the patient, who remained blinded to the results of the tests carried out as part of the study, so as not to bias their decision. There was also an independent 'events adjudication committee' who classified all events as primary or secondary by assessessing blinded clinic letters of referral.

7.3 Primary outcome

7.3.1 Demographic data

The demographic data for the overall population, as well as those with and without a primary outcome, is shown in Table 53.

The outcome group had a greater proportion of females, higher NT-proBNP, lower BSA, Hb and eGFR than those without an outcome. There was no difference in resting haemodynamics, co-morbidities and medication between the two groups.

Table 53. Demographic data for those with and without a Primary outcome

	Primary outcome (n=39)	No primary outcome (n=135)	p-value
Age (years)	68.4 ± 12.0	65.6 ± 13.7	0.245
Male (n (%))	22 (56.4)	111 (82.2)	<0.001*
BSA (m^2)	1.9 ± 0.19	2.0 ± 0.21	0.011*
BMI (kg/m^2)	27.4 ± 4.1	28.2 ± 4.2	0.299
Resting HR (bpm)	70.6 ± 14.3	70.2 ± 10.5	0.894
Resting SBP (mmHg)	147.4 ± 22.9	146.7 ± 20.6	0.861
Resting DBP (mmHg)	74.9 ± 10.4	77.8 ± 10.7	0.128
Diabetes (n (%))	8 (20.5)	17 (12.6)	0.214
Hypertension (n (%))	20 (51.3)	73 (54.1)	0.758
Hyperlipidaemia (n (%))	17 (43.6)	75 (55.6)	0.404
ACE-I/ARB (n (%))	14 (35.9)	63 (46.7)	0.233
Beta-blocker (n (%))	18 (46.2)	36 (26.7)	0.021
Statin	21 (53.8)	84 (62.2)	0.346
NT-proBNP (pmol/L)	120.8 (38.3, 278.7)	50.3 (17.2, 132.0)	0.006*
Hb (g/dL)	13.8 ± 1.2	14.4 ± 1.2	0.005*
Hct	0.415 ± 0.036	0.428 ± 0.034	0.037*
Hba1c (%)	6.0 ± 0.68	5.9 ± 0.85	0.594
eGFR (ml/min)	79 ± 18.7	90 ± 30.5	0.008*

Abbreviations: BSA=body surface area, HR=heart rate, SBP/DBP=systolic/diastolic blood pressure, ACE-I=angiotensin converting enzyme inhibitor, ARB=angiotensin II receptor blocker, NT-proBNP=N terminal brain natriuretic peptide, Hb=haemoglobin, Hct=haematocrit, eGFR=estimated glomerular filtration rate

7.3.2 Echocardiographic and ECG data

Table 54 demonstrates the echocardiographic and ECG data. Patients who reached a primary outcome had more severe AS, higher resting and LVRPP. The increase in VAI was of borderline significance.

Table 54. Echocardiographic and ECG data for those with and without a Primary outcome

	Primary outcome (n=39)	No primary outcome (n=135)	p-value
AV Vmax (m/s)	4.17 ± 0.63	3.77 ± 0.51	<0.001*
MPG (mmHg)	42.6 ± 14.8	33.3 ± 10.9	<0.001*
AVAI (cm^2/m^2)	0.50 ± 0.15	0.59 ± 0.13	<0.001*
E/A	0.86 ± 0.32	0.89 ± 0.28	0.690
Septal E/e'	13.36 ± 6.01	11.97 ± 4.46	0.198
Lateral E/e'	10.70 ± 3.58	9.65 ± 3.75	0.129
DPT (ms)	584.4 ± 145.3	624.7 ± 160.3	0.161
Longitudinal PSS (%)	-18.05 ± 2.46	-18.21 ± 2.84	0.796
Longitudinal PSSR (1/s)	-1.00 ± 0.23	-1.00 ± 0.20	0.939
Longitudinal PEDSR (1/s)	0.80 ± 0.19	0.78 ± 0.22	0.672
Resting LVRPP ($mmHg.bpm.10^{-4}$)	1.48 ± 0.34	1.34 ± 0.27	0.024*
VAI (Echo) ($mmHg/ml/m^2$)	4.24 ± 1.15	3.88 ± 1.02	0.059
Sokolow criteria (n(%))	2 (5.1)	16 (11.9)	0.370
Cornell criteria (n(%))	9 (23.1)	22 (16.3)	0.330

Abbreviations: AV Vmax=peak aortic jet velocity, MPG=mean pressure gradient, AVAI=aortic valve area indexed to BSA, DPT=diastolic perfusion time, PSS=peak systolic strain, PSSR=peak systolic strain rate, PEDSR=peak early diastolic strain rate, LVRPP=left ventricular rate pressure product, VAI=valvulo-arterial impedance

7.3.3 Cardiopulmonary exercise testing data

CPET data are shown in Table 55. As mentioned in the previous chapter, two patients did not complete a CPET (equipment unavailability and knee replacement). There was no significant difference in the total exercise duration between those with and without a primary outcome. Although the peak workload achieved was lower in the outcome group, there was no significant difference in the percentage predicted workload or exercise duration between the two groups, suggesting a similar level of exercise achieved when accounting for age, sex and weight.

Table 55. CPET data for those with and without a Primary outcome

	Primary outcome (n=38)	No primary outcome (n=134)	p-value
Exercise duration (min)	8.02 ± 2.45	8.63 ± 1.86	0.163
% predicted HR (%)	86.5 ± 12.5	86.9 ± 11.7	0.869
Rise in SBP (mmHg)	34.0 ± 22.3	44.0 ± 21.9	0.018*
Exercise LVRPP (mmHg.bpm.10^{-4})	3.49 ± 0.71	3.53 ± 0.74	0.764
Peak VO_2 (ml/kg/min)	14.8 ± 5.3	18.4 ± 5.4	0.002*
% Predicted VO_2 (%)	65.2 ± 19.2	75.0 ± 16.2	0.005*
Peak workload achieved (W)	90 ± 32.1	116 ± 40.4	<0.001*
% Predicted workload (%)	83.0 ± 27.3	87.3 ± 27.5	0.391
Peak RER	1.11 ± 0.13	1.12 ± 0.15	0.683
Positive test (strict) (n(%))	8 (21.1)	11 (8.2)	0.026*
Positive test (conventional) (n(%))	17 (44.7)	38 (28.4)	0.056
Reason for stopping (n(%)):			0.163
Chest pain	1 (2.6)	3 (2.2)	
Dyspnoea	14 (36.8)	29 (21.6)	
General fatigue	2 (5.3)	20 (14.9)	
Leg fatigue	15 (39.5)	58 (43.3)	
Arrhythmia	1 (2.6)	0 (0.0)	
Hypertension	0 (0.0)	1 (0.7)	
Other	5 (13.2)	23 (17.2)	

Abbreviations: HR=heart rate, SBP=systolic blood pressure, LVRPP=left ventricular rate pressure product, VO2=oxygen uptake, RER=respiratory exchange ratio.

However, the rise in systolic blood pressure and the peak / percentage predicted VO_2 achieved was significantly lower in the outcome group. There were also a significantly greater proportion of positive tests using the strict, but not the conventional definition in the outcome group, which was of borderline statistical significance.

7.3.4 Cardiac Magnetic Resonance imaging data

All included patients completed a stress CMR scan, with no complications.

7.3.4.1 CMR volumetric, myocardial deformation and distensibility data

Volumetric, myocardial deformation and distensibility data are shown in Table 56.

Table 56. CMR volumetric, myocardial deformation and distensibility data for those with and without a Primary outcome

	Primary outcome (n=39)	No primary outcome (n=135)	p-value
LVEDVI (ml/m^2)	82.87 ± 14.94	88.94 ± 18.95	0.068
LVESVI (ml/m^2)	35.22 ± 8.99	39.17 ± 10.95	0.041*
LVSV (ml)	90.0 ± 16.6	99.0 ± 24.4	0.008*
LVSVI (ml/m^2)	47.65 ± 7.82	49.79 ± 9.67	0.207
LVEF (%)	57.8 ± 4.80	56.4 ± 4.96	0.103
LVMI (g/m^2)	56.32 ± 12.22	58.09 ± 14.3	0.484
LV mass/volume (g/ml)	0.69 ± 0.12	0.66 ± 0.11	0.165
LAVI (ml/m^2)	57.76 ± 18.16	54.12 ± 13.54	0.252
RVEDVI (ml/m^2)	84.58 ± 15.35	89.28 ± 14.98	0.087
VAI (MRI) (mmHg/ml/m^2)	4.08 ± 0.78	3.74 ± 0.81	0.020*
Longitudinal PSS (%)	-18.77 ± 3.39	-18.40 ± 2.91	0.495
Longitudinal PSSR (1/s)	-1.12 ± 0.23	-1.09 ± 0.24	0.483
Longitudinal PEDSR (1/s)	1.16 ± 0.31	1.07 ± 0.27	0.072
Circumferential PSS (%)	-29.52 ± 4.42	-27.68 ± 4.66	0.029*
Circumferential PSSR (1/s)	-1.82 ± 0.35	-1.71 ± 0.40	0.110
Circumferential PEDSR (1/s)	1.79 ± 0.38	1.64 ± 0.41	0.042*
AA distensibility (10^{-3}mmHg^{-1})	1.84 ± 1.04	1.94 ± 1.23	0.652
DA distensibility (10^{-3}mmHg^{-1})	2.30 ± 1.62	2.06 ± 1.44	0.397
PWV (m/s)	7.45 ± 3.02	8.66 ± 3.67	0.072

Abbreviations: LVEDVI=left ventricular end-diastolic volume indexed to BSA, LVESVI=left ventricular end systolic volume indexed to BSA, LVSV=left ventricular stroke volume, LVSVI=LVSV indexed to BSA, LVEF=left ventricular ejection fraction, LVMI=left ventricular mass indexed to BSA, LAVI=left atrial volume indexed to BSA, RVESVI=right ventricular end diastolic volume indexed to BSA, VAI=valvulo-arterial impedance, PSS=peak systolic strain, PSSR=peak systolic strain rate, PEDSR=peak early diastolic strain rate, AA=ascending aorta, DA=descending aorta, PWV=pulse wave velocity

There was no significant difference in end-diastolic volume, mass and EF. The indexed end-systolic volume was lower in the outcome group, as was the absolute stroke volume, though when indexed to BSA, there was no difference. The VAI using CMR-derived stroke volume was significantly higher in those with a primary outcome, suggesting more severe haemodynamic load. Overall, there

was no difference in the CMR measured myocardial deformation data, with the exception of a higher circumferential PSS and PEDSR in the primary outcome group (measured using endocardial contours only on Feature Tracking). There was no significant difference in measures of aortic stiffness between the two groups.

7.3.4.2 Contrast Enhanced CMR

The contrast-enhanced CMR data is presented in Table 57. The total MBF was calculated by multiplying the MBF by the LVMI. The primary outcome group had a significantly lower global MPR and total stress MBF, with similar rest MBF. There was no significant difference in either LGE, native T1 time or ECV between those with and without a primary outcome.

Table 57. CMR perfusion and fibrosis data for those with and without a Primary outcome

	Primary outcome (n=39)	No primary outcome (n=135)	p-value
Global stress MBF (ml/min/g)	2.07 ± 0.66	2.19 ± 0.71	0.373
Global rest MBF (ml/min/g)	1.07 ± 0.39	0.95 ± 0.21	0.089
Total stress MBF (ml/min/m^2)	111.50 ± 29.06	125.59 ± 47.96	0.029*
Total rest MBF (ml/min/m^2)	57.68 ± 17.12	54.92 ± 16.39	0.366
Global MPR	2.04 ± 0.63	2.33 ± 0.71	0.026*
LGE present (n,%)	18 (46.2)	64 (47.4)	0.890
% LGE (%)	4.0 ± 3.03	4.3 ± 3.95	0.714
Native myocardial T1 (ms)	1116.8 ± 64.21	1137.1 ± 70.88	0.162
ECV (%)	25.52 ± 2.52	24.59 ± 2.37	0.074

Abbreviations: MPR=myocardial perfusion reserve, MBF=myocardial blood flow, LGE=late gadolinium enhancement, ECV=extracellular volume fraction

7.3.5 CT data

Results are shown in Table 58. There was wide range present, with no significant difference in AV or coronary calcium scores between the two groups.

Table 58. CT data for those with and without a Primary outcome

	Primary outcome (n=39)	No primary outcome (n=133)	p-value
AoV Ca^{2+} score	2107.0 (1275, 3398)	1864.0 (1169, 3034)	0.515
Coronary artery Ca^{2+} score	400.5 (6.8, 934.0)	276.5 (5.5, 950.0)	0.678

Abbreviations: AoV Ca^{2+} score= aortic valve calcium score (median and inter-quartile range displayed)

7.3.6 Univariate associations with primary outcome

Table 59. Univariate associations of primary outcome (adjusted for gender)

Variable	HR (95% CI)	p-value
AV Vmax	3.17 (1.87 - 5.39)	<0.001*
MPG	1.05 (1.03 - 1.08)	<0.001*
AVA	0.08 (0.02-0.29)	<0.001*
AVAI	0.60 (0.46 - 0.79)	<0.001*
VAI (Echo)	1.35 (1.05 - 1.74)	0.020*
VAI (CMR)	1.50 (1.04 - 2.17)	0.030*
LV mass / Volume (CMR)	1.38 (1.06 - 1.80)	0.017*
MPR	0.58 (0.35-0.95)	0.032*
AoV Ca^{2+} score	1.00 (1.01-1.21)	0.025*
Log (AoV Ca^{2+} score)	1.92 (1.18-3.13)	0.009*
Log (NT-proBNP)	1.33 (1.07-1.66)	0.010*
Positive CPET (strict)	4.76 (2.05 - 11.03)	<0.001*
Positive CPET (conventional)	1.78 (0.93 - 3.38)	0.080
Peak VO_2	0.90 (0.83-0.97)	0.007*
% Predicted workload achieved	0.98 (0.97 - 1.00)	0.019*
% Predicted VO_2 achieved	0.96 (0.94 - 0.98)	<0.001*
Resting LVRPP	3.14 (1.17-8.39)	0.023*

Abbreviations: AV Vmax=peak aortic jet velocity, MPG=mean pressure gradient, AVA=aortic valve area, AVAI=AVA indexed to BSA, VAI=valvulo-arterial impedance, MPR=myocardial perfusion reserve, AoV Ca^{2+} score=aortic valve calcium score, CPET=cardiopulmonary exercise test, VO_2=oxygen consumption, LVRPP=left ventricular rate pressure product

The univariate associations of the primary outcome, adjusted for gender, are displayed in Table 59. These include measures of AS severity, LV remodeling,

MPR, AV calcification, NT-proBNP, positive CPET (using strict definition) and measures of exercise capacity.

7.3.7 Multivariate associations of primary outcome

Stepwise multivariate analysis was performed separately for strict (Table 60) and conventionally (Table 61) defined positive CPET. Given the relatively low number of events, a maximum of five variables were entered into the model in addition to gender, and included: AVAI, MPR, LVM/volume, positive CPET and NT-proBNP.

Multivariate predictors using strict CPET were female gender, low AVAI and positive (strict) CPET.

Table 60. Multivariate associations of primary outcome (strict definition CPET)

Variable	HR (95% CI)	p-value
Gender (male)	0.32 (0.16 - 0.64)	0.001
AVAI	0.55 (0.40 - 0.75)	<0.001
Positive CPET (strict)	4.39 (1.89 - 10.21)	<0.001

Abbreviations: AVAI=AVA indexed to BSA, CPET=cardiopulmonary exercise test.

Multivariate predictors using conventional CPET were: female gender, low AVAI and high NT-ptoBNP.

Table 61. Multivariate associations of primary outcome (conventional definition CPET)

Variable	HR (95% CI)	p-value
Gender (male)	0.43 (0.22 - 0.83)	0.012
AVAI	0.56 (0.52 - 0.75)	<0.001
Log(NT-proBNP)	1.25 (1.01 - 1.54)	0.038

Abbreviations: AVAI=AVA indexed to BSA, NT-proBNP=N-terminal pro-brain natriuretic peptide.

7.4 Secondary outcome-1: composite primary endpoint over entire study period

The demographic, exercise and imaging data for those with and without a secondary outcome-1 (composite primary endpoint over entire study period, n=47) are tabulated in Appendix-2 (section 9.2).

7.4.1 Univariate and multivariate associations of secondary outcome-1

The univariate associations of secondary outcome-1, adjusted for gender, are shown in Table 62. Similar to the primary outcome, these include measures of AS severity, LV remodeling, MPR, AV calcification, NT-proBNP, positive CPET (using strict and conventional definitions this time) and measures of exercise capacity.

Table 62. Univariate associations of secondary outcome-1

Variable	HR (95% CI)	p-value
AV Vmax	3.25 (1.99 - 5.31)	<0.001
MPG	1.05 (1.03 - 1.07)	<0.001
AVA	0.10 (0.03 - 0.33)	<0.001
AVAI	0.63 (0.50 - 0.80)	<0.001
VAI (Echo)	1.30 (1.04 - 1.63)	0.024
VAI (CMR)	1.42 (1.02 - 1.98)	0.035
LVMI group (high *vs.* low)	1.85 (1.02 - 3.34)	0.042
LV mass/volume	1.32 (1.04 - 1.68)	0.023
MPR	0.62 (0.39 - 0.97)	0.035
AoV Ca^{2+} score	1.08 (1.00-1.18)	0.047
Log (AoV Ca^{2+} score)	1.75 (1.13 - 2.73)	0.013
Log (NT-proBNP)	1.28 (1.05 - 1.56)	0.015
Positive CPET (strict)	4.17 (1.92 - 9.05)	<0.001
Positive CPET (conventional)	1.90 (1.06 - 3.42)	0.032
Peak VO_2	0.91 (0.85 - 0.98)	0.011
% Predicted VO_2 achieved	0.97 (0.95 - 0.99)	0.003
Resting LVRPP	2.89 (1.14 - 7.37)	0.026

Abbreviations: AV Vmax=peak aortic jet velocity, MPG=mean pressure gradient, AVA=aortic valve area, AVAI=AVA indexed to BSA, VAI=valvulo-arterial impedance, LVMI=left ventricular mass indexed to BSA, MPR=myocardial perfusion reserve, AoV Ca^{2+} score=aortic valve calcium score, CPET=cardiopulmonary exercise test, VO_2=oxygen consumption, LVRPP=left ventricular rate pressure product

Table 63 and Table 64 show the results of stepwise multivariate analysis for the secondary outcome-1, after entering the following variables: gender, AVAI, MPR, LVM/volume, positive CPET, NT-proBNP.

Table 63. Multivariate associations of secondary outcome-1 (strict definition CPET)

Variable	HR (95% CI)	p-value
Gender (male)	0.42 (0.22 - 0.79)	0.008
AVAI	0.61 (0.47 - 0.80)	<0.001
Positive CPET (strict)	3.41 (1.55 - 7.50)	0.002

Abbreviations: AVAI=AVA indexed to BSA, CPET=cardiopulmonary exercise test

Table 64. Multivariate associations of secondary outcome-1 (conventional definition CPET)

Variable	HR (95% CI)	p-value
Gender (male)	0.54 (0.29 - 0.99)	0.045
AVAI	0.60 (0.47 - 0.77)	<0.001
Log(NT-proBNP)	1.22 (1.00 - 1.48)	0.048

Abbreviations: AVAI=AVA indexed to BSA, NT-proBNP=N-terminal pro-brain natriuretic peptide.

Multivariate associations of the secondary outcome-1 using strict definition CPET included gender, AVAI and positive CPET. Using the conventional definition of CPET, these included gender, AVAI and NT-proBNP.

7.5 Secondary outcome-2: all AVRs, deaths, MACE at 12 months

The demographic, exercise and imaging data for those with and without a secondary outcome-2 (all AVR's, deaths and MACE at 12 months, n=49) are tabulated in Appendix-3 (section 9.3).

7.5.1 Univariate and multivariate associations of secondary outcome-2

The univariate associations of secondary outcome-2, adjusted for gender, are listed in Table 65. Once again, these include measures of AS severity, LV

remodeling, MPR, AV calcification, NT-proBNP, positive CPET (using strict definition only) and measures of exercise capacity.

Table 65. Univariate associations of secondary outcome-2

Variable	HR (95% CI)	p-value
AV Vmax	3.50 (2.18 - 5.62)	<0.001
MPG	1.06 (1.04 - 1.08)	<0.001
AVA	0.05 (0.02 - 0.18)	<0.001
AVAI	0.56 (0.44 - 0.72)	<0.001
VAI (Echo)	1.33 (1.06 - 1.67)	0.013
VAI (CMR)	1.48 (1.07 - 2.06)	0.019
LVMI group (high *vs.* low)	1.96 (1.10 - 3.51)	0.023
LVMI (continuous)	1.02 (1.00 - 1.04)	0.040
LV mass/volume	1.40 (1.11 – 1.77)	0.005
LAVI	1.02 (1.00 – 1.04)	0.037
MPR	0.55 (0.35 – 0.86)	0.009
Stress MBF	0.63 (0.40 – 0.99)	0.045
Total rest MBF (MBF x LVMI)	1.02 (1.00 - 1.04)	0.028
AoV Ca^{2+} score	1.12 (1.04-1.21)	0.003
Log (AoV Ca^{2+} score)	2.06 (1.31 - 3.23)	0.002
Log (NT-proBNP)	1.29 (1.07 - 1.56)	0.008
Positive CPET (strict)	4.03 (1.93 - 8.41)	<0.001
Positive CPET (conventional)	1.62 (0.91 - 2.88)	0.103
Peak VO_2	0.89 (0.83 - 0.96)	0.002
% Predicted VO_2 achieved	0.96 (0.94 - 0.98)	<0.001
% Predicted workload achieved	0.98 (0.97 - 1.00)	0.011
Resting LVRPP	2.74 (1.11 - 6.72)	0.028

Abbreviations: AV Vmax=peak aortic jet velocity, MPG=mean pressure gradient, AVA=aortic valve area, AVAI=AVA indexed to BSA, VAI=valvulo-arterial impedance, LVMI=left ventricular mass indexed to BSA, LAVI=left atrial volume indexed to BNSA, MPR=myocardial perfusion reserve, MBF=myocardial blood flow, AoV Ca^{2+} score=aortic valve calcium score, CPET=cardiopulmonary exercise test, VO_2=oxygen consumption, LVRPP=left ventricular rate pressure product

The results of stepwise multivariate analysis for the secondary outcome-2 are shown in Table 66 and Table 67, after entering the following variables: gender, AVAI, MPR, LVM/volume, positive CPET, NT-proBNP.

Multivariate associations of the secondary outcome-2 using strict definition CPET included gender, AVAI, MPR and positive CPET. Using the conventional definition of CPET, these included AVAI, MPR and positive CPET.

Table 66. Multivariate associations of secondary outcome-2 (strict definition CPET)

Variable	HR (95% CI)	p-value
Gender (male)	0.52 (0.27 - 0.98)	0.042
AVAI	0.54 (0.51 - 0.71)	<0.001
MPR	0.58 (0.35 - 0.96)	0.035
Positive CPET (strict)	3.64 (1.75 - 7.59)	<0.001

Abbreviations: AVAI=AVA indexed to BSA, MPR=myocardial perfusion reserve, CPET= cardiopulmonary exercise test

Table 67. Multivariate associations of secondary outcome-2 (conventional definition CPET)

Variable	HR (95% CI)	p-value
AVAI	0.53 (0.41 - 0.69)	<0.001
MPR	0.49 (0.30 - 0.82)	0.007
Positive CPET (conventional)	1.86 (1.00 - 3.44)	0.049

Abbreviations: AVAI=AVA indexed to BSA, MPR=myocardial perfusion reserve, CPET= cardiopulmonary exercise test

7.6 Secondary outcome-3: all AVRs, deaths, MACE over entire study period

The demographic, exercise and imaging data for those with and without a secondary outcome-3 (all AVR's, deaths and MACE over entire study period, n=60) are tabulated in Appendix-4 (section 9.4).

7.6.1 Univariate and multivariate associations of secondary outcome-3

The univariate associations of secondary outcome-3, adjusted for gender, are listed in Table 68. These include measures of AS severity, LV remodeling, MPR, longitudinal strain/strain rates, AV calcification, NT-proBNP, positive CPET (using strict definition only) and measures of exercise capacity.

Table 68. Univariate associations of secondary outcome-3

Variable	HR (95% CI)	p-value
AV Vmax	3.53 (2.28 - 5.46)	<0.001
MPG	1.06 (1.04 - 1.08)	<0.001
AVA	0.08 (0.03 - 0.23)	<0.001
AVAI	0.60 (0.49 - 0.74)	<0.001
VAI (Echo)	1.29 (1.05 - 1.57)	0.013
VAI (CMR)	1.41 (1.06 - 1.89)	0.020
LVMI group (high *vs.* low)	2.01 (1.19 - 3.40)	0.010
LVMI (continuous)	1.02 (1.00 - 1.04)	0.025
LV mass/volume	1.37 (1.12 - 1.69)	0.003
LAVI	1.02 (1.00 - 1.04)	0.030
MPR	0.60 (0.40 - 0.89)	0.012
Total rest MBF (MBF x LVMI)	1.02 (1.00 - 1.04)	0.010
Longitudinal PSS (CMR)	1.11 (1.01 - 1.23)	0.027
Longitudinal PSSR (CMR)	3.23 (1.02 - 10.20)	0.046
AoV Ca^{2+} score	1.11 (1.03-1.18)	0.003
Log (AoV Ca^{2+} score)	1.95 (1.30 - 2.92)	0.001
Log (NT-proBNP)	1.22 (1.03 - 1.44)	0.021
Positive CPET (strict)	3.47 (1.75 - 6.88)	<0.001
Positive CPET (conventional)	1.62 (0.96 - 2.75)	0.071
Peak VO_2	0.90 (0.85 - 0.97)	0.004
% Predicted VO_2 achieved	0.97 (0.95 - 0.99)	0.002
Change in MPG>18 mmHg on exercise	1.95 (1.01 - 3.77)	0.048
Resting LVRPP	2.94 (1.27 - 6.80)	0.012

Abbreviations: AV Vmax=peak aortic jet velocity, MPG=mean pressure gradient, AVA=aortic valve area, AVAI=AVA indexed to BSA, VAI=valvulo-arterial impedance, LVMI=left ventricular mass indexed to BSA, LAVI=left atrial volume indexed to BNSA, MPR=myocardial perfusion reserve, MBF=myocardial blood flow, PSS=peak systolic strain, PSSR=peak systolic strain rate, AoV Ca^{2+} score=aortic valve calcium score, CPET=cardiopulmonary exercise test, VO_2=oxygen consumption, LVRPP=left ventricular rate pressure product

The results of stepwise multivariate analysis for the secondary outcome-3 are shown in Table 69 and Table 70, after entering the following variables: gender, AVAI, MPR, LVM/volume, positive CPET, NT-proBNP.

Multivariate associations of the secondary outcome-3 using strict definition CPET included AVAI, MPR and positive CPET. Using the conventional definition of CPET, these included AVAI, MPR and positive CPET.

Table 69. Multivariate associations of secondary outcome-3 (strict definition CPET)

Variable	HR (95% CI)	p-value
AVAI	0.60 (0.48 - 0.75)	<0.001
MPR	0.57 (0.36 - 0.89)	0.013
Positive CPET (strict)	2.56 (1.31 - 5.01)	0.006

Abbreviations: AVAI=AVA indexed to BSA, MPR=myocardial perfusion reserve, CPET= cardiopulmonary exercise test

Table 70. Multivariate associations of secondary outcome-3 (conventional definition CPET)

Variable	HR (95% CI)	p-value
AVAI	0.59 (0.47 - 0.74)	<0.001
MPR	0.52 (0.33 - 0.83)	0.006
Positive CPET (conventional)	1.77 (1.02 - 3.09)	0.043

Abbreviations: AVAI=AVA indexed to BSA, MPR=myocardial perfusion reserve, CPET= cardiopulmonary exercise test

7.7 Comparison of MPR and symptomatic CPET as predictors of outcome

The primary hypothesis of the PRIMID-AS study was that MPR would be a better predictor of outcome than symptom-limited exercise testing.

7.7.1 Kaplan-Meier survival curves

The Kaplan-Meier survival curves for MPR (above and below optimal MPR cut-point of 2.098 from ROC analysis) and CPET (positive *vs.* all others) for the ***primary outcome*** are shown in Figure 51. Event-free survival was significantly lower in those with low MPR (p=0.014) and a positive CPET, using both strict (p=0.003) and conventional (p=0.035) definitions.

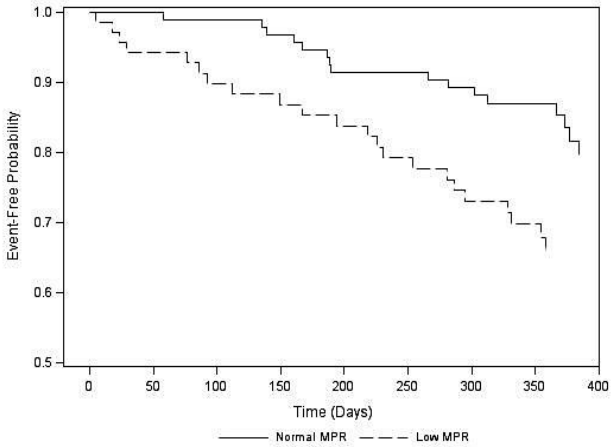
Event-Free Probability
1.0
0.9
0.8
0.7
0.6
0.5
0
50
100
150
200
250
300
350
400
Time (Days)
Normal MPR
Low MPR

a.

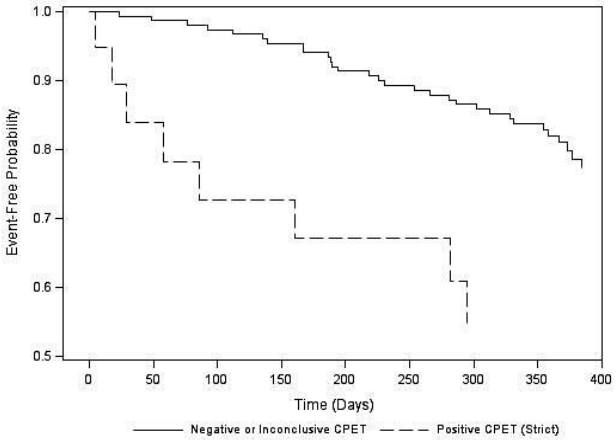
Event-Free Probability
1.0
0.9
0.8
0.7
0.6
0.5
0
50
100
150
200
250
300
350
400
Time (Days)
Negative or Inconclusive CPET
Positive CPET (Strict)

b.

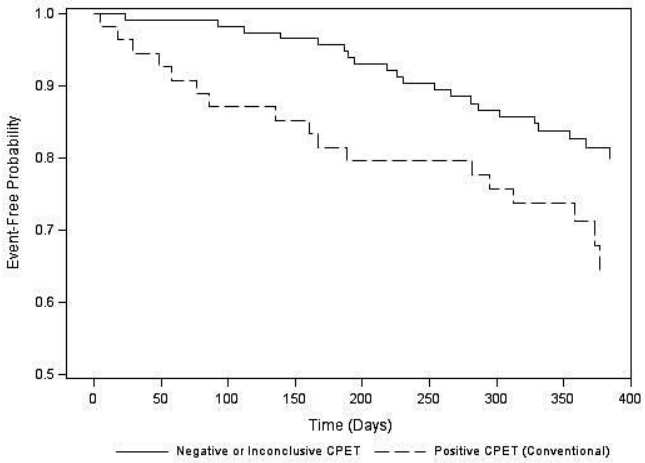
Event-Free Probability
1.0
0.9
0.8
0.7
0.6
0.5
0
50
100
150
200
250
300
350
400
Time (Days)
Negative or Inconclusive CPET
Positive CPET (Conventional)

c.

	Survival probability estimates at 12 months		
MPR	Normal: 0.87 (0.78,0.92)	Low: 0.66 (0.53, 0.76)	Difference: 0.21 (0.08, 0.33) p=0.002
CPET (strict)	Pos: 0.55 (0.30, 0.74)	Neg/inc: 0.82 (0.75, 0.87)	Difference: -0.27(-0.47,-0.07) p=0.008
CPET (conventional)	Pos: 0.71 (0.57, 0.82)	Neg/inc: 0.83 (0.74,0.89)	Difference: -0.12 (-0.25, 0.02) p=0.093

Figure 51. Kaplan-Meier survival curves for the primary outcome for a.) above and below MPR cut-point (Log-Rank p=0.014), b.) positive *vs.* negative/inconclusive CPET (strict definition) (Log-Rank p=0.003), c.) positive *vs.* negative/inconclusive CPET (conventional definition) (Log-Rank p=0.035)

7.7.2 Sensitivity, Specificity, Positive predictive value and Negative predictive value of MPR and CPET

The sensitivity, specificity, positive predictive value (PPV) and negative predictive value (NPV) of MPR and symptom-limited CPET for predicting the ***primary outcome*** are shown in Table 71. Both parameters had a very high NPV but a low PPV, suggesting their utility as a 'rule-out test', rather than predicting the onset of symptoms. The strict definition CPET in particular, had a very high specificity but very low sensitivity.

Table 71. Sensitivity, specificity, PPV and NPV of MPR and CPET for primary outcome

Parameter	Sensitivity	Specificity	PPV	NPV
MPR	0.605	0.622	0.324	0.840
Positive Exercise Test (strict)	0.211	0.918	0.421	0.804
Positive Exercise Test (conventional)	0.447	0.716	0.309	0.821

Similar data for the ***secondary outcomes*** is shown in Table 72. Similar trends were noted for the secondary outcomes as the primary outcome.

Table 72. Sensitivity, specificity, PPV and NPV of MPR and CPET for secondary outcomes

Parameter	Sensitivity	Specificity	PPV	NPV
***Secondary outcome-1**: Composite primary endpoint over entire study period*				
MPR	0.587	0.630	0.380	0.798
Positive Exercise Test (strict)	0.196	0.921	0.474	0.758
Positive Exercise Test (conventional)	0.457	0.730	0.382	0.786
***Secondary outcome-2**: All AVRs/deaths/MACE at 12 months*				
MPR	0.625	0.650	0.423	0.809
Positive Exercise Test (strict)	0.208	0.927	0.526	0.752
Positive Exercise Test (conventional)	0.417	0.718	0.364	0.761
***Secondary outcome-3**: All AVRs/deaths/MACE over entire study period*				
MPR	0.603	0.664	0.493	0.755
Positive Exercise Test (strict)	0.186	0.929	0.579	0.686
Positive Exercise Test (conventional)	0.407	0.726	0.436	0.701

7.7.3 Receiver Operator Characteristic (ROC) analysis and area under curve (AUC)

7.7.3.1 Primary outcome ROC and AUC analysis

In order to assess the predictive accuracy of the two variables, logistic regressions and Receiver Operator Characteristic (ROC) analysis, with calculation of the area under the curves (AUC), was performed (Figure 52).

The AUC was 0.62 (0.52-0.71, p=0.019) for *MPR*, 0.58 (0.49-0.67, p=0.071) for *conventional CPET*, and 0.56 (0.50-0.63, p=0.071) for *strict CPET*. Therefore, both MPR and CPET had moderate accuracy for predicting outcome, with only MPR being statistically significant.

For the above analysis, positive CPET was compared against all others, i.e., negative and inconclusive tests combined. We also looked at the effect of combining positive and inconclusive tests against the truly negative test. This increased the AUC for CPET to significant values (AUC=0.62 (0.55-0.70, p=0.002

for *conventional CPET*, and AUC=0.60 (0.51-0.69, p=0.024) for *strict CPET*), suggesting a better role of CPET in identifying the low-risk population, rather than predicting those who go on to develop symptoms within 12 months.

The AUC's of MPR and CPET were compared using correlated ROC analysis. There was no significant difference between the AUC's of MPR and CPET when predicting the primary outcome: (0.05(-0.06-0.17, p=0.375) for strict definition and 0.05(-0.10-0.19, p=0.516) for conventional definition). The MPR cut-point for predicting primary outcome was also selected to match the sensitivity of symptomatic CPET, and paired comparisons of the specificities of the two techniques were carried out using McNemar's Test. There was no significant difference between the two parameters as predictors of primary outcome using this approach (p>0.05).

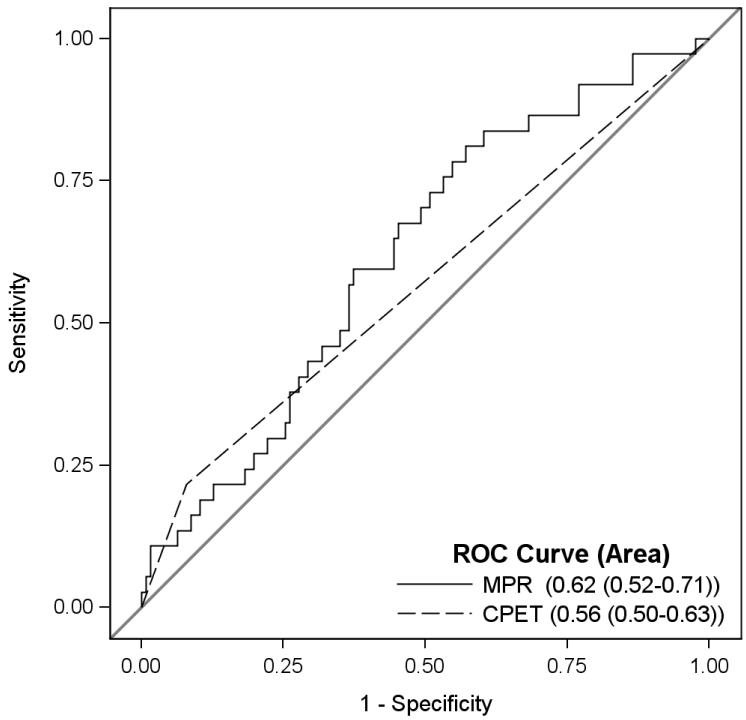

a.

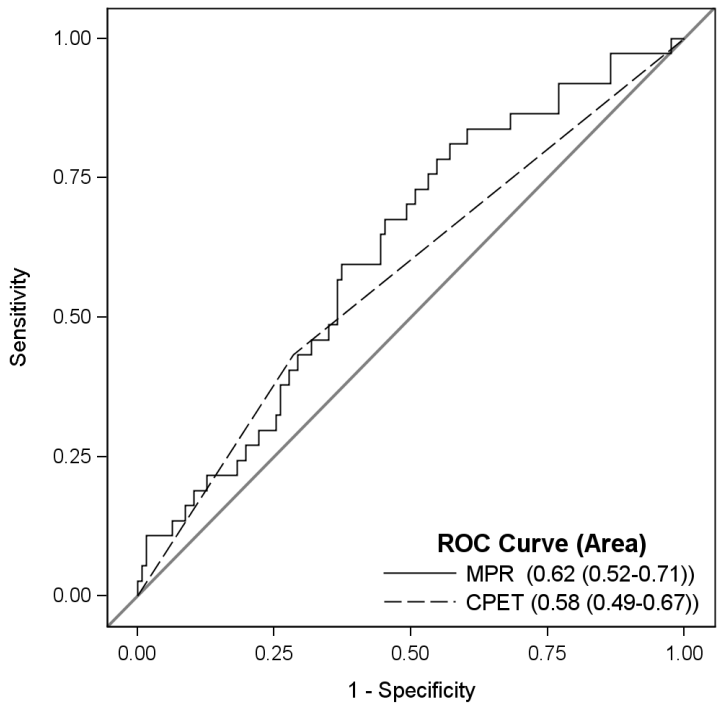

b.

Figure 52. ROC curves for MPR and symptom-limited Exercise Test (a.) strict definition, b.) conventional definition) for predicting the primary outcome

7.7.3.2 Secondary outcomes ROC and AUC analysis

The AUC's for MPR and symptomatic CPET for predicting the secondary outcomes are listed in Table 73. As can be seen, the AUC for MPR remained statistically significant for all secondary endpoints, with moderate predictive accuracy, while only the conventional definition CPET was significant for secondary outcome-1 and only the strict definition CPET was significant for secondary outcomes 2 and 3.

Table 73. Predictive accuracy of MPR and CPET for secondary outcomes

Parameter	AUC (95% CI)	p-value
***Secondary outcome-1**: Composite primary endpoint over entire study period*		
MPR	0.612 (0.52-0.71)	0.020*
Positive Exercise Test (strict)	0.558 (0.50-0.62)	0.069
Positive Exercise Test (conventional)	0.593 (0.51-0.68)	0.027*
***Secondary outcome-2**: All AVRs/deaths/MACE at 12 months*		
MPR	0.641 (0.55-0.73)	0.002*
Positive Exercise Test (strict)	0.568 (0.51-0.63)	0.033*
Positive Exercise Test (conventional)	0.567 (0.49-0.65)	0.104
***Secondary outcome-3**: All AVRs/deaths/MACE over entire study period*		
MPR	0.632 (0.54-0.72)	0.004*
Positive Exercise Test (strict)	0.558 (0.50-0.61)	0.041*
Positive Exercise Test (conventional)	0.566 (0.49-0.64)	0.086

7.8 Discussion

A number of studies have linked the development of LV remodeling, and particularly myocardial fibrosis measured with CMR, with adverse outcome in AS. This is the first prospective study to explore the hypothesis that CMR could predict the development of symptoms in asymptomatic patients with AS, who may benefit from early surgical intervention. It has been shown previously that MPR is an independent predictor of exercise capacity and inversely associated with NYHA class in patients with severe AS undergoing AVR(108). In this study we have confirmed that low MPR in initially asymptomatic patients with moderate-

severe AS is also associated with the development of symptoms within 12 months. However, the accuracy of MPR to predict outcome was moderate at best and, contrary to our primary hypothesis, not significantly better than exercise testing.

This is the largest cohort of patients with asymptomatic moderate-severe AS to date to have undergone both exercise testing and CMR, as well as the largest cohort looking at the prognostic value of exercise testing in AS. The primary endpoint occurred in 22% of patients at 12-months and the secondary endpoints in 27-35%, and is comparable to that seen in previous reports(42), (33) .

7.8.1 Exercise testing

It may be surprising that exercise testing to identify 'pre-symptomatic patients' performed poorly in this study, given the now class-I indication for surgery for this finding in the major International guidelines. Though, it is worth noting that the 2014 AHA/ACC guidelines re-classified symptoms on exercise testing from a class IIb indication to a class I indication for AVR, without any randomised trials, and after the commencement of our study, when exercise testing was not widely adopted in our institutions. However, our results are largely consistent with the published literature. A normal exercise test has a high negative predictive accuracy (ranging from 0.86-1.00 in previous studies compared to 0.82 in ours)(32, 33, 43), suggesting that patients who do well on exercise testing can be safely managed conservatively. However, although patients who develop symptoms on exercise testing are at higher risk of developing spontaneous symptoms or experiencing MACE, the specificity of a positive test is low (0.60-0.78 in previous studies compared to 0.72 in ours)(42, 43). In this study, only 17 of 55 patients who had a positive test, using a conventional definition of symptoms at any stage, developed spontaneous symptoms within 12 months. The results were consistent in a sensitivity analysis (Appendix-5: section 9.5) of patients with severe AS only (specificity 0.69). If current guidelines were followed, our data suggest that many patients may be sent for early surgery unnecessarily, as the

majority of patients with a positive test did not develop spontaneous symptoms within 12 months. One further limitation was the high proportion of patients in our study with inconclusive results (30%), despite restricting inclusion to those who can exercise. This highlights another real-world limitation of exercise testing, and the potential risk of wrongly categorising patients who are unable to perform a minimal level of exercise.

As previously demonstrated(33, 36, 127), echocardiographic measures of severity are important predictors of outcome although there is wide overlap between groups. Only one other study has identified female gender as increasing risk of symptoms(50). Female patients may have a different remodeling process, as suggested by lower cardiac volumes and more concentric LV geometry than men(192, 209). Similar pressure gradients despite lower stroke volumes may therefore indicate more severe disease in females compared to men. This may suggest a need for gender-specific cut-offs for definition of severity. Female patients also tend to perform less well on exercise testing(210), and may therefore be more likely to be labelled as having an inconclusive test, and not identified as high risk until a later stage.

7.8.2 CMR predictors of outcome

7.8.2.1 LV remodeling

Our patient cohort clearly showed evidence of remodeling compared to controls, despite all being asymptomatic and 29% with moderate AS, as shown in Chapter-5. However, LVEDV and mass were not significantly higher in the outcome group. The lack of association of mass and volumes with outcome in this study is likely to be related to the high event rate in female patients, who have smaller hearts even when indexed to body size(192, 209).

7.8.2.2 Longitudinal and circumferential myocardial deformation

There were no significant differences seen in longitudinal strain parameters, whilst circumferential PSS and PEDSR were actually higher in the primary

outcome group. Comparison of our patient cohort with matched controls has already suggested that these asymptomatic patients are still at an early stage of 'compensated' hypertrophy, with impaired longitudinal but not circumferential strain parameters and no difference in exercise capacity compared to controls (Chapter-5). This might also explain the higher circumferential parameters in the outcome group.

Work by Carasso *et al* using TTE to assess myocardial deformation in severe AS patients undergoing AVR *vs.* controls showed the mid-PSS-C and mid-PEDSR-C to be higher in patients than controls pre-AVR, which returned close to normal values early post-AVR. The longitudinal parameters however, were lower pre-AVR, and increased post-AVR(211). They went on to assess the effect of low LVEF on this, and once again found supra-normal mid-PSS-C in those with preserved LVEF, whilst both longitudinal and circumferential strain were reduced in those with impaired LVEF(212). More recently, the same group has published data looking at strain parameters in asymptomatic *vs.* symptomatic AS with preserved LVEF and controls, and shown that asymptomatic AS demonstrated a smaller reduction in PSS-L than symptomatic, a supra-normal apical-PSS-C and supra-normal apical rotation, compared to controls(213). Taken together, these data suggest that there is an initial increase in circumferential deformation to compensate for the loss of longitudinal function resulting from sub-endocardial ischaemia, in order to maintain normal LVEF (Figure 53). Whilst there is a steady decline in longitudinal strain parameters with increasing LV afterload(196), circumferential strain initially increases to 'supra-normal' levels before declining with progressive disease.

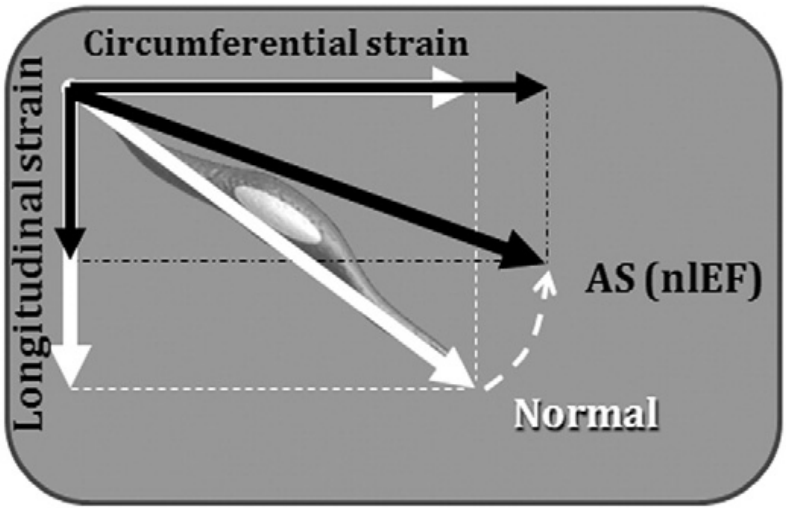

Figure 53. A schematic showing interaction of longitudinal and circumferential strain in order to maintain a normal LVEF: as longitudinal strain decreases, circumferential strain increases to maintain a normal shortening vector and therefore LVEF. (Reproduced from (212))

7.8.2.3 Markers of fibrosis

LGE and ECV in this study were not associated with the primary outcome. This was despite LGE being found in 47% of our patients, affecting a mean of 4.2% of the LV mass. However, we did not exclude patients with infarct-pattern LGE (n=26), which may have over-estimated the amount of LGE, though it is within the range reported in previous studies of AS (3.0-7.3% of LV)(25, 89, 91, 93). However, the incidence and amount of LGE reported in AS has been variable, which may partly be due to differences in quantification method used, and symptom status of patients have not always been specified. In one study with severe, mostly symptomatic AS, LGE was reported in as high as 79% of patients, affecting 19.7% of the LV(205). Although LGE has been shown to be associated with poor outcome, this has been almost exclusively in patients with severe AS who have undergone AVR(89, 92). In that context LGE represents replacement fibrosis and is likely indicative of irreversible LV remodeling, rather than predictor of symptom onset.

There has been intense interest in quantification of ECV, as a surrogate of diffuse interstitial fibrosis, and the relationship to clinical outcomes in a range of cardiac conditions, especially AS(101, 214). We saw only a very small difference in ECV (1%) between those who did and did not develop symptoms and have also shown that ECV is not increased in asymptomatic patients with AS, compared to age and sex-matched controls(197). This highlights one of the limitations of ECV. The normal range of ECV is in the order of 25%, and there is very wide overlap between patients and healthy controls and therefore it is likely to be insensitive to small increases in interstitial fibrosis(99, 100). So, although ECV may detect differences in populations, it is unlikely to be of clinical value in individual patients unless they have extreme values, such as in amyloidosis(99).

7.8.2.4 Myocardial perfusion

Both global MPR and total stress MBF were significantly lower in the primary outcome group, with no difference in rest MBF. MPR was also a univariate predictor of outcome, as well as there being significant survival difference in those with a low and high MPR on Kaplen-Meier analysis. Finally, ROC analysis demonstrated statistically significant AUC for MPR to predict the primary outcome, though with moderate accuracy. Despite the above, MPR did not come out as an independent predictor of the primary outcome on stepwise multivariate analysis. Interestingly however, MPR was an independent predictor of the secondary outcomes that included all AVR's despite being asymptomatic. This may reflect the factors that influence Clinicians to refer patients for surgery despite being asymptomatic, which in turn may be determinants of a low MPR. For example, patients with higher gradients/lower AVA and more LVH on TTE are more likely to be referred, which are factors that have been shown to be associated with a low MPR / CFR in AS in previous studies(24, 108, 205).

There are still limitations in quantitative MBF analysis, with time-consuming post-processing and complex, non-standardised algorithms in use. As a result, the test-retest repeatability of MBF and MPR was found to be relatively poor (section 3.5),

which may limit its predictive accuracy for outcome. However, there was a clear incremental decline in MPR between our controls, asymptomatic AS patients and previously studied severe mostly symptomatic AS patients(108) (3.16±0.65, 2.27±0.70 and 2.03±0.55 respectively). The only other study looking at CMR-measured MPR in severe AS showed it to be an independent predictor of aerobic exercise capacity and inversely related to NYHA class symptoms(108). There have been no studies looking at the prognostic value of MPR in AS. We have shown for the first time that MPR is associated with symptom onset in initially asymptomatic AS, albeit with moderate predictive accuracy.

7.8.3 MPR *vs*. Exercise Testing

The primary hypothesis of the PRIMID-AS study was that MPR would be a better predictor of outcome than exercise testing in asymptomatic patients with moderate to severe AS. We found MPR and strict-definition positive CPET (but not conventional-definition) to be univariate predictors of the primary outcome, and only strict-definition CPET to be an independent predictor on multivariate analysis. In addition, on ROC analysis, the AUC for CPET was not statistically significant but MPR was. However, both had moderate predictive accuracy (AUC around 0.60), with no significant difference between the two. Overall therefore, we cannot conclude that MPR is a better predictor of outcome.

As mentioned, 'symptoms on exercise testing' has been upgraded to a class-I indication for AVR (from previous IIb) by ACC/AHA guidelines, to align with the ESC guidelines(5, 215). However, our findings of exercise testing performing poorly as a predictor of symptom onset and outcome seriously call into question this recommendation, which is not based on randomised trials, but mainly on single-centre observational studies with small numbers of patients (30 to 160)(32, 33, 39, 43). Clearly, there is need for better risk stratification of patients with severe AS to select those who may benefit from early operative intervention without unnecessarily subjecting patients to the risks of major surgery. Ideally, randomised control trials of exercise / imaging markers would be the best way to

address this, but this may not be easily possible. Perhaps, a stratified approach using a combination of risk-stratification strategies including biomarkers, exercise and imaging may be the way forward, as discussed in the final chapter (Figure 54).

7.8.4 Summary

Our data suggest that this cohort of patients may be in a state of 'compensated remodeling', with clear evidence of LV remodeling in patients compared to controls, yet without significant differences in exercise capacity. Amongst the patient group, there were no significant differences in markers of LV remodeling between those with and without an outcome, which may partly be due to more females in the outcome group, but there was lower MPR and higher circumferential strain values, suggesting the presence of subendocardial ischaemia, with compensation, prior to decompensation leading to symptom onset and decline in LVEF. No differences were demonstrated in LGE and ECV in our cohort, which also did not predict symptom onset. The main finding of the PRIMID-AS study is the moderate predictive accuracy of both symptom-limited exercise testing and MPR for symptom onset, which may have important implications for current clinical guidelines.

Perhaps, symptom onset remains the current best marker of poor outcome in AS, necessitating AVR, but studying only those who already have symptoms does not advance our understanding of the pathophysiology of this complex disease. The need remains to identify those patients at the brink of changing to decompensation, just prior to symptom onset and irreversible changes within the myocardium. Further refinement of risk-stratification and management is clearly required in asymptomatic AS.

7.8.5 Strengths and limitations

Our prospective study has a number of strengths compared to previous work in asymptomatic AS patients. It was multicentre and although observational, was

run from outset to the same standards as a randomised controlled trial. The CMR and CPET results were blinded to the clinicians, imaging tests were analysed in a core lab, and there was independent event adjudication and statistical analysis. We also recruited a well-described population who were regarded as low risk (in whom prophylactic AVR may be offered) and were prepared to have surgery should symptoms develop. Finally, the primary endpoint was carefully defined and excluded those being referred for AVR prior to the onset of spontaneous symptoms, which is a soft endpoint.

Although this study was large for it's kind, the number of clinical events up during follow-up period was relatively small, especially hard clinical endpoints (MACE and deaths), and this limits the number of variables that could be entered into the multivariate models. The short follow-up time is therefore a limitation, however, longer-term follow-up is planned and this may address some of these limitations. The inclusion of patients with moderate disease may be criticised, however, these patients do have high event rates and the results of the study were consistent when only the 123 patients with severe AS were analysed. There was also missing data (T1 mapping) due to technical problems during the study, but his did not affect the primary outcome analysis.

7.8.6 Conclusions

CMR measured MPR and symptom-limited exercise testing were associated with clinical outcome at 12 months in initially asymptomatic patients with moderate-severe AS. However, predictive accuracy was moderate at best and MPR was not superior to symptom-limited exercise testing. LGE and ECV did not predict outcome.

CHAPTER EIGHT

8 THESIS CONCLUSIONS AND RECOMMENDATIONS FOR FUTURE RESEARCH

8.1 Reproducibility of novel CMR techniques in AS

Rationale: The purpose of this chapter was to establish the reproducibility, especially the test-retest repeatability of the variours CMR techniques. This was because good reproducibility is important for serial assessment of patients, as well as in differentiating abnormal from normal, and it has not previously been well established in this particular cohort of patients. It also helped us decide what analysis techniques to use going forward within this thesis, with the exception of the Ranolazine sub-study, the methodology for which had been pre-planned.

8.1.1 Myocardial deformation: a comparison between Tagging and Feature Tracking at 1.5 T and 3 T

-The total time for tagging analysis is approximately double that required for FT (50 minutes *vs.* 25 minutes), which is even quicker if only endocardial contours are utilised.

-PSS and PEDSR values derived using FT are higher than those using tagging, regardless of field strength and whether only endocardial, or both endocardial and epicardial contours are used for FT. FT and tagging strain measures are therefore not interchangeable.

-The inter-observer variability of circumferential PSS and PEDSR using both tagging and FT at both field strengths was good. The inter-observer variability of longitudinal PSS and PEDSR was better with FT than tagging at 3T.

-The test-retest repeatability of circumferential PSS is excellent using FT and good using tagging at 1.5T and 3T. The repeatability of circumferential PEDSR assessed by FT and tagging at 1.5T is good when only basal and mid slices are used but moderate to poor at 3T. Tagging appears to offer no significant advantages over FT for the assessment of strain and diastolic strain rate in patients with AS.

8.1.1.1 Original Hypothesis

H_0: MRI measured strain and strain rate, using tagging and Feature Tracking, does not have good reproducibility at 3T (CoV > 20%): ***rejected***.

8.1.1.2 Future implications

Based on these findings, in future studies where the primary outcome relates to the assessment of circumferential PEDSR, measurement at basal and mid slices at 1.5T would be recommended, which was not possible for the Ranolazine sub-study as the methodology had been pre-planned, whilst MPR was the primary outcome measure of interest for the PRIMID-AS study, which is better assessed at 3T.

Ideally, for direct comparison of 1.5T with 3T, test-retest repeatability should be assessed in the same cohort of patients.

8.1.2 T1 mapping using MOLLI at 3T: parametric map *vs.* full MOLLI series

-The intra- and inter-observer variability for native T1 and ECV is excellent using the parametric T1 maps for assessment and good using the full MOLLI series.

-The test-retest repeatability of T1 quantification using MOLLI is excellent in patients with AS, and is higher when outlining the myocardium on a single T1 parametric map rather than on each individual MOLLI image.

8.1.2.1 Original Hypothesis

H_0: MRI measured T1 / ECV does not have good reproducibility (CoV > 20%): ***rejected***.

8.1.2.2 Future implications

These results suggest that this technique is robust and repeatable, and could be used reliably for serial monitoring of AS patients. It also confirms that using parametric T1 maps is quicker and as robust as the full dataset acquired.

8.1.3 MPR at 3T: a comparison of MOCO *vs.* raw image analysis

-The average time taken to contour the MOCO images is about half that for the raw images, due to less manual adjustment required (22 minutes *vs.* 10.6 minutes).

-There is excellent correlation between the MBF and MPR values obtained using the MOCO and raw images.

-The intra- and inter-observer variability of MBF and MPR quantification is good to moderate, and not much different between raw and MOCO images.

-The test-retest repeatability is moderate to poor for the overall cohort, and best for rest MBF.

8.1.3.1 Original Hypothesis

H_0: Both MOCO and raw images are equally reproducible for measurement of MPR: ***accepted***.

8.1.3.2 Future implications

The results call into question the utility of quantitative MBF / MPR as a reliable outcome measure in interventional clinical trials, using the current complex post-processing and quantification techniques. There is a need for simplification and semi-automation of post-processing, as well as a more standardised approach to absolute MBF quantification, which would hopefully lead to better reproducibility of this important CMR technique.

Future work comparing the reproducibility of single-bolus *vs.* dual-bolus technique, or single-contrast *vs.* dual-contrast in the same cohort of patients may help refine the technique further.

8.2 Effect of Ranolazine on CMR measured diastolic function and MPR in asymptomatic AS

Rationale: Ranolazine has been shown to improve diastolic function and myocardial perfusion in animal models and small clinical studies. The purpose of this sub-study was therefore to assess its effect on diastolic function and MPR in asymptomatic patients with moderate to severe AS who already have evidence of diastolic dysfunction.

Conclusions:

-There was no conclusive evidence that Ranolazine improved PEDSR or MPR, though some interesting trends were demonstrated. There was a non-significant trend for PEDSR to increase from the baseline value to a higher value after 6 weeks of oral Ranolazine, and then reduce to a lower value at week-10, after stopping Ranolazine. On sub-group analysis, these differences were more apparent in the high-PPG (with a statistically significant increase in PEDSR at week-6 for the mid-slice and the average of basal and mid slice values) and low-MPR sub-groups.

-The total exercise duration showed a trend towards increasing at week-6, with a lower exercise LVRPP. The trend for the exercise LVRPP to reduce at week-6 was mirrored in the same sub-groups that demonstrated an increase in PEDSR (high-PPG and low-MPR).

8.2.1 Original Hypothesis

H_0: Short-term treatment with Ranolazine does not lead to an improvement in MPR and diastolic strain rate in patients with moderate to severe AS: ***accepted***.

8.2.2 Future implications

Given the low power of the current study, a larger study in patients with severe AS and diastolic dysfunction is warranted and preferably conducted at 1.5T (given

the findings of the previous chapter), with consideration of feature tracking or tissue tracking for strain analysis, to avoid data loss with tagging.

8.3 Comparison of asymptomatic patients with moderate to severe AS and healthy controls

Rationale: Most CMR studies that have compared patient groups to controls have recruited younger subjects with no co-morbidities. We wanted to establish normal reference values for the novel CMR techniques assessed as part of this thesis in age matched controls, without excluding common co-morbidities, in order to assess the incremental value of AS on these parameters. Secondly, as our patients were asymptomatic and at an early stage of disease, we also wanted to confirm whether they demonstrate changes in LV remodeling and exercise capacity compared to matched controls.

Conclusions:

-Patients with AS demonstrated evidence of higher myocardial workload (LVRPP), LV remodeling, impaired longitudinal function, reduced stress MBF / MPR, and a greater degree of focal myocardial fibrosis than matched controls, despite being asymptomatic. However, there was no significant difference in exercise capacity (VO_2), circumferential strain / strain rates, rest MBF and ECV.

8.3.1 Original Hypothesis

H_0: Asymptomatic patients with moderate to severe AS do not show evidence of LV remodeling and impaired exercise capacity compared to controls: ***partially rejected***.

8.3.2 Implications

We have established normal reference values for novel CMR parameters in an ilder group of controls with common co-morbidities. We have also shown patients

at an earlier asymptomatic stage of AS are in a state of compensated hypertrophy, with some evidence of LV remodeling and other changes, but with preserved exercise capacity. Therefore, there is a need for better risk stratification and further studies are needed at this early asymptomatic phase, in order to prevent further irreversiblr remodelling and exercise limitation.

8.4 Determinants of exercise capacity, MBF and MPR in asymptomatic AS

Rationale: An understanding of the determinants of exercise capacity in theses patients will enhance our understanding of the pathophysiology of symptom development in AS. MPR has previously been shown to be independenly associated with exercise capacity in AS, and establishing its determinants would also further aid our understanding of the pathophysiology of AS.

8.4.1 Determinants of age- and sex-corrected peak VO_2

-Univariate: Peak VO_2 was directly correlated with AVAI, longitudinal and circumferential strain, MPR and PWV, while inversely correlated with NT-proBNP, VAI, LV mass/volume, rest MBF, coronary calcium score and Cornell LVH criteria on ECG.

-Multivariate: The independent associates of age and sex-corrected peak VO_2 were gender, PSS-L(TTE) and MPR.

8.4.2 Determinants of age- and sex-corrected peak workload

-Univariate: This was positively associated with MPR and negatively with NT-proBNP, lateral E/e' and rest MBF.

-Multivariate: The independent associations of peak workload were log(NT-proBNP) and VAI(CMR), in addition to age and gender.

8.4.3 Determinants of MPR

-Univariate: MPR was inversely related to age, NT-proBNP, AS severity, LV mass/volume, ECV, AoV and coronary calcium scores, VAI (CMR) and resting LVRPP. It was directly related to longitudinal strain and diastolic strain rate on echo and exercise LVRPP.

-Multivariate: AV Vmax and ECV remained independently associated with MPR.

8.4.4 Original Hypotheses

H_0: MPR does not predict peak VO_2 measured on CPET: ***rejected***.

H_0: MPR is not related to LV mass or myocardial fibrosis in asymptomatic AS: ***partially rejected*** (not related to LVMI or LGE, but was related to ECV).

8.4.5 Future implications

We have confirmed for the first time that MPR is an independent predictor of exercise capacity in asymptomatic patients with AS, similar to what was shown by our group for more advanced AS. In addition, longitudinal strain and global afterload (VAI) were also associated. This may suggest that the increased global afterload caused by the AS adds to reduced MPR, which in turn causes subendocardial ishaemia and impaired longitudinal function. All these changes ultimately lead to reduced exercise capacity, even in the early compensated phase of the disease. Ideally, randomised controlled trials of early AVR *vs.* continued monitoring in those with and without these changes would be the ultimate way to test their value in risk-stratification of these patients, but may be difficult to achieve. Larger phase III studies addressing novel therapeutic targets in AS, especially LV remodeling, fibrosis and calcification, some of which are already under way, will provide further insights into the pathophysiology of symptom onset and improve management of asymptomatic patients with AS.

8.5 A comparison of exercise testing and stress CMR to predict outcomes in asymptomatic AS

Rationale: This chapter outlines the results of the PRIMID-AS study, the aim of which was to directly compare the prognostic value of MPR with symptom-limited exercise testing in asymptomatic AS. This was because exercise testing is the best-studied risk-stratification tool so far, whilst our group previously showed that MPR was an independent predictor of exrcise capacity in those with more advanced AS. We therefore wanted to assess the role of MPR in tgose at an earlier stage of AS.

Conclusions:

-CMR measured MPR and symptom-limited exercise testing were both associated with clinical outcome at 12 months in initially asymptomatic patients with moderate-severe AS.

-The predictive accuracy for both was moderate at best, and MPR was not superior to symptom-limited exercise testing.

-LGE and ECV did not predict outcome.

-Amongst the patient group, there were no significant differences in markers of LV remodeling between those with and without an outcome, which may partly be due to more females in the outcome group, but there was lower MPR and higher circumferential strain values, suggesting the presence of subendocardial ischaemia, with compensation, prior to decompensation leading to symptom onset and decline in LVEF.

-Multivariate predictors of the primary outcome were gender, AVAI and positive CPET using the strict definition only, but NT-proBNP instead of positive CPET, when entering the conventional definition CPET into the model.

8.5.1 Original Hypothesis

H_0: MPR is not a better predictor of outcome in moderate to severe AS than exercise testing: ***accepted*** (but both equally poor).

8.5.2 Future implications

For the first time we have shown the importance of CMR measured MPR in predicting symptom onset and outcome in patients with AS at an earlier asymptomatic phase of the disease. However, both MPR and exercise testing only demonstrated moderate predictive accuracy for outcome. Our findings therefore call into question the current class-I recommendation of AVR for symptoms on exercise testing in asymptomatic AS, which is not based on randomised trials, but mainly on single-centre observational studies with small numbers of patients. We have shown a greater potential of exercise testing in identifying the low-risk population, rather than those who go on to develop symptoms within 12 months.

There is need for further refinement of risk stratification of asymptomatic patients with severe AS to select those who may benefit from early operative intervention. Our data suggest that some of these patients are actually still in a 'compensated' phase of disease, implying that a 'wait and watch' policy is the correct approach for them. However, identifying those who are at the brink of 'decompensating' would be the ideal goal in improving management of these patients. Ideally, randomised control trials of exercise / imaging markers would be the best way to address this, but this may not be easily possible. Perhaps, a stratified approach using a combination of risk-stratification strategies including biomarkers, exercise and imaging, such as the one suggested below, may be the way forward (Figure 54).

Figure 54. Stratified approach to risk-stratification of asymptomatic patients with moderate to severe AS

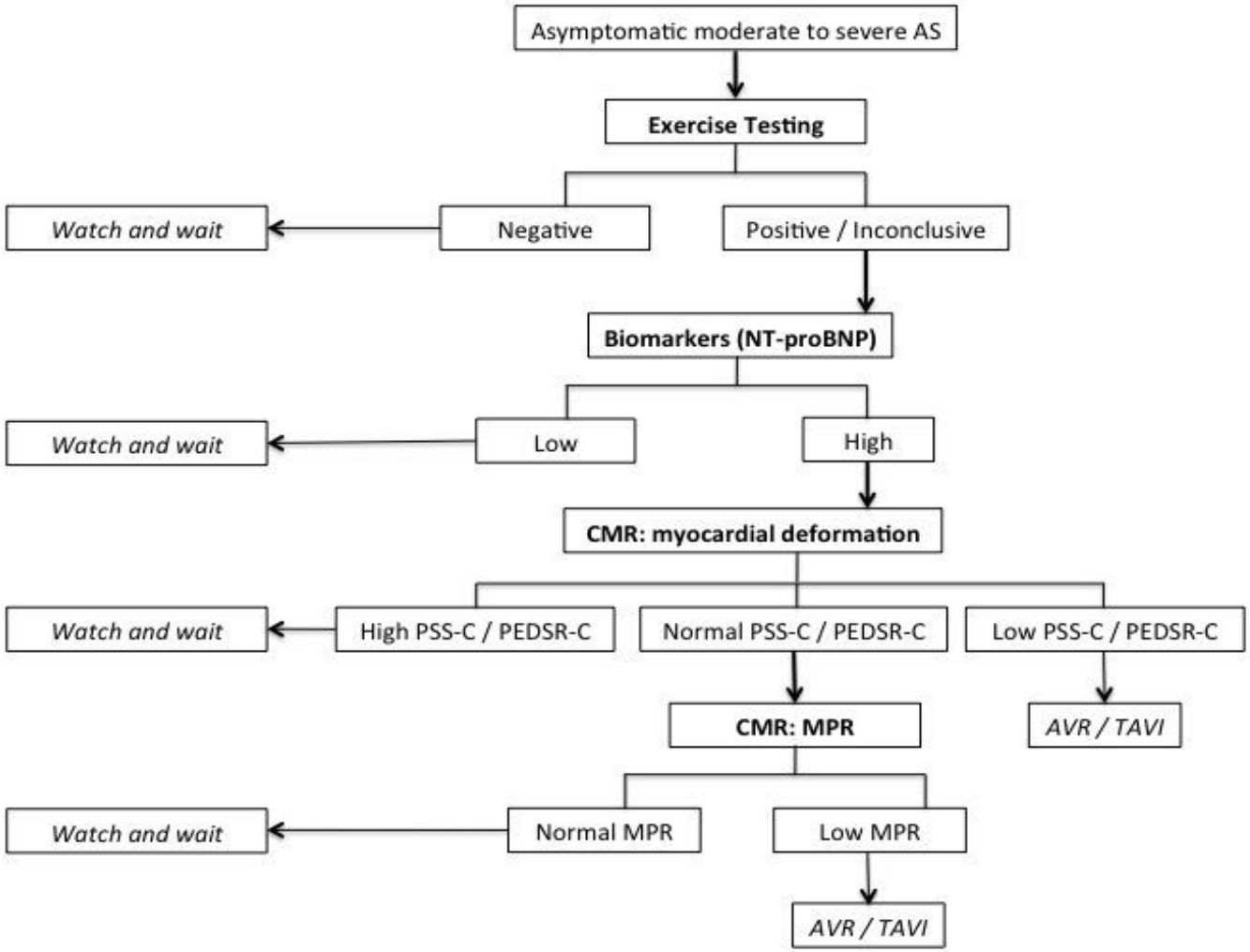

8.6 Other planned analyses

-Longer-term follow-up: We plan to look at determinants of longer-term outcome (2 year, 5 year), as this would increase the number of hard endpoints and allow more variables to be entered in the multivariate models.

-Gender differences in exercise capacity and its determinants in AS: This will give us more insight into gender differences in the response to AS and the pathophysiology of exercise limitation and symptom onset in male and female patients.

-Gender differences in LV remodeling in response to AS / determinants of MPR: There is a potential need for different definitions of 'severe AS' in females.

-Progression of LV remodeling in asymptomatic AS: We have acquired additional CMR in 50 patients who remained asymptomatic at 12 months. This analysis will give us further insights into the progression of LV remodeling in these patients.

-Differences in aortic stiffness between bicuspid and tri-leaflet AS: We plan to look at aortic distensibility and PWV in patients split according to their AV morphology.

-Role of biomarkers / troponin / ECG strain in asymptomatic AS: The stored plasma from our cohort is going to be used in a BHF-funded study looking at the role of other biomarkers (e.g., Galectin-3, MMP's, TIMP's), as well as collaborative work with Edinburgh looking at the role of troponin / ECG strain in these patients.

CHAPTER NINE

9 APPENDICES AND SUPPLEMENTARY DATA

9.1 Appendix-1: Summary of risk-stratification studies in Aortic Stenosis

Table 74. Summary of risk-stratification studies in AS

Author (year)	Number	Severity	Investigations	CAD excluded	Outcome measure	Follow-up	AVR / outcome	Total/ Cardiac Deaths	SCD	Outcome predictor
Pellikka 1990 (127)	143 (30 early AVR, **113** other)	Severe (Vmax >4m/s). Asymptomatic	**TTE**	History of MI, CABG	Death, symptoms.	Mean 20 months (range 6-48)	20 AVR (6 still asymp.), 37 developed symps, 14 deaths	14 (6 cardiac)	2	AV **Vmax**, **EF**.
Otto 1997 (36)	123	Vmax >2.5 m/s. Asymptomatic	**TTE**, treadmill **ETT** (104)	No	Death, AVR	2.5±1.4 years	56: 48 AVR (6 asymptomatic), 8 deaths	8 (4 cardiac- 2 refused AVR)	0	AV **Vmax**, **rate of change** of AV Vmax, **functional** status score.
Rosenhek 2000 (37)	128	Severe (Vmax >4m/s). Asymptomatic	**TTE**	No	Death, symptom-driven AVR	22±18 months	67 (59 symptom-driven AVR, 8 deaths) + 22 had AVR without symptoms	8 (6 cardiac- 3 refused AVR)	1	AV **calcification**, rapid **progression**
Amato 2001 (32)	66	Severe (AVA <1cm2). Asymptomatic	**TTE**, treadmill **ETT**	Excluded (angio)	Sudden death, symptoms	15±12 months	38 (34 symptoms, 4 SCD)	4	4	**AVA** < 0.7cm^2, positive **ETT**.
Alborino 2002 (43)	30	Moderate to severe (MPG>30 mmHg); Asymptomatic	Upright bike ergometry **ETT**	No	Cardiac death, symptom-driven AVR	12 months	10 symptom-driven AVR	0	0	Positive **ETT**.
Lancellotti 2005 (33)	69	Severe (AVA <1cm2). Asymptomatic	**TTE** (rest & exercise), semi-supine bike **ETT**	No	Symptoms, cardiac death, AVR	15±7 months	18 (Symptoms: 4, AVR: 12, death: 2)	3 cardiac (1 post AVR)	2	Increase in **exercise MPG>18 mmHg**, +ve **ETT**, **AVA**<0.75cm^2

Pellikka 2005 (38)	622	Severe (Vmax >4m/s). Asymptomatic	**TTE**	History of MI, PCI, CABG	Symptoms, AVR, death	5.4±4 years	Symps: 297; AVR: 352 (131 asymp); Death: 265.	265 (117 cardiac)	11	**AVA**, **LVH** (symptom development). **Age**, **CRF**, **inactivity**, **AV Vmax** (mortality)
Das 2005 (42)	125	Moderate to severe (AVA <1.4cm2)	**TTE**, treadmill **ETT**	No	Symptoms, cardiovascular death	12 months	36 developed symptoms	0	0	**Exercise symptoms** (no additional benefit of BP/ST changes)
Monin 2009 (50)	107 (development cohort)	Moderate to severe (Vmax >3m/s, AVA <1.5cm), Asymptomatic	**TTE**, bike **ETT** (89), **BNP**	RWMA excluded	AVR (symptoms, +ve ETT), all cause death	24 months	62: 58 AVR (37 for symps.), 1 refused despite symptoms, 3 deaths	3 (1 cardiac), +1 post AVR	0	**Female** sex, **BNP**, AV **Vmax**.
Hachicha 2009 (40) Retrospective	544	Moderate to severe (Vmax > 2.5 m/s)	**TTE**	No	Overall mortality (regardless of AVR or medical Rx)	2.5±1.8 years	N/A	91 (51 cardiac)	Not specified	**Zva** (>3.5), **age**, **LVMI**.
Rosenhek 2010 (34)	116	Very severe (Vmax >5m/s)	**TTE**	No	Symptom-driven AVR, cardiac death	41 (26-63) months (median)	AVR indicated 90, cardiac death in 6. -10 refused AVR, 10 referred without symptoms.	17 (6 cardiac): 9 in no surgery grp., 8 post AVR.	1	AV **Vmax** >5.5m/s, **diabetes**, **hyperlipidaemia**.
Kang 2010 (35)	197: 102 early AVR, 95 conventional (at clinician's discretion)	Very severe (Vmax >4.5m/s, AVA <0.75cm^2), Asymptomatic	**TTE**	History or RWMA	Death (operative mortality and cardiac death)	1501 days (median)	148: 102 early grp, 46 conventional grp	3 (0 cardiac) early grp, 28 (18 cardiac) conventional grp.	9 (2 after symptoms) conventional grp, 0 early grp	AV **Vmax** >5m/s.
Lancellotti 2010 (39)	163	Moderate to severe (AVA<0.6 cm^2/m^2)	**TTE**, bike **ETT**	No	Symptoms, AVR, Cardiac Death	20±19 months	57 AVR (44 symptomatic), additional 11 symps (3 refused AVR, 8 on waiting list)	6 cardiac (+ 2 others not included in analysis)	3	AV **Vmax** (>4.4), LV **longitudinal deformation** (<15.9%), **VAI**, **LA** area.

Cioffi 2011 (18)	209	Severe (AVA<1cm^2 or MPG>40 mmHg)	**TTE**	History	Death, AVR, MI, HF hospitalisation	22±13 months	72 AVR (59 symptomatic); 15 hospitalisations, 7 refused AVR	20 (16 cardiac)	2	Inappropriately high **LVMI**, AV **Vmax**, **calcification**.
Greve 2012 (51)	1533 (SEAS study)	Mild to moderate (Vmax 2.5-4.0 m/s), Asymptomatic	**ECG** (LVH-Sokolow-Lyon & Cornell voltage-duration; strain-T inversion V4-6)	No	1st of MI, CVA, HF, AVR, cardiovascular death	4.3±0.8 years	627 events	146 (72 cardiac)	27	**ECG strain** (predicted MI) and **LVH** (predicted HF, AVR and combined endpoint of MI/HF/CV death).
Shah 2014 (52)	140 (outcome cohort)	Outcome cohort: moderate to severe (AVA 0.7-1.3 cm^2), asymptomatic	**ECG**, **TTE, CT Ca^{2+} score, TnT**	No	Cardiovascular death, AVR	10.6 years (outcome cohort)	63 AVRs, 22 CV deaths	36 (22 cardiac)		**ECG strain** (≥1-mm concave down- sloping ST depression with asymmetrical T inversion in lateral leads).
Chin 2014 (53)	133 (outcome cohort)	Outcome cohort: moderate to severe, asymptomatic	**TTE**, **TnI, NT-proBNP**, **CT Ca^{2+} score**	No	Cardiovascular death, AVR	10.6 years (outcome cohort)	60 AVR, 24 cardiovascular deaths	71 (24 cardiac)		**TnI** concentration.
Weidemann 2009 (92)	58	Severe AS (symptomatic)-planned AVR	**TTE, CMR (LGE)** in 46, **Histology**	Yes	Death (post-AVR), functional improvement (NYHA class)	9 months	4 deaths (3 within 30 days post-AVR)- all in high fibrosis group			No significant change in LGE 9 mths post-AVR, Improved NYHA in no **fibrosis** / preserved **longitudinal** function

Azevedo 2010 (89)	54	Severe AS / AR (symptomatic)-planned AVR	**CMR (LGE) + Histology** (f/u CMR at 27±22 mths post-AVR in 25)	Yes (angio in >40 yrs)	Death (post-AVR)	52±17 months	16 deaths	16 deaths (4 early post-op)		**Age, LGE amount (g)**
Dweck 2011 (93)	143	Moderate-severe AS (symptom status not mentioned)	**CMR (LGE-**absent / mid-wall / infarct pattern**)**	No	All-cause mortality	2±1.4 years	27 deaths (72 AVR's)	27	3	**Mid-wall fibrosis** & **EF:** independent predictors of mortality
Flett 2012 (101)	63 AS + 30 controls	Severe AS-planned AVR	**CMR (T1 mapping** Vd**, LGE** (pre- & post-AVR), **TTE**, **6-min walk, BNP**	No	LVH regression post-op	6 months (194±24 days)	5 deaths (4 in high DMF group)			6MWT ass with DMF & BNP at baseline. LVH regression post-op is cellular rather than fibrosis resolution

9.2 Appendix-2 (Supplementary data): Demographic, Exercise and Imaging data for those with and without Secondary outcome-1 (composite primary endpoint over entire study period)

9.2.1 Demographic data

Table 75. Demographic data for those with and without a secondary outcome-1

	Secondary outcome 1 (n=47)	**No secondary outcome 1** (n=127)	**p-value**
Demographic data			
Age (years)	68.7 ± 11.54	65.3 ± 13.89	0.144
Male (n (%))	29 (61.7)	104 (81.9)	0.005*
BSA (m^2)	1.9 ± 0.18	2.0 ± 0.21	0.034*
BMI (kg/m^2)	27.5 ± 3.91	28.2 ± 4.23	0.292
Resting HR (bpm)	70.1 ± 13.80	70.4 ± 10.47	0.918
Resting SBP (mmHg)	147.3 ± 22.80	146.8 ± 20.51	0.886
Resting DBP (mmHg)	75.2 ± 10.80	77.9 ± 10.54	0.148
Diabetes (n (%))	8 (17.0)	17 (13.4)	0.544
Hypertension (n (%))	25 (53.2)	68 (53.5)	0.967
Hyperlipidaemia (n (%))	22 (46.8)	70 (55.1)	0.577
ACE-I/ARB (n (%))	18 (38.3)	59 (46.5)	0.336
Beta-blocker (n (%))	19 (40.4)	35 (27.6)	0.103
Statin	27 (57.4)	78 (61.4)	0.635
NT-proBNP (pmol/L)	129.97 (36.86, 254.31)	48.69 (17.18, 124.47)	0.008*
Hb (g/dL)	13.9 ± 1.14	14.4 ± 1.25	0.016*
Hct	0.42 ± 0.04	0.43 ± 0.04	0.144
eGFR (ml/min)	79 ± 19.2	91 ± 30.8	0.004*

Abbreviations: BSA=body surface area, HR=heart rate, SBP/DBP=systolic/diastolic blood pressure, ACE-I=angiotensin converting enzyme inhibitor, ARB=angiotensin II receptor blocker, NT-proBNP=N terminal brain natriuretic peptide, Hb=haemoglobin, Hct=haematocrit, eGFR=estimated glomerular filtration rate

There were a greater proportion of females in the outcome group, who also had a higher NT-proBNP and a lower Hb and eGFR. There was no difference in resting haemodynamics, co-morbidities and medication between the two groups.

9.2.2 Echocardiographic and ECG data

Table 76. Echocardiographic and ECG data for those with and without a secondary outcome-1

	Secondary outcome 1 (n=47)	**No secondary outcome 1** (n=127)	**p-value**
Echocardiography data			
AV Vmax (m/s)	4.13 ± 0.61	3.76 ± 0.51	<0.001*
MPG (mmHg)	41.5 ± 14.15	33.1 ± 11.04	<0.001*
AVAI (cm^2/m^2)	0.51 ± 0.15	0.59 ± 0.13	0.001*
E/A	0.85 ± 0.30	0.89 ± 0.28	0.388
Septal E/e'	13.23 ± 5.61	11.92 ± 4.52	0.125
Lateral E/e'	10.59 ± 3.44	9.62 ± 3.80	0.137
DPT (ms)	590.5 ± 136.5	624.9 ± 164.2	0.202
Longitudinal PSS (%)	-18.18 ± 2.60	-18.17 ± 2.83	0.989
Longitudinal PSSR (1/s)	-1.01 ± 0.21	-1.00 ± 0.20	0.940
Longitudinal PEDSR (1/s)	0.78 ± 0.18	0.79 ± 0.22	0.863
Resting LVRPP ($mmHg.bpm.10^{-4}$)	1.45 ± 0.33	1.34 ± 0.27	0.030*
VAI (Echo) ($mmHg/ml/m^2$)	4.18 ± 1.18	3.88 ± 1.00	0.096
ECG data			
Sokolow criteria (n(%))	3 (6.4)	15 (11.8)	0.405
Cornell criteria (n(%))	9 (19.1)	22 (17.3)	0.780

Abbreviations: AV Vmax=peak aortic jet velocity, MPG=mean pressure gradient, AVAI=aortic valve area indexed to BSA, DPT=diastolic perfusion time, PSS=peak systolic strain, PSSR=peak systolic strain rate, PEDSR=peak early diastolic strain rate, LVRPP=left ventricular rate pressure product, VAI=valvulo-arterial impedance

9.2.3 CPET data

Those in the outcome group had lower peak VO_2 and workload, but with similar percentage VO_2 and workload achieved. There was a greater proportion of positive CPET's using both the strict and conventional definitions.

Table 77. CPET data for those with and without a secondary outcome-1

	Secondary outcome 1 (n=47)	**No secondary outcome 1** (n=127)	**p-value**
Cardiopulmonary Exercise Test data			
Exercise duration (min)	8.45 ± 2.55	8.51 ± 1.79	0.892
% predicted HR (%)	87.4 ± 11.9	86.5 ± 11.8	0.657
Rise in SBP (mmHg)	37 ± 24.8	43 ± 21.0	0.098
Exercise LVRPP ($mmHg.bpm.10^{-4}$)	3.54 ± 0.68	3.51 ± 0.75	0.800
Peak VO_2 (ml/kg/min)	15.6 ± 5.44	18.3 ± 5.48	0.012*
% predicted VO_2 (%)	68.0 ± 19.9	74.5 ± 16.1	0.054
Peak workload (W)	96 ± 33.7	115 ± 41.2	0.006*
% predicted workload (%)	85.4 ± 25.6	86.7 ± 28.2	0.775
Peak RER	1.11 ± 0.12	1.12 ± 0.15	0.517
Positive test (strict) (n(%))	9 (19.6)	10 (7.9)	0.031*
Positive test (conventional) (n(%))	21 (45.7)	34 (27.0)	0.020*
Reason for stopping (n(%)):			0.066
Chest pain	2 (4.3)	2 (1.6)	
Dyspnoea	16 (34.8)	27 (21.4)	
General fatigue	2 (4.3)	20 (15.9)	
Leg fatigue	17 (37)	56 (44.4)	
Arrhythmia	1 (2.2)	0 (0)	
Hypertension	0 (0)	1 (0.8)	
Other	8 (17.4)	20 (15.9)	

Abbreviations: HR=heart rate, SBP=systolic blood pressure, LVRPP=left ventricular rate pressure product, VO2=oxygen uptake, RER=respiratory exchange ratio

9.2.4 CMR data

9.2.4.1 CMR volumetric, myocardial deformation and distensibility data

There was no significant difference in LV remodeling, myocardial deformation and distensibility measures between those with and without a secondary outcome-1.

Table 78. CMR volumetric, myocardial deformation and distensibility data for those with and without a secondary outcome-1

	Secondary outcome 1 (n=47)	**No secondary outcome 1** (n=127)	**p-value**
CMR Volumetric data			
LVEDVI (ml/m^2)	84.47 ± 15.38	88.73 ± 19.16	0.173
LVESVI (ml/m^2)	36.15 ± 9.20	39.07 ± 11.07	0.109
LVSV (ml)	92 ± 16.2	99 ± 25.1	0.033*
LVSVI (ml/m^2)	48.29 ± 7.79	49.68 ± 9.82	0.383
LVEF (%)	57.5 ± 4.60	56.4 ± 5.05	0.167
LVMI (g/m^2)	57.14 ± 12.15	57.90 ± 14.46	0.750
LV mass/volume (g/ml)	0.68 ± 0.13	0.66 ± 0.10	0.146
LAVI (ml/m^2)	57.31 ± 17.33	54.05 ± 13.61	0.251
RVEDVI (ml/m^2)	86.26 ± 14.75	88.96 ± 15.29	0.299
VAI (MRI) (mmHg/ml/m^2)	4.00 ± 0.80	3.74 ± 0.82	0.065
CMR Myocardial Deformation data			
Longitudinal PSS (%)	-18.54 ± 3.20	-18.46 ± 2.96	0.873
Longitudinal PSSR (1/s)	-1.09 ± 0.23	-1.09 ± 0.25	0.977
Longitudinal PEDSR (1/s)	1.11 ± 0.30	1.08 ± 0.27	0.496
Circumferential PSS (%)	-29.17 ± 4.48	-27.69 ± 4.68	0.064
Circumferential PSSR (1/s)	-1.79 ± 0.37	-1.71 ± 0.39	0.211
Circumferential PEDSR (1/s)	1.74 ± 0.38	1.65 ± 0.41	0.191
CMR Distensibility data			
AA distensibility (10^{-3}mmHg^{-1})	1.77 ± 0.97	1.98 ± 1.26	0.325
DA distensibility (10^{-3}mmHg^{-1})	2.09 ± 1.54	2.12 ± 1.46	0.934
PWV (m/s)	7.63 ± 2.83	8.67 ± 3.77	0.060

Abbreviations: LVEDVI=left ventricular end-diastolic volume indexed to BSA, LVESVI=left ventricular end systolic volume indexed to BSA, LVSV=left ventricular stroke volume, LVSVI=LVSV indexed to BSA, LVEF=left ventricular ejection fraction, LVMI=left ventricular mass indexed to BSA, LAVI=left atrial volume indexed to BSA, RVESVI=right ventricular end diastolic volume indexed to BSA, VAI=valvulo-arterial impedance, PSS=peak systolic strain, PSSR=peak systolic strain rate, PEDSR=peak early diastolic strain rate, AA=ascending aorta, DA=descending aorta, PWV=pulse wave velocity

9.2.4.2 Contrast Enhanced CMR

Table 79. CMR perfusion and fibrosis data for those with and without a secondary outcome-1

	Secondary outcome 1 (n=47)	**No secondary outcome 1** (n=127)	**p-value**
CMR Perfusion data			
Global MPR	2.06 ± 0.65	2.34 ± 0.70	0.022*
Global stress MBF (ml/min/g)	2.05 ± 0.64	2.20 ± 0.72	0.216
Global rest MBF (ml/min/g)	1.05 ± 0.36	0.96 ± 0.22	0.119
Total stress MBF (ml/min/m^2)	112.71 ± 30.68	126.06 ± 48.58	0.037*
Total rest MBF (ml/min/m^2)	57.63 ± 16.42	54.76 ± 16.59	0.318
CMR Fibrosis data			
LGE present (n,%)	24 (51.1)	58 (45.7)	0.527
% LGE (%)	4.4 ± 3.19	4.2 ± 3.96	0.683
Native T1 (ms)	1114.3 ± 61.13	1139.4 ± 71.85	0.070
ECV (%)	25.35 ± 2.53	24.60 ± 2.37	0.132

Abbreviations: MPR=myocardial perfusion reserve, MBF=myocardial blood flow, LGE=late gadolinium enhancement, ECV=extracellular volume fraction

Global MPR and total stress MBF were significantly lower in the outcome group. There was no difference in measures of fibrosis between those with and without a secondary outcome-1.

9.2.5 CT data

Table 80. CT data for those with and without a secondary outcome-1

	Secondary outcome 1 (n=47)	**No secondary outcome 1** (n=127)	**p-value**
CT data			
AoV Ca^{2+} score	2145 (1290, 3119)	1833 (1147, 3157)	0.443
Coronary Ca^{2+} score	380.5 (10.0, 926.0)	276.5 (3.8, 988.0)	0.749

Abbreviations: AoV Ca^{2+} score= aortic valve calcium score (median and inter-quartile range displayed)

9.3 Appendix-3 (Supplementary data): Demographic, Exercise and Imaging data for those with and without Secondary outcome-2 (all AVRs, deaths, MACE at 12 months)

9.3.1 Demographic data

Table 81. Demographic data for those with and without a secondary outcome-2

	Secondary outcome 2 (n=49)	**No secondary outcome 2** (n=125)	**p-value**
Demographic data			
Age (years)	68.3 ± 11.62	65.4 ± 13.92	0.208
Male (n (%))	31 (63.3)	102 (81.6)	0.010*
BSA (m^2)	1.9 ± 0.20	2.0 ± 0.20	0.024*
BMI (kg/m^2)	27.5 ± 4.27	28.2 ± 4.10	0.301
Resting HR (bpm)	69.8 ± 13.02	70.5 ± 10.78	0.703
Resting SBP (mmHg)	147.4 ± 21.10	146.7 ± 21.17	0.840
Resting DBP (mmHg)	75.9 ± 10.21	77.7 ± 10.82	0.326
Diabetes (n (%))	9 (18.4)	16 (12.8)	0.346
Hypertension (n (%))	25 (51.0)	68 (54.4)	0.688
Hyperlipidaemia (n (%))	23 (46.9)	69 (55.2)	0.226
ACE-I/ARB (n (%))	18 (36.7)	59 (47.2)	0.211
Beta-blocker (n (%))	20 (40.8)	34 (27.2)	0.081
Statin	28 (57.1)	77 (61.6)	0.589
NT-proBNP (pmol/L)	104.27 (22.88, 266.50)	50.25 (15.33, 130.65)	0.009*
Hb (g/dL)	13.9 ± 1.17	14.4 ± 1.24	0.019*
Hct	0.42 ± 0.04	0.43 ± 0.03	0.090
eGFR (ml/min)	81 ± 20.3	91 ± 31.0	0.027*

Abbreviations: BSA=body surface area, HR=heart rate, SBP/DBP=systolic/diastolic blood pressure, ACE-I=angiotensin converting enzyme inhibitor, ARB=angiotensin II receptor blocker, NT-proBNP=N terminal brain natriuretic peptide, Hb=haemoglobin, Hct=haematocrit, eGFR=estimated glomerular filtration rate

There was a greater proportion of females in the outcome group, with higher NT-proBNP and lower Hb and eGFR.

9.3.2 Echocardiographic and ECG data

Table 82. Echocardiographic and ECG data for those with and without a secondary outcome-2

	Secondary outcome 2 (n=49)	**No secondary outcome 2** (n=125)	**p-value**
Echocardiography data			
AV Vmax (m/s)	4.20 ± 0.61	3.73 ± 0.48	<0.001*
MPG (mmHg)	43.5 ± 14.44	32.1 ± 10.00	<0.001*
AVAI (cm^2/m^2)	0.49 ± 0.14	0.60 ± 0.13	<0.001*
E/A	0.86 ± 0.30	0.89 ± 0.28	0.555
Septal E/e'	13.63 ± 5.71	11.75 ± 4.40	0.046*
Lateral E/e'	10.78 ± 3.61	9.53 ± 3.72	0.050
DPT (ms)	601.5 ± 149.3	621.2 ± 160.9	0.460
Longitudinal PSS (%)	-17.62 ± 2.60	-18.40 ±2.80	0.161
Longitudinal PSSR (1/s)	-0.98 ± 0.23	-1.01 ± 0.19	0.498
Longitudinal PEDSR (1/s)	0.80 ± 0.19	0.79 ± 0.22	0.817
Resting LVRPP ($mmHg.bpm.10^{-4}$)	1.46 ± 0.33	1.34 ± 0.27	0.012*
VAI (Echo) ($mmHg/ml/m^2$)	4.25 ± 1.05	3.85 ± 1.04	0.025*
ECG data			
Sokolow criteria (n(%))	4 (8.2)	14 (11.2)	0.783
Cornell criteria (n(%))	11 (22.4)	20 (16.0)	0.317

Abbreviations: AV Vmax=peak aortic jet velocity, MPG=mean pressure gradient, AVAI=aortic valve area indexed to BSA, DPT=diastolic perfusion time, PSS=peak systolic strain, PSSR=peak systolic strain rate, PEDSR=peak early diastolic strain rate, LVRPP=left ventricular rate pressure product, VAI=valvulo-arterial impedance

Those with a secondary outcome-2 had more severe AS and higher septal E/e' and resting LVRPP than those without.

9.3.3 CPET data

Table 83. CPET data for those with and without a secondary outcome-2

	Secondary outcome 2 (n=49)	No secondary outcome 2 (n=125)	p-value
Cardiopulmonary Exercise Test data			
Exercise duration (min)	8.00 ± 2.40	8.69 ± 1.82	0.080
% predicted HR (%)	86.8 ± 12.7	86.8 ± 11.5	0.986
Rise in SBP (mmHg)	37 ± 23.2	43 ± 21.7	0.081
Exercise LVRPP ($mmHg.bpm.10^{-4}$)	3.54 ± 0.79	3.51 ± 0.71	0.770
Peak VO_2 (ml/kg/min)	14.9 ± 4.94	18.6 ± 5.50	<0.001*
% predicted VO_2 (%)	65.4 ± 18.5	75.5 ± 16.2	0.002*
Peak workload (W)	94 ± 38.6	117 ± 39.1	<0.001*
% predicted workload (%)	81.8 ± 27.5	88.2 ± 27.3	0.174
Peak RER	1.10 ± 0.13	1.13 ± 0.15	0.387
Positive test (strict) (n(%))	10 (20.8)	9 (7.3)	0.011*
Positive test (conventional) (n(%))	20 (41.7)	35 (28.2)	0.090
Reason for stopping (n(%)):			0.194
Chest pain	1 (2.1)	3 (2.4)	
Dyspnoea	17 (35.4)	26 (21.0)	
General fatigue	3 (6.3)	19 (15.3)	
Leg fatigue	19 (39.6)	54 (43.5)	
Arrhythmia	1 (2.1)	0 (0)	
Hypertension	0 (0)	1 (0.8)	
Other	7 (14.6)	21 (16.9)	

Abbreviations: HR=heart rate, SBP=systolic blood pressure, LVRPP=left ventricular rate pressure product, VO2=oxygen uptake, RER=respiratory exchange ratio

Patients with a secondary outcome-2 had a significantly lower peak VO_2, $\%VO_2$ and peak workload, and a greater proportion of positive CPET's using the strict definition only.

9.3.4 CMR data

9.3.4.1 CMR volumetric, myocardial deformation and distensibility data

Table 84. CMR volumetric, myocardial deformation and distensibility data for those with and without a secondary outcome-2

	Secondary outcome 2 (n=49)	**No secondary outcome 2** (n=125)	**p-value**
CMR Volumetric data			
LVEDVI (ml/m²)	85.34 ± 16.38	88.46 ± 18.95	0.313
LVESVI (ml/m²)	37.28 ± 10.42	38.67 ± 10.75	0.438
LVSV (ml)	91 ± 18.8	99 ± 24.4	0.035*
LVSVI (ml/m²)	48.08 ± 8.01	49.79 ± 9.76	0.277
LVEF (%)	56.8 ± 5.34	56.7 ± 4.81	0.883
LVMI (g/m²)	56.86 ± 14.68	57.24 ± 13.54	0.489
LV mass/volume (g/ml)	0.69 ± 0.12	0.65 ± 0.10	0.030*
LAVI (ml/m²)	57.60 ± 17.52	53.55 ± 13.36	0.079
RVEDVI (ml/m²)	85.76 ± 14.87	89.20 ± 15.20	0.179
VAI (MRI) (mmHg/ml/m²)	4.07 ± 0.77	3.71 ± 0.82	0.010*
CMR Myocardial Deformation data			
Longitudinal PSS (%)	-18.45 ± 3.45	-18.50 ± 2.85	0.920
Longitudinal PSSR (1/s)	-1.08 ± 0.24	-1.10 ± 0.24	0.644
Longitudinal PEDSR (1/s)	1.11 ± 0.32	1.08 ± 0.26	0.479
Circumferential PSS (%)	-28.91 ± 4.67	-27.77 ± 4.64	0.149
Circumferential PSSR (1/s)	-1.76 ± 0.39	-1.72 ± 0.39	0.586
Circumferential PEDSR (1/s)	1.71 ± 0.41	1.66 ± 0.40	0.497
CMR Distensibility data			
AA distensibility	1.86 ± 0.97	1.94 ± 1.27	0.658
DA distensibility	2.17 ± 1.49	2.09 ± 1.48	0.764
PWV (m/s)	7.63 ± 3.31	8.69 ± 3.63	0.087

Abbreviations: LVEDVI=left ventricular end-diastolic volume indexed to BSA, LVESVI=left ventricular end systolic volume indexed to BSA, LVSV=left ventricular stroke volume, LVSVI=LVSV indexed to BSA, LVEF=left ventricular ejection fraction, LVMI=left ventricular mass indexed to BSA, LAVI=left atrial volume indexed to BSA, RVESVI=right ventricular end diastolic volume indexed to BSA, VAI=valvulo-arterial impedance, PSS=peak systolic strain, PSSR=peak systolic strain rate, PEDSR=peak early diastolic strain rate, AA=ascending aorta, DA=descending aorta, PWV=pulse wave velocity

Those with a secondary outcome-2 demonstrated a lower absolute stroke volume and a higher mass/volume ratio and CMR-derived VAI (Table 84). There was no difference in CMR measures of myocardial deformation or distensibility.

9.3.4.2 Contrast Enhanced CMR

Table 85. CMR perfusion and fibrosis data for those with and without a secondary outcome-2

	Secondary outcome 2 (n=49)	**No secondary outcome 2** (n=125)	**p-value**
CMR Perfusion data			
Global MPR	2.03 ± 0.63	2.36 ± 0.70	0.005*
Global stress MBF (ml/min/g)	2.03 ± 0.65	2.22 ± 0.72	0.107
Global rest MBF (ml/min/g)	1.04 ± 0.35	0.95 ± 0.22	0.108
Total stress MBF (ml/min/m^2)	114.27 ± 35.51	125.66 ± 47.63	0.094
Total rest MBF (ml/min/m^2)	59.09 ± 17.05	54.14 ± 16.20	0.079
CMR Fibrosis data			
LGE present (n,%)	25 (51.0)	57 (45.6)	0.520
% LGE (%)	4.3 ± 3.26	4.2 ± 3.95	0.943
Native T1 (ms)	1121.1 ± 64.93	1136.4 ± 71.22	0.274
ECV (%)	25.24 ± 2.49	24.65 ± 2.40	0.244

Abbreviations: MPR=myocardial perfusion reserve, MBF=myocardial blood flow, LGE=late gadolinium enhancement, ECV=extracellular volume fraction

Those with a secondary outcome-2 demonstrated a significantly lower global MPR than those without, with no difference in measures of myocardial fibrosis.

9.3.5 CT data

Table 86. CT data for those with and without a secondary outcome-2

	Secondary outcome 2 (n=49)	**No secondary outcome 2** (n=125)	**p-value**
CT data			
AoV Ca^{2+} score	2198 (1275, 3610)	1832 (1147, 2873)	0.128
Coronary Ca^{2+} score	400.5 (8.4, 946.0)	257.5 (5.4, 934.0)	0.454

Abbreviations: AoV Ca^{2+} score= aortic valve calcium score (median and inter-quartile range displayed)

There was no significant difference in the over all calcium scores between those with and without a secondary outcome-2.

9.4 Appendix-4 (Supplementary data): Demographic, Exercise and Imaging data for those with and without Secondary outcome-3 (all AVRs, deaths, MACE over entire study period)

9.4.1 Demographic data

Table 87. Demographic data for those with and without a secondary outcome-3

	Secondary outcome 3 (n=60)	**No secondary outcome 3** (n=114)	**p-value**
Demographic data			
Age (years)	68.5 ± 11.34	65.1 ± 14.19	0.111
Male (n (%))	41 (68.3)	92 (80.7)	0.068
BSA (m^2)	1.9 ± 0.20	2.0 ± 0.21	0.069
BMI (kg/m^2)	27.5 ± 4.12	28.2 ± 4.16	0.293
Resting HR (bpm)	70.1 ± 12.74	70.4 ± 10.73	0.865
Resting SBP (mmHg)	147.8 ± 20.96	146.4 ± 21.23	0.673
Resting DBP (mmHg)	76.7 ± 10.67	77.4 ± 10.68	0.649
Diabetes (n (%))	10 (16.7)	15 (13.2)	0.530
Hypertension (n (%))	31 (51.7)	62 (54.4)	0.733
Hyperlipidaemia (n (%))	28 (46.7)	64 (56.1)	0.025*
ACE-I/ARB (n (%))	23 (38.3)	54 (47.4)	0.254
Beta-blocker (n (%))	24 (40.0)	30 (26.3)	0.064
Statin	36 (60.0)	69 (60.5)	0.946
NT-proBNP (pmol/L)	103.06 (21.19, 243.13)	50.51 (16.75, 124.47)	0.031*
Hb (g/dL)	14.0 ± 1.12	14.4 ± 1.28	0.042*
Hct	0.42 ± 0.03	0.43 ± 0.04	0.261
eGFR (ml/min)	81 ± 21.5	91 ± 31.3	0.016*

Abbreviations: BSA=body surface area, HR=heart rate, SBP/DBP=systolic/diastolic blood pressure, ACE-I=angiotensin converting enzyme inhibitor, ARB=angiotensin II receptor blocker, NT-proBNP=N terminal brain natriuretic peptide, Hb=haemoglobin, Hct=haematocrit, eGFR=estimated glomerular filtration rate

There was a greater proportion of females in those with a secondary outcome-3, though this did not reach statistical significance for this group. As before, the NT-proBNP was significantly higher and the Hb and eGFR were significantly lower in the outcome group.

9.4.2 Echocardiographic and ECG data

Table 88. Echocardiographic and ECG data for those with and without a secondary outcome-3

	Secondary outcome 3 (n=60)	**No secondary outcome 3** (n=114)	**p-value**
Echocardiography data			
AV Vmax (m/s)	4.15 ± 0.58	3.71 ± 0.48	<0.001*
MPG (mmHg)	42.3 ± 13.73	31.7 ± 10.10	<0.001*
AVAI (cm^2/m^2)	0.51 ± 0.15	0.60 ± 0.12	<0.001*
E/A	0.84 ± 0.29	0.90 ± 0.29	0.228
Septal E/e'	13.50 ± 5.46	11.62 ± 4.39	0.017*
Lateral E/e'	10.81 ± 3.67	9.38 ± 3.67	0.018*
DPT (ms)	597.1 ± 141.6	625.4 ± 165.1	0.262
Longitudinal PSS (%)	-17.78 ± 2.65	-18.40 ± 2.81	0.231
Longitudinal PSSR (1/s)	-0.99 ± 0.21	-1.01 ± 0.20	0.611
Longitudinal PEDSR (1/s)	0.77 ± 0.19	0.80 ± 0.22	0.449
Resting LVRPP ($mmHg.bpm.10^{-4}$)	1.45 ± 0.31	1.33 ± 0.27	0.011*
VAI (Echo) ($mmHg/ml/m^2$)	4.21 ± 1.11	3.83 ± 1.01	0.026*
ECG data			
Sokolow criteria (n(%))	5 (8.3)	13 (11.4)	0.609
Cornell criteria (n(%))	11 (18.3)	20 (17.5)	0.897

Abbreviations: AV Vmax=peak aortic jet velocity, MPG=mean pressure gradient, AVAI=aortic valve area indexed to BSA, DPT=diastolic perfusion time, PSS=peak systolic strain, PSSR=peak systolic strain rate, PEDSR=peak early diastolic strain rate, LVRPP=left ventricular rate pressure product, VAI=valvulo-arterial impedance

Those who achieved a secondary outcome-3 had more severe AS, with a significantly higher septal and lateral E/e', resting LVRPP and echo-derived VAI.

9.4.3 CPET data

Table 89. CPET data for those with and without a secondary outcome-3

	Secondary outcome 3 (n=60)	**No secondary outcome 3** (n=114)	**p-value**
Cardiopulmonary Exercise Test data			
Exercise duration (min)	8.40 ± 2.44	8.55 ± 1.76	0.686
% predicted HR (%)	88.1 ± 12.4	86.1 ± 11.5	0.273
Rise in SBP (mmHg)	39 ± 24.8	43 ± 20.7	0.255
Exercise LVRPP ($mmHg.bpm.10^{-4}$)	3.60 ± 0.74	3.47 ± 0.72	0.295
Peak VO_2 (ml/kg/min)	15.6 ± 5.12	18.5 ± 5.56	0.004*
% predicted VO_2 (%)	67.8 ± 19.2	75.0 ± 16.1	0.024*
Peak workload (W)	101 ± 39.0	115 ± 40.0	0.022*
% predicted workload (%)	84.4 ± 25.7	87.4 ± 28.3	0.500
Peak RER	1.10 ± 0.13	1.13 ± 0.15	0.279
Positive test (strict) (n(%))	11 (18.6)	8 (7.1)	0.022*
Positive test (conventional) (n(%))	24 (40.7)	31 (27.4)	0.077
Reason for stopping (n(%)):			0.064
Chest pain	2 (3.4)	2 (1.8)	
Dyspnoea	19 (32.2)	24 (21.2)	
General fatigue	3 (5.1)	19 (16.8)	
Leg fatigue	22 (37.3)	51 (45.1)	
Arrhythmia	1 (1.7)	0 (0)	
Hypertension	0 (0)	1 (0.9)	
Other	12 (20.3)	16 (14.2)	

Abbreviations: HR=heart rate, SBP=systolic blood pressure, LVRPP=left ventricular rate pressure product, VO2=oxygen uptake, RER=respiratory exchange ratio

Those with a secondary outcome-3 had a significantly lower peak VO_2, % peak VO_2 and peak workload achieved, and a greater incidence of a positive exercise test using the strict definition only.

9.4.4 CMR data

9.4.4.1 CMR volumetric, myocardial deformation and distensibility data

Table 90. CMR volumetric, myocardial deformation and distensibility data for those with and without a secondary outcome-3

	Secondary outcome 3 (n=60)	**No secondary outcome 3** (n=114)	**p-value**
CMR Volumetric data			
LVEDVI (ml/m^2)	86.11 ± 16.01	88.36 ± 19.37	0.442
LVESVI (ml/m^2)	37.44 ± 10.14	38.72 ± 10.92	0.453
LVSV (ml)	93 ± 18.6	99 ± 25.2	0.125
LVSVI (ml/m^2)	48.66 ± 7.84	49.65 ± 10.02	0.474
LVEF (%)	56.9 ± 5.18	56.6 ± 4.85	0.630
LVMI (g/m^2)	59.44 ± 14.11	56.78 ± 13.68	0.229
LV mass/volume (g/ml)	0.69 ± 0.13	0.65 ± 0.10	0.013*
LAVI (ml/m^2)	57.68 ± 16.58	53.53 ± 13.57	0.083
RVEDVI (ml/m^2)	87.24 ± 14.12	88.75 ± 15.70	0.534
VAI (MRI) (mmHg/ml/m^2)	4.00 ± 0.77	3.72 ± 0.83	0.030*
CMR Myocardial Deformation data			
Longitudinal PSS (%)	-18.11 ± 3.30	-18.68 ± 2.86	0.243
Longitudinal PSSR (1/s)	-1.06 ± 0.23	-1.11 ± 0.25	0.152
Longitudinal PEDSR (1/s)	1.08 ± 0.30	1.09 ± 0.27	0.756
Circumferential PSS (%)	-28.46 ± 4.72	-27.90 ± 4.64	0.458
Circumferential PSSR (1/s)	-1.74 ± 0.39	-1.73 ± 0.39	0.913
Circumferential PEDSR (1/s)	1.66 ± 0.40	1.68 ± 0.41	0.790
CMR Distensibility data			
AA distensibility	1.80 ± 0.92	1.98 ± 1.31	0.296
DA distensibility	2.01 ± 1.40	2.16 ± 1.52	0.513
PWV (m/s)	7.81 ± 3.12	8.70 ± 3.76	0.125

Abbreviations: LVEDVI=left ventricular end-diastolic volume indexed to BSA, LVESVI=left ventricular end systolic volume indexed to BSA, LVSV=left ventricular stroke volume, LVSVI=LVSV indexed to BSA, LVEF=left ventricular ejection fraction, LVMI=left ventricular mass indexed to BSA, LAVI=left atrial volume indexed to BSA, RVESVI=right ventricular end diastolic volume indexed to BSA, VAI=valvulo-arterial impedance, PSS=peak systolic strain, PSSR=peak systolic strain rate, PEDSR=peak early diastolic strain rate, AA=ascending aorta, DA=descending aorta, PWV=pulse wave velocity

There was no significant difference in markers of LV remodeling between those with and without a secondary outcome-3, except a significantly higher LV mass/volume

ratio in those with an outcome. The CMR-derived VAI was also significantly higher, with no difference in measures of myocardial deformation or distensibility.

9.4.4.2 Contrast Enhanced CMR

Table 91. CMR perfusion and fibrosis data for those with and without a secondary outcome-3

	Secondary outcome 3 (n=60)	**No secondary outcome 3** (n=114)	**p-value**
CMR Perfusion data			
Global MPR	2.06 ± 0.65	2.38 ± 0.70	0.005*
Global stress MBF (ml/min/g)	2.05 ± 0.66	2.22 ± 0.72	0.146
Global rest MBF (ml/min/g)	1.04 ± 0.33	0.95 ± 0.22	0.074
Total stress MBF (ml/min/m^2)	118.46 ± 41.62	124.45 ± 46.27	0.412
Total rest MBF (ml/min/m^2)	59.76 ± 17.17	53.28 ± 15.82	0.015*
CMR Fibrosis data			
LGE present (n,%)	32 (53.3)	50 (43.9)	0.234
% LGE (%)	4.5 ± 3.30	4.1 ± 3.99	0.420
Native T1 (ms)	1116.7 ± 61.16	1140.0 ± 72.68	0.079
ECV (%)	24.96 ± 2.53	24.74 ± 2.39	0.646

Abbreviations: MPR=myocardial perfusion reserve, MBF=myocardial blood flow, LGE=late gadolinium enhancement, ECV=extracellular volume fraction

The global MPR was significantly lower and the total rest MBF was significantly higher in those with a secondary outcome-3. There was no difference in measures of fibrosis.

9.4.5 CT data

Table 92. CT data for those with and without a secondary outcome-3

	Secondary outcome 3 (n=49)	**No secondary outcome 3** (n=125)	**p-value**
CT data			
AoV Ca^{2+} score	2393 (1359, 3620)	1749 (1122, 2829)	0.033*
Coronary Ca^{2+} score	389.0 (10.0, 934.0)	256.0 (2.1, 968.0)	0.513

Abbreviations: AoV Ca^{2+} score= aortic valve calcium score (median and inter-quartile range displayed)

The AV calcium score was significantly higher in those with a secondary outcome-3.

9.5 Appendix-5 (Supplementary data): Sensitivity analysis in patients with severe AS only

Additional sensitivity analyses were performed in the 123 (71%) patients, who met at least one criterion for severe AS. The below tables summarise the results of ROC analysis and the sensitivity, specificity, positive predictive value (PPV) and negative predictive value (NPV) of MPR and exercise testing in predicting the primary (Table 93) and secondary outcomes (Table 94 to Table 96) in the severe-AS population.

(Abbreviations for all tables in **Appendix-5**: PPV= positive predictive value, NPV=negative predictive value, MPR=myocardial perfusion reserve, CPET=cardiopulmonary exercise test.)

Table 93. Sensitivity, specificity, PPV and NPV of MPR and CPET in predicting the Primary Outcome (symptom-driven AVR, MACE, cardiovascular death at 12 months) in severe AS group

Parameter	Sensitivity	Specificity	PPV	NPV	AUC	p-value
MPR	0.629	0.590	0.393	0.790	0.597 (0.49-0.71)	0.081
Positive CPET (strict)	0.206	0.909	0.467	0.748	0.557 (0.48-0.63)	0.135
Positive CPET (conventional)	0.441	0.693	0.357	0.763	0.567 (0.47-0.67)	0.177

Table 94. Sensitivity, specificity, PPV and NPV of MPR and CPET in predicting the Secondary Outcome-1 (symptom-driven AVR, MACE, cardiovascular death over entire study period) in severe AS group

Parameter	Sensitivity	Specificity	PPV	NPV	AUC	p-value
MPR	0.610	0.597	0.446	0.742	0.590 (0.48-0.70)	0.099
Positive CPET (strict)	0.200	0.915	0.533	0.701	0.557 (0.49-0.63)	0.107
Positive CPET (conventional)	0.450	0.707	0.429	0.725	0.579 (0.49-0.67)	0.095

Table 95. Sensitivity, specificity, PPV and NPV of MPR and CPET in predicting the Secondary Outcome-2 (all AVR, MACE, cardiovascular death at 12 months) in severe AS group

Parameter	Sensitivity	Specificity	PPV	NPV	AUC	p-value
MPR	0.644	0.630	0.518	0.742	0.628 (0.52-0.73)	0.015
Positive CPET (strict)	0.205	0.923	0.600	0.673	0.564 (0.50-0.63)	0.063
Positive CPET (conventional)	0.409	0.692	0.429	0.675	0.551 (0.46-0.64)	0.268

Table 96. Sensitivity, specificity, PPV and NPV of MPR and CPET in predicting the Secondary Outcome-3 (all AVR, MACE, cardiovascular death over entire study period) in severe AS group

Parameter	Sensitivity	Specificity	PPV	NPV	AUC	p-value
MPR	0.623	0.646	0.589	0.677	0.617(0.51-0.72)	0.026*
Positive CPET (strict)	0.189	0.928	0.667	0.598	0.558 (0.50-0.62)	0.064
Positive CPET (conventional)	0.396	0.696	0.500	0.600	0.546(0.46-0.63)	0.296

9.6 Appendix-6: PUBLICATIONS ARISING FROM THIS THESIS

Paper-1: Review article

Singh A, Steadman CD, McCann GP. Advances in the Understanding of the Pathophysiology and Management of Aortic Stenosis: Role of Novel Imaging Techniques. Can J Cardiol. 2014 Sep;30(9):994-1003.

Paper-2: Protocol paper (PRIMID-AS)

Singh A, Ford I, Greenwood JP, Khan JN, Uddin A, Berry C, Neubauer S, Prendergast B, Jerosch-Herold M, Williams B, Samani NJ, McCann GP. Rationale and design of the PRognostic Importance of MIcrovascular Dysfunction in asymptomatic patients with Aortic Stenosis (PRIMID-AS): a multicentre observational study with blinded investigations. BMJ Open. 2013;3(12):e004348

Paper-3: Tagging *vs.* Feature Tracking: reproducibility

Singh A, Steadman CD, Khan JN, Horsfield MA, Bekele S, Nazir SA, Kanagala P, Masca NG, Clarysse P, McCann GP. Intertechnique agreement and interstudy reproducibility of strain and diastolic strain rate at 1.5 and 3 Tesla: a comparison of feature-tracking and tagging in patients with aortic stenosis. J Magn Reson Imaging. 2015 Apr;41(4):1129-37

Paper-4: T1 mapping in AS: reproducibility and comparison with controls

Singh A, Horsfield MA, Bekele S, Khan JN, Greiser A, McCann GP. Myocardial T1 and extracellular volume fraction measurement in asymptomatic patients with aortic stenosis: reproducibility and comparison with age-matched controls. Eur Heart J Cardiovasc Imaging. 2015 Jul;16(7):763-70

Paper-5: Ranolazine in AS

Singh A, Steadman CD, Khan JN, Reggiardo G, McCann GP. Effect of late sodium current inhibition on MRI measured diastolic dysfunction in aortic stenosis: a pilot study. BMC Res Notes. 2016;9(1):64

10 REFERENCES

1. Ward C. Clinical significance of the bicuspid aortic valve. Heart. 2000;83(1):81-5.

2. Bridgewater B, Kinsman R, Walton P, Keogh B. Demonstrating Quality: The sixth National Adult Cardiac Surgery database report. Henley-on-Thames: Society for Cardiothoracic Surgery in Great Britain & Ireland.; 2008.

3. Lindroos M, Kupari M, Heikkila J, Tilvis R. Prevalence of aortic valve abnormalities in the elderly: an echocardiographic study of a random population sample. J Am Coll Cardiol. 1993;21(5):1220-5.

4. Nkomo V, Gardin J, Skelton T, Gottdiener J, Scott C, Enriquez-Sarano M. Burden of valvular heart diseases: a population-based study. Lancet. 2006;368(9540):1005-11.

5. Vahanian A, Alfieri O, Andreotti F, Antunes MJ, Baron-Esquivias G, Baumgartner H, Borger MA, Carrel TP, De Bonis M, Evangelista A, Falk V, Iung B, Lancellotti P, Pierard L, Price S, Schafers HJ, Schuler G, Stepinska J, Swedberg K, Takkenberg J, Von Oppell UO, Windecker S, Zamorano JL, Zembala M. Guidelines on the management of valvular heart disease (version 2012). Eur Heart J. 2012;33(19):2451-96.

6. Camm A, Luscher T, Serruys P. The ESC Textbook of Cardiovascular Medicine. Second ed: Oxford University Press; 2009.

7. Purcell H, Kalra PR. Specialist training in cardiology. Edinburgh: Mosby; 2005.

8. Faggiano P, Aurigemma GP, Rusconi C, Gaasch WH. Progression of valvular aortic stenosis in adults: literature review and clinical implications. Am Heart J. 1996;132(2 Pt 1):408-17.

9. Pibarot P, Dumesnil JG. Improving assessment of aortic stenosis. J Am Coll Cardiol. 2012;60(3):169-80.

10. Nistri S, Grande-Allen J, Noale M, Basso C, Siviero P, Maggi S, Crepaldi G, Thiene G. Aortic elasticity and size in bicuspid aortic valve syndrome. Eur Heart J. 2008;29(4):472-9.

11. Cohn JN, Ferrari R, Sharpe N. Cardiac remodeling--concepts and clinical implications: a consensus paper from an international forum on cardiac remodeling. Behalf of an International Forum on Cardiac Remodeling. J Am Coll Cardiol. 2000;35(3):569-82.

12. Kupari M, Turto H, Lommi J. Left ventricular hypertrophy in aortic valve stenosis: preventive or promotive of systolic dysfunction and heart failure? Eur Heart J. 2005;26(17):1790-6.

13. Dweck MR, Joshi S, Murigu T, Gulati A, Alpendurada F, Jabbour A, Maceira A, Roussin I, Northridge DB, Kilner PJ, Cook SA, Boon NA, Pepper J, Mohiaddin RH, Newby DE, Pennell DJ, Prasad SK. Left ventricular remodeling and hypertrophy in patients with aortic stenosis: insights from cardiovascular magnetic resonance. J Cardiovasc Magn Reson. 2012;14:50.

14. Ganau A, Devereux RB, Roman MJ, de Simone G, Pickering TG, Saba PS, Vargiu P, Simongini I, Laragh JH. Patterns of left ventricular hypertrophy and geometric remodeling in essential hypertension. J Am Coll Cardiol. 1992;19(7):1550-8.

15. Chambers J. The left ventricle in aortic stenosis: evidence for the use of ACE inhibitors. Heart. 2006;92(3):420-3.

16. Carabello BA. The relationship of left ventricular geometry and hypertrophy to left ventricular function in valvular heart disease. J Heart Valve Dis. 1995;4 Suppl 2:S132-8; discussion S8-9.

17. Esposito G, Rapacciuolo A, Naga Prasad SV, Takaoka H, Thomas SA, Koch WJ, Rockman HA. Genetic alterations that inhibit in vivo pressure-overload hypertrophy prevent cardiac dysfunction despite increased wall stress. Circulation. 2002;105(1):85-92.

18. Cioffi G, Faggiano P, Vizzardi E, Tarantini L, Cramariuc D, Gerdts E, de Simone G. Prognostic effect of inappropriately high left ventricular mass in asymptomatic severe aortic stenosis. Heart. 2011;97(4):301-7.

19. Trenouth RS, Phelps NC, Neill WA. Determinants of left ventricular hypertrophy and oxygen supply in chronic aortic valve disease. Circulation. 1976;53(4):644-50.

20. Hess OM, Ritter M, Schneider J, Grimm J, Turina M, Krayenbuehl HP. Diastolic stiffness and myocardial structure in aortic valve disease before and after valve replacement. Circulation. 1984;69(5):855-65.

21. Galiuto L, Lotrionte M, Crea F, Anselmi A, Biondi-Zoccai GG, De Giorgio F, Baldi A, Baldi F, Possati G, Gaudino M, Vetrovec GW, Abbate A. Impaired coronary and myocardial flow in severe aortic stenosis is associated with increased apoptosis: a transthoracic Doppler and myocardial contrast echocardiography study. Heart. 2006;92(2):208-12.

22. Hein S, Arnon E, Kostin S, Schonburg M, Elsasser A, Polyakova V, Bauer EP, Klovekorn WP, Schaper J. Progression from compensated hypertrophy to failure in the pressure-overloaded human heart: structural deterioration and compensatory mechanisms. Circulation. 2003;107(7):984-91.

23. Garcia D, Camici PG, Durand LG, Rajappan K, Gaillard E, Rimoldi OE, Pibarot P. Impairment of coronary flow reserve in aortic stenosis. J Appl Physiol. 2009;106(1):113-21.

24. Rajappan K, Rimoldi OE, Dutka DP, Ariff B, Pennell DJ, Sheridan DJ, Camici PG. Mechanisms of coronary microcirculatory dysfunction in patients with aortic stenosis and angiographically normal coronary arteries. Circulation. 2002;105(4):470-6.

25. Rudolph A, Abdel-Aty H, Bohl S, Boye P, Zagrosek A, Dietz R, Schulz-Menger J. Noninvasive detection of fibrosis applying contrast-enhanced cardiac magnetic resonance in different forms of left ventricular hypertrophy relation to remodeling. J Am Coll Cardiol. 2009;53(3):284-91.

26. Hoffman JI. Determinants and prediction of transmural myocardial perfusion. Circulation. 1978;58(3 Pt 1):381-91.

27. Lafitte S, Perlant M, Reant P, Serri K, Douard H, DeMaria A, Roudaut R. Impact of impaired myocardial deformations on exercise tolerance and prognosis in patients with asymptomatic aortic stenosis. Eur J Echocardiogr. 2009;10(3):414-9.

28. Petersen SE, Jerosch-Herold M, Hudsmith LE, Robson MD, Francis JM, Doll HA, Selvanayagam JB, Neubauer S, Watkins H. Evidence for microvascular dysfunction in hypertrophic cardiomyopathy: new insights from multiparametric magnetic resonance imaging. Circulation. 2007;115(18):2418-25.

29. Elsasser A, Suzuki K, Schaper J. Unresolved issues regarding the role of apoptosis in the pathogenesis of ischemic injury and heart failure. J Mol Cell Cardiol. 2000;32(5):711-24.

30. Gaudino M, Anselmi A, Abbate A, Galiuto L, Luciani N, Glieca F, Possati G. Myocardial apoptosis predicts postoperative course after aortic valve replacement in patients with severe left ventricular hypertrophy. J Heart Valve Dis. 2007;16(4):344-8.

31. Mewton N, Liu CY, Croisille P, Bluemke D, Lima JA. Assessment of myocardial fibrosis with cardiovascular magnetic resonance. J Am Coll Cardiol. 2011;57(8):891-903.

32. Amato MC, Moffa PJ, Werner KE, Ramires JA. Treatment decision in asymptomatic aortic valve stenosis: role of exercise testing. Heart. 2001;86(4):381-6.

33. Lancellotti P, Lebois F, Simon M, Tombeux C, Chauvel C, Pierard LA. Prognostic importance of quantitative exercise Doppler echocardiography in asymptomatic valvular aortic stenosis. Circulation. 2005;112(9 Suppl):I377-82.

34. Rosenhek R, Zilberszac R, Schemper M, Czerny M, Mundigler G, Graf S, Bergler-Klein J, Grimm M, Gabriel H, Maurer G. Natural history of very severe aortic stenosis. Circulation. 2010;121(1):151-6.

35. Kang DH, Park SJ, Rim JH, Yun SC, Kim DH, Song JM, Choo SJ, Park SW, Song JK, Lee JW, Park PW. Early surgery versus conventional treatment in asymptomatic very severe aortic stenosis. Circulation. 2010;121(13):1502-9.

36. Otto CM, Burwash IG, Legget ME, Munt BI, Fujioka M, Healy NL, Kraft CD, Miyake-Hull CY, Schwaegler RG. Prospective study of asymptomatic valvular aortic stenosis. Clinical, echocardiographic, and exercise predictors of outcome. Circulation. 1997;95(9):2262-70.

37. Rosenhek R, Binder T, Porenta G, Lang I, Christ G, Schemper M, Maurer G, Baumgartner H. Predictors of outcome in severe, asymptomatic aortic stenosis. N Engl J Med. 2000;343(9):611-7.

38. Pellikka PA, Sarano ME, Nishimura RA, Malouf JF, Bailey KR, Scott CG, Barnes ME, Tajik AJ. Outcome of 622 adults with asymptomatic, hemodynamically significant aortic stenosis during prolonged follow-up. Circulation. 2005;111(24):3290-5.

39. Lancellotti P, Donal E, Magne J, Moonen M, O'Connor K, Daubert JC, Pierard LA. Risk stratification in asymptomatic moderate to severe aortic stenosis: the importance of the valvular, arterial and ventricular interplay. Heart. 2010;96(17):1364-71.

40. Hachicha Z, Dumesnil JG, Pibarot P. Usefulness of the valvuloarterial impedance to predict adverse outcome in asymptomatic aortic stenosis. J Am Coll Cardiol. 2009;54(11):1003-11.

41. Gibbons RJ, Balady GJ, Bricker JT, Chaitman BR, Fletcher GF, Froelicher VF, Mark DB, McCallister BD, Mooss AN, O'Reilly MG, Winters WL, Jr., Gibbons RJ, Antman EM, Alpert JS, Faxon DP, Fuster V, Gregoratos G, Hiratzka LF, Jacobs AK, Russell RO, Smith SC, Jr. ACC/AHA 2002 guideline update for exercise testing: summary article: a report of the American College of Cardiology/American Heart Association Task

Force on Practice Guidelines (Committee to Update the 1997 Exercise Testing Guidelines). Circulation. 2002;106(14):1883-92.

42. Das P, Rimington H, Chambers J. Exercise testing to stratify risk in aortic stenosis. Eur Heart J. 2005;26(13):1309-13.

43. Alborino D, Hoffmann JL, Fournet PC, Bloch A. Value of exercise testing to evaluate the indication for surgery in asymptomatic patients with valvular aortic stenosis. J Heart Valve Dis. 2002;11(2):204-9.

44. Nishimura RA, Otto CM, Bonow RO, Carabello BA, Erwin JP, 3rd, Guyton RA, O'Gara PT, Ruiz CE, Skubas NJ, Sorajja P, Sundt TM, 3rd, Thomas JD. 2014 AHA/ACC guideline for the management of patients with valvular heart disease: a report of the American College of Cardiology/American Heart Association Task Force on Practice Guidelines. J Am Coll Cardiol. 2014;63(22):e57-185.

45. Steadman CD, Ray S, Ng LL, McCann GP. Natriuretic peptides in common valvular heart disease. J Am Coll Cardiol. 2010;55(19):2034-48.

46. de Lemos JA, McGuire DK, Drazner MH. B-type natriuretic peptide in cardiovascular disease. Lancet. 2003;362(9380):316-22.

47. Bergler-Klein J, Klaar U, Heger M, Rosenhek R, Mundigler G, Gabriel H, Binder T, Pacher R, Maurer G, Baumgartner H. Natriuretic peptides predict symptom-free survival and postoperative outcome in severe aortic stenosis. Circulation. 2004;109(19):2302-8.

48. Nessmith MG, Fukuta H, Brucks S, Little WC. Usefulness of an elevated B-type natriuretic peptide in predicting survival in patients with aortic stenosis treated without surgery. Am J Cardiol. 2005;96(10):1445-8.

49. Gerber IL, Legget ME, West TM, Richards AM, Stewart RA. Usefulness of serial measurement of N-terminal pro-brain natriuretic peptide plasma levels in asymptomatic patients with aortic stenosis to predict symptomatic deterioration. Am J Cardiol. 2005;95(7):898-901.

50. Monin JL, Lancellotti P, Monchi M, Lim P, Weiss E, Pierard L, Gueret P. Risk score for predicting outcome in patients with asymptomatic aortic stenosis. Circulation. 2009;120(1):69-75.

51. Greve AM, Boman K, Gohlke-Baerwolf C, Kesaniemi YA, Nienaber C, Ray S, Egstrup K, Rossebo AB, Devereux RB, Kober L, Willenheimer R, Wachtell K. Clinical implications of electrocardiographic left ventricular strain and hypertrophy in asymptomatic patients with aortic stenosis: the Simvastatin and Ezetimibe in Aortic Stenosis study. Circulation. 2012;125(2):346-53.

52. Shah AS, Chin CW, Vassiliou V, Cowell SJ, Doris M, Kwok TC, Semple S, Zamvar V, White AC, McKillop G, Boon NA, Prasad SK, Mills NL, Newby DE, Dweck MR. Left ventricular hypertrophy with strain and aortic stenosis. Circulation. 2014;130(18):1607-16.

53. Chin CW, Shah AS, McAllister DA, Joanna Cowell S, Alam S, Langrish JP, Strachan FE, Hunter AL, Maria Choy A, Lang CC, Walker S, Boon NA, Newby DE, Mills NL, Dweck MR. High-sensitivity troponin I concentrations are a marker of an advanced hypertrophic response and adverse outcomes in patients with aortic stenosis. Eur Heart J. 2014.

54. McCann GP, Steadman CD, Ray SG, Newby DE. Managing the asymptomatic patient with severe aortic stenosis: randomised controlled trials of early surgery are overdue. Heart. 2011;97(14):1119-21.

55. Lancellotti P, Karsera D, Tumminello G, Lebois F, Pierard LA. Determinants of an abnormal response to exercise in patients with asymptomatic valvular aortic stenosis. Eur J Echocardiogr. 2008;9(3):338-43.

56. Marechaux S, Hachicha Z, Bellouin A, Dumesnil JG, Meimoun P, Pasquet A, Bergeron S, Arsenault M, Le Tourneau T, Ennezat PV, Pibarot P. Usefulness of exercise-stress echocardiography for risk stratification of true asymptomatic patients with aortic valve stenosis. Eur Heart J. 2010;31(11):1390-7.

57. Lancellotti P, Magne J, Pierard LA. The role of stress testing in evaluation of asymptomatic patients with aortic stenosis. Curr Opin Cardiol. 2013;28(5):531-9.

58. Iung B, Baron G, Butchart EG, Delahaye F, Gohlke-Barwolf C, Levang OW, Tornos P, Vanoverschelde JL, Vermeer F, Boersma E, Ravaud P, Vahanian A. A prospective survey of patients with valvular heart disease in Europe: The Euro Heart Survey on Valvular Heart Disease. Eur Heart J. 2003;24(13):1231-43.

59. Bruch C, Stypmann J, Grude M, Gradaus R, Breithardt G, Wichter T. Tissue Doppler imaging in patients with moderate to severe aortic valve stenosis: clinical usefulness and diagnostic accuracy. Am Heart J. 2004;148(4):696-702.

60. Wang B, Chen H, Shu X, Hong T, Lai H, Wang C, Cheng L. Emerging role of echocardiographic strain/strain rate imaging and twist in systolic function evaluation and operative procedure in patients with aortic stenosis. Interact Cardiovasc Thorac Surg. 2013;17(2):384-91.

61. Delgado V, Tops LF, van Bommel RJ, van der Kley F, Marsan NA, Klautz RJ, Versteegh MI, Holman ER, Schalij MJ, Bax JJ. Strain analysis in patients with severe aortic stenosis and preserved left ventricular ejection fraction undergoing surgical valve replacement. Eur Heart J. 2009;30(24):3037-47.

62. Marechaux S, Carpentier E, Six-Carpentier M, Asseman P, LeJemtel TH, Jude B, Pibarot P, Ennezat PV. Impact of valvuloarterial impedance on left ventricular longitudinal deformation in patients with aortic valve stenosis and preserved ejection fraction. Arch Cardiovasc Dis. 2010;103(4):227-35.

63. Ng AC, Delgado V, Bertini M, Antoni ML, van Bommel RJ, van Rijnsoever EP, van der Kley F, Ewe SH, Witkowski T, Auger D, Nucifora G, Schuijf JD, Poldermans D, Leung DY, Schalij MJ, Bax JJ. Alterations in multidirectional myocardial functions in patients with aortic stenosis and preserved ejection fraction: a two-dimensional speckle tracking analysis. Eur Heart J. 2011;32(12):1542-50.

64. Yingchoncharoen T, Gibby C, Rodriguez LL, Grimm RA, Marwick TH. Association of myocardial deformation with outcome in asymptomatic aortic stenosis with normal ejection fraction. Circ Cardiovasc Imaging. 2012;5(6):719-25.

65. Agatston AS, Janowitz WR, Hildner FJ, Zusmer NR, Viamonte M, Jr., Detrano R. Quantification of coronary artery calcium using ultrafast computed tomography. J Am Coll Cardiol. 1990;15(4):827-32.

66. Messika-Zeitoun D, Aubry MC, Detaint D, Bielak LF, Peyser PA, Sheedy PF, Turner ST, Breen JF, Scott C, Tajik AJ, Enriquez-Sarano M. Evaluation and clinical implications of aortic valve calcification measured by electron-beam computed tomography. Circulation. 2004;110(3):356-62.

67. Koos R, Mahnken AH, Kuhl HP, Muhlenbruch G, Mevissen V, Stork L, Dronskowski R, Langebartels G, Autschbach R, Ortlepp JR. Quantification of aortic valve calcification using multislice spiral computed tomography: comparison with atomic absorption spectroscopy. Invest Radiol. 2006;41(5):485-9.

68. Morgan-Hughes GJ, Owens PE, Roobottom CA, Marshall AJ. Three dimensional volume quantification of aortic valve calcification using multislice computed tomography. Heart. 2003;89(10):1191-4.

69. Koos R, Mahnken AH, Sinha AM, Wildberger JE, Hoffmann R, Kuhl HP. Aortic valve calcification as a marker for aortic stenosis severity: assessment on 16-MDCT. AJR Am J Roentgenol. 2004;183(6):1813-8.

70. Cueff C, Serfaty JM, Cimadevilla C, Laissy JP, Himbert D, Tubach F, Duval X, Iung B, Enriquez-Sarano M, Vahanian A, Messika-Zeitoun D. Measurement of aortic valve calcification using multislice computed tomography: correlation with haemodynamic severity of aortic stenosis and clinical implication for patients with low ejection fraction. Heart. 2011;97(9):721-6.

71. Clavel MA, Messika-Zeitoun D, Pibarot P, Aggarwal SR, Malouf J, Araoz PA, Michelena HI, Cueff C, Larose E, Capoulade R, Vahanian A, Enriquez-Sarano M. The complex nature of discordant severe calcified aortic valve disease grading: new insights from combined Doppler echocardiographic and computed tomographic study. J Am Coll Cardiol. 2013;62(24):2329-38.

72. Utsunomiya H, Yamamoto H, Kitagawa T, Kunita E, Urabe Y, Tsushima H, Hidaka T, Awai K, Kihara Y. Incremental prognostic value of cardiac computed tomography angiography in asymptomatic aortic stenosis: Significance of aortic valve calcium score. Int J Cardiol. 2013;168(6):5205-11.

73. Marie–Annick C, Pibarot P, Messika–Zeitoun D, Aggarwal S, Maalouf Y, Araoz P, Michelena H, Caroline C, Larose E, Capoulade R, Vahanian A, Sarano M. Impact of aortic valve calcification measured by multidetector CT on the outcome of patients with aortic stenosis. J Am Coll Cardiol. 2013;61:10_S.

74. Cowell SJ, Newby DE, Prescott RJ, Bloomfield P, Reid J, Northridge DB, Boon NA. A randomized trial of intensive lipid-lowering therapy in calcific aortic stenosis. N Engl J Med. 2005;352(23):2389-97.

75. Mohler ER, 3rd, Wang H, Medenilla E, Scott C. Effect of statin treatment on aortic valve and coronary artery calcification. J Heart Valve Dis. 2007;16(4):378-86.

76. Rossebo AB, Pedersen TR, Boman K, Brudi P, Chambers JB, Egstrup K, Gerdts E, Gohlke-Barwolf C, Holme I, Kesaniemi YA, Malbecq W, Nienaber CA, Ray S, Skjaerpe T, Wachtell K, Willenheimer R. Intensive lipid lowering with simvastatin and ezetimibe in aortic stenosis. N Engl J Med. 2008;359(13):1343-56.

77. Dweck MR, Joshi NV, Rudd JH, Newby DE. Imaging of inflammation and calcification in aortic stenosis. Curr Cardiol Rep. 2013;15(1):320.

78. Marincheva-Savcheva G, Subramanian S, Qadir S, Figueroa A, Truong Q, Vijayakumar J, Brady TJ, Hoffmann U, Tawakol A. Imaging of the aortic valve using fluorodeoxyglucose positron emission

tomography increased valvular fluorodeoxyglucose uptake in aortic stenosis. J Am Coll Cardiol. 2011;57(25):2507-15.

79. Dweck MR, Jones C, Joshi NV, Fletcher AM, Richardson H, White A, Marsden M, Pessotto R, Clark JC, Wallace WA, Salter DM, McKillop G, van Beek EJ, Boon NA, Rudd JH, Newby DE. Assessment of valvular calcification and inflammation by positron emission tomography in patients with aortic stenosis. Circulation. 2012;125(1):76-86.

80. Bottini PB, Carr AA, Prisant LM, Flickinger FW, Allison JD, Gottdiener JS. Magnetic resonance imaging compared to echocardiography to assess left ventricular mass in the hypertensive patient. Am J Hypertens. 1995;8(3):221-8.

81. Grothues F, Smith GC, Moon JC, Bellenger NG, Collins P, Klein HU, Pennell DJ. Comparison of interstudy reproducibility of cardiovascular magnetic resonance with two-dimensional echocardiography in normal subjects and in patients with heart failure or left ventricular hypertrophy. Am J Cardiol. 2002;90(1):29-34.

82. Myerson SG, Bellenger NG, Pennell DJ. Assessment of left ventricular mass by cardiovascular magnetic resonance. Hypertension. 2002;39(3):750-5.

83. Childs H, Ma L, Ma M, Clarke J, Cocker M, Green J, Strohm O, Friedrich MG. Comparison of long and short axis quantification of left ventricular volume parameters by cardiovascular magnetic resonance, with ex-vivo validation. J Cardiovasc Magn Reson. 2011;13:40.

84. John AS, Dill T, Brandt RR, Rau M, Ricken W, Bachmann G, Hamm CW. Magnetic resonance to assess the aortic valve area in aortic stenosis: how does it compare to current diagnostic standards? J Am Coll Cardiol. 2003;42(3):519-26.

85. Krayenbuehl HP, Hess OM, Monrad ES, Schneider J, Mall G, Turina M. Left ventricular myocardial structure in aortic valve disease before, intermediate, and late after aortic valve replacement. Circulation. 1989;79(4):744-55.

86. Flett AS, Hayward MP, Ashworth MT, Hansen MS, Taylor AM, Elliott PM, McGregor C, Moon JC. Equilibrium contrast cardiovascular magnetic resonance for the measurement of diffuse myocardial fibrosis: preliminary validation in humans. Circulation. 2010;122(2):138-44.

87. Simonetti OP, Kim RJ, Fieno DS, Hillenbrand HB, Wu E, Bundy JM, Finn JP, Judd RM. An improved MR imaging technique for the visualization of myocardial infarction. Radiology. 2001;218(1):215-23.

88. Moon JC, Reed E, Sheppard MN, Elkington AG, Ho SY, Burke M, Petrou M, Pennell DJ. The histologic basis of late gadolinium enhancement cardiovascular magnetic resonance in hypertrophic cardiomyopathy. J Am Coll Cardiol. 2004;43(12):2260-4.

89. Azevedo CF, Nigri M, Higuchi ML, Pomerantzeff PM, Spina GS, Sampaio RO, Tarasoutchi F, Grinberg M, Rochitte CE. Prognostic significance of myocardial fibrosis quantification by histopathology and magnetic resonance imaging in patients with severe aortic valve disease. J Am Coll Cardiol. 2010;56(4):278-87.

90. Flett AS, Hasleton J, Cook C, Hausenloy D, Quarta G, Ariti C, Muthurangu V, Moon JC. Evaluation of techniques for the quantification of myocardial scar of differing etiology using cardiac magnetic resonance. J Am Coll Cardiol Img. 2011;4(2):150-6.

91. Debl K, Djavidani B, Buchner S, Lipke C, Nitz W, Feuerbach S, Riegger G, Luchner A. Delayed hyperenhancement in magnetic resonance imaging of left ventricular hypertrophy caused by aortic stenosis and hypertrophic cardiomyopathy: visualisation of focal fibrosis. Heart. 2006;92(10):1447-51.

92. Weidemann F, Herrmann S, Stork S, Niemann M, Frantz S, Lange V, Beer M, Gattenlohner S, Voelker W, Ertl G, Strotmann JM. Impact of myocardial fibrosis in patients with symptomatic severe aortic stenosis. Circulation. 2009;120(7):577-84.

93. Dweck MR, Joshi S, Murigu T, Alpendurada F, Jabbour A, Melina G, Banya W, Gulati A, Roussin I, Raza S, Prasad NA, Wage R, Quarto C, Angeloni E, Refice S, Sheppard M, Cook SA, Kilner PJ, Pennell DJ, Newby DE, Mohiaddin RH, Pepper J, Prasad SK. Midwall fibrosis is an independent predictor of mortality in patients with aortic stenosis. J Am Coll Cardiol. 2011;58(12):1271-9.

94. Iles L, Pfluger H, Phrommintikul A, Cherayath J, Aksit P, Gupta SN, Kaye DM, Taylor AJ. Evaluation of diffuse myocardial fibrosis in heart failure with cardiac magnetic resonance contrast-enhanced T1 mapping. J Am Coll Cardiol. 2008;52(19):1574-80.

95. Ugander M, Oki AJ, Hsu LY, Kellman P, Greiser A, Aletras AH, Sibley CT, Chen MY, Bandettini WP, Arai AE. Extracellular volume imaging by magnetic resonance imaging provides insights into overt and sub-clinical myocardial pathology. Eur Heart J. 2012;33(10):1268-78.

96. Miller CA, Naish JH, Bishop P, Coutts G, Clark D, Zhao S, Ray SG, Yonan N, Williams SG, Flett AS, Moon JC, Greiser A, Parker GJ, Schmitt M. Comprehensive validation of cardiovascular magnetic resonance techniques for the assessment of myocardial extracellular volume. Circ Cardiovasc Imaging. 2013;6(3):373-83.

97. White SK, Sado DM, Fontana M, Banypersad SM, Maestrini V, Flett AS, Piechnik SK, Robson MD, Hausenloy DJ, Sheikh AM, Hawkins PN, Moon JC. T1 mapping for myocardial extracellular volume measurement by CMR: bolus only versus primed infusion technique. JACC Cardiovasc Imaging. 2013;6(9):955-62.

98. Bull S, White SK, Piechnik SK, Flett AS, Ferreira VM, Loudon M, Francis JM, Karamitsos TD, Prendergast BD, Robson MD, Neubauer S, Moon JC, Myerson SG. Human non-contrast T1 values and correlation with histology in diffuse fibrosis. Heart. 2013;99(13):932-7.

99. Sado DM, Flett AS, Banypersad SM, White SK, Maestrini V, Quarta G, Lachmann RH, Murphy E, Mehta A, Hughes DA, McKenna WJ, Taylor AM, Hausenloy DJ, Hawkins PN, Elliott PM, Moon JC. Cardiovascular magnetic resonance measurement of myocardial extracellular volume in health and disease. Heart. 2012;98(19):1436-41.

100. Chin CW, Semple S, Malley T, White AC, Mirsadraee S, Weale PJ, Prasad S, Newby DE, Dweck MR. Optimization and comparison of myocardial T1 techniques at 3T in patients with aortic stenosis. Eur Heart J Cardiovasc Imaging. 2014;15(5):556-65.

101. Flett AS, Sado DM, Quarta G, Mirabel M, Pellerin D, Herrey AS, Hausenloy DJ, Ariti C, Yap J, Kolvekar S, Taylor AM, Moon JC. Diffuse myocardial fibrosis in severe aortic stenosis: an equilibrium contrast cardiovascular magnetic resonance study. Eur Heart J Cardiovasc Imaging. 2012;13(10):819-26.

102. Hess OM, Villari B, Krayenbuehl HP. Diastolic dysfunction in aortic stenosis. Circulation. 1993;87(5 Suppl):IV73-6.

103. Moon JC, Messroghli DR, Kellman P, Piechnik SK, Robson MD, Ugander M, Gatehouse PD, Arai AE, Friedrich MG, Neubauer S, Schulz-Menger J, Schelbert EB. Myocardial T1 mapping and extracellular volume quantification: a Society for Cardiovascular Magnetic Resonance (SCMR) and CMR Working Group of the European Society of Cardiology consensus statement. J Cardiovasc Magn Reson. 2013;15(1):92.

104. Mahmod M, Bull S, Suttie JJ, Pal N, Holloway C, Dass S, Myerson SG, Schneider JE, De Silva R, Petrou M, Sayeed R, Westaby S, Clelland C, Francis JM, Ashrafian H, Karamitsos TD, Neubauer S. Myocardial steatosis and left ventricular contractile dysfunction in patients with severe aortic stenosis. Circ Cardiovasc Imaging. 2013;6(5):808-16.

105. Brindley DN, Kok BP, Kienesberger PC, Lehner R, Dyck JR. Shedding light on the enigma of myocardial lipotoxicity: the involvement of known and putative regulators of fatty acid storage and mobilization. Am J Physiol Endocrinol Metab. 2010;298(5):E897-908.

106. Doucette JW, Corl PD, Payne HM, Flynn AE, Goto M, Nassi M, Segal J. Validation of a Doppler guide wire for intravascular measurement of coronary artery flow velocity. Circulation. 1992;85(5):1899-911.

107. Rajappan K, Rimoldi OE, Camici PG, Bellenger NG, Pennell DJ, Sheridan DJ. Functional changes in coronary microcirculation after valve replacement in patients with aortic stenosis. Circulation. 2003;107(25):3170-5.

108. Steadman CD, Jerosch-Herold M, Grundy B, Rafelt S, Ng LL, Squire IB, Samani NJ, McCann GP. Determinants and functional significance of myocardial perfusion reserve in severe aortic stenosis. J Am Coll Cardiol Img. 2012;5(2):182-9.

109. Jerosch-Herold M, Seethamraju RT, Swingen CM, Wilke NM, Stillman AE. Analysis of myocardial perfusion MRI. J Magn Reson Imaging. 2004;19(6):758-70.

110. Jerosch-Herold M. Quantification of myocardial perfusion by cardiovascular magnetic resonance. J Cardiovasc Magn Reson. 2010;12:57.

111. Lee DC, Johnson NP. Quantification of absolute myocardial blood flow by magnetic resonance perfusion imaging. JACC Cardiovasc Imaging. 2009;2(6):761-70.

112. Pai RG, Kapoor N, Bansal RC, Varadarajan P. Malignant natural history of asymptomatic severe aortic stenosis: benefit of aortic valve replacement. Ann Thorac Surg. 2006;82(6):2116-22.

113. Bonow RO, Carabello BA, Chatterjee K, de Leon AC, Jr., Faxon DP, Freed MD, Gaasch WH, Lytle BW, Nishimura RA, O'Gara PT, O'Rourke RA, Otto CM, Shah PM, Shanewise JS. 2008 focused update incorporated into the ACC/AHA 2006 guidelines for the management of patients with valvular heart disease: a report of the American College of Cardiology/American Heart Association Task Force on Practice

Guidelines (Writing Committee to revise the 1998 guidelines for the management of patients with valvular heart disease). Endorsed by the Society of Cardiovascular Anesthesiologists, Society for Cardiovascular Angiography and Interventions, and Society of Thoracic Surgeons. J Am Coll Cardiol. 2008;52(13):e1-142.

114. Vahanian A, Baumgartner H, Bax J, Butchart E, Dion R, Filippatos G, Flachskampf F, Hall R, Iung B, Kasprzak J, Nataf P, Tornos P, Torracca L, Wenink A. Guidelines on the management of valvular heart disease: The Task Force on the Management of Valvular Heart Disease of the European Society of Cardiology. Eur Heart J. 2007;28(2):230-68.

115. Leon MB, Smith CR, Mack M, Miller DC, Moses JW, Svensson LG, Tuzcu EM, Webb JG, Fontana GP, Makkar RR, Brown DL, Block PC, Guyton RA, Pichard AD, Bavaria JE, Herrmann HC, Douglas PS, Petersen JL, Akin JJ, Anderson WN, Wang D, Pocock S. Transcatheter aortic-valve implantation for aortic stenosis in patients who cannot undergo surgery. N Engl J Med. 2010;363(17):1597-607.

116. Chan KL, Teo K, Dumesnil JG, Ni A, Tam J. Effect of Lipid lowering with rosuvastatin on progression of aortic stenosis: results of the aortic stenosis progression observation: measuring effects of rosuvastatin (ASTRONOMER) trial. Circulation. 2010;121(2):306-14.

117. Study Investigating the Effect of Drugs Used to Treat Osteoporosis on the Progression of Calcific Aortic Stenosis. (SALTIRE II). NCT02132026 [database on the Internet]. ClinicalTrials.gov. Available from: https://clinicaltrials.gov/show/NCT02132026.

118. Liu PY, Tsai WC, Lin CC, Hsu CH, Haung YY, Chen JH. Invasive measurements of pulse wave velocity correlate with the degree of aortic valve calcification and severity associated with matrix metalloproteinases in elderly patients with aortic valve stenosis. Clin Sci (Lond). 2004;107(4):415-22.

119. Chaitman BR, Pepine CJ, Parker JO, Skopal J, Chumakova G, Kuch J, Wang W, Skettino SL, Wolff AA. Effects of ranolazine with atenolol, amlodipine, or diltiazem on exercise tolerance and angina frequency in patients with severe chronic angina: a randomized controlled trial. JAMA. 2004;291(3):309-16.

120. Chaitman BR, Skettino SL, Parker JO, Hanley P, Meluzin J, Kuch J, Pepine CJ, Wang W, Nelson JJ, Hebert DA, Wolff AA. Anti-ischemic effects and long-term survival during ranolazine monotherapy in patients with chronic severe angina. J Am Coll Cardiol. 2004;43(8):1375-82.

121. Sossalla S, Wagner S, Rasenack EC, Ruff H, Weber SL, Schondube FA, Tirilomis T, Tenderich G, Hasenfuss G, Belardinelli L, Maier LS. Ranolazine improves diastolic dysfunction in isolated myocardium from failing human hearts--role of late sodium current and intracellular ion accumulation. J Mol Cell Cardiol. 2008;45(1):32-43.

122. Lovelock JD, Monasky MM, Jeong EM, Lardin HA, Liu H, Patel BG, Taglieri DM, Gu L, Kumar P, Pokhrel N, Zeng D, Belardinelli L, Sorescu D, Solaro RJ, Dudley SC, Jr. Ranolazine improves cardiac diastolic dysfunction through modulation of myofilament calcium sensitivity. Circ Res. 2012;110(6):841-50.

123. Coppini R, Ferrantini C, Yao L, Fan P, Del Lungo M, Stillitano F, Sartiani L, Tosi B, Suffredini S, Tesi C, Yacoub M, Olivotto I, Belardinelli L, Poggesi C, Cerbai E, Mugelli A. Late sodium current inhibition

reverses electromechanical dysfunction in human hypertrophic cardiomyopathy. Circulation. 2013;127(5):575-84.

124. Venkataraman R, Belardinelli L, Blackburn B, Heo J, Iskandrian AE. A study of the effects of ranolazine using automated quantitative analysis of serial myocardial perfusion images. J Am Coll Cardiol Img. 2009;2(11):1301-9.

125. Shah PK. Severe aortic stenosis should not be operated on before symptom onset. Circulation. 2012;126(1):118-25.

126. Carabello BA. Aortic valve replacement should be operated on before symptom onset. Circulation. 2012;126(1):112-7.

127. Pellikka PA, Nishimura RA, Bailey KR, Tajik AJ. The natural history of adults with asymptomatic, hemodynamically significant aortic stenosis. J Am Coll Cardiol. 1990;15(5):1012-7.

128. Lund O, Nielsen TT, Emmertsen K, Flo C, Rasmussen B, Jensen FT, Pilegaard HK, Kristensen LH, Hansen OK. Mortality and worsening of prognostic profile during waiting time for valve replacement in aortic stenosis. Thorac Cardiovasc Surg. 1996;44(6):289-95.

129. Yarbrough WM, Mukherjee R, Ikonomidis JS, Zile MR, Spinale FG. Myocardial remodeling with aortic stenosis and after aortic valve replacement: mechanisms and future prognostic implications. J Thorac Cardiovasc Surg. 2012;143(3):656-64.

130. Hatle L, Angelsen BA, Tromsdal A. Non-invasive assessment of aortic stenosis by Doppler ultrasound. Br Heart J. 1980;43(3):284-92.

131. Feigenbaum H, Armstrong WF, Ryan T. Feigenbaum's echocardiography. 6th ed. / Harvey Feigenbaum, William F. Armstrong, Thomas Ryan. ed. Philadelphia, Pa. ; London: Lippincott Williams & Wilkins; 2005.

132. Currie PJ, Seward JB, Reeder GS, Vlietstra RE, Bresnahan DR, Bresnahan JF, Smith HC, Hagler DJ, Tajik AJ. Continuous-wave Doppler echocardiographic assessment of severity of calcific aortic stenosis: a simultaneous Doppler-catheter correlative study in 100 adult patients. Circulation. 1985;71(6):1162-9.

133. Zoghbi WA, Farmer KL, Soto JG, Nelson JG, Quinones MA. Accurate noninvasive quantification of stenotic aortic valve area by Doppler echocardiography. Circulation. 1986;73(3):452-9.

134. Oh JK, Taliercio CP, Holmes DR, Jr., Reeder GS, Bailey KR, Seward JB, Tajik AJ. Prediction of the severity of aortic stenosis by Doppler aortic valve area determination: prospective Doppler-catheterization correlation in 100 patients. J Am Coll Cardiol. 1988;11(6):1227-34.

135. Fokkema DS, VanTeeffelen JW, Dekker S, Vergroesen I, Reitsma JB, Spaan JA. Diastolic time fraction as a determinant of subendocardial perfusion. Am J Physiol Heart Circ Physiol. 2005;288(5):H2450-6.

136. Wasserman K, Hanson J, Sue D, Casaburi R, Whipp B. Principles of exercise testing and interpretation. Third ed: Lippincott Williams and Wilkins; 1999.

137. Okin PM, Ameisen O, Kligfield P. A modified treadmill exercise protocol for computer-assisted analysis of the ST segment/heart rate slope: methods and reproducibility. J Electrocardiol. 1986;19(4):311-8.

138. Borg G. Perceived exertion as an indicator of somatic stress. Scand J Rehabil Med. 1970;2(2):92-8.

139. Borg GA. Psychophysical bases of perceived exertion. Med Sci Sports Exerc. 1982;14(5):377-81.

140. Christian TF, Bell SP, Whitesell L, Jerosch-Herold M. Accuracy of cardiac magnetic resonance of absolute myocardial blood flow with a high-field system: comparison with conventional field strength. J Am Coll Cardiol Img. 2009;2(9):1103-10.

141. Messroghli DR, Greiser A, Frohlich M, Dietz R, Schulz-Menger J. Optimization and validation of a fully-integrated pulse sequence for modified look-locker inversion-recovery (MOLLI) T1 mapping of the heart. J Magn Reson Imaging. 2007;26(4):1081-6.

142. Xue H, Shah S, Greiser A, Guetter C, Littmann A, Jolly MP, Arai AE, Zuehlsdorff S, Guehring J, Kellman P. Motion correction for myocardial T1 mapping using image registration with synthetic image estimation. Magn Reson Med. 2012;67(6):1644-55.

143. Papavassiliu T, Kuhl HP, Schroder M, Suselbeck T, Bondarenko O, Bohm CK, Beek A, Hofman MM, van Rossum AC. Effect of endocardial trabeculae on left ventricular measurements and measurement reproducibility at cardiovascular MR imaging. Radiology. 2005;236(1):57-64.

144. Schaefer BM, Lewin MB, Stout KK, Gill E, Prueitt A, Byers PH, Otto CM. The bicuspid aortic valve: an integrated phenotypic classification of leaflet morphology and aortic root shape. Heart. 2008;94(12):1634-8.

145. Bland JM, Altman DG. Statistical methods for assessing agreement between two methods of clinical measurement. Lancet. 1986;1(8476):307-10.

146. McGraw KO, Wong SP. Forming inferences about some intraclass correlation coefficients. Psychological Methods. 1996;1:30-46.

147. MeSH. The National Center for Biotechnology Information: Medical subject headings. Available from: http://www.ncbi.nlm.nih.gov/mesh/68015588.

148. McNaught AD, Wilkinson A. Compendium of chemical terminology : IUPAC recommendations. 2nd ed / compiled by Alan D. McNaught and Andrew Wilkinson. ed. Oxford: Blackwell Science; 1997.

149. Miller CA, Borg A, Clark D, Steadman CD, McCann GP, Clarysse P, Croisille P, Schmitt M. Comparison of local sine wave modeling with harmonic phase analysis for the assessment of myocardial strain. J Magn Reson Imaging. 2013;38(2):320-8.

150. Dalsgaard M, Kjaergaard J, Pecini R, Iversen KK, Kober L, Moller JE, Grande P, Clemmensen P, Hassager C. Predictors of exercise capacity and symptoms in severe aortic stenosis. Eur J Echocardiogr. 2010;11(6):482-7.

151. Hor KN, Gottliebson WM, Carson C, Wash E, Cnota J, Fleck R, Wansapura J, Klimeczek P, Al-Khalidi HR, Chung ES, Benson DW, Mazur W. Comparison of magnetic resonance feature tracking for strain calculation with harmonic phase imaging analysis. J Am Coll Cardiol Img. 2010;3(2):144-51.

152. Schuster A, Kutty S, Padiyath A, Parish V, Gribben P, Danford DA, Makowski MR, Bigalke B, Beerbaum P, Nagel E. Cardiovascular magnetic resonance myocardial feature tracking detects quantitative wall motion during dobutamine stress. J Cardiovasc Magn Reson. 2011;13:58.

153. Schuster A, Paul M, Bettencourt N, Morton G, Chiribiri A, Ishida M, Hussain S, Jogiya R, Kutty S, Bigalke B, Perera D, Nagel E. Cardiovascular magnetic resonance myocardial feature tracking for quantitative viability assessment in ischemic cardiomyopathy. Int J Cardiol. 2013;166(2):413-20.

154. Morton G, Schuster A, Jogiya R, Kutty S, Beerbaum P, Nagel E. Inter-study reproducibility of cardiovascular magnetic resonance myocardial feature tracking. J Cardiovasc Magn Reson. 2012;14:43.

155. Augustine D, Lewandowski AJ, Lazdam M, Rai A, Francis J, Myerson S, Noble A, Becher H, Neubauer S, Petersen SE, Leeson P. Global and regional left ventricular myocardial deformation measures by magnetic resonance feature tracking in healthy volunteers: comparison with tagging and relevance of gender. J Cardiovasc Magn Reson. 2013;15:8.

156. Harrild DM, Han Y, Geva T, Zhou J, Marcus E, Powell AJ. Comparison of cardiac MRI tissue tracking and myocardial tagging for assessment of regional ventricular strain. Int J Cardiovasc Imaging. 2012;28(8):2009-18.

157. Schuster A, Morton G, Hussain ST, Jogiya R, Kutty S, Asrress KN, Makowski MR, Bigalke B, Perera D, Beerbaum P, Nagel E. The intra-observer reproducibility of cardiovascular magnetic resonance myocardial feature tracking strain assessment is independent of field strength. Eur J Radiol. 2013;82(2):296-301.

158. Valeti VU, Chun W, Potter DD, Araoz PA, McGee KP, Glockner JF, Christian TF. Myocardial tagging and strain analysis at 3 Tesla: comparison with 1.5 Tesla imaging. J Magn Reson Imaging. 2006;23(4):477-80.

159. Kuijer JP, Jansen E, Marcus JT, van Rossum AC, Heethaar RM. Improved harmonic phase myocardial strain maps. Magn Reson Med. 2001;46(5):993-9.

160. Fischer SE, McKinnon GC, Maier SE, Boesiger P. Improved myocardial tagging contrast. Magn Reson Med. 1993;30(2):191-200.

161. Swoboda PP, Larghat A, Zaman A, Fairbairn TA, Motwani M, Greenwood JP, Plein S. Reproducibility of myocardial strain and left ventricular twist measured using complementary spatial modulation of magnetization. J Magn Reson Imaging. 2013.

162. Gotte MJ, Germans T, Russel IK, Zwanenburg JJ, Marcus JT, van Rossum AC, van Veldhuisen DJ. Myocardial strain and torsion quantified by cardiovascular magnetic resonance tissue tagging: studies in normal and impaired left ventricular function. J Am Coll Cardiol. 2006;48(10):2002-11.

163. Liu S, Han J, Nacif MS, Jones J, Kawel N, Kellman P, Sibley CT, Bluemke DA. Diffuse myocardial fibrosis evaluation using cardiac magnetic resonance T1 mapping: sample size considerations for clinical trials. J Cardiovasc Magn Reson. 2012;14:90.

164. Fontana M, White SK, Banypersad SM, Sado DM, Maestrini V, Flett AS, Piechnik SK, Neubauer S, Roberts N, Moon JC. Comparison of T1 mapping techniques for ECV quantification. Histological validation

and reproducibility of ShMOLLI versus multibreath-hold T1 quantification equilibrium contrast CMR. J Cardiovasc Magn Reson. 2012;14:88.

165. Rogers T, Dabir D, Mahmoud I, Voigt T, Schaeffter T, Nagel E, Puntmann VO. Standardization of T1 measurements with MOLLI in differentiation between health and disease--the ConSept study. J Cardiovasc Magn Reson. 2013;15:78.

166. Kellman P, Hansen MS. T1-mapping in the heart: accuracy and precision. J Cardiovasc Magn Reson. 2014;16:2.

167. Morton G, Jogiya R, Plein S, Schuster A, Chiribiri A, Nagel E. Quantitative cardiovascular magnetic resonance perfusion imaging: inter-study reproducibility. Eur Heart J Cardiovasc Imaging. 2012;13(11):954-60.

168. Larghat AM, Maredia N, Biglands J, Greenwood JP, Ball SG, Jerosch-Herold M, Radjenovic A, Plein S. Reproducibility of first-pass cardiovascular magnetic resonance myocardial perfusion. J Magn Reson Imaging. 2013;37(4):865-74.

169. Elkington AG, Gatehouse PD, Ablitt NA, Yang GZ, Firmin DN, Pennell DJ. Interstudy reproducibility of quantitative perfusion cardiovascular magnetic resonance. J Cardiovasc Magn Reson. 2005;7(5):815-22.

170. Chih S, Macdonald PS, Feneley MP, Law M, Graham RM, McCrohon JA. Reproducibility of adenosine stress cardiovascular magnetic resonance in multi-vessel symptomatic coronary artery disease. J Cardiovasc Magn Reson. 2010;12:42.

171. Muhling OM, Dickson ME, Zenovich A, Huang Y, Wilson BV, Wilson RF, Anand IS, Seethamraju RT, Jerosch-Herold M, Wilke NM. Quantitative magnetic resonance first-pass perfusion analysis: inter- and intraobserver agreement. J Cardiovasc Magn Reson. 2001;3(3):247-56.

172. Jerosch-Herold M, Vazquez G, Wang L, Jacobs DR, Jr., Folsom AR. Variability of myocardial blood flow measurements by magnetic resonance imaging in the multi-ethnic study of atherosclerosis. Invest Radiol. 2008;43(3):155-61.

173. Rastogi S, Sharov VG, Mishra S, Gupta RC, Blackburn B, Belardinelli L, Stanley WC, Sabbah HN. Ranolazine combined with enalapril or metoprolol prevents progressive LV dysfunction and remodeling in dogs with moderate heart failure. Am J Physiol Heart Circ Physiol. 2008;295(5):H2149-55.

174. Figueredo VM, Pressman GS, Romero-Corral A, Murdock E, Holderbach P, Morris DL. Improvement in left ventricular systolic and diastolic performance during ranolazine treatment in patients with stable angina. J Cardiovasc Pharmacol Ther. 2011;16(2):168-72.

175. Maier LS, Layug B, Karwatowska-Prokopczuk E, Belardinelli L, Lee S, Sander J, Lang C, Wachter R, Edelmann F, Hasenfuss G, Jacobshagen C. RAnoLazIne for the Treatment of Diastolic Heart Failure in Patients With Preserved Ejection FractionThe RALI-DHF Proof-of-Concept Study. JACC: Heart Failure. 2013;1(2):115-22.

176. Sossalla S, Maurer U, Schotola H, Hartmann N, Didie M, Zimmermann WH, Jacobshagen C, Wagner S, Maier LS. Diastolic dysfunction and arrhythmias caused by overexpression of CaMKIIdelta(C) can be reversed by inhibition of late Na(+) current. Basic Res Cardiol. 2011;106(2):263-72.

177. Hayashida W, van Eyll C, Rousseau MF, Pouleur H. Effects of ranolazine on left ventricular regional diastolic function in patients with ischemic heart disease. Cardiovasc Drugs Ther. 1994;8(5):741-7.

178. D'Elia E, Fiocca L, Ferrero P, Iacovoni A, Baio P, Medolago G, Duino V, Gori M, Gavazzi A, Senni M. Ranolazine in heart failure with preserved left ventricular ejection fraction and microvascular dysfunction: case report and literature review. J Clin Pharmacol. 2013;53(6):665-9.

179. Singh A, Steadman CD, Khan JN, Horsfield MA, Bekele S, Nazir SA, Kanagala P, Masca NG, Clarysse P, McCann GP. Intertechnique agreement and interstudy reproducibility of strain and diastolic strain rate at 1.5 and 3 tesla: A comparison of feature-tracking and tagging in patients with aortic stenosis. J Magn Reson Imaging. 2014.

180. Venkataraman R, Aljaroudi W, Belardinelli L, Heo J, Iskandrian AE. The effect of ranolazine on the vasodilator-induced myocardial perfusion abnormality. J Nucl Cardiol. 2011;18(3):456-62.

181. Villano A, Di Franco A, Nerla R, Sestito A, Tarzia P, Lamendola P, Di Monaco A, Sarullo FM, Lanza GA, Crea F. Effects of ivabradine and ranolazine in patients with microvascular angina pectoris. Am J Cardiol. 2013;112(1):8-13.

182. Wilson SR, Scirica BM, Braunwald E, Murphy SA, Karwatowska-Prokopczuk E, Buros JL, Chaitman BR, Morrow DA. Efficacy of ranolazine in patients with chronic angina observations from the randomized, double-blind, placebo-controlled MERLIN-TIMI (Metabolic Efficiency With Ranolazine for Less Ischemia in Non-ST-Segment Elevation Acute Coronary Syndromes) 36 Trial. J Am Coll Cardiol. 2009;53(17):1510-6.

183. Clyne CA, Arrighi JA, Maron BJ, Dilsizian V, Bonow RO, Cannon RO, 3rd. Systemic and left ventricular responses to exercise stress in asymptomatic patients with valvular aortic stenosis. Am J Cardiol. 1991;68(15):1469-76.

184. Donal E, Thebault C, O'Connor K, Veillard D, Rosca M, Pierard L, Lancellotti P. Impact of aortic stenosis on longitudinal myocardial deformation during exercise. Eur J Echocardiogr. 2011;12(3):235-41.

185. Hawkins S, Wiswell R. Rate and mechanism of maximal oxygen consumption decline with aging: implications for exercise training. Sports Med. 2003;33(12):877-88.

186. Grotenhuis HB, Ottenkamp J, Westenberg JJ, Bax JJ, Kroft LJ, de Roos A. Reduced aortic elasticity and dilatation are associated with aortic regurgitation and left ventricular hypertrophy in nonstenotic bicuspid aortic valve patients. J Am Coll Cardiol. 2007;49(15):1660-5.

187. Yap SC, Nemes A, Meijboom FJ, Galema TW, Geleijnse ML, ten Cate FJ, Simoons ML, Roos-Hesselink JW. Abnormal aortic elastic properties in adults with congenital valvular aortic stenosis. Int J Cardiol. 2008;128(3):336-41.

188. Celik S, Durmus I, Korkmaz L, Gedikli O, Kaplan S, Orem C, Baykan M. Aortic pulse wave velocity in subjects with aortic valve sclerosis. Echocardiography. 2008;25(10):1112-6.

189. El-Chilali K, Farouk H, Abdelhafez M, Neumann T, Alotaibi S, Wendt D, Thielmann M, Jakob HG, Ashour Z, Sorour K, Kahlert P, Erbel R. Predictors of aortic pulse wave velocity in the elderly with severe aortic stenosis. Aging Clin Exp Res. 2015.

190. Nemes A, Galema TW, Geleijnse ML, Soliman OI, Yap SC, Anwar AM, ten Cate FJ. Aortic valve replacement for aortic stenosis is associated with improved aortic distensibility at long-term follow-up. Am Heart J. 2007;153(1):147-51.

191. Meimoun P, Germain AL, Elmkies F, Benali T, Boulanger J, Espanel C, Clerc J, Zemir H, Luycx-Bore A, Tribouilloy C. Factors associated with noninvasive coronary flow reserve in severe aortic stenosis. J Am Soc Echocardiogr. 2012;25(8):835-41.

192. Hudlicka O, Brown M, Egginton S. Angiogenesis in skeletal and cardiac muscle. Physiol Rev. 1992;72(2):369-417.

193. Takeda S, Rimington H, Smeeton N, Chambers J. Long axis excursion in aortic stenosis. Heart. 2001;86(1):52-6.

194. Dinh W, Nickl W, Smettan J, Koehler T, Bansemir L, Lankisch M, Scheffold T, Barroso MC, Gulker JE, Futh R. Relation of global longitudinal strain to left ventricular geometry in aortic valve stenosis. Cardiol J. 2011;18(2):151-6.

195. Nakano K, Corin WJ, Spann JF, Jr., Biederman RW, Denslow S, Carabello BA. Abnormal subendocardial blood flow in pressure overload hypertrophy is associated with pacing-induced subendocardial dysfunction. Circ Res. 1989;65(6):1555-64.

196. Donal E, Bergerot C, Thibault H, Ernande L, Loufoua J, Augeul L, Ovize M, Derumeaux G. Influence of afterload on left ventricular radial and longitudinal systolic functions: a two-dimensional strain imaging study. Eur J Echocardiogr. 2009;10(8):914-21.

197. Duncan AI, Lowe BS, Garcia MJ, Xu M, Gillinov AM, Mihaljevic T, Koch CG. Influence of concentric left ventricular remodeling on early mortality after aortic valve replacement. Ann Thorac Surg. 2008;85(6):2030-9.

198. Das P, Rimington H, Smeeton N, Chambers J. Determinants of symptoms and exercise capacity in aortic stenosis: a comparison of resting haemodynamics and valve compliance during dobutamine stress. Eur Heart J. 2003;24(13):1254-63.

199. Rajani R, Rimington H, Nabeebaccus A, Chowienczyk P, Chambers JB. Asymptomatic aortic stenosis: the influence of the systemic vasculature on exercise time. J Am Soc Echocardiogr. 2012;25(6):613-9.

200. Dulgheru R, Magne J, Capoulade R, Davin L, Vinereanu D, Pierard LA, Pibarot P, Lancellotti P. Impact of global hemodynamic load on exercise capacity in aortic stenosis. Int J Cardiol. 2013;168(3):2272-7.

201. Dulgheru R, Magne J, Davin L, Nchimi A, Oury C, Pierard LA, Lancellotti P. Left ventricular regional function and maximal exercise capacity in aortic stenosis. Eur Heart J Cardiovasc Imaging. 2016;17(2):217-24.

202. Briand M, Dumesnil JG, Kadem L, Tongue AG, Rieu R, Garcia D, Pibarot P. Reduced systemic arterial compliance impacts significantly on left ventricular afterload and function in aortic stenosis: implications for diagnosis and treatment. J Am Coll Cardiol. 2005;46(2):291-8.

203. Herrmann S, Stork S, Niemann M, Lange V, Strotmann JM, Frantz S, Beer M, Gattenlohner S, Voelker W, Ertl G, Weidemann F. Low-gradient aortic valve stenosis myocardial fibrosis and its influence on function and outcome. J Am Coll Cardiol. 2011;58(4):402-12.

204. Carroll JD, Carroll EP, Feldman T, Ward DM, Lang RM, McGaughey D, Karp RB. Sex-associated differences in left ventricular function in aortic stenosis of the elderly. Circulation. 1992;86(4):1099-107.

205. Mahmod M, Francis JM, Pal N, Lewis A, Dass S, De Silva R, Petrou M, Sayeed R, Westaby S, Robson MD, Ashrafian H, Neubauer S, Karamitsos TD. Myocardial perfusion and oxygenation are impaired during stress in severe aortic stenosis and correlate with impaired energetics and subclinical left ventricular dysfunction. J Cardiovasc Magn Reson. 2014;16(1):29.

206. Burwash IG, Lortie M, Pibarot P, de Kemp RA, Graf S, Mundigler G, Khorsand A, Blais C, Baumgartner H, Dumesnil JG, Hachicha Z, DaSilva J, Beanlands RS. Myocardial blood flow in patients with low-flow, low-gradient aortic stenosis: differences between true and pseudo-severe aortic stenosis. Results from the multicentre TOPAS (Truly or Pseudo-Severe Aortic Stenosis) study. Heart. 2008;94(12):1627-33.

207. Banovic MD, Vujisic-Tesic BD, Kujacic VG, Callahan MJ, Nedeljkovic IP, Trifunovic DD, Aleksandric SB, Petrovic MZ, Obradovic SD, Ostojic MC. Coronary flow reserve in patients with aortic stenosis and nonobstructed coronary arteries. Acta Cardiol. 2011;66(6):743-9.

208. Diez J, Querejeta R, Lopez B, Gonzalez A, Larman M, Martinez Ubago JL. Losartan-dependent regression of myocardial fibrosis is associated with reduction of left ventricular chamber stiffness in hypertensive patients. Circulation. 2002;105(21):2512-7.

209. Villar AV, Llano M, Cobo M, Exposito V, Merino R, Martin-Duran R, Hurle MA, Nistal JF. Gender differences of echocardiographic and gene expression patterns in human pressure overload left ventricular hypertrophy. J Mol Cell Cardiol. 2009;46(4):526-35.

210. Nemes A, Balazs E, Csanady M, Forster T. Long-term prognostic role of coronary flow velocity reserve in patients with aortic valve stenosis - insights from the SZEGED Study. Clin Physiol Funct Imaging. 2009;29(6):447-52.

211. Carasso S, Cohen O, Mutlak D, Adler Z, Lessick J, Reisner SA, Rakowski H, Bolotin G, Agmon Y. Differential effects of afterload on left ventricular long- and short-axis function: insights from a clinical model of patients with aortic valve stenosis undergoing aortic valve replacement. Am Heart J. 2009;158(4):540-5.

212. Carasso S, Cohen O, Mutlak D, Adler Z, Lessick J, Aronson D, Reisner SA, Rakowski H, Bolotin G, Agmon Y. Relation of myocardial mechanics in severe aortic stenosis to left ventricular ejection fraction and response to aortic valve replacement. Am J Cardiol. 2011;107(7):1052-7.

213. Carasso S, Mutlak D, Lessick J, Reisner SA, Rakowski H, Agmon Y. Symptoms in severe aortic stenosis are associated with decreased compensatory circumferential myocardial mechanics. J Am Soc Echocardiogr. 2015;28(2):218-25.

214. Wong TC, Piehler K, Meier CG, Testa SM, Klock AM, Aneizi AA, Shakesprere J, Kellman P, Shroff SG, Schwartzman DS, Mulukutla SR, Simon MA, Schelbert EB. Association between extracellular matrix expansion quantified by cardiovascular magnetic resonance and short-term mortality. Circulation. 2012;126(10):1206-16.

215. Nishimura RA, Otto CM, Bonow RO, Carabello BA, Erwin JP, 3rd, Guyton RA, O'Gara PT, Ruiz CE, Skubas NJ, Sorajja P, Sundt TM, 3rd, Thomas JD. 2014 AHA/ACC Guideline for the Management of Patients With Valvular Heart Disease: executive summary: a report of the American College of Cardiology/American Heart Association Task Force on Practice Guidelines. Circulation. 2014;129(23):2440-92.